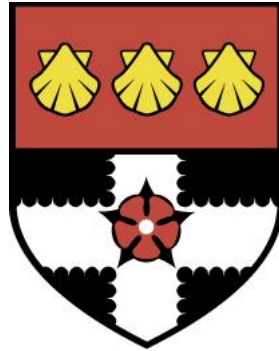UNIVERSITY OF READING

Department of Meteorology

The impact of climate variability and climate change on the GB power system

Hannah C. Bloomfield

A thesis submitted for the degree of Doctor of Philosophy

April 2017

Declaration

I confirm that this is my own work and the use of all material from other sources has been properly and fully acknowledged.

Hannah Bloomfield

Abstract

Recent trends in global energy systems have seen a rapid uptake in renewable generation, however, few studies have investigated the impacts of inter-annual climate variability and climate change on power system operation. This thesis aims to explore these impacts for the GB power system. Multi-decadal re-analysis and climate model datasets are used to create demand and wind power time-series as inputs for a load duration curve based power system assessment.

Using the MERRA reanalysis, it was found that all aspects of the GB power system are impacted by inter-annual climate variability, but the impacts are most pronounced for baseload generation. The impacts of climate variability are amplified by increasing onshore wind power capacity, and decreased by increasing offshore wind power capacity. The GB power system model is most sensitive to winter weather. A system with no installed wind power capacity is driven by inter-annual variability in temperatures. As the amount of installed wind power capacity is increased, the power system becomes increasingly sensitive to variability in winds. It was found that more than 10 years of climate data are required to adequately sample the impacts of inter-annual variability of climate on the power system.

In the HiGEM 4XCO_2 climate scenario, mean winter demand reduces (-6%) while mean summer demand increases (+5%) primarily due to warmer temperatures. These changes result in a reduction in the use of conventional generation (-30%) and peak load (-6%). Furthermore, suggesting that climate change may somewhat counteract the increases in inter-annual power system variability which would otherwise be associated with increasing installed wind power capacity.

Acknowledgements

Contents

List of Acronyms

Acronym	Definition
CCC	Committee on Climate Change
CDD	Cooling Degree Day
CMIP5	Coupled Model Intercomparison Project 5
DECC	Department of Energy and Climate Change
DNW	Demand-net-wind
EA	East Atlantic
EA-WR	East Atlantic West Russian
ENTSOe	European Network of Transmission System Operators for Electricity
GB	Great Britain
GCM	Global Climate Model
HDD	Heating Degree Day
HiGEM	HIgh Resolution Global Environmental Model
HIGH	A scenario with 45GW of installed wind power capacity (mostly offshore)
HIGH*	A scenario with 45GW of installed wind power capacity (mostly onshore)
LDC	Load Duration Curve
LOW	A scenario with 15GW of installed wind power capacity
MED	A scenario with 30GW of installed wind power capacity
MERRA	Modern-Era Retrospective Analysis for Research and Applications
MLR	Minimum Load Requirement
NAO	North Atlantic Oscillation
NERC	National Environmental Research Council
NO-WIND	A scenario with no installed wind power capacity
NREL	National Renewable Energy Laboratory
PB	Parsons Brinckerhoff
RMSE	Root Mean Square Error
RCP	Relative Concentration Pathway
SAT	Surface air temperature
SCA	Scandinavian
TAER	Total Annual Energy Requirement
TVE	Total Volume of Energy
UK	United Kingdom

Chapter 1:

Introduction

An international effort is currently being made to combat global warming by reducing CO_2 emissions. To achieve this, national targets have been set which require carbon reductions in all sectors. The electricity sector is one of the largest sources of greenhouse-gas emissions (accounting 27% of the United Kingdom's 2015 total; DECC (2016)). Present day power systems are not sustainable within these targets, due to a heavy reliance on fossil fuel technology, which causes large emissions of greenhouse gases. Within the electricity sector technologically mature, cost-effective options to meet carbon reduction targets are available, which are not so easily applicable in other sectors (such as agriculture and industry). Accordingly, power systems across the world are undergoing rapid decarbonisation in order to limit the impact of human induced climate change (CCC (2008)). An example of widely used decarbonisation is the installation of renewable energy generation. However, this results in an increasing level of weather-dependence, and consequent increases in the weather-dependent power system variability.

1.1 Weather-dependence in present day power systems

Within power systems weather-dependence is present in both demand (which is dependent on temperature; Baker et al. (1985)) and supply (due to renewable generation). In particular, wind power generation is predominantly dependent on wind speed, solar power generation is predominantly dependent on incoming solar radiation, and large hydropower generation is predominantly dependent on the amount of precipitation. Power system infrastructure can also be impacted by extreme events such as storms, lightning, and flooding (Dowling (2013)).

Weather can impact power systems on a number of timescales. On operational

timescales (of seconds-days) changes in synoptic conditions, such as the passing of an extra-tropical cyclone, can lead to localised changes in temperature and wind speed. These changes impact demand and renewable generation, which have implications for plant scheduling and grid management.

On timescales of days-months, seasonal forecasts are used to indicate anomalous demand behaviour, to plan wholesale energy contracts, and to confirm the maintenance schedules of power stations. A seasonal forecast showing that there may be a cold spell within summer could alert a coal or gas plant which operates exclusively in winter to the possibility of an additional opportunities to generate.

On timescales of years-decades (which are of interest to this project) the long-term patterns of demand or renewable generation can be characterised. There has been growing research interest in the inter-annual variability of wind power production due to the information being needed for wind farm site assessment (e.g. Brayshaw et al. (2011b), Cannon et al. (2015)). If a single year of data is used to assess the output of a potential wind farm site this could lead to problems in terms of wind farm financing. If a anomalously low wind year is chosen for analysis the site will be deemed unsuitable, whereas if a anomalously high wind year is chosen then the farm owners may struggle to make loan payments based on overly high expected generation.

The impacts of weather-dependant variability described above are all experienced by present day power systems. However, as the level of weather-dependence within power systems is increased (through the installation of more renewable generation capacity) a greater potential for variability at all temporal scales is seen.

1.2 Weather dependence in future power systems

Section 1.1 described some of the impacts that weather currently has on power systems. However, climate change may result in changes to the amount of weather-dependent power system variability (at all previously discussed timescales) and therefore differences in the operational requirements of power systems. Increasing temperatures may result in a reduction in heating-induced demand and an increase in cooling-induced demand across Europe (Isaac and van Vuuren (2009), Golombek et al. (2011)). Climate change may also cause changes to European wind speeds, with previous studies showing the potential for increasing average winter wind speeds and decreasing average summer wind speeds, which may cause changes in wind power generation on seasonal and inter-annual

timescales (Cradden et al. (2012), Hueging et al. (2013)). The combination of these factors (and multiple others discussed in section 2.4.7) results in a complex system response to climate change, which must be well understood in order for system operators to reliably meet consumer demand.

1.3 Thesis Motivation

It is challenging to perform analysis on weather-dependent power system components due to a number of issues (Dowling (2013)) including:

- A lack of available climate data at suitable temporal and spatial resolutions

- Difficulties translating climate data into energy-system-relevant data

- A lack of detail in energy system models where climate impacts act

- The non-stationarity of the power systems that must be represented

This study is believed to be the first to use multi-decadal time series of climate data, to assess the impact of inter-annual climate variability on the generation characteristics of a power system as a whole. Previous studies in this area have seldom used more than 10 years of data in their analysis (e.g. POYRY (2009), Green and Vasilakos (2010)), often claiming there is not enough multi-decadal climate data available in a usable format (Dowling (2013)). This thesis demonstrates a method for incorporating considerable amounts of climate data into a power system modelling framework in a transparent and reproducible way.

This study characterises the meteorological drivers of multiple aspects of power system behaviour. This is motivated by the growing weather-dependence of power systems, which means there is a need to understand the aspects of weather and climate variability that most strongly determine the expected annual or seasonal operation of conventional energy generation. The growing use of climate model data for power system modelling studies also requires the knowledge of the important characteristics of weather and climate that must be well represented in climate models, if they are to provide useful information.

Previous studies investigating the impact of climate change on power systems have either been part of global or continental scale studies, where limited amounts of climate model data have been used (Isaac and van Vuuren (2009), Golombek et al. (2011)) or studies where significant amounts of climate model data have been used to study a single

power system component, such as wind power generation (Hueging et al. (2013), Tobin et al. (2015)). This study investigates the impact of climate change on multiple aspects of power system operation, at country scale, using multi-decadal climate model data from a high resolution climate model (the High Resolution Global Environmental Model, HiGEM; Shaffrey et al. (2009)).

1.4   Thesis Aim and Objectives

The overarching aim of this thesis is:

To estimate the impact of inter-annual climate variability and climate change on the GB power system and understand its meteorological drivers.

This is accomplished by fulfilling a number of objectives. The chapter in which they are addressed given in brackets.

1. To construct a modelling framework in which multi-decadal meteorological data series can be used to evaluate the impacts of inter-annual climate variability on the GB power system. [Ch3]

2. To quantify the impacts of inter-annual climate variability on the GB power system. [Ch4]

3. To characterise the meteorological drivers of GB power system behaviour. [Ch5]

4. To assess the suitability of the High Resolution Global Environmental Model (HiGEM) for use in a study of the impacts of climate change on the GB power system. [Ch6]

5. To quantify the impact of climate change on the GB power system. [Ch6]

The first of these objectives is methodological, with the remainder being scientific objectives, forming the basis of the discussion in chapter 7. In completing these objectives this thesis provides information on the importance of robustly accounting for the impacts of inter-annual climate variability and climate change within power system planning. The thesis provides guidance on the important meteorological phenomena relevant to current and future power system operation and explores the barriers to the use of climate model data within power system modelling.

1.5 Study Scope

Great Britain (GB) is an island nation with limited interconnection. Physical links allowing for the transfer of electricity exist with: Ireland (1GW), the Netherlands (1GW) and France (2GW). GB therefore represents a reasonably isolated system. The GB power system is mature, with a well established installed wind power capacity of ∼15GW circa January 2017, and an increasing amount of installed solar power capacity, due to recent government subsidies (∼9GW of solar power was installed by the end of 2015; DECC (2016)). For context, the peak demand GB in 2015 was ∼53GW (DECC (2016)).

GB has committed to meet European Union targets of 20% of energy from renewable resources by 2020, resulting in a target of ∼30% for electricity generation (CCC (2008)). The GB system operator, National Grid, has created a set of four scenarios for power system development, in order to meet carbon reduction targets (National Grid (2015)). All four scenarios show increases in installed wind power and solar power capacity out to 2040. The scenario contributing the highest percentage of installed renewable generation is the *Gone Green* scenario (shown in Figure 1.1) and is the basis for analysis in this thesis.
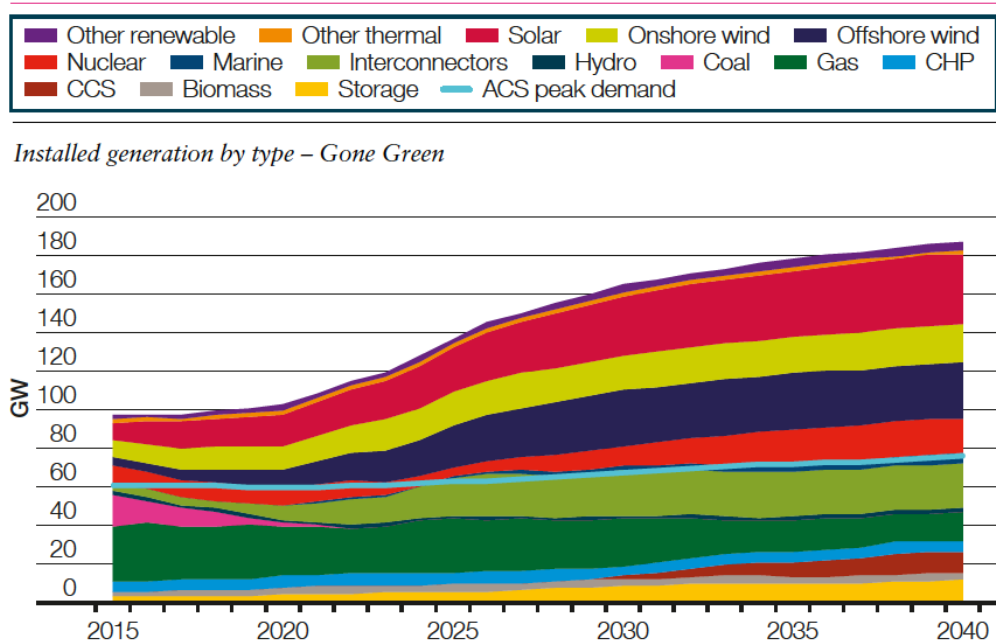
Figure 1.1 GB power system projected installed capacity in the *Gone Green* scenario. Source: National Grid (2015)

The weather-dependent components of this study have been limited to demand and wind power generation. At the beginning of this project (2013) less than 2GW of solar power capacity was installed in GB (with limited expectation of early growth) providing

~0.3% of annual electricity consumption (DECC (2016)). The amount of solar capacity installed on the GB system has increased considerably during the course of this study (~11.5GW of solar power capacity was installed by the end of 2016 providing 3.5% of total electricity consumption; DECC (2016)). Section 2.3 notes this gap, and argues for the inclusion of solar power generation in future projects.

1.6   Thesis Outline

The objectives given in section 1.5 are addressed in this thesis as follows:

Chapter 2 provides a literature review covering:

1. The power systems modelling literature, the weather-dependent power system components relevant to this study (demand and wind power production), and how they may be impacted by climate variability and change.

2. The meteorological drivers of GB power system variability

3. The drivers of European climate variability, which have the potential to impact current and future power system operation.

Chapter 3 describes the framework for analysis used in this thesis, and argues for the use of Load Duration Curves (LDCs) to model the GB power system. Weather-dependent demand and wind power models are created using meteorological re-analysis data. A series of metrics are also identified to be used as explanatory variables for inter-annual power system variability.

Chapter 4 focusses on quantifying the impacts of observed inter-annual climate variability on the GB power system. The first half of the chapter demonstrates the impact of inter-annual climate variability on the GB power system with varying levels of installed wind power capacity. Following this, sensitivity tests are conducted in order to understand how the distribution of wind farms used in the study may influence the amount of inter-annual variability experienced by the power system. This chapter concludes by discussing how previous studies may have been limited by their choice of meteorological data, with analysis performed in order to understand the amount of uncertainty that short meteorological records introduce into power system modelling studies.

Chapter 5 investigates the meteorological drivers of the inter-annual power system variability observed in chapter 4. The meteorological phenomena related to the inter-annual variability of five of the power system metrics (defined in chapter 3) are studied

and the implications of increasing the amount of installed wind power capacity on the GB power system are discussed.

In the first half of chapter 6 the ability of the chosen climate model, HiGEM, to simulate the meteorological drivers of inter-annual power system variability is assessed. Appropriate bias correction techniques are applied to ensure that the model is able to accurately simulate these metrological phenomena. The second half of chapter 6 quantifies the impact of climate change on the GB power system. The impact of climate change on demand and wind power generation are first examined separately. Following this the impact of climate change on the GB power system as a whole is quantified.

Chapter 7 explores the wider implications of key results from chapters 4 to 6. The thesis is then concluded and suggestions for future work are given.

Chapter 2:

Literature Review

This literature review introduces the meteorology and power systems background relevant for this thesis, written with a focus on the GB power system (a schematic overview of which is given in Figure 2.1). The focus of this thesis is on the impact of inter-annual climate variability and climate change on the GB power system. Inter-annual climate variability impacts the weather-dependent power system components, which are connected to the distribution grid (low voltage) or transmission grid (high voltage; see Figure 2.1). Section 2.1 focuses on electricity demand and section 2.2 on wind power production. A short section on solar power generation is included (section 2.3) to summarise how current research in this area relates to this thesis. In each section, the fundamentals of modelling each phenomena are discussed first; following this the impacts of inter-annual climate variability and climate change are summarised. While reviewing these weather-dependent components, challenges in understanding the impact of inter-annual climate variability and climate change on the relevant system components are highlighted, as well as gaps in the current research. This motivates the work which is completed in chapter 3 and 4 of this thesis.

Relevant methods used to model the GB power system as a whole (such as the system in Figure 2.1) are then discussed in section 2.4. After reviewing these methods the motivation for the choice of technique used to model the GB power system is given. The impact of inter-annual climate variability on the GB power system as a whole is the topic of chapter 4 therefore current work in this area, and gaps in the field are highlighted in section 2.4.5. Studies investigating the impact of climate change on the GB power system are highlighted in section 2.4.7, the limited amount of research in this area focussed on GB motivates the work which is completed in chapter 6 of this thesis.

The green and yellow power system components of Figure 2.1 are dependent on me-
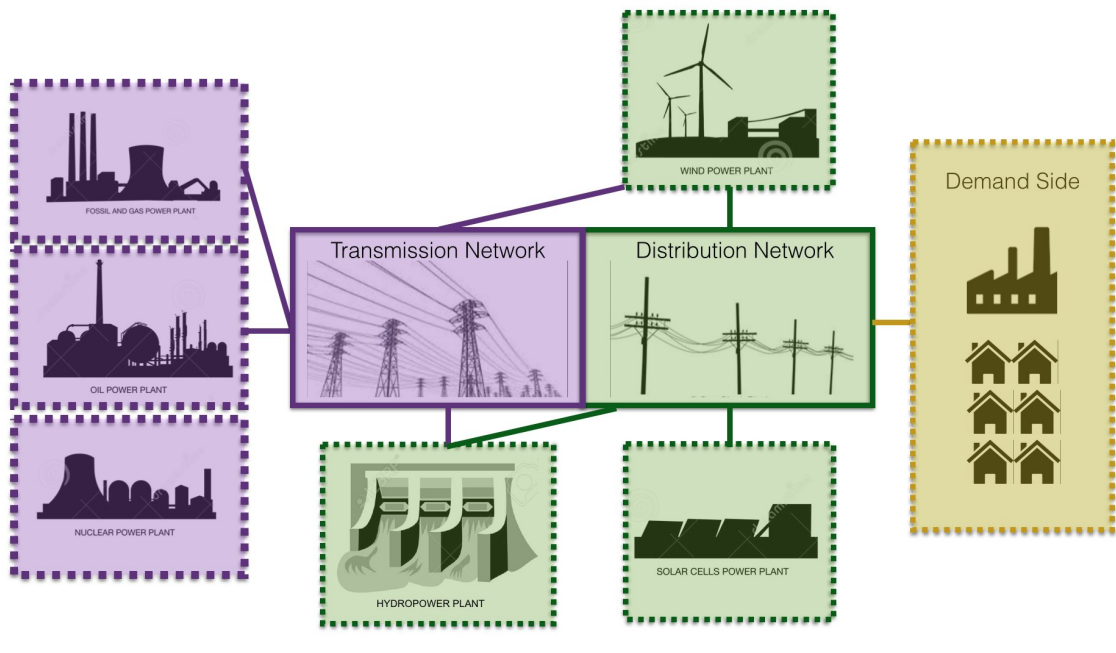
Figure 2.1   A schematic of the GB power system.

teorological variables, which vary on inter-annual timescales. Section 2.5 describes the previously published research on the meteorological drivers of GB power system variability. This research is reasonably sparse, motivating section 2.6 which describes the large scale drivers of European climate variability. These meteorological phenomena are of relevance to chapter 5 of this thesis, which builds on current research into the meteorological drivers of GB power system variability.

The chapter concludes in section 2.7 by summarising previous literature on the impacts of inter-annual climate variability on the GB power system, which this thesis aims to build upon.

2.1   Electricity Demand

Electricity demand is the total consumption of (electrical) energy from a number of sectors such as: industrial, residential and transport. In GB, national demand for electricity follows a number of regular and (to some extent) predictable patterns. These include a seasonal cycle (Figure 2.2a), a weekly cycle (Figure 2.2b) and a diurnal cycle (Figure 2.2c). The seasonal cycle of demand is predominantly dependent on temperature and will be discussed further in section 2.1.1. The weekly cycle of demand is controlled by human behaviour, with demand being higher on the week-days than at the weekends.

The diurnal cycle is also controlled by human behaviour, with a daily peak between 4pm and 10pm (Psiloglou et al. (2009)).
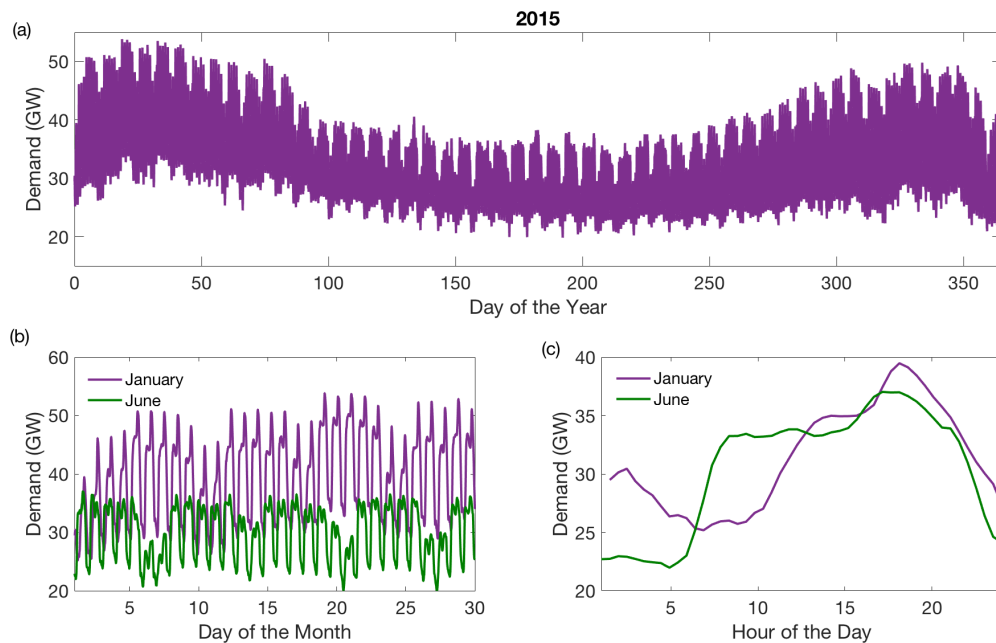
Figure 2.2   Example GB hourly demand data from 2015 for (a) the whole year (b) The months of January (purple) and June (green) (c) The first day of January (purple) and June (green). Source: National Grid (2015)

A range of model types have been used to study demand, these include: regression-based models (Taylor and Buizza (2003), Bessec and Fouquau (2008), Psiloglou et al. (2009), neural network models (Hippert et al. (2002)), and fuzzy logic models (Liu et al. (2002), Filik et al. (2011)). Demand has also been modelled on a range of spatial scales, from the demand in individual buildings (Yao and Steemers (2005)) to the national aggregate demand (Bessec and Fouquau (2008) and Thornton et al. (2016)). The majority of studies are aimed at the accurate forecasting of demand from hourly (Hippert et al. (2002), Taylor and Buizza (2003), Yao and Steemers (2005)) to seasonal (Felice et al. (2009)) timescales. However some also aim to understand the weather-dependencies of demand (e.g. Bessec and Fouquau (2008) Thornton et al. (2016)).

Demand models include a number of weather-dependent and non-weather dependent parameters. Examples of non-weather-dependent parameters include: hour of the day, day of the week, month of the year, public holidays, block industrial holidays and economic growth (Taylor and Buizza (2003), Psiloglou et al. (2009)). The aim of this thesis is to understand the impact of inter-annual climate variability on the GB power system. This involves the isolation of the weather-dependent components of national aggregate demand. The possible weather sensitivities of GB demand are discussed in the following

section.

2.1.1   Weather-sensitivities of demand

Near surface air temperature (from here-on referred to as temperature) is commonly considered to be the most significant meteorological variable impacting electricity demand from hourly to annual timescales (see Table 2.1). The statistical relationship between electricity demand and temperature is well established (Baker et al. (1985), Valor et al. (2001), Sailor (2001)). Temperature data is often weighted by population centres to more accurately reflect the sources of demand in large countries (Sailor and Munoz (1997), Valor et al. (2001)). *Effective temperature* is sometimes used rather than temperature (Baker et al. (1985) and Taylor and Buizza (2003)). This can be expressed as shown in Equation 2.1.

$$TE_t = TO_t + TE_{t-24} \tag{2.1}$$

Where TE represents an effective temperature, TO is the mean temperature over the last four hours and t is the hourly time-step (Taylor and Buizza (2003)). The definition of TO as the average of the last four hours temperatures is used as this is the timescale of heat transfer from external surroundings to within buildings (see Baker et al. (1985)). TE accounts for the implied time lag in the response of heating appliances within buildings to changes in external temperature (Baker et al. (1985)).

The relationship between demand and temperature has a characteristic *u-shaped* response (as shown in Figure 2.3). This u-shaped response reflects the winter-time heating-induced demands and summer-time cooling induced demands. There is a *dead zone* from ∼15-25°C where demand is not very sensitive to temperature. The characteristics of this u-shape differ by country, with southern European countries experiencing larger cooling-induced demand than Northern European countries (see Figure 2.3 and Bessec and Fouquau (2008)).

The u-shaped relationship between temperature and demand can be modelled using a quadratic or quartic term (Taylor and Buizza (2003)). An alternative method commonly used is to calculate heating degree days (HDD) and cooling degree days (CDD). HDD and CDD are calculated by fitting a linear curve to either side of the u-shape. An annual value for HDD and CDD is commonly described by Equations 2.2 and 2.3 respectively.
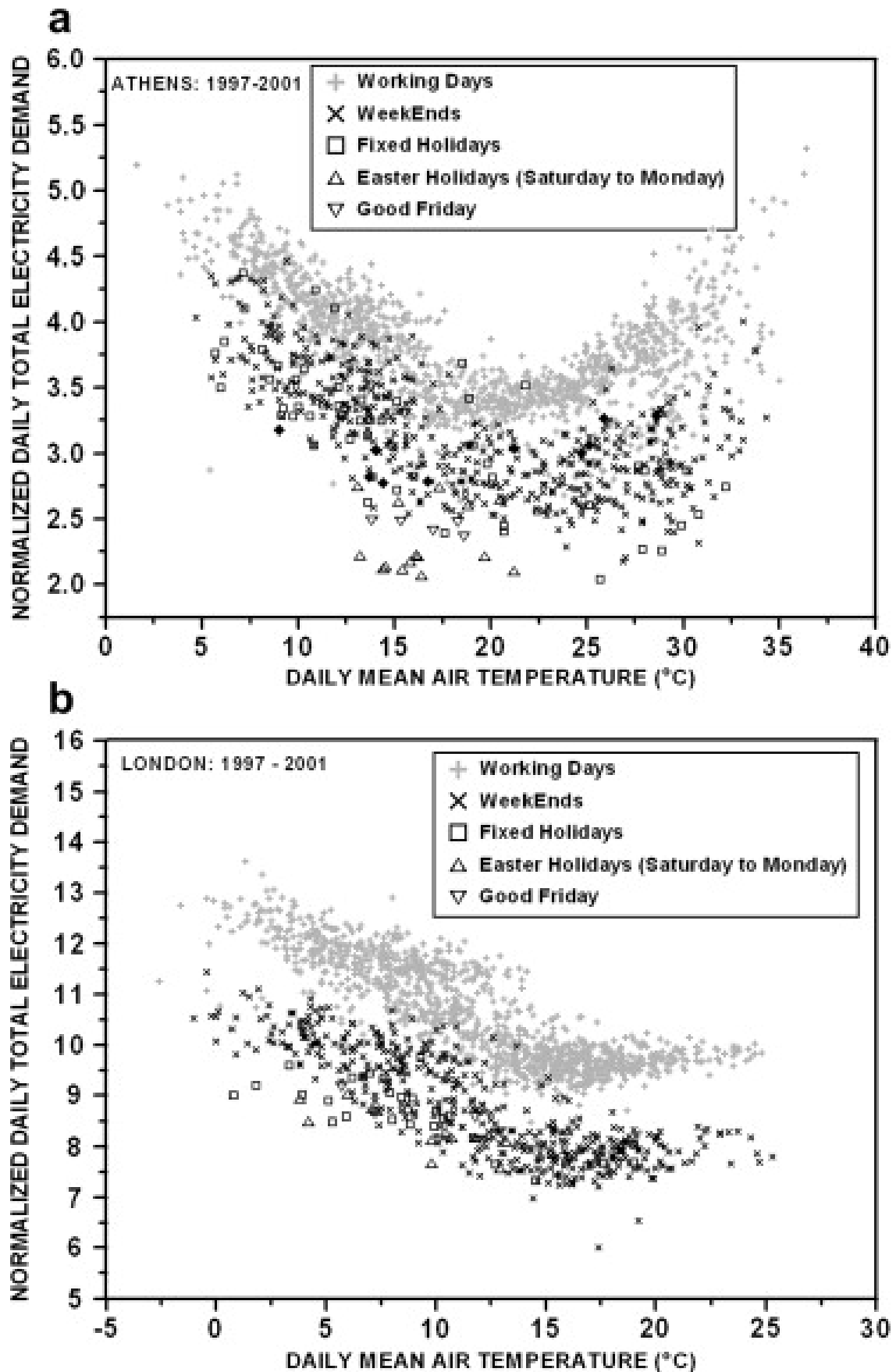
Figure 2.3 Scatter plot of normalised daily total electricity demand vs. daily mean air temperature, for (a) Athens, Greece and (b) London, UK, for the period 1997-2001. Source: Psiloglou et al. (2009)

Study	Country	Data period	Data source	Lead time	Weather-dependencies
Isaac and van Vuuren (2009)	Global	1970-1990	IMAGE Pattern scaling of Met Office climate model	Monthly	T, HDD, CDD, $T_b = 18$
Golombek et al. (2011)	European (including GB)	2000 and 2085	multiples GCM's downscaled using re-analysis data	Monthly	T, HDD $T_b = 18$, CDD, $T_b = 22$
Baker et al. (1985)	UK	1947-1958	MetOffice Forecast	Hourly	T_e, WC, EI
Taylor and Buizza (2003)	UK	1998-2000	ECMWF Forecast	Hourly	T_e, WC, CC
Hor et al. (2005)	England and Wales	1989-2003	UK CET	Monthly	T, HDD, CDD, ELD, RH $T_b = 20$
Psiloglou et al. (2009)	London	1997-2001	UK Met Office station	Hourly	T, HDD, CDD $T_b = 16$
Thornton et al. (2016)	GB	1975-2013	UK CET	Daily	T
Howden and Crimp (2001)	Australia	1999-2001	SILO datadrill	Weekly	HDD, CDD $T_b = 16$-18
Thatcher (2007)	Australia	2001-2004	Weather Station	Half-hourly	HDD, CDD $T_b = 17$-19
Apadula et al. (2012)	Italy	1994-2009	Stations	Monthly	T, u, RH, CC, HDD, CDD
Felice et al. (2013)	Italy	2003-2009	NWP forecast	Daily	T
Felice et al. (2009)	Italy	1990-2007	ECMWF seasonal forecast	Seasonal	T
Mirasgedis et al. (2007)	Greece	1993-2003	WMO station PRECIS climate model	Monthly	HDD, CDD, $T_b = 18.5$
Psiloglou et al. (2009)	Athens	1997-2001	UK Met Office station	Hourly	T, HDD, CDD, $T_b = 20$
Valor et al. (2001)	Spain	1992-1999	Weather stations	Daily	T, HDD, CDD $T_b = 18$
Sailor and Munoz (1997)	USA	1984-1993	weather stations	Monthly	T, RH, u, HDD, CDD $T_b = 18.3$
Sailor (2001)	USA	1984-2000	weather stations	Monthly	T, RH, u, HDD, CDD $T_b = 18.3$
Beenstock et al. (1999)	Israel	1973-1994	Weather station	Quarterly	HDD $T_b = 10$, CDD $T_b = 25$

Table 2.1 Details of a selection of the regression based models included in this literature review. Weather-dependencies are listed in order of significance. Terms include temperature (T), Heating-degree-days (HDD), cooling-degree-days (CDD), Base temperature (T_b), Effective temperature (T_e), Cooling power of the wind (WC), Effective Illumination (EI), Cloud cover (CC), enthalpy latent heat days ELD, relative humidity (RH), wind speed (u). See section 2.1.1 for definitions of terms.

$$\begin{aligned} \text{HDD} &= \sum_{i=1}^{365}(T_b - T_i) \quad &\text{for} = T_i < T_b \\ \text{HDD} &= 0 \quad &\text{for} = T_i > T_b \end{aligned} \quad (2.2)$$

$$\begin{aligned} \text{CDD} &= \sum_{i=1}^{365}(T_i - T_b) \quad &\text{for} = T_i > T_b \\ \text{CDD} &= 0 \quad &\text{for} = T_i < T_b \end{aligned} \quad (2.3)$$

Here T_i is the temperature at daily time-step and T_b is the base temperature. T_b can vary between countries depending on their sensitivity to the requirement for heating or cooling, with a range of 16-25°C found in the literature (Bessec and Fouquau (2008); Table 2.1). Countries with a large requirement for cooling tend to have a strong relationship between CDD and demand (Parkpoom and Harrison (2008), Beenstock et al. (1999)) whereas countries with a large requirement for heating tend to have a strong relationship with HDD (Hor et al. (2005) and Psiloglou et al. (2009)).

Temperature is not the only meteorological variable demand is dependent on. Other meteorological variables used in demand modelling include: relative humidity, rainfall rate, wind speed and cloud cover (see Table 2.1). These are sometimes viewed as correction terms for the relationship between temperature and demand (Li and Sailor (1995)), but mostly they are viewed as independent meteorological relationships (see Table 2.1).

Relative humidity can be significant in the determination of air-conditioning demands in warm countries such as the southern USA (Sailor and Munoz (1997)) Thailand (Wangpattarapon et al. (2008)) and Hong-Kong (Lam (1998), Lam et al. (2008)). When relative humidity is high, more energy is required to cool and de-humidify the air to indoor comfort levels (Sailor and Munoz (1997)). Precipitation rate can also be a significant variable in countries experiencing a rainy season, for example Wangpattarapon et al. (2008) found that a 1mm increase in average monthly rainfall results in 0.12GWh increase in monthly demand for Bangkok, this is due to the increase in relative humidity causing a higher cooling-induced demand. Rather than using relative humidity, some studies have used more complex variables such as enthalpy latent heat days (Sailor and Munoz (1997), Hor et al. (2005)). An enthalpy latent heat day can be described as the amount of energy required to lower the humidity to a desired comfort level without reducing the air temperature. Using this variable allows of the complete separation of the temperature and humidity impacts on demand (Hor et al. (2005)).

Heating-induced demand (such as experienced by GB) has been shown to be sensitive to wind speed and cloud cover (Taylor and Buizza (2003), Apadula et al. (2012)). The *cooling power of the wind* (WC) has been used in studies of GB electricity demand (Baker et al. (1985) and Taylor and Buizza (2003)). The cooling power of the wind is an empirical combination of temperature and wind speed. This relationship (taken from Baker et al. (1985)) is given in Equation 2.4.

$$WC(t) = \begin{cases} u^{0.5}(t)(18.3 - TO(t)) & \text{for} \quad TO(t) < 18.3^oC \\ 0 & \text{for} \quad TO(t) > 18.3^oC \end{cases} \tag{2.4}$$

Here u is the 10m wind speed and the other symbols are as defined in equation 2.1. This formulation is used as it adequately accounts for increases in residential demand caused by draughts within buildings. More complex methods could include information on wind direction (Baker et al. (1985)). Both cloud cover and precipitation have been shown to be related to lighting demand, with increases in both cloud cover and precipitation causing increases in demand for lighting (Taylor and Buizza (2003)).

2.1.2 Impact of climate variability on demand

One of the objectives of this thesis is to quantify the impact of inter-annual climate variability on the GB power system. To do this the impact of climate variability on GB demand must be well understood, with current research on this forming the focus of this

section. It is well known that a large proportion of the variability in demand is dependent on weather (Thatcher (2007)). However, the impacts of inter-annual climate variability and climate change on demand have been less well documented in the literature (Sailor and Munoz (1997), Mideksa and Kallbekken (2010)). The studies that have been found within the literature that are relevant to GB are discussed below.

Bessec and Fouquau (2008) analysed data from 1985-2000 to investigate the relationship between demand and temperature for multiple countries including GB. A large amount of inter-annual variability in temperatures is seen in this period, with a range of 0.6^oC between the mean temperatures of the consecutive five year periods, leading to inter-annual variability in demand.

Hor et al. (2005) created a monthly demand model based on weather and non-weather dependent parameters for GB from the period of 1970-1995. Hor et al. (2005) note in their discussion that including the hot summers of 1995 and the warm winter of 1989 in the training period of their model allowed for the inter-annual variability of demand to be both well modelled and understood.

Thornton et al. (2016) studied a multi-decadal time series of daily demand data (1772-present) in order to estimate the return periods of extreme, weather-induced demands which could impact the GB power system. The study found that the winter demand of 2010 (the highest on record, once socio-economic factors are removed by de-trending for the slowly varying background state) is estimated to be a 1 in 18 year event (with a 95% confidence interval of 12-27 years). This study showed that modelled multi-decadal demand data can be used to provide useful context to extreme system conditions.

2.1.3   Challenges in quantifying the impact of inter-annual climate variability on GB demand

One of the key challenges in investigating the impact of inter-annual climate variability on electricity demand is data availability (Dowling (2013)), with the quality of a statistical model being highly dependent on the quality and the quantity of data that is used in its development (Filik et al. (2011)). Demand models are generally developed with as much observed meteorological and demand data as is possible. Operational forecasts of demand incorporate output from numerical weather prediction models on timescales of a few hours to 1 day ahead (Taylor and Buizza (2003), Thatcher (2007), Felice et al. (2013)). Seasonal meteorological forecasts are beginning to be used to generate forecasts of demand (Felice et al. (2013)). Weather-station observations are commonly used to

investigate the impact of inter-annual climate variability on demand (Hor et al. (2005), Psiloglou et al. (2009), Thornton et al. (2016)). To the best of the authors knowledge re-analysis data has not been used to investigate the impact of climate variability on demand within the literature (see section 2.2.2 for more details on re-analysis data). The inputs for demand models running on multi-decadal timescales are commonly from global climate model (GCM) data sets (Mirasgedis et al. (2007), Isaac and van Vuuren (2009), Golombek et al. (2011)).

There presently are much longer records of weather data than demand data. Taking GB as an example, hourly demand data is available from 2006-present via ENTSOE (2016), whereas decades of meteorological data are available from meteorological stations or re-analysis datasets. Demand modellers are aware that the choice of meteorological period used for model training and analysis will influence the results from a study, and longer datasets are beginning to become more widely used (Hor et al. (2005), Bessec and Fouquau (2008)).

There tends to be a general trade off between demand modelling studies where either high temporal resolution data (e.g. hourly data) is used in models for a short time period, or low temporal resolution data (e.g. daily or monthly data) is used for a long time period (see Table 2.1). Both model types have their advantages and disadvantages. Demand models of high temporal resolution data ran over a short time period allow for an accurate representation of the diurnal cycle, and therefore a more accurate assessment of the human drivers of demand, with only a few years of data required to understand the behaviour at bank holidays or weekends (Taylor and Buizza (2003)). Conversely, demand models run for years-decades at lower temporal resolution allow for the impacts of interannual climate variability and climate change to be investigated (Thornton et al. (2016)). Using long series of meteorological data allows for the distinction between changes in demand due to climate variability or due to socio-economic factors, such as GDP or energy usage.

The only study within the literature that has been found to use multi-decadal records of meteorological data to generate a multi-decadal time series of demand is Thornton et al. (2016) (see Table 2.1). Thornton et al. (2016) is however limited to daily resolution, and therefore does not account for the diurnal cycle of demand, which introduces daily variability of the order of ∼15GW into the data (see Figure 2.2). There is therefore room for further modelling work in this area in order to understand the influences of inter-annual variability of GB demand using hourly resolution data. This would allow for a more accurate representation of the timing of peak demand events, and an assessment of

the variability that the GB power systems supply mix may be required to meet.

Another challenge in quantifying the impacts of inter-annual climate variability on demand is the ability to isolate the weather-dependent influences on demand. As Hekkenberg et al. (2009) state 'without removing variation due to weekdays, holidays and economic activity it is hard to isolate the impacts of temperature variability on demand'. Multiple methods to isolate these weather-impacts on demand have been used in the literature to remove long run trends due to economic growth. A commonly used technique for this is to divide demand by population (Sailor and Munoz (1997), Bessec and Fouquau (2008)). The influence of weekly cycles of demand (controlled by human behaviour) is removed in Thornton et al. (2016) by fitting and removing fourier modes to the demand data. The exclusion of exogenous demand variability is not common practice in the literature, therefore in studies which discuss the variability of demand it is difficult to know if this is due to weather or exogenous drivers.

Research into understanding the impact of inter-annual climate variability on demand is in its early stages of development, with it becoming increasingly common to isolate the impacts of weather on demand. The availability of reanalysis datasets means that there are consistent multi-decadal records of meteorological data that can be used to create long time series of demand, which to the best of the authors knowledge have not yet been utilised by the demand modelling community.

2.1.4 Impact of climate change on demand

The pace of research on the potential impacts of climate change on demand has accelerated in recent years as global climate change has become better understood, and the degree of spatial resolution available in climate projections has increased (Franco and Stanstad (2007)).

The literature on the impact of climate change on energy demand is primarily focussed on how changes in temperatures may impact the number of HDD or CDD experienced by a given country (Mirasgedis et al. (2007), Golombek et al. (2011), Isaac and van Vuuren (2009)). The general result found in all studies is that heating-induced demands may reduce (in countries such as Northern Europe, GB, and parts of the U.S.A.) whereas cooling-demands may increase (particularly in countries such as Southern Europe, and parts of Asia; Isaac and van Vuuren (2009), Golombek et al. (2011))

Mirasgedis et al. (2007) examined the changes in intra-seasonal variability of demand for Greece in a future climate, finding a larger increase in demand variability in summer

than in winter. This was due to the increasing temperature-dependence of demand in summer (with more months of data present within the up-tick of the u-shaped relationship between temperature and demand) and decreasing temperature dependence in winter.

Research on the impact of climate change on GB electricity demand is reasonably sparse, with most results relevant to GB coming from global (Isaac and van Vuuren (2009)) or European (Golombek et al. (2011), Mideksa and Kallbekken (2010)) studies. Increasing temperatures due to climate change may cause a reduced GB winter heating demand (e.g. Isaac and van Vuuren (2009), Golombek et al. (2011), CCC (2017)), although GB winter demands are still predicted to remain high (CCC (2017)).

A gap in this literature is highlighted for a more focussed analysis on the potential impacts of climate change on GB electricity demand. All of the studies discussed above are focused on how a mean change in temperature may impact a mean change in demand (usually using HDD or CDD as a proxy). No studies have investigated how a changing climate may influence the inter-annual variability of demand.

2.1.5 Challenges in quantifying the impact of climate change on GB demand.

In a future climate there may be changes in demand due to factors that are both weather-dependent and non-weather-dependent. Changes in demand which are not due to weather include: efficiency improvements of household appliances and lighting, and the electrification of heat and transport sectors (Bossmann and Staffell (2015)). NERC (2016) estimate that the electrification of the transport sector (due to increased uptake of electric vehicles) could increase GB demand by 26TWh. Future economic uncertainty, such as changing energy prices and regional population changes have been suggested to have much larger impacts on future energy use than climate change (Hor et al. (2005), Mirasgedis et al. (2007), Hekkenberg et al. (2009)). Isaac and van Vuuren (2009) discuss how although climate change may have a large impact on demand in countries such as India, the magnitude of this change is strongly dependent on changes in gross-domestic-product and the affordability of cooling appliances to the population.

One of the main challenges in quantifying the impact of climate change on GB demand is that the future climate is uncertain. Potential changes in a future climate can be modelled using global climate models (GCM's). GCM's include both an atmosphere and ocean component, which can be coupled together. The large scale circulation within a GCM is described by the equations for mass, momentum and energy conservation in the

atmosphere and ocean (known as the primitive equations). These can be discretised over the chosen model grid. GCMs are generally run at a coarse resolution due to their high computational expense. Therefore processes which happen at smaller scales than the chosen model grid are then represented by parameterisations (these include: convection, radiation and gravity wave drag).

GCM output is stored at relatively low temporal resolution (typically daily, due to data storage limitations), and therefore is not naturally suited for modelling the sub-daily variability of demand. The horizontal resolution of early GCM's was highlighted as a limitation of climate models for use in demand modelling in Li and Sailor (1995). Changes in demand patterns over GB may be driven by changes in meteorological conditions over small areas, where the grid box values from climate models may not be representative of an area of high population density (and therefore high demand) such as a city (Mirasgedis et al. (2007)).

The large scale circulation within a GCM is described by the equations for mass, momentum and energy conservation in the atmosphere and ocean (known as the primitive equations). These can be discretised over the chosen model grid. GCMs are generally run at a coarse resolution due to their high computational expense. Therefore processes which happen at smaller scales than the chosen model grid are then represented by parameterisations (these include: convection, radiation and gravity wave drag). Ocean-only GCM's and Atmosphere-only GCM's are used to model the ocean and atmosphere respectively. Coupled GCM's combine these two types of models and are the basis of model predictions of future climate.

The simplest approach used in some of the earliest studies of the impact of climate change on demand involved taking observed temperature data and adding on the difference between climate models control runs and future scenarios over the area of interest (Sailor (2001), Parkpoom and Harrison (2008)). Slightly more complex approaches include *pattern scaling* techniques, such as employed in Isaac and van Vuuren (2009) where the climate change signal from surface temperatures from a Hadley centre climate model was imposed onto present day temperature data. An alternative approach is to use the GCM data itself to represent the current and future climate. This has been done in Thatcher (2007), where GCM data from the CSIRO Mk2 model (ran at 1.8 degree resolution ($\approx$200km over Europe; Gordon et al. (2002)) was dynamically down-scaled to 60km resolution (using CSIRO's conformal cubic atmospheric model; McGregor (2004)). Dynamical downscaling is a method for obtaining increased resolution climate model data

from relatively coarse-resolution GCM's using a limited-area, high-resolution model (i.e. a regional climate model) which is driven by boundary conditions from a GCM. Following the dynamical downscaling temperature data from the time period 2001-2010 was com-pared to 2051-2060 within the model.

This has been done in Thatcher (2007), where GCM data from the CSIRO Mk2 model (Gordon et al. (2002)) was dynamically downscaled to 60km resolution (using CSIRO's conformal cubic atmospheric model; McGregor (2004)). Dynamical downscaling is a method for obtaining increased resolution climate model data from relatively coarse-resolution GCM's using a limited-area, high-resolution model (i.e. a regional climate model) which is driven by boundary conditions from a GCM. Following the dynamical downscaling temperature data from the time period 2001-2010 was compared to 2051-2060 within the model.

GCM output contains biases, which must be both understood and accounted for if the results from studies using climate model data are to provide meaningful information to the power systems modelling community. Biases arise due to the coarse spatial resolution of the models (which is required for mutli-decadal simulations) which results in a number of small scale processes being parameterised, and therefore not always accurately represented.

In Mirasgedis et al. (2007) the control run of the climate model simulations which are used is compared to station-based observations (see Figure 4 in Mirasgedis et al. (2007)). This study could have been improved by attempting to correct the biases in spring and autumn temperatures which were identified. Franco and Stanstad (2007) use bias correction techniques to account for the differences between the control run of the regional climate model and observations used in their study of electricity demand in California. The comparison of climate model data to observations allows for more physically meaningful results, and an understanding of the weaknesses of the climate model over the study area (although it is noted that observations may also contain biases).

Climate models are a useful tool to understand the impacts of potential changes in weather and climate on demand, however, there are a lack of studies within the literature which make use of current generation, high resolution climate models for this purpose. The bias present in climate model data used for demand modelling is also rarely evaluated.

2.2 Wind power generation

This section discusses the instantaneous relationship between wind speed and wind power generation. The following subsections then summarise current literature on the impacts of inter-annual climate variability and climate change on GB wind power production, and the challenges associated with accurately modelling this.

Wind speeds experienced at wind turbine locations are strongly influenced by passing weather systems (e.g. extra-tropical cyclones and anti-cyclones), local terrain (e.g. the presence of mountains, valleys, buildings or trees) and the differential heating of the land and sea (Freris and Infield (2008)).

The energy availability to a wind turbine is proportional to the cube of the wind speed and is described as in Equation 2.5.

$$\text{WP} = \frac{1}{2}\rho \text{A} u^3 c_p \tag{2.5}$$

where ρ is the density of air, A is the swept area of the turbine, u is the hub-height wind speed and c_p is the betz limit (0.59; this describes the aerodynamic efficiency of the wind turbine (Freris and Infield (2008)). Commonly wind speed observations are taken at heights of 10m, whereas wind turbine hub-heights range from 60-100m (Kubik et al. (2013)). In order to get wind speeds to hub-height, scaling relationships are applied. Two commonly used methods of extrapolating surface winds to hub-height are given in Equations 2.6 and 2.7. The first is the Hellman exponential law shown in Equation 2.6:

$$\frac{u_{hub}}{u_{ref}} = (\frac{z_{hub}}{z_{ref}})^\alpha \tag{2.6}$$

where u_{hub} is the wind speed at hub-height, u_{ref} is the reference height wind speed (usually 10m). z_{hub} and z_{ref} represent wind turbine hub-height and reference height respectively. α is an empirically derived wind shear coefficient which accounts for the local surface roughness and stability conditions. The Hellman exponential law is known as the wind profile power law if a value of $\alpha = \frac{1}{7}$ is used. The wind profile power law has been used in multiple studies of wind power generation over GB (e.g. Hueging et al. (2013), Tobin et al. (2015), Hdidouan and Staffell (2017)).

The second method of extrapolating wind speeds to hub-height is the logarithmic wind profile law shown in Equation 2.7:

$$\frac{u_{hub}}{u_{ref}} = \frac{ln(\frac{z_{hub}}{z_0})}{ln(\frac{z_{ref}}{z_0})} \tag{2.7}$$

where terms are defined as in equation 2.6 and z_0 is the roughness length of the terrain near the turbine. Both equations have been shown to perform similarly for a mean wind speed profile, however, Kubik et al. (2013) showed that the max-min range of extrapolated wind speeds at 60m is considerably larger for the wind profile power law than the logarithmic wind profile law. For sites which mainly exhibit stable boundary layer conditions the two laws perform similarly. However, in neutral and unstable conditions the profiles differ more considerably and the power law is believed to be more correct (Emeis and Turk (2007)).

If wind speeds at multiple heights are available then other methods to calculate hub-height wind speed can be used. In Cannon et al. (2015) a logarithmic profile was fitted between 2m, 10m and 50m wind speeds from the MERRA re-analysis (Rienecker et al. (2011)) at each wind farm location. The logarithmic profiles were then used to extrapolate the 50m winds to hub-height.

The cubic relationship between wind speed and wind power generation implies that wind power varies substantially more than wind speed. Figure 2.4 shows the power curve used in Cannon et al. (2015) which characterises the relationship between wind speed and wind power capacity factor. Capacity factor is defined as the amount of power that is being generated as a percentage of the maximum possible generation during the time period (Freris and Infield (2008)). A power curve is a commonly used method for calculating wind power generation of a turbine. Below the cut-in speed the turbine is not operational (due to there not being sufficient torque to overcome frictional forces and generate useful power). Between the cut-in speed and the rated-wind-speed of the wind turbine the cubic relationship shown in equation 2.5 holds. Once at the rated-wind-speed the turbine will generate at maximum (rated) power output unless the wind speed exceeds the cut-out wind speed or drops below the rated-wind-speed. Most modern turbines have the requirement that if the cut-out wind speed is exceeded then there is a limit lower than the cut-out-speed which must be reached before power can be generated again. This is a safety precaution to reduce the possibility of costly damage to turbines at high wind speeds (Cannon et al. (2015)).
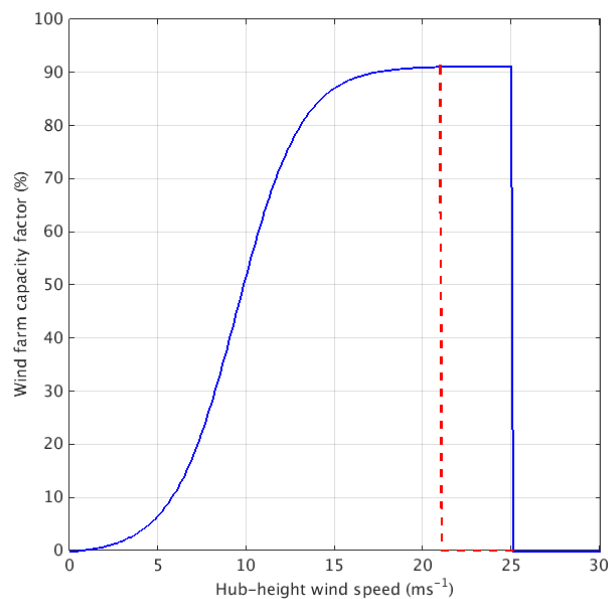
Figure 2.4 The power curve used in Cannon et al. (2015) is shown in blue. The cut-in speed is shown in the red dashed line. If wind speeds greater than 25m^{-1} are experienced then the cut-in speed is the level that wind speed must reduce to before the wind farm can generate power again.

2.2.1 Impact of inter-annual climate variability on GB wind power generation

The addition of installed wind power capacity to a power system increases the amount of weather-dependent-variability present. Variations in wind power generation range from the turbulent scale (where second to second variations in wind speed cause changes in wind power generation) to climate scale (where inter-annual changes in annual average wind speed impact aggregate power generation). Between these there are a number of other timescales of variability such as diurnal, with wind speeds being higher on average during the day than the night (Sinden (2007)), synoptic, with passing weather systems impacting wind power output (Oswald et al. (2008)), or seasonal (with wind speeds being higher in winter than summer; Cannon et al. (2015), Sinden (2007)). The timescale of interest to this study is the climate scale (i.e. year-year) so this will be the focus of the remainder of this section.

The long term variability of GB wind power was first considered by Golding and Stodhart (1949) where wind speed records from 12 weather stations across GB were analysed with fluctuations in wind speeds ranging from 65-130% of the long term average. Multiple studies have been conducted since this, using station based observations. Palutikof et al. (1987) found that between 1962-1981 there were three phases of fluctuating wind speed which could lead to as much as a 50% reduction in wind power output be-

tween high and low years. Sinden (2007) examined the period from 1970-2003 showing that the period had a long term average capacity factor of 30%. Sinden (2007), Earl et al. (2013) (who studied the period from 1980-2010) and Fruh (2013) (with the study period from 1969-2013) found the maximum year to year swing in capacity factor was from 1986-1987, with an approximately 10% difference in wind power generation. Fruh (2013) show Scottish wind power output typically varies by 10-15% per year with much larger variations being possible in individual pairs of years. Fruh (2013) states this could lead to large deviations in wind farm income between years.

Many studies have made use of re-analysis data to study the impact of climate variability on wind power generation. A re-analysis dataset is a data product in which observations are combined with a numerical model to provide a consistent gridded dataset spanning an extended period, usually multiple decades. Studies based on re-analysis data find a general increase in annual-mean wind speeds from 1940-1980 (Pryor et al. (2006)) followed by a general weakening in annual wind speeds since the early 1980s (Cannon et al. (2015), Earl et al. (2013)). Large changes in the observing system were seen from 1940-1980 with increasing volumes of data becoming available, which could be the reason for the increasing winds during this period (see Bengtsson et al. (2004) for further details). From 1980 large volumes of satellite data are available for assimilation within re-analysis datasets which should result in less uncertainty in the data from this point, especially over regions which have not been previously well observed (e.g. the southern hemisphere). However, there is still some uncertainty due to changes in the observation quality and quantity over time and differences in data assimilation.

Cannon et al. (2015) used the MERRA (Rienecker et al. (2011)) and ERA-interim (Dee et al. (2011)) re-analysis products to examine the impact of climate variability on GB aggregate wind power production from 1980-2012. An annual average capacity factor of 32% is found in the period, with interannual swings comparable to Earl et al. (2013) and Sinden (2007). Drew et al. (2015) extended the work of Cannon et al. (2015) to investigate how GB wind power production may change with increased offshore wind generation. A significant rise in annual mean capacity factor was suggested (from 32.7% to 39%) due to the windier locations of offshore farms. The inter-annual variability of annual capacity factor in Drew et al. (2015) remains comparable to Cannon et al. (2015).

Bett et al. (2013) investigated inter-annual wind speed variability over the last 140 years using the 20th Century re-analysis (Compo et al. (2011)). Bett et al. (2013) show that 2010 is the lowest mean wind speed year within the 140 year record, which could

have made it the lowest wind power production year in the last century. These results should however be interpreted with caution due to the large increases in the quantity and quality of the mean sea-level pressure observations that are assimilated within the 140 year period in the 20th Century re-analysis.

There is a vast amount of literature on the impact of inter-annual climate variability on wind power generation with mature techniques and modelling tools available for future research in this area. The bulk of these studies (with the exception of Drew et al. (2015)) have focussed on current distributions of wind farms, therefore the impact of inter-annual climate variability on GB wind power production in a power system with large amounts of offshore wind generation is less well understood.

2.2.2 Challenges in modelling the impact of inter-annual climate variability on GB wind power generation

Many studies on the impact of wind speed variability on wind power output are based on station observations (Palutikof et al. (1987), Sinden (2007), Earl et al. (2013), Fruh (2013)). These studies all include long observational records of data, however they are limited to onshore monitoring sites, which is not reflective of the planned wind farm developments for GB (Drew et al. (2015)). The wind mast data also may not have been located in relevant wind generation sites, which may have distorted the wind generation profiles (Kubik et al. (2013)). There may also have been changes in the recording instrumentation at sites, which may impact the resultant wind power output (Kubik et al. (2013)).

A method of dealing with the lack of observation data at wind farm location is to use re-analysis data (Pryor et al. (2006), Bett et al. (2013), Cannon et al. (2015), Drew et al. (2015)). In a re-analysis product, model fields are combined with irregularly distributed observations (both spatially and temporally) in order to create a complete, gridded meteorological dataset. In doing this the model and analysis system is kept constant over the whole period of interest. (Kubik et al. (2013)). The parameterisations within a re-analysis dataset may not be able to exactly represent sub-grid scale effects such as local topography, but can provide a consistent time series which is commonly much longer than the wind mast records which are available.

Re-analysis data-sets are not the perfect solution to model wind power generation as they do not include sub-hourly resolution wind speed variability and have parameterised, sub-grid scale processes (Kubik et al. (2013)). Re-analysis products are also not without

inherent bias. This bias can be due to the quantity and quality of observations which are assimilated within the re-analysis, and this not being constant in time. The bias in the MERRA re-analysis has been examined in Rose and Apt (2015) and Staffell and Pfenninger (2016) with a focus on wind power modelling. Staffell and Pfenninger (2016) found that MERRA over-estimates wind speed over GB, which without bias correction, lead to an over-estimation in wind power generation. Understanding the causes of the wind speed bias was beyond the scope of this study but is suggested in the study as a useful avenue for further work.

Although re-analysis datasets are able to provide long records of data for analysis they are still limited to observational recording periods. One way to address this problem is to use long control runs from climate models (Pryor et al. (2006)). A problem with the use of climate model data for calculating wind power generation over GB is models contain biases, which must be well understood for results to be used meaningfully.

2.2.3 Impact of climate change on GB wind power generation

GCM's are a useful tool to investigate the impacts of climate change on wind power production (see section 2.1.5 for a description of a GCM). When using GCM's, wind power generation is commonly calculated for a country as a whole, rather than calculating individual wind farm output, due to the coarse spatial resolution of climate models (Pryor et al. (2006), Hueging et al. (2013), Tobin et al. (2016)). Wind energy indices are often used for analysis at country level (such as wind speed cubed, commonly termed wind energy density; Hueging et al. (2013)).

Some studies have found moderate reductions in annual wind power generation over GB in a future climate (<5%; Barstad et al. (2012), Tobin et al. (2016)), whilst some find moderate increase in wind power generation. These changes are predominantly associated with reductions in summer wind power generation, but larger increases in winter wind power generation (Cradden et al. (2012), Hueging et al. (2013), Tobin et al. (2015)). Hueging et al. (2013) find that the inter-annual variability of wind power generation may increase over GB in a future climate. These results are all regarded as highly uncertain, as studies conducted using an ensemble of GCM's show a large spread over GB (Pryor et al. (2006), Hueging et al. (2013)). The large spread between GCM simulations is due to uncertainty in the representation of both large scale features (such as the North Atlantic storm track; see Woollings (2010)) and small scale features (such as cyclones; see Catto et al. (2010)).

2.2.4 Challenges in modelling the impact of climate change on GB wind power generation.

The large spread in potential future wind power generation discussed in section 2.2.3 is due to the large spread in future wind speed responses to climate change over GB in GCM's. GB wind speeds are impacted by the passing of storms. Zappa et al. (2013b) showed the spread in North Atlantic storm track locations in an ensemble of climate models (CMIP5 ensemble) to be of the same order of magnitude as the signal of change in storm track location when the multi-model means are analysed. If GCM's are to be used to understand the impact of inter-annual climate variability on GB wind power generation then the biases within the models must be well understood and potentially corrected for. Bias correction could however be complex if model dynamics are fundamentally wrong (for example a too zonal representation of the North Atlantic storm track).

Within the wind power modelling literature there are many studies which use GCM data to calculate future wind power generation. Various bias correction techniques are used in future wind power modelling, with the correction normally performed on the wind speed field (e.g. Tobin et al. (2015)). Methods include corrections of Weibull parameters (Hdidouan and Staffell (2017)) or cumulative frequency distribution transforms (e.g. Barstad et al. (2012), Tobin et al. (2015)).

There are also a number of studies which do not use bias correction techniques (e.g. Nolan et al. (2012), Cradden et al. (2012) Hueging et al. (2013), Tobin et al. (2016)). Tobin et al. (2016) choose not to use bias correction due to a lack of high resolution observations to perform the correction against, stating that correcting to satellite data or re-analysis data does not alter the results seen in the study, which is focused on potential *changes* in wind power generation in a future climate, rather than the magnitudes of generation.

Pryor et al. (2006) also examine the validity of the climate model they are using to make statements about changes in the wind climate by comparing its output statistically to the NCEP re-analysis and ERA-40 re-analysis. Pryor et al. (2006) comment that if the model in question did not have a good representation of the large scale atmospheric circulation (and consequently the near surface flow) then it would not provide reliable estimates of wind energy indices. Their chosen climate model was picked due to its good representation of the North Atlantic Oscillation, which had been shown to be important for analysing wind power variability in the European climate (see Section 2.5.2).

There are multiple studies examining the impact of climate change on GB wind

power production. however, even with the large variety of models and techniques used, the magnitude and direction of future changes in GB wind power production is still uncertain. This motivates the need for further analysis in this area so that more robust conclusions can be drawn.

2.3   Solar power generation

Solar power provided 7.5TWh of energy to GB in 2015, meeting 2.5% of total electricity consumption (DECC (2016)). This is a small contribution compared to the 40TWh of generation from wind power (11% of total electricity consumption; DECC (2016)). However, the amount of solar power generation installed on the GB power system is increasing, and solar power is set to become an important resource to decarbonise the GB power system (National Grid (2015)). Some relevant background and important studies within the current GB solar power literature are outlined below.

Solar power generation is dependent on the amount of incoming solar radiation incident on the solar panel. The efficiency of a solar panel is also proportional to the air temperature around the panel (Bett and Thornton (2016)). Solar power generation is generally modelled by combining a *clear sky* model and a *radiation* model. The clear sky model calculates the amount of solar power generation at a site in clear sky conditions, incorporating the effects of latitude, solar zenith angle and shadowing. The radiation model incorporates the effects of aerosols and clouds (for more details see Antonanzas et al. (2016)).

Solar power has a strong diurnal cycle with generation only possible during daylight hours. It also has a large seasonal cycle (larger than seen for wind power generation Bett and Thornton (2016)) with significantly more potential for solar power generation during summer than winter due to the angle that the earth is incident to the sun (Antonanzas et al. (2016)).

As solar power is a relatively new technology, which is commonly input onto the grid at distribution level rather than transmission level (Freris and Infield (2008)) there are limited records of metered solar power data available to use in power system modelling. Modellers have therefore began to use re-analysis data (Heide et al. (2010), Jurus et al. (2013), Bett and Thornton (2016), Pfenninger and Staffell (2016)) and satellite observations (Jurus et al. (2013), Pfenninger and Staffell (2016)) to model solar power generation.

When using re-analysis data, solar power has been modelled using the global horizontal irradiance field (Jurus et al. (2013), Pfenninger and Staffell (2016)). There are problems with using re-analysis for solar power modelling due to the coarse grid resolution (Boilley and Wald (2015)). Satellite data has been shown to give a more accurate representation of global horizontal irradiance, than re-analysis data (Boilley and Wald (2015)), however hourly satellite data has only recently become available so has not commonly been used for solar power generation modelling (Pfenninger and Staffell (2016)).

The co-variability of wind power and solar power generation over GB has been investigated by Bett and Thornton (2016) using re-analysis data. A weak tendency was found for days of high wind power generation to have low solar power generation, particularly on the west coast of GB. Bett and Thornton (2016) also found that the daily variability of wind power generation is reduced by incorporating solar capacity. This is useful knowledge for system balancing.

Including solar power generation in the GB power system has been found to significantly change the GB load profile, and impact the ramping requirements of plants (Pfenninger and Staffell (2016)). More modelling studies are needed to further quantify these impacts and understand how inter-annual variations in demand, wind power and solar power may impact the GB power system.

Research into the modelling and understanding of the solar power resource and its impacts on the GB power system is in its relative infancy, with only a handful of studies focussed on GB specifically (Pfenninger and Staffell (2016), Bett and Thornton (2016)). The quality of modelled solar power data from re-analysis is a topic of current interest, with further work needed to fully understand the usefulness of re-analysis data for country specific solar power modelling. For this reason solar power has not been considered in the current thesis, but would provide an interesting avenue for future work.

2.4 GB Power system modelling

This section presents a summary of the fundamental methods used to model the GB power system and its weather-dependent components, both on operational timescales (hours-months) and investment timescales (years-decades). As the aim of this thesis is to understand the impact of inter-annual climate variability on the GB power system, a summary of the current research in this area is presented for both operational and investment power system modelling (section 2.4.5). The impact of climate change on the

GB power system as a whole is also discussed in sections 2.4.7. Within each subsection the challenges in modelling the impacts of inter-annual climate variability on the GB power system are highlighted, motivating the need for studies such as this thesis.

2.4.1 Operational timescale power system modelling

Power system models exploring operational timescales (i.e. hourly to weekly timescales) decide on the most economically efficient way to operate a set of known generators within a power system. The main two operational modelling techniques are *unit-commitment* and *economic dispatch.*

A unit commitment model schedules the most appropriate mix of generation to meet a forecast load. Unit-commitment models are typically cost-optimised (although it is possible to optimise for other variables such as CO_2 emissions) over a number of days-weeks to quantify the times at which different plants are needed to turn on and off. A number of constraints could be present in a unit commitment model which may restrict plant output. These constraints make unit commitment a complex non-linear optimisation problem which is computationally expensive to solve. Some examples of these include:

- **Start up times:** Some plants (such as large coal fired power stations) will take a number of hours to initially switch on. This is known as cold operation.

- **Ramping rates:** The maximum rate of change in output that a generator is capable of.

- **Minimum loading of a plant:** For a plant (such as a coal or gas power station) there are lower limits to the operational efficiency. Minimum loading is typically 30-50% for a plant (Freris and Infield (2008)).

- **System non-synchronous penetrable limits:** The amount of power that must be supplied by large synchronous generation sources. The large spinning parts in these conventional plant aids in balancing grid frequency. In GB the current limit is 30% of generation to come from non-synchronous sources, however there are future plans for this limit to move towards 50% as more renewables are incorporated, such as with the Irish power system. (McGarrigle et al. (2013))

- **Storage:** This may be present in the form of large pumped hydropower plants or as smaller battery units. Both can be used to ease the ramping requirements

of conventional plants, to shift loading requirements through the day or for rapid frequency response.

Unit commitment models commonly use the principle of *merit order* (Green (2005)). To do this each generation unit is ranked according to the price of generation. The price is typically characterised by the short-run costs of production (usually the cost of the fuel to generate an extra unit of electricity) and the amount of energy that can be provided (Stoft (2002)). A schematic showing the principle of merit order is given in Figure 2.5. The gradient of the cost-curves in Figure 2.5 gives the marginal cost of generating another unit of power. This marginal cost is sometimes known as the *variable cost* and includes: fuel and maintenance costs (Stoft (2002)). In reality the marginal cost is not a linear function (as is seen in Figure 2.5a) due to plants operating at different efficiencies at different output levels (Freris and Infield (2008)).
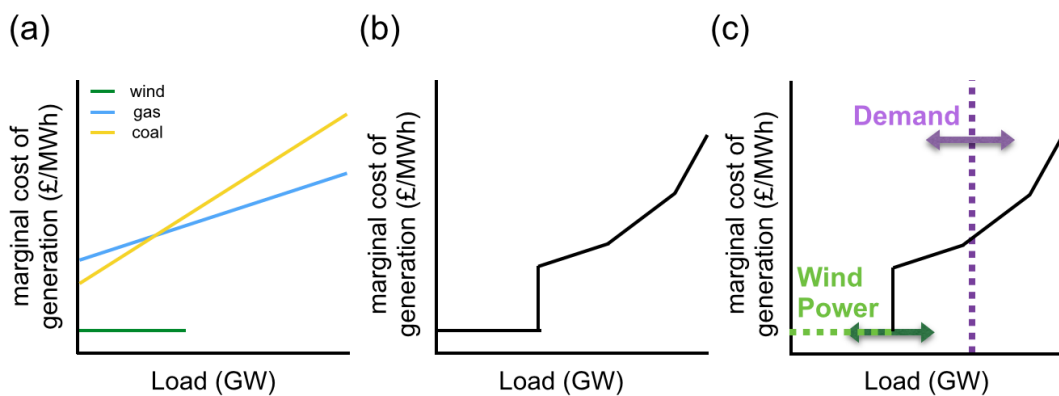
Figure 2.5 A schematic of the economic-dispatch problem for the GB power system. Adapted from Green and Vasilakos (2010) (a) screening curves showing the marginal cost of each plant type to meet a given load. (b) A merit-order stack showing the minimum marginal cost to meet a given value of load. (c) as in (b) but showing how weather-dependent demand (purple) and wind power generation (green) may impact the merit-order stack.

Figure 2.5a indicates that the marginal cost for wind power generation is constant and low, as it does not cost the wind farm owner money for fuel, and the cost of operation and maintenance is relatively low. The demand that must be met is not perfectly forecastable (due to uncertainty in the future weather conditions and the amount of embedded generation which may be produced) therefore there is uncertainty in the amount of load that must be met. There is also uncertainty in the amount of renewable energy that may be produced. This means that the generation-stack may shift forwards or backwards (see Figure 2.5c). The generators which are used are then determined by the intersection of the demand level with the generation-stack.

An economic dispatch model determines the cost-optimal level of power generation

for each plant which will be operational (which could have previously been decided from a unit-commitment model). The variable efficiency of plant at different operating levels is one of the main constraints considered within an economic dispatch model.

Operational timescale power system models have been commonly used in the energy-meteorology literature to investigate the impacts of changing power system structure on system operation and running costs. A popular topic within the literature currently is the impact of increasing amounts of wind power generation on system operation. The questions that can be answered with the operational timescale models become more complex with increasing model complexity. For example De Jonghe et al. (2011) used a simplified unit-commitment model for the UK power system to show that increasing wind power generation (therefore increased variability in system load) results in reduced baseload plant operation. Whereas McGarrigle et al. (2013) used PLEXOS (a complex power system model) to investigate the impact of the system non-synchronous penetrable limit on the amount of wind power curtailment, showing annual total wind power curtailment drops from 14% to 7% as the system non-synchronous penetrable limit is raised from 60% to 75%. Operational timescale power system models have the advantages of including multiple power system constraints, and therefore a more realistic spatial and temporal representation of the power system.

2.4.2   Challenges in operational power system modelling

Many power system models exist within the literature which can be used for focussed analysis on renewable integration (see Connolly et al. (2010) for a review of commonly used models). However, it is rare for models to be run with more than one year of meteorological data within their simulations, due to the high computational cost (Pfenninger and Staffell (2016)). This has the potential to severely bias model results dependent on the state of the climate present during the simulation. For example a simulation year chosen without comparison to climatology may experience anomalous demand or renewable generation, resulting in unrealistic conclusions. There is therefore the need for modelling studies which attempt to address the amount of uncertainty inherent in studies based on just one year of data and how this may impact the operation of conventional generation.

2.4.3   The investment-timescale power system modelling problem

Investment timescale modelling differs from operational timescale modelling in the sense that it allows modellers to quantify the impacts of policy options on technologi-

cal development or natural resource depletion (MARKAL (2008)). Investment-timescale problems are usually computed using a whole energy system model (rather than the operational-timescale models which are more focused on the electricity sector). An energy system model includes the electricity market and also includes other markets, such as gas and liquified petroleum gas. The inclusion of multiple sectors results in a reduction in both the amount and the temporal resolution of data from the electricity sector which is used (Connolly et al. (2010)). Models used in long-range power system planning are often limited to calculations at annual time-steps (e.g. the LEAP model (Heaps (2012)), based on typical daily profiles of demand and renewable generation (LEAP, Heaps (2012) and MARKAL, MARKAL (2008)), this makes them less suited to systems with a large volume of renewable energy (Connolly et al. (2010), Deane et al. (2012))

The investment-timescale problem can be analysed more simply, using a tool called Load Duration Curves (LDCs). LDCs focus on changes in the power sector exclusively, without incorporating changes in heating and transport sectors. The simplicity of this method means that there are not computational limits to the volume of data that can be used for analysis (i.e. due to data storage issues or model run times). LDCs are a popular tool used in the literature to analyse GB power system operation and how this may change with increasing renewable generation (George and Banerjee (2011), De Jonghe et al. (2011), Ueckerdt et al. (2013), Buttler et al. (2016)).

An LDC is built by creating a cumulative frequency distribution of load data for a certain country or region. This is typically done for a time period of one year. This representation allows the calculation of the number of hours where demand is above or below a certain threshold (Stoft (2002)). Previous studies have taken reference points on the LDCs to represent the operation of key generation types such as baseload generation (plant that generates for a large percentage of the year) or peaking plant generation (plant that operates for only a small percentage of the year; Buttler et al. (2016)) or analysed gross changes in the shape and gradient of the curves (Ueckerdt et al. (2015)). This simplified investment modelling methodology can provide useful information on the impact of inter-annual climate variability on the GB power system due to their limited computation requirements.

Within the literature multiple studies have used LDC analysis to show the impact of increasing renewable generation on European power systems (e.g. George and Banerjee (2011), De Jonghe et al. (2011), Ueckerdt et al. (2013), Buttler et al. (2016)) finding that increasing the amount of installed wind power generation results in a reduction in

the total use of baseload plant, and increases in the total use of peaking plant (Ueckerdt et al. (2013), Buttler et al. (2016)). However, multiple LDC based studies have limited themselves to using one year of hourly demand and renewable generation data for analysis (George and Banerjee (2011), De Jonghe et al. (2011), Ueckerdt et al. (2013), Buttler et al. (2016)). A gap is therefore present in the literature where multiple years of demand and renewable generation could be used to quantify the impacts of inter-annual climate variability on the GB power system in both a present day and future power system configuration.

2.4.4   Challenges in investment-timescale power system modelling

A large challenge for investment timescale models used in renewable resource assessment is the quantity of data which is able to be input to the power systems component of the model. It is common for time slices of demand and renewable generation data to be used to represent typical operating conditions for a power system. For example MARKAL (MARKAL (2008)) commonly uses six time slices for its power system analysis. These slices are taken as two days from three seasons. This accounts for some of the seasonal and diurnal variability in demand, but does not account well for the large variability present in wind power generation. This type of time slicing is typical across multiple energy system models (Nahmmacher et al. (2016)).

An alternative methodology for accounting for wind and solar variability within investment models is presented by Nahmmacher et al. (2016) in which cluster analysis is performed on co-varying time series of demand, wind power and solar power data to select a diverse set of operating conditions, representing characteristic fluctuations of the input data to run through the investment model.

It is useful to incorporate information from operational-timescale power system models into investment timescale models for a more accurate simulation of the behaviour of conventional generation in systems including large amounts of renewable generation. This is referred to as *soft-linking*, which allows the detailed results calculated from operational timescale power system models, using high resolution data, to be transferred to energy system models. Deane et al. (2012) showed that the absence of key technical constraints in energy system models can result in the under-valuing of flexible resources in energy system models, for example the use of baseload plant is commonly over-estimated and the amount of wind power curtailment under-estimated.

Soft-linking is becoming more common in the literature, however one year of data is

still commonly used for simulations within the operational timescale power system model (Deane et al. (2012)). This motivates the need to understand the impact of climate variability on power system operation in order for more meaningful results to be provided by investment modelling studies using selected data periods.

2.4.5 The impact of inter-annual climate variability on the GB power system

Within the literature it is becoming increasingly common to investigate the impact of inter-annual climate variability on power systems. This is motivated by the large volume of literature showing that wind power generation is strongly impacted by inter-annual climate variability (Earl et al. (2013), Bett et al. (2013), Cannon et al. (2015)) and may therefore impact the operation of a power system. A summary of results focussed on the GB power system are given below.

POYRY (2009) studied the impact of renewable generation variability of the GB and Irish electricity markets, finding that the max-min range of annual wind power production was 11% of the total generation (between 2000-2007). The inter-annual variability in wind power generation then lead to price volatility in the Northern European energy market. POYRY (2009) was the first study in the literature to attempt to quantify how inter-annual variations in renewable generation may impact electricity price.

Green and Vasilakos (2010) examined the study period from 1993-2004 and found that the variability of electricity price significantly increases in a power system including wind power generation (∼25% increase in the standard deviation of electricity price).

The impact of inter-annual climate variability on the potential for large scale energy storage was investigated in Grünewald et al. (2011) using data from 2003-2009. Even within these six years of data a large amount of uncertainty was found in the year-year revenues of storage. This was shown to be largely due to changes in the amount of renewable energy generation rather than due to changes in demand (Grünewald et al. (2011)).

2.4.6 Challenges in modelling the impact of climate variability on the GB power system

All the studies from section 2.4.5 are based on metered demand data, hence the study period being limited to a ∼10 year period. Recent developments have seen power system

modellers using re-analysis data to create wind power and solar power time series for use in power system modelling (Pfenninger and Keirstead (2015), Bett and Thornton (2016)). However, the full re-analysis record is not always used to analyse the impact of climate variability on power system operation, with the use of single years of data for analysis still being common (such as in Pfenninger and Keirstead (2015)). This limitation is not peculiar to GB - with many other studies internationally adopting the same approach (e.g., [NREL (2010), NREL (2011), Santos-Alamillos et al. (2012), MacGill (2010), MacDonald et al. (2016), Buttler et al. (2016) each contain less than a decade of data). This is due to the studies using measured data (of which there are only short records; e.g. Buttler et al. (2016)) or due to *typical meteorological years* being chosen due to data processing and storage restrictions (e.g. NREL (2010), NREL (2011)).

A few GB based studies have included multiple years of data in an attempt to account for the impacts of climate variability (e.g. POYRY (2009), Green and Vasilakos (2010), Grünewald et al. (2011) use 8, 13 and 7 years of data respectively limited to the period between 2000 and 2011). However, given these short records, none of these studies are capable of robustly assessing the impact of inter-annual climate variability on the GB power system.

It is difficult to isolate the power system variability due to climate alone, due to the large inter-annual variability in other system components. For example, Green and Vasilakos (2010) show that the inter-annual variability of electricity price due to the presence of future wind power generation is significantly lower than the variability due to uncertainty in future fuel costs.

2.4.7 The impact of climate change on the GB power system

There are many studies examining the impacts of climate change on individual components of the power system such as wind power generation (Cradden et al. (2012), Hueging et al. (2013), Tobin et al. (2015)) and demand (Golombek et al. (2011), Isaac and van Vuuren (2009)). These have been discussed in sections 2.1.4 and 2.2.3 respectively so are not discussed again.

Increasing heavy rain in Northern Europe may result in changes in hydropower generation potential (Dowling (2013)) with increasing permafrost thaw causing problems with transport routes (IEA (2013)). An increasing probability of droughts may mean that water resources for power plant cooling may be limited (Mideksa and Kallbekken (2010), Dowling (2013)). The thermal efficiency of power stations may also be impacted, with

a reduction in efficiency seen as cooling water temperature increases (Golombek et al. (2011)).

GB energy infrastructure may become more at risk of damage in a future climate due to an increasing likelihood of strong winds (CCC (2017)) and lightning (CCC (2017), McColl et al. (2012)). There is however predicted to be a reduction in the amount of maintenance required on the transmission system in GB due to snow, sleet and blizzards (McColl et al. (2012)).

Although there are a wealth of studies on how components of the power system may be impacted by climate change very few studies have focussed on how these impacts combine together to impact the GB power system as a whole, and how they may impact the cost of electricity (Mideksa and Kallbekken (2010)).

Golombek et al. (2011) find the combined impacts of climate change on European demand, thermal plant efficiency and hydropower generation cause a maximum change in electricity price of 2%, and their impacts are therefore deemed small. Dowling (2013) find an average change in electricity price of 1.5% when averaged over a number of potential climate responses. Dowling (2013) also show that the demand-side impacts of climate change are larger than the supply side impacts (i.e. changes in wind power generation or operation of conventional generation). The ARIES ($http://www.arcc-network.org.uk/aries/$) and RESNET ($http://www.arcc-network.org.uk/resnet/$) projects are currently investigating the whole system impacts of climate change on GB.

No studies have been found which examine the changes in inter-annual variability of operation of power system components within the literature. The focus is instead directed in changes in the mean state of relevant variables.

2.4.8 Challenges in modelling the impact of climate change on the GB power system

There are a number of large uncertainties involved in future power system modelling. These include uncertainty in terms of: available generation, power system configuration, the costs of fuels, and the impact of climate change on weather-dependent power system components (Mideksa and Kallbekken (2010)). Gross assumptions have to be made in order to run investment models (e.g. assuming no changes are made to the current system in a future climate). The vast amount of assumptions mean that the results from models are used more an a scientific exercise than as a plausible future power system. The problems in using climate model data discussed in sections 2.2.4 and 2.1.5 are also still

relevant here.

2.5 Meteorological Drivers of Power system variability

This section summarises previous literature aiming to understand the meteorological drivers of power system variability. Previous studies in this area can be grouped into two parts. Section 2.5.1 discusses meteorological drivers of extreme events. Section 2.5.2 investigates meteorological drivers of long term GB power system variability, and how this relates to the climate-scale variations in wind speed and temperature (section 2.5.2).

2.5.1 Extreme events

This section focuses on the meteorological conditions associated with peak demand (section 2.5.1.1) and wind power curtailment (section 2.5.1.2) as these are the events which cause the most immediate problems for power system operation. Peak demand and wind power curtailment are not the only extreme power system events which have distinct meteorological conditions associated with them. For more examples of extreme meteorological events which could impact power system operation see section 2.4.7.

2.5.1.1 Peak Demand

The main extreme event which has been analysed for the GB power system is peak demand, with much of the analysis being completed since 2010, when the most extreme winter demand on record was experienced (ENTSOE (2016)). The cold winters of 2009-10 and 2010-11 highlighted the need for the system operator to understand what meteorologically causes the most extreme high demands. It is also important to know if wind power is able to provide generation at these times.

The general view in the literature is that peak demands are related to *low wind cold snaps*, which happen when high pressure is located over GB (Brayshaw et al. (2012)). Leah and Foley (2012) and Hawkins et al. (2011) analysed the synoptic situation present during the peak demand event of 2010, showing that it was associated with high pressure centred over the north of GB. This resulted in low wind speeds over GB and Ireland but high demand, which was a problem for security of supply (Leah and Foley (2012)).

Brayshaw et al. (2012) suggested there are three synoptic conditions which are commonly present during peak demand events over GB (see Figure 2.6). High pressure over GB was found as one of the three synoptic conditions (as seen in Leah and Foley (2012)

and Hawkins et al. (2011)). High pressure to the north of GB and a trough to the south of GB were the other two synoptic situations found (see Figure 2.6). These both result in higher wind speeds over GB (due to increased horizontal pressure gradients), with the advection of cold air from continental Europe, leading to the most extreme peak demands (Brayshaw et al. (2012)).
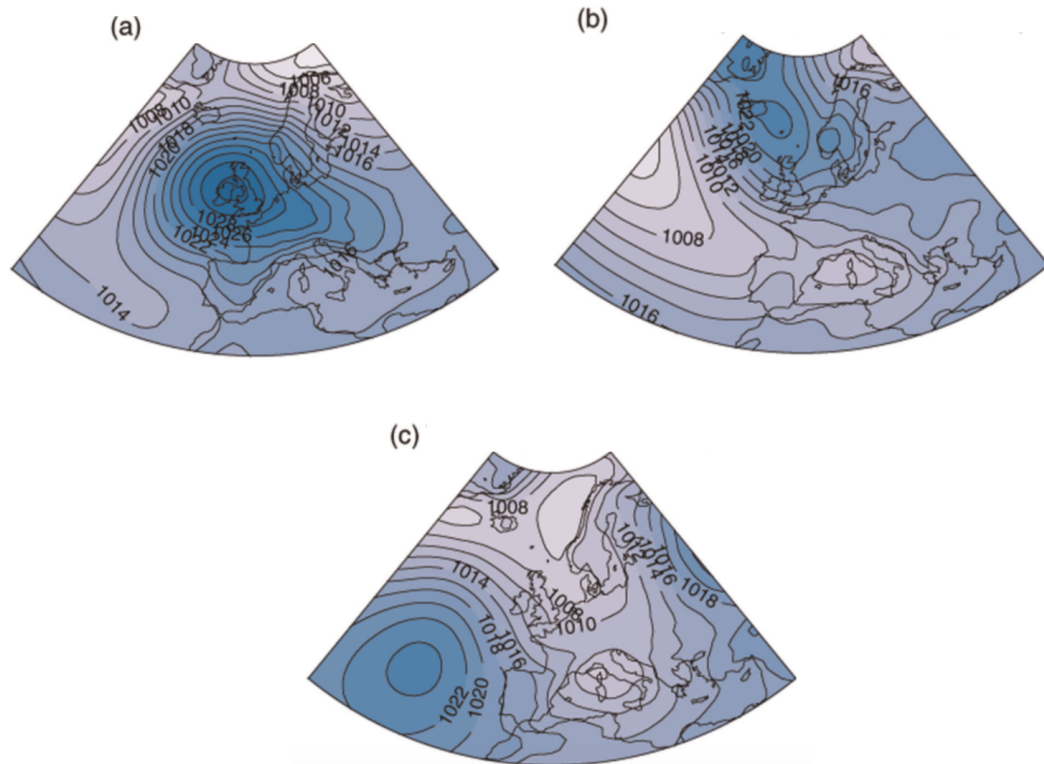
Figure 2.6 Mean sea level pressure patterns associated with the three main synoptic weather-patterns present during GB peak demand events (units hPa). (a) High pressure over GB, (b) High pressure over Iceland and Scandinavia, (c) A trough over GB. refinement, Source: Brayshaw et al. (2012))

Thornton et al. (In review) found a series of synoptic patterns which are present during the upper 5% of demand days from GB. These are: high pressure to the north of GB, high pressure over central and northern Europe and high pressure over the North Atlantic. These cause the advection of cold air over GB by easterly, south-easterly and northerly flows respectively. Anomalously low temperatures are present over GB in all of the synoptic situations, however the amount of wind power generation is variable.

The diverse set of synoptic conditions present during times of peak demand suggest that the relationship between wind power and peak demand is complex. This promotes the need for further research in this area, with Zachary et al. (2011) highlighting the need for long time series of data to be used to better understand the extreme events in

the power system. Understanding the weather conditions present during peak demand is important for the assessment of wind power capacity credit (this is the amount of firm capacity wind power can provide at times of peak demand).

All of the studies mentioned above consider current levels of wind power generation within the GB power system. No studies have investigated how these conditions may change in future power systems, with large increases in installed wind power capacity.

2.5.1.2   Wind Power Curtailment

Wind power curtailment can be defined as times when wind power generation is reduced or restricted. This can be due to wind power generation being greater than demand or due to transmission system constraints (i.e. difficulties transporting the electricity from the point of generation to demand). High wind power generation (required for curtailment) is associated times of highest wind speeds. These are discussed below.

Extra-tropical cyclones are low pressure systems, primarily gaining energy from the horizontal temperature contrasts that exist in the atmosphere. Extra-tropical cyclones are one of the main causes of high wind speeds over GB, with the highest wind speed being found to the south of the cyclone centres when the cyclones are at maximum intensity (Catto et al. (2010)). This is due to the superposition of the cyclonic flow and the direction of the storm motion (Dacre et al. (2012)).

The relationship between wind speed and wind power suggests that the regions of highest wind power generation (and therefore highest potential for curtailment) could be associated with strong pressure gradients and high wind speeds to the south of a cyclone centre. This was confirmed by Oswald et al. (2008) (for a case study in January 2001) and Quest (2013) (analysing periods of high capacity factor within the MERRA re-analysis), with the incidences of highest capacity factor over GB being associated with a strong pressure gradient. This pressure gradient was caused by a low pressure centre located to the North of GB, and higher pressure over southern Europe.

The relationship between temperature and demand (discussed in section 2.1) results in the lowest GB demand being present in summer. Quest (2013) confirmed the largest curtailment events occur when low demands are coupled with high wind power capacity factors. There is minimal literature which examines the synoptic situations associated with wind power curtailment (compared to the number of studies which have examined peak demand).

2.5.2 Climate-scale impacts of weather on the power system

This section discusses how climate-scale fluctuations in meteorological variables can cause large scale power system variability, motivating the need to use long time series of data for power system analysis.

The relative frequency of westerly or anticyclonic wind conditions has been shown to be related to the variability of wind energy output, with wind farms located to the west of GB being the most strongly influenced by the strength of prevailing westerly flow (Palutikof et al. (1987)). Very small latitudinal shifts in the storm tracks have also been shown to have large consequences for European wind speed output (Barstad et al. (2012)).

The majority of research into the impact of climate variability on GB wind power output has related wind power generation to the state of the North Atlantic Oscillation (NAO; this is a metric which describes the pressure difference between Iceland and the Azores (see section 2.6.1). In brief, the NAO is associated with the shifting in the path of North Atlantic jet stream, which impacts the path extra-tropical cyclones travelling across the North Atlantic (Gulev et al. (2001), Pinto et al. (2009)). A positive NAO index is associated with storms passing over central-northern Europe, therefore warm, wet and windy conditions being present over GB Brayshaw et al. (2011b) and an increasing probability of extreme cyclone events (Pinto et al. (2009)). The negative phase of the NAO index is associated with a southward deflection of the path of weather-systems, resulting in cold, dry and calm conditions over GB (Brayshaw et al. (2011b), Zubiate et al. (2016). The state of the NAO has been shown to have a significant impact on the monthly mean GB wind power output, with higher wind speeds over GB (and therefore higher wind power generation) being present in a positive NAO state (Brayshaw et al. (2011b), Ely et al. (2013), Bett et al. (2013)).

Ely et al. (2013) showed that there is a strong correlation between the winter NAO index and demand, with years of higher NAO index having lower mean temperatures and therefore lower demands. Demand-net-wind (demand - wind power generation; DNW) is considered in Ely et al. (2013), in order to show the combined relationship between wind power generation, demand and NAO index. Winters with above average DNW (i.e. experiencing high demands and low wind power generation) have a more negative NAO state than winters with below average DNW (experiencing low demands and high wind power generation). This is due to the positive NAO index winters being warmer (i.e. lower demand) and windier due to the increased frequency of weather systems passing over GB (therefore more wind power generation).

Colantuono et al. (2014) have shown that the NAO can also be related to GB solar power generation, with a negative value of the winter NAO index leading to a 9% more solar generation in south-west England (where the majority of solar generation is located) compared to a year with a positive winter NAO index. Combining this with Ely et al. (2013) suggests that negative NAO years have: higher than average demand, below average wind power generation and above average solar power generation.

Curtis et al. (2016) extend the previous studies for the Irish power system. A switch from a negative to positive NAO state has been shown to reduce thermal generation costs to the GB power system by 8%, reduce wholesale electricity prices by as much as £1.5/MWh, and increase wind power generators' revenue by 12% (Curtis et al. (2016)).

There is a minimal amount of literature from the energy-meteorology community which investigates the relationship between other large scale meteorological features which may drive European temperatures and wind speeds (such other modes of European climate variability, the location of the North Atlantic jet, or frequency of blocking events).

2.6   Atmospheric drivers of European weather and climate

Section 2.5 has presented the current knowledge of the meteorological conditions which are associated with extreme power system events and the variability of both demand and wind power generation. The literature in this area is relatively sparse, although there is a multitude of literature from the meteorological community on the drivers of European climate variability. Research which may be relevant to the operation of the GB power system is described in subsequent sections.

The first area of focus of this section is the teleconnection patterns relevant to European climate variability (section 2.6.1), as much of the literature on the meteorological drivers of power system variability is currently focussed around the variability of the North Atlantic Oscillation. Following this the North Atlantic Jet stream (section 2.6.2), and the North Atlantic Storm Track (section 2.6.3) are discussed. This is due to their relationship to the teleconnection patterns which have previously been shown to be important to power system variability. European Blocking is discussed in section 2.6.4 as blocking events have been highlighted as one of the potential drivers of peak demand events. The relevant processes are first described for the present climate, and then evidence of what may happen in a future climate is presented.

2.6.1 Atmospheric modes of European climate variability

The current research described in section 2.5.2 on the long-term meteorological drivers of power system variability is conducted using data at daily to annual timescales. At longer timescales it can be useful to characterise the large scale climate over Europe using *modes of atmospheric variability*. A mode of atmospheric variability has a coherent spatial structure, which is preserved through time, while the amplitude and phase (and sometimes geographical location) is able to change (National Research Council (1998)).

There are two main methods of calculating the atmospheric modes of variability. The first is a teleconnection based approach which involves finding the temporal correlation between a meteorological parameter at one given geographical location and all others in the domain. This produces many correlation patterns of which the highest amplitude, most well defined correlations (called teleconnection patterns) are accepted as centres of action of the modes of variability (Barnston and Livezey (1986)).

The second method is to use rotated principle component analysis. In this method eigenvectors of the cross-correlation matrix are scaled according to the total amount of variance in the data which they are able to explain. These eigenvectors are then rotated (under certain constraints) to obtain the main patterns of large scale variability over a domain (Barnston and Livezey (1986)).

Over Europe the four largest modes of variability are the North Atlantic Oscillation (NAO), the East-Atlantic pattern (EA), the Scandinavian pattern (SCAN) and the East-Atlantic/West-Russian pattern (EAWR). These patterns can be seen visually in Figure 2.7. This is not an exhaustive set of teleconnections which impact European climate, with others including the Arctic Oscillation (sometimes known as the Northern Annular Mode; see Thompson and Wallace (2013)).

The dominant mode of atmospheric variability over Europe is the NAO. Figure 2.7 shows the NAO has a dipole structure with centres of action over Iceland and the Azores. The NAO is able to explain a large portion of the variability of the North Atlantic Jet stream (Woollings (2010)). During the positive phase of the NAO the jet stream is northward shifted, and intensified, with the North Atlantic storm track experiencing a stronger south-west to north-east tilt (Woollings (2010)). This results in above average temperatures and above average wind speeds for GB (Hurrell et al. (2003)). This has been shown to cause decreased demand and increased wind power generation over GB (Ely et al. (2013)). In the negative phase of the NAO the jet stream is shifted further south (Woollings et al. (2010)), located over southern Europe and Northern Africa. This
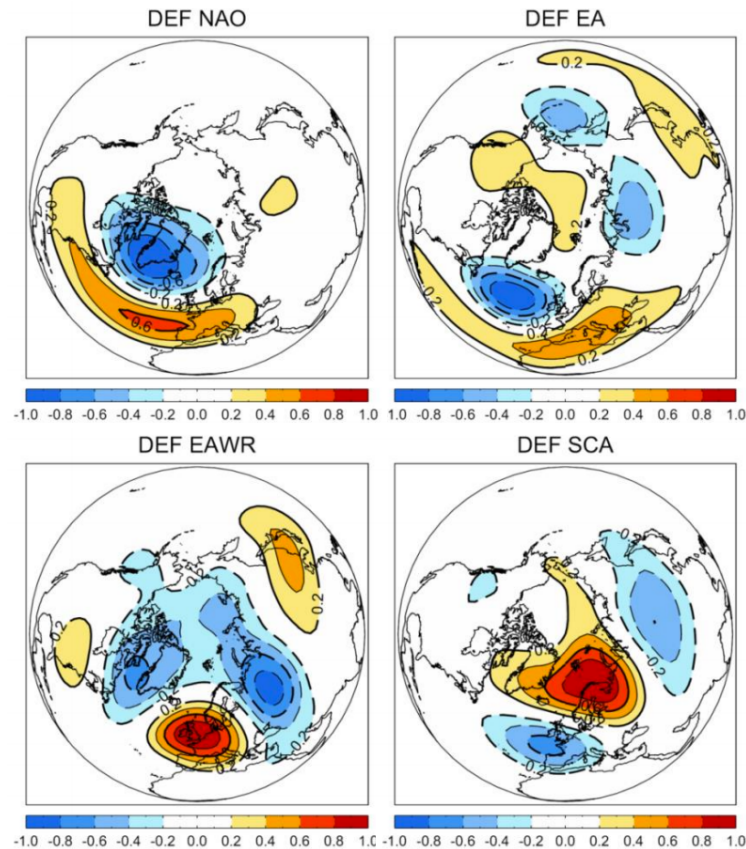
Figure 2.7 Normalised 500hPa geopotential height projections of the first four principal components of variability of the North Atlantic and Europe, The North Atlantic Oscillation (NAO), East Atlantic Pattern (EA) Atlantic Ridge(EAWR) and Scandinavian pattern (SCA). Source $http://www.c3.urv.cat/climate-es/session3/03_barriopedro.pdf$

results in GB experiencing below average temperatures and wind speeds. This may result in decreased demand and increased wind power generation over GB (Ely et al. (2013)). The negative phase of the NAO is strongly coupled to enhanced blocking in western Europe (Luo et al. (2015)).

The next largest modes of variability in the North Atlantic found from principal component analysis is the EA pattern. Figure 2.7 shows that the EA pattern describes an eastward extension of the eddy-driven jet stream (Barnston and Livezey (1986)). The positive phase of the EA pattern results in higher wind speeds and warmer temperatures over GB. These conditions could lead to higher wind power generation (Zubiate et al. (2016)).

The Atlantic Ridge pattern (EAWR) seen in Figure 2.7 is associated with high pressure centred over GB. The presence of this ridge creates a wave train and limits the progression of the jet stream into central Europe. This results in low winds over GB and warmer temperatures (Cassou et al. (2004)). This could result in low wind power

generation over GB.

The Scandinavian pattern (SCA) is associated with high pressure over Northern Europe, while a trough extends south-eastward from the North Atlantic towards southern Europe (Figure 2.7). This leads to moderate temperatures over GB and strong winds due to the high pressure gradient (Comas-Bru and McDermott (2014)).

The teleconnection patterns are not independent of each-other. Comas-Bru and McDermott (2014) and Zubiate et al. (2016) have shown how different combinations of NAO-EA pattern and NAO-SCA pattern influence winter european temperatures, wind speeds and precipitation. Zubiate et al. (2016) show that the interaction of teleconnection patterns has an important role in modifying wind speeds over Europe. When the positive phase of the NAO is combined with the negative phase of the SCA pattern then there are anomalously high wind speeds over GB compared to when the neutral, or positive phase of the SCA pattern is present in a positive phase of the NAO (Zubiate et al. (2016)), this large wind speed anomaly could have a large impact on GB wind power generation.

2.6.1.1 The impact of climate change on atmospheric modes of variability

Any projected changes in the dominant phase of the NAO (or other atmospheric modes of variability) could potentially result in changes in GB power system behaviour. From 1960 to 1990 the NAO index experienced a marked increase, with surface pressure over Iceland falling by around 7hPa over the period (Gillett et al. (2008)). During the period from 1960-1990 there was a rapid increase in the concentrations of greenhouse gases. This lead to a number of studies investigating if a positive NAO index would be more common in a future climate.

Studies generally found that there is not a trend for the positive phase of the NAO in a future climate, however the centres of action of NAO were found to shift north-eastward (Ulbrich and Christoph (1999), Hu and Wu (2004)). Studies which do suggest a positive trend in NAO index in a future climate (such as Woollings and Hannachi (2010)) note in their conclusions that the model used has deficiencies in simulating the NAO so results should be viewed with caution.

2.6.2 The North Atlantic jet

The global zonally averaged circulation shows the presence of two westerly jet streams (one in each hemisphere) extending through the whole depth of the troposphere. Both

jet-streams experience maximum zonally averaged velocities in the region of 30-35°N with upper-level wind speeds in these regions reaching $90 \mathrm{ms}^{-1}$ or greater (Holton (2004)). A number of jet streams make up this zonally averaged picture, these include the North Atlantic jet and pacific jet. The North Atlantic jet is the focus of this section due to the relevance to European climate.

The North Atlantic jet is strongest in winter due to the largest temperature gradients being present in this season. There are two mechanisms which cause the North Atlantic jet stream to be present, both are fundamentally due to the large scale meridional gradient in temperature, due to the differences in incoming solar radiation between the equator and the poles. One results in an *eddy-driven* component of the jet stream and one results in a *thermally driven* component (Holton (2004)). The thermally driven component of the jet stream (often called the sub-tropical jet) rarely extends past 40°N, and is present in the upper-troposphere. The eddy-driven component of the jet stream is present throughout the whole depth of the troposphere, anywhere between 40°N and 70°N (Woollings et al. (2010)). The eddies act to transfer both heat and momentum from the equator to the pole.

A schematic of the zonal-mean perspective of the formation of the sub-tropical jet is given in Figure 2.8. The increased amounts of incoming solar radiation in equatorial regions compared to polar regions drives a thermally direct circulation in the troposphere, transporting heat and momentum poleward between approximately 0 and 30N. This zonal mean picture is known as the Hadley circulation (Holton (2004)). Conservation of angular momentum results in the deflection of the poleward branch of the Hadley cell to the East, therefore creating a jet stream, known as the sub-tropical jet. The Hadley cell edge has a strong temperature gradient on its poleward side, which is baroclinically unstable (Held and Hou (1980)). Eddies grow on this baroclinic instability which drives the formation of a second overturning cell, the Ferrel cell (see Figure 2.8). The second mechanism for jet formation relies on the meridional temperature gradient driving transient eddy behaviour. The movement of these eddies leads to the transport of momentum and heat polewards and has the effect of accelerating westerly winds. The maximum of this poleward heat flux is at approximately 50°N, at which latitude the eddy-driven jet component can be seen (Holton (2004)).

In reality the North Atlantic jet differs substantially from the zonal-mean picture described above due to a set of complex spatial asymmetries in the Northern Hemisphere. The presence of the Rocky mountains results in the deflection of the zonal mean flow

around the mountains. This deflection acts to strengthen the temperature gradient over the continent as cold dry air from the north is deflected southwards towards warm, moist, tropical air. This acts to strengthen the baroclinicity in the area and leads to increased eddy-development (Brayshaw et al. (2009)). The sharp sea surface temperature gradients present in the gulf stream combined with the deflection of the zonal flow around the Rockies, and the shape of the North American continent combine to be responsible for the southwest to north-east tilt in the North Atlantic storm track (Nakamura et al. (2008), Brayshaw et al. (2011a)), this drives the location of the eddy-driven jet.

The latitudinal variability in the North Atlantic jet is also altered due to Rossby wave breaking events. Anti-cyclonic wave breaking has been shown to move the jet northwards, and cyclonic wave breaking is shown to move the jet southwards (Masato et al. (2012)).
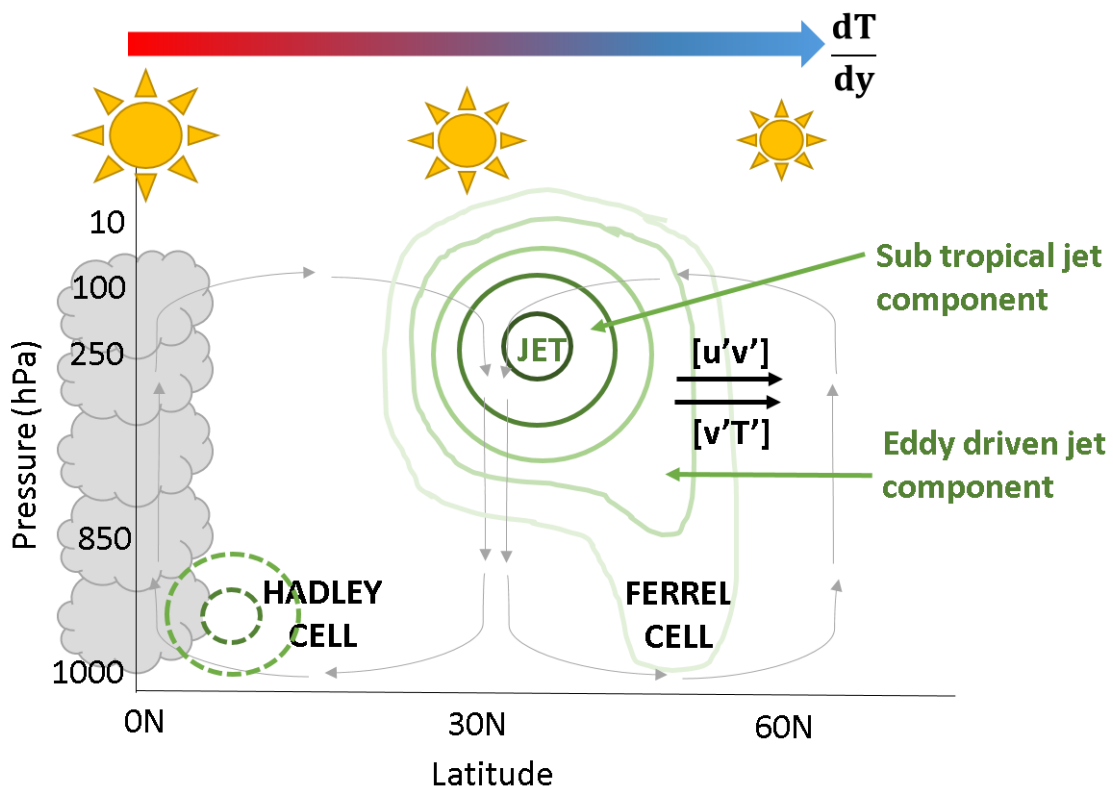
Figure 2.8 An annual-mean schematic of the Hadley circulation and how this leads to subtropical and eddy driven jet formation. Green contours show the westerly jet with dashed contours showing the easterly trade winds. Adapted from Holton (2004)

Fluctuations in the location of the eddy-driven component of the jet are responsible for much of the variability in European climate. The eddy driven jet has been shown to have three preferred positions during winter: A Northerly, Central and southern position centred on 60N, 45N and 35N respectively (see Figure 2.9; Woollings et al. (2010)). These three positions have different downstream impacts on European weather. The southern-jet

is generally associated with high-latitude blocking over Greenland, with GB experiencing cold temperatures and reduced wind speeds. A northern jet location results in high wind speeds over GB, with moderate wind speeds over GB when the jet is located in the central position (Woollings et al. (2010)).

The fluctuations in the location of the eddy-driven jet could have a large impact on the amount of wind power generation over GB. Although the relationship between the NAO and GB wind power generation has been established (Brayshaw et al. (2011b)) and the relationship between the eddy-driven jet and the NAO is also known (Woollings et al. (2010)) no study has yet investigated how the different locations of the eddy-driven jet may impact the amount of wind power generation over GB, and how this may cause further impacts to the GB power system.
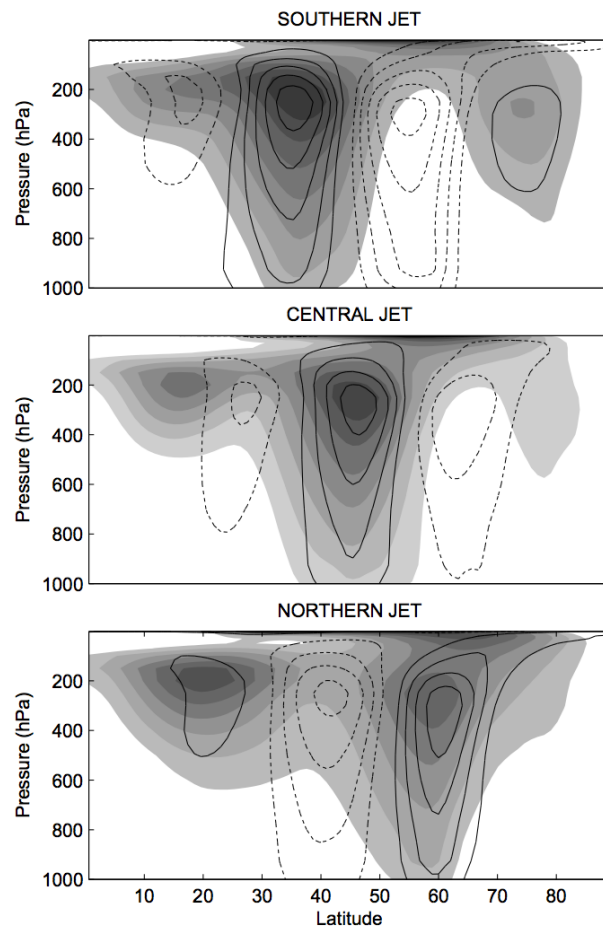
Figure 2.9 Composites of the zonal wind averaged over 0-60W for the three jet stream locations. Shading shows the full field contoured every 5 ms^{-1}, with the lowest contour drawn at 5 ms^{-1}. Contour lines show anomalies from the DJF climatology at 3 ms^{-1} intervals, with negative contours dashed and the zero contour omitted. Source: Woollings et al. (2010)

.

2.6.2.1   The impact of climate change on the North Atlantic Jet

The subtropical jet stream may be impacted by the increased upper-tropospheric warming near the equator in a warmer climate (Kirtman et al. (2013)). This warming may cause the edge of the Hadley cell to expand both poleward and upwards in the troposphere. This is due to an increase in the sub-tropical static stability of the atmosphere (due to enhanced upper level heating) which results in a poleward movement of the point at which this thermally driven jet first becomes baroclinically unstable (Lu et al. (2007), Solomon et al. (2007)). Large changes in precipitation may be felt by the latitudes at the edge of the Hadley Cell as the sub-tropical dry zone may move further north (Seidel et al. (2008)).

A potential warming at the poles and a reduction of the low level meridional temperature gradient may cause there to be a poleward shift in the location of the transient eddy forcing (and therefore baroclinicity), which could cause a poleward shift of the North Atlantic jet (Woollings (2010), Solomon et al. (2007)). Climate change could also result in the eddy-driven jet extending further east into continental Europe, however, there is considerable spread between the jet stream responses to climate change over Europe within models (Woollings (2010)). Changes in the location of the North Atlantic jet could have consequences for the amount of wind power generation present over GB.

2.6.3   North Atlantic Storm Track

Synoptic-scale disturbances tend to develop preferentially in the regions of maximum time-mean zonal winds, and propagate downstream along *storm tracks* that approximately follow the jet axis (Holton (2004)). The North Atlantic storm track is the name given to the groups of weather systems which are transported across the North Atlantic from west to east. This process acts to stir warm and cold air masses and plays a huge part in the transport of heat, moisture, and momentum from the tropics to the poles (Blackmon (1976)). Storm activity is mainly located over the North Atlantic, however, there is also a secondary region over the Mediterranean. The North Atlantic storm track has a characteristic south-west to north-east tilt, meaning that warm tropical air is transported across the North Atlantic. This tilting is responsible for the milder climate experienced by Europe compared to other countries at equivalent latitudes (Brayshaw et al. (2009)).

The North Atlantic storm track is strongest in winter. In the summer the storm track is weaker and is located slightly further polewards (following the seasonal fluctuations in the jet stream). The storm track exhibits variations from winter to winter in its strength

(i.e., number of depressions) and position (i.e., the median route taken by that winter's storms), but a particularly recurrent variation is for the storm track to be either strong with a north-eastward orientation taking depressions into NW Europe or weaker with an east-west orientation taking depressions into Mediterranean Europe (Holton (2004)). The North Atlantic storm track has a strong influence on European precipitation patterns and temperatures (Zappa et al. (2013a)), which could lead to impacts on GB power system operation. The direct influences of the North Atlantic storm track on the GB power system have not been quantified in the literature.

2.6.3.1 Impact of climate change on the North Atlantic Storm Track

Early studies from Solomon et al. (2007) predicted that storm tracks could shift polewards in line with changes in the jet stream, however models predicted a large spread around this change (Yin (2005), Harvey et al. (2015)). Studies from Kirtman et al. (2013) showed a tri-polar pattern of change in winter storm track location (e.g. Chang et al. (2012), Zappa et al. (2013b)). There is a reduction in the number of storms in the Norwegian and the Mediterranean sea and an increase in Central Europe, particularly over GB (see Figure 2.10a, Zappa et al. (2013b)) which is also seen in summer Dong et al. (1998). The Mediterranean basin has been shown to be particularly impacted by climate change with a strong reduction in winter cyclone activity (Bengtsson et al. (2009), Zappa et al. (2013a)). The North Atlantic storm track is different to those in other regions as its response to climate change is to strengthen and extend further east, particularly on its southern flank (Zappa et al. (2013a)). This is associated with the extension and intensification of the eddy-driven jet across Europe. In summer a poleward shift of the storm track is seen, accompanied by a reduction of storms on the southern flank and an increase in storms over Greenland.

A general result from modelling is that there may be less cyclones occurring in a warmer climate (Catto et al. (2011), Chang et al. (2012)) consistent with a weaker low level meridional temperature gradient (Harvey et al. (2015)), and therefore decreased baroclinicity (Bengtsson et al. (2009), Catto et al. (2011)). When the full CMIP5 climate model ensemble is analysed Zappa et al. (2013a) find a potential reduction in the total number of cyclones over Europe in winter (-4%) and summer (-2%) with a slight reduction in the number of cyclones associated with strong winds (see Figure 2.10b). Conversely, an increase in cyclones associated with strong precipitation is seen (Figure 2.10c, Li et al. (2014)).

In winter a potential increase in the number of cyclones over GB is seen in Lehmann et al. (2014). A moderate increase in the number and intensity of cyclones associated with strong wind speeds and intense precipitation is suggested over GB specifically in Zappa et al. (2013a) (see Figure 2.10b and c respectively). This could have potential impacts for wind power generation and damage to the GB transmission system as highlighted in CCC (2017).
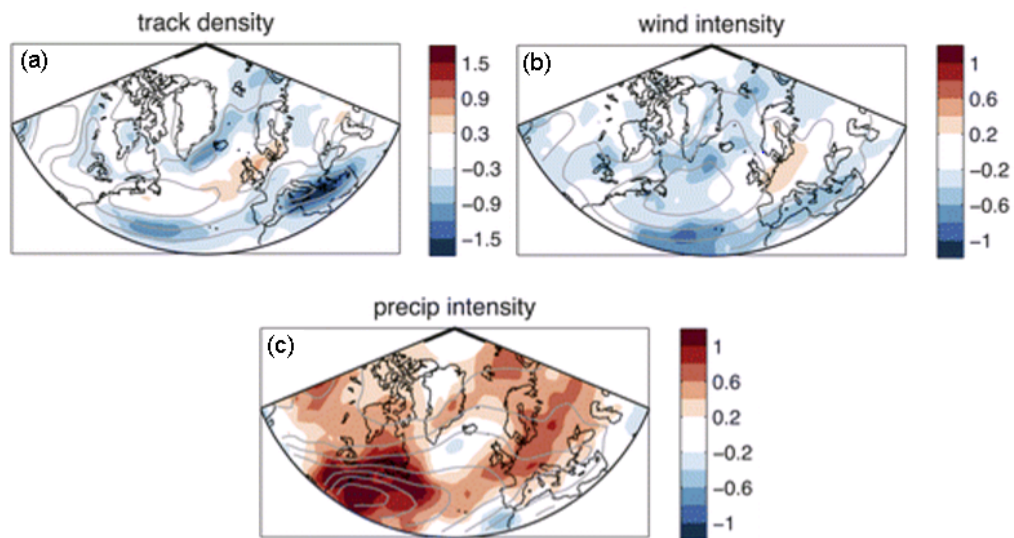
Figure 2.10 CMPI5 multi-model mean winter response for the RCP 4.5 scenario (a) track density (b) mean cyclone dynamical intensity measured by 850-hPa wind speed, and (c) mean precipitation intensity. The grey contours show the multi-model-mean values in the historical (1986-2005) simulations with contour intervals of four cyclones per month per unit area, 4 m s^1, and 2 mm/day for (a),(b), and (c), respectively. Source: Zappa et al. (2013a). ©American Meteorological Society. Used with permission.

2.6.4 European Blocking

Blocking is a weather regime which is commonly present over Europe. During such an event westerly winds are *blocked* by a persistent stationary anomaly, which is generally an anticyclone (Woollings (2010)). This anomaly is present due to a mass of sub-tropical air moving to higher latitudes, and associated wave-breaking occurring (Pelly and Hoskins (2003)). Cyclones will be diverted to the North of the blocking event in this case, generally following the contours of the time-mean flow (Woollings (2010)). The mass of sub-tropical air may become cut off from and isolated from the sub-tropics, in this case cyclones are able to pass to the North and South of the system.

Blocking frequency is normally modelled using a blocking index, which is commonly

based on the reversal of the meridional gradient of the mid-tropospheric geopotential height (Tibaldi and Molenti (1990)). Europe is defined as the region of most frequent blocking by many of these indices, and much work as been completed on understanding the causes and variability of Euoprean Blocking (Woollings (2010)).

Blocking events can persist for longer than a few days (the typical lifetime of a storm) and can last several weeks. The impacts of blocking are very dependent on the system and the time of year, but blocking is commonly associated with extreme weather events (Pfhal and Wernli (2012)). Persistent blocking can cause extended cold snaps over Europe in winter, when the land surface cools under clear skies and often easterly winds from the cold European continent (Trigo et al. (2004)). An example of this was experienced by the UK in 2010, where blocking events led to extreme low temperatures and also low wind speeds (Cattiaux et al. (2010)). These are conditions which are associated with high winter demand over GB (Brayshaw et al. (2012)). Conversely, in summer blocking leads to long dry spells and heatwaves such as seen in Europe in 2003 (Schar et al. (2004)). This could also potentially be associated with high demand over GB although this has not been confirmed in the literature.

2.6.4.1 Impact of climate change on European Blocking

Climate models in the past have universally underestimated the occurrence of blocking, in particular in the Euro-Atlantic sector (Scaife et al. (2010)). Recent work has shown that models with high horizontal resolution have a better representation of blocking due to the improved representation of orography and atmospheric dynamics (Woollings (2010)). However, most of the CMIP5 models still significantly underestimate winter Euro-Atlantic blocking (Kirtman et al. (2013), Zappa et al. (2014)).

Previous research has shown that under climate change the frequency of blocking events may be decreased (Zappa et al. (2014)), Kennedy et al. (2016)), however blocks that do occur may be longer lasting and more intense (Zappa et al. (2014)). This could have potential consequences for the GB power system, as blocking has previously been shown to be associated with periods of high demand (Brayshaw et al. (2012)).

2.7 Chapter Summary

The fundamental relationships between meteorological variables and the individual weather-dependent power system components of the GB power system (i.e. demand and

wind power generation) are well understood. The impact of climate variability and climate change on these components is also well understood. However, the impact of inter-annual climate variability on the operation of the GB power system as an integrated whole has received relatively little research attention, with studies tending to use short records of meteorological data to represent multi-decadal power system variability. These modelling studies have been limited by the availability of data and the computational expense of running multi-year power system simulations. An assessment is therefore required of how important using multi-decadal data records is to power system modelling studies.

The meteorological drivers of peak demand have been well studied within the literature, with peak demand typically associated with blocking in the region of the UK. However, little research attention has been given to the meteorological drivers of total power system behaviour, or individual plant operation. It is important that the meteorological drivers of all system components are understood in order to quantify the phenomena which climate models must be able to represent well if they are to be used to study the impact of climate change on the GB power system. Such validation of climate models is not present in the literature.

Chapter 3:

Methods

This chapter presents the modelling framework, which allows the input of multi-decadal meteorological data sets to investigate the impacts of climate variability and change on the GB power system (section 1.4, objective 1). The set of tools described allow for the remaining thesis objectives to be addressed in subsequent chapters. Section 3.1 describes the multi-decadal data inputs used to create weather-dependent demand and wind power models (sections 3.2 and 3.3 respectively). Section 3.4 describes the creation of load duration curves (LDCs) which are used to analyse the weather-dependent power system inputs. Following this a series of metrics for power system analysis are presented in section 3.4.2 which allow for the study of GB power system components. The chapter concludes with a summary of the framework, highlighting reasons why it has been chosen for this thesis (section 3.5).

3.1 Data description

In this thesis both the MERRA (Modern-Era Retrospective analysis for Research and Applications) re-analysis (Rienecker et al. (2011), section 3.1.1) and the HIgh resolution Global Environment Model (HiGEM, Shaffrey et al. (2009), section 3.1.2) are used to create mutually consistent reconstructions of weather-dependent demand and wind power generation. HiGEM data representing both the present day, and two future climate scenarios (section 3.1.3) are used.

3.1.1 The MERRA re-analysis

Re-analysis datasets are commonly used within the meteorological community as they provide a multi-decadal dataset of consistent spatial and temporal resolution including

hundreds of variables. Re-analysis data is produced by combining a short range forecast with all available observations, using data assimilation within the assimilation window (typically 6-12 hours). This process is performed sequentially (see Rienecker et al. (2011) for further details). This results in a dynamically consistent estimate of the climate state at each time step. Types of observations include: radiosondes, buoys, aircraft, ship reports and satellites (Rienecker et al. (2011)). A potential limitation of re-analysis data is that the quality and quantity of observations varies spatially and temporally over the grid. This can lead to local biases and trends within the data (see Bengtsson et al. (2004) for further details).

In this study the main source of data is the MERRA re-analysis (Rienecker et al. (2011)). MERRA is a global product developed by the National Aeronautical and Space Agency Global Modelling and Assimilation Office (NASA-GMAO). MERRA is chosen for this study due to the availability of hourly data for analysis. It is however noted that the hourly data is created using the incremental analysis update method, which gradually forces the model integration throughout the 6 hour analysis period (Bloom et al. (1996)). MERRA is freely available for download (at: $http://disc.sci.gsfc.nasa.gov/mdisc/$) and is frequently used within the energy-meteorology community (Jurus et al. (2013), Kubik et al. (2013), Cannon et al. (2015), Drew et al. (2015), Pfenninger and Keirstead (2015), Hdidouan and Staffell (2017)). MERRA has also been shown to perform well for wind power modelling (Cannon et al. (2015)).

The MERRA re-analysis starts from the beginning of the modern satellite era, covering the period from January 1979 - February 2016. MERRA was generated with version 5.2.0 of the Goddard Earth Observing System atmospheric model and data assimilation system (Rienecker et al. (2011)). Observations from satellites, radiosondes, weather stations, ships, ocean buoys, and aircraft are used in its construction (Rienecker et al. (2011)). The resolution of MERRA is $\frac{1}{2}^{\circ}$ latitude by $\frac{2}{3}^{\circ}$ longitude (approximately 55km by 74km respectively over GB), with 72 vertical levels. The GCM used to create MERRA is based on finite volume dynamics and uses three-dimensional variational data assimilation. Details on the parameterisations used for long-wave radiation, short wave radiation, boundary layer mixing, gravity wave drag are given in section 2 of Rienecker et al. (2011).

MERRA calculates meteorological fields every six hours with incremental analysis updates applied between these time steps so that fields are available for download at hourly resolution. The MERRA re-analysis includes 2m, 10m and 50m wind speeds as outputs (which are calculated by extrapolating the lowest model level wind speed to the

relevant height). This makes it the only re-analysis product that outputs multiple wind speeds below 100m (the exception to this being the MERRA2 re-analysis, available at: $https://gmao.gsfc.nasa.gov/reanalysis/MERRA-2/$ discussed in Appendix 8.2). This is useful for wind power modelling as it allows a more accurate calculation of the hub-height winds speeds needed to model wind power. Methods for these calculations are discussed in Section 2.2.

3.1.2   HiGEM: The control run

In this study the High Resolution Global Environmental Model (HiGEM) is used (Shaffrey et al. (2009)). HiGEM is based on the Met Office Hadley Centre coupled ocean-atmosphere climate model, HADGEM1 (Martin et al. (2006)). HiGEM has a spatial resolution of $1.25°$ longitude by $0.83°$ latitude and 38 vertical levels in the atmosphere, with a spatial resolution of $\frac{1}{3}°$ by $\frac{1}{3}°$ in the ocean. HiGEM's atmospheric component is very similar to HADGEM1. HiGEM has a non-hydrostatic dynamical core, with semi-lagrangian transport (Davies et al. (2005)), details of the boundary layer and convective parameterisations used in HiGEM are given in Shaffrey et al. (2009). The ocean component within HiGEM is the same as in HADGEM1 but with increased resolution and improvements to some of the model physics. The ocean model has 40 unevenly spaced vertical levels, with enhanced resolution close to the surface.

HiGEM is chosen for this study due to its relatively high spatial resolution and its ability to resolve and simulate meteorological phenomena that impact GB, such as: the structure of intense extratropical storms (Catto et al. (2010)), the climatological location (Catto (2009)) and tilt (Shaffrey et al. (2009), Woollings (2010)) of the North Atlantic storm track and the North Atlantic Oscillation (Keeley et al. (2009)). Further details on HiGEM can be found in Shaffrey et al. (2009). The relatively high spatial resolution of HiGEM means that there are many improvements compared to HADGEM1 and other lower resolution climate models. These include better estimations of: sea surface height variability, the amount of arctic sea ice, the simulation of ENSO, and the partial resolution of oceanic eddies (Shaffrey et al. (2009)).

The HiGEM control run is used in this project. This was run using present day radiative forcing with the concentrations of greenhouse gases held at a constant level (345 ppmv for CO_2, 1656 ppbv for CH_4 and 307 ppbv for NO_2). The net top of atmosphere radiation and the upper ocean are considered to be spun up after 20 years (see Shaffrey et al. (2009)). For this reason the first 20 years of the integration have been rejected.

The data used in this study come from years 21-70 of the control integration (as used in Catto et al. (2010)). Before the HiGEM data can be used in this thesis, the bias present within the near-surface temperature and wind speed data is assessed, and corrected. This is addressed in the first half of chapter 6.

3.1.3 HiGEM: Climate change scenarios

GCM's can be used to understand quantitively the affects of climate change on our atmosphere. As well as this they can be used to understand how these changes may cause socio-economic impacts, such as on power systems. Simulating a future climate in a GCM is performed by changing the amount of external forcing present within the atmosphere (i.e. green house gases, solar forcing, volcanic eruptions and aerosols) and allowing the system to respond.

Two idealised future climate scenario runs are used from HiGEM in this study. These scenarios can be seen schematically in Figure 3.1 and are described in Catto et al. (2011). In the first HiGEM future climate scenario CO_2 levels in the control run are increased by 2% a year for 35 years until the amount of CO_2 present in the atmosphere is doubled (to 690 ppm). The climate within HiGEM then stabilises resulting in a new equilibrium state being reached. The stabilised run is known as the $2xCO_2$ experiment. The second HiGEM future climate scenario follows a similar methodology, but CO_2 levels are increased for 70 years, so reaching 4x CO_2 levels (1380 ppm). The $2xCO_2$ scenario occurs at $\sim$2070 in RCP8.5, whereas $4xCO_2$ occurs at $\sim$2100; Kirtman et al. (2013).

The $2xCO_2$ and $4xCO_2$ simulations both show strongly enhanced surface warming at the winter pole and reduced lower tropospheric warming over the North Atlantic Ocean (due to the slowdown of the Meridional overturning circulation; Catto et al. (2011)). The largest warming is found near the pole due to the sea ice albedo feedback. An upward shift in the North Atlantic jet stream is found in both the $2xCO_2$ and $4xCO_2$ experiments (Catto et al. (2011)).

The $2xCO_2$ and $4xCO_2$ experiments differ in their mean sea level pressure and zonal wind responses to increasing CO_2. In the North Atlantic the competing effects of surface warming at high latitudes, upper level warming in the tropics, and the slow-down of the meridional over-turning circulation combine to give a different pattern of change in each scenario (Catto et al. (2011)). A North-East shift in the storm track is found in the $2xCO_2$ experiment due to enhanced surface polar warming and enhanced tropical upper tropospheric warming. A poleward shift is not seen in the $4xCO_2$ experiment, due to a
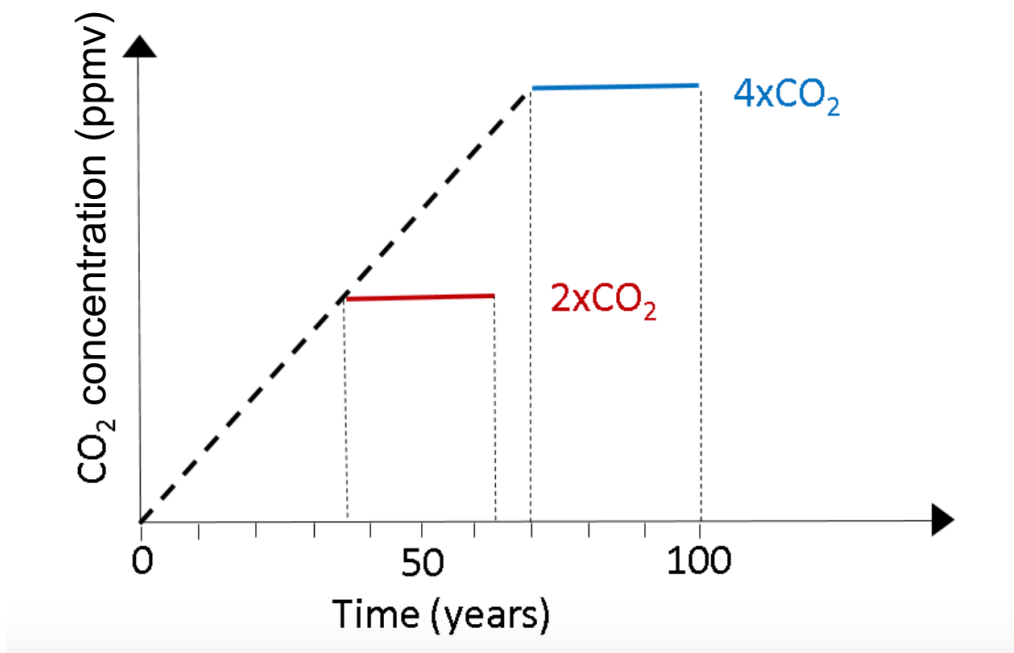
Figure 3.1 A schematic showing the CO_2 forcing in the HiGEM model runs.

reduction in low level warming caused by the meridional overturning circulation slowdown (see Catto (2009) for further details).

3.2 Demand Model

Within the energy-meteorology literature, electricity demand models contain various degrees of weather-dependence (see section 2.1 for details). In this study two models of GB electricity demand are created. The first is a model of the total GB electricity demand (section 3.2.1) and the second is a purely weather-dependent GB electricity demand model (section 3.2.2) which is used in this study. Both the full electricity demand model and weather-dependent electricity demand model have two main methodological steps. Firstly the daily-mean demand is estimated using a regression based technique. Secondly, the resulting daily field is then interpolated to hourly resolution using a set of fixed diurnal cycles, created from recorded hourly electricity demand data.

3.2.1 Full demand model description

A daily multiple linear regression model similar to Taylor and Buizza (2003) is created, of the form:

$$
\begin{aligned}
Demand(t) \;=\;& \alpha_1 + \alpha_2 t + \alpha_3 sin(\omega t) + \alpha_4 cos(\omega t) + \alpha_5 Te(t) + \alpha_6 Te^2(t) \\
& + \sum_{k=7}^{8} \alpha_k WE(t) + \sum_{l=9}^{12} \alpha_l WD(t) + \alpha_{13} HOL(t)
\end{aligned}
\tag{3.1}
$$

In Equation 3.1 α's represent regression coefficients. α_2 represents an exogenous time trend that could typically be associated with changes in GDP, population, energy efficiency, or the amount of embedded wind and solar power generation (Mirasgedis et al. (2007)). α_3 and α_4 correspond to the magnitude of the mean annual cycle of the drivers of demand, which are both exogenous (e.g. human behaviour and lighting use) and weather-dependent (e.g. temperature). α_5 and α_6 correspond to the weather-dependent drivers of demand, where the *effective temperature*, Te is defined as:

$$
Te(t) = \frac{1}{2} T(t) + \frac{1}{2} Te(t-1)
\tag{3.2}
$$

where T is the land-only, spatially-averaged, daily-mean, 2m temperature at the current time step (t). In this study land-only temperatures are defined as grid boxes which have a land fraction greater or equal to 50%. All of the relevant boxes over GB are then averaged to get the daily-mean temperature. Land-only, daily-mean temperature is insensitive to the land fraction used between 30 and 70% (see appendix 8.1 for further details).

Within Equation 3.1 the effective temperature term is quadratic to account for the *u shaped* temperature response to demand. Effective temperature is used rather than temperature as Taylor and Buizza (2003) showed it to be more effective in capturing the lagged relationship between temperature and demand (see section 2.1.1 for details).

α_7 to α_{13} are binary values which represent behavioural demand factors, these are: weekends, (with WE1 representing Saturdays and WE2 representing Sundays) and holidays (HOL, this includes Christmas, Easter and any English bank holidays).

The regression model is trained against metered daily electricity demand data from 2006-2015 (ENTSOE (2016)) with regression coefficients given in Table 3.1. Cross validation is carried out to understand how sensitive the model is to the choice of training period. This is done by excluding each year from the 10 year sample and examining the impact on the regression coefficients (see Table 3.1). This cross validation analysis shows that the weather-dependent terms in the model (bold terms in Table 3.1) are the most

sensitive to the training period. The R^2 and RMSE of the model with each different train-
ing period are however comparable. The small fluctuations in RMSE (e.g. the increase
when 2009 is excluded) are a result of days classed as christmas holidays in the model
having anomalous weather (not shown). As the accurate representation of these days is
not the focus of the project then the fit of this model is deemed acceptable. The full
electricity demand model performs well compared to models of a similar type (Thatcher
(2007)) with an R^2 of 0.95 and RMSE of 1.09GW when the training period of 2006-2015
is used.

In order to get hourly demand data the daily-mean electricity demand is then in-
terpolated to hourly values using prescribed diurnal cycle anomaly curves. A different
diurnal cycle is determined for each meteorological season by compositing the recorded
2006-2015 hourly demand data (see Figure 3.2). Each of the four diurnal cycles are simi-
lar except for the period from 17:00-21:00 where higher demands are seen in autumn and
winter, consistent with the increased demand for heating and lighting use during this part
of the day. Tests confirm that the characteristics of these diurnal cycle anomaly curves
are insensitive to the choice of year used for creation (not shown). A linear combination
of the relevant diurnal cycle anomaly curves is used to interpolate the daily demand to
hourly resolution. For example:

- The daily demand for the first of December is interpolated to hourly resolution using
  a 50%-50% weighting of the diurnal cycle anomaly curves from autumn and winter.

- The daily demand for the first of January has a 100% weighting of the winter diurnal
  cycle anomaly curve.

- The daily demand for the first of February has a 50%-50% weighting of the winter
  and spring diurnal cycle anomaly curves.

At hourly resolution the resulting demand model still performs well with an R^2 of
0.78 and RMSE of 3.35GW. The increase in RMSE with respect to the daily-mean model
is due to the crude approximation of the diurnal cycle. However the resulting R^2 still sits
within the range of literature values reported. (R^2 values are generally between 0.6 and
0.7, Thatcher (2007).) The crude representation of the diurnal cycle is deemed sufficient
for this study as the focus is on the weather-dependent component of demand. Much of the
behaviour within the diurnal cycle of demand is driven by human behaviour (Bossmann
and Staffell (2015) and see section 2.1) therefore standardising this throughout each year
still allows the interaction of wind power and demand at hourly resolution, but without

the added complication of human-induced diurnal variability.

Table 3.1 Demand model regression coefficients for different training periods. Data used is from 2006 (06) to 2015 (10). The 06-15 model coefficients are used for this study. The terms are described as in Equation 3.1. Weather dependent terms are shown in bold. R^2 and RMSE terms are calculated using the excluded year of data except for 06-15 where they are the model values.

Regression Variable						Model training period						
	06-15	07-15	06-14	06, 08-15	06-07, 09-15	06-08, 10-15	06-09, 11-15	06-10, 12-15	06-11, 13-15	06-12, 14-15	06-13, 15
Intercept	1416	1405	1366	1374	1393	1453	1416	1414	1431	1440	1444
time trend	-0.70	-0.68	-0.66	-0.67	-0.67	-0.70	-0.69	-0.68	-0.69	-0.70	-0.70
cos term	**2.94**	**2.86**	**2.95**	**2.94**	**2.91**	**2.92**	**2.94**	**3.02**	**3.06**	**2.94**	**2.93**
sin term	**-0.16**	**-0.20**	**-0.12**	**-0.08**	**-0.26**	**-0.18**	**-0.16**	**-0.13**	**-0.12**	**-0.17**	**-0.20**
TE	**-118.50**	**-113.70**	**-112.92**	**-112.40**	**-116.60**	**-113.20**	**-118.50**	**-110.20**	**-109.20**	**-110.30**	**-117.70**
TE ^{2}	**46.00**	**42.82**	**42.87**	**46.4**	**45.84**	**42.48**	**45.99**	**44.19**	**44.56**	**40.98**	**43.32**
WK1	-4.03	-3.98	-4.07	-4.00	-4.02	-4.02	-4.03	-4.05	-4.05	-4.04	-4.05
WK2	-4.93	-4.87	-5.02	-4.89	-4.92	-4.93	-4.93	-4.93	-4.96	-4.94	-4.94
HOL	-5.58	-5.46	-5.57	-5.50	-5.52	-5.71	-5.58	-5.60	-5.68	-5.53	-5.69
WD1	0.32	0.33	0.30	0.33	0.30	0.32	0.32	0.32	0.33	0.34	0.39
WD2	0.56	0.59	0.60	0.62	0.57	0.55	0.59	0.59	0.59	0.58	0.60
WD3	0.66	0.65	0.67	0.68	0.65	0.63	0.66	0.66	0.66	0.67	0.67
WD4	0.64	0.63	0.65	0.63	0.65	0.62	0.64	0.63	0.63	0.64	0.64
RMSE	1.09	1.01	1.21	1.13	1.08	1.64	1.00	0.89	1.16	1.08	0.98
R^2	0.95	0.97	0.93	0.95	0.95	0.93	0.97	0.96	0.94	0.96	0.95

Relative humidity, amount of precipitation, and cloud cover have been shown to be significant variables in previous demand modelling studies (see section 2.1). When including these variables as parameters within the regression model none of were found to have a statistically significant impact (i.e. all had a p value > 0.1, not shown). As these meteorological impacts on GB demand are small compared to the impact of temperature (Taylor and Buizza (2003)) the model is kept purely temperature-dependent, for simplicity.
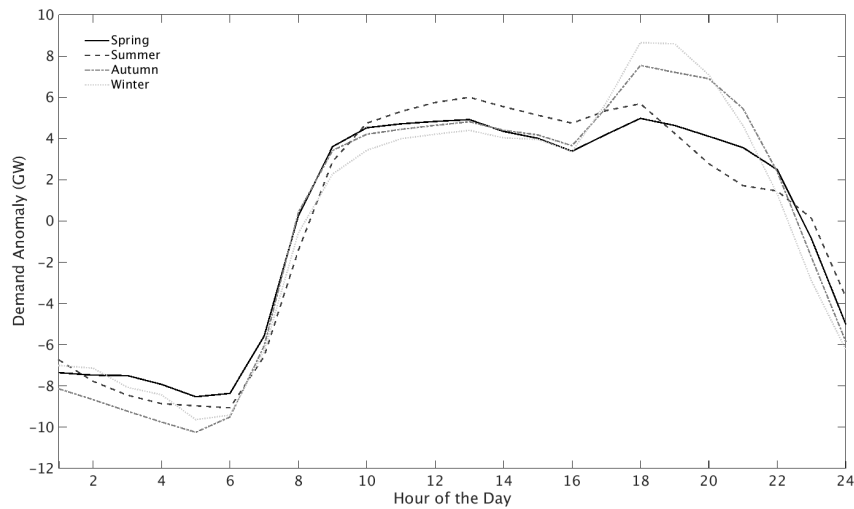
Figure 3.2 Seasonal anomaly curves used for interpolation of daily demand data to hourly resolution. The meteorological seasons are used where spring represents March April and May, summer represents June, July and August, autumn represents September October and November and winter represents December, January and February.

3.2.2 Weather-dependent model description

The full demand model (Equation 3.1) provides a reasonably accurate reconstruction of the observed demand during the recent period. However, the primary aim of this study is to isolate the impact of *weather and climate variability* on the power system. It is therefore useful to remove the variability due to non-meteorological factors (such as weekends and holidays). The daily full demand model is therefore reduced to Equation 3.3:

$$Demand = \alpha_1 + \alpha_3 sin(\omega t) + \alpha_4 cos(\omega t) + \alpha_5 Te(t) + \alpha_6 Te^2(t) \tag{3.3}$$

Here the regression coefficients are defined as in Equation 3.1 with values as given in Table 3.1. The resulting daily time series is interpolated to hourly resolution as previously described. This model is used to create hourly demand data from 1980-2015 using the

MERRA re-analysis as an input for use in chapters 4 and 6.

3.2.3   Future demand model description

The demand model described in section 3.2.2 is used in order to model demand in a future climate using the future HiGEM data. It is assumed that the same quadratic relationship between temperature and demand that is present in a current climate will hold in a future climate. This is a common assumption in the literature (Howden and Crimp (2001), Thatcher (2007) and Isaac and van Vuuren (2009)).

The shape of the diurnal cycle of demand is also assumed to remain constant in the future. This is an assumption, which previous studies have suggested will not be valid, due to the electrification of transport, and increases in demand-side response (Bossmann and Staffell (2015)). However, as the accurate representation of changes in demand due to human behaviour are not the aim of this project, it is deemed acceptable here. Possible changes in demand shown in chapter 6 are therefore related solely to changing temperatures, rather than any changes in policy, or human behaviour.

3.3   Wind Power Model

The wind power model from Cannon et al. (2015) is used to simulate hourly time series of GB aggregated wind power capacity factor from 1980-2015. This model uses the 2m, 10m and 50m wind speeds from the MERRA re-analysis (Rienecker et al. (2011)). In this model wind speeds are spatially interpolated onto the locations of the 2012 GB wind farm distribution (see Figure 3.3a for the distribution). A logarithmic profile is then created from the 2m, 10m, and 50m wind speeds at each farm location. These profiles are used to scale the 50m wind speeds to wind turbine hub-heights.

Wind speeds from each site are converted into wind power using a standardised wind power curve (see Figure 2.4) and aggregated across GB to produce an hourly capacity factor time series. Within this model a cut out speed of $25\mathrm{ms}^{-1}$ is used, with a cut in speed of $21\mathrm{ms}^{-1}$. This means that once wind speeds are over $25\mathrm{ms}^{-1}$ then the wind power generation will be zero and the wind speed must drop back below $21\mathrm{ms}^{-1}$ before generation can recommence. The resulting capacity factor time series can then be converted into total GB hourly wind power generation by multiplying by the total installed wind power capacity.

As discussed in Cannon et al. (2015), extensive validation was conducted on both the
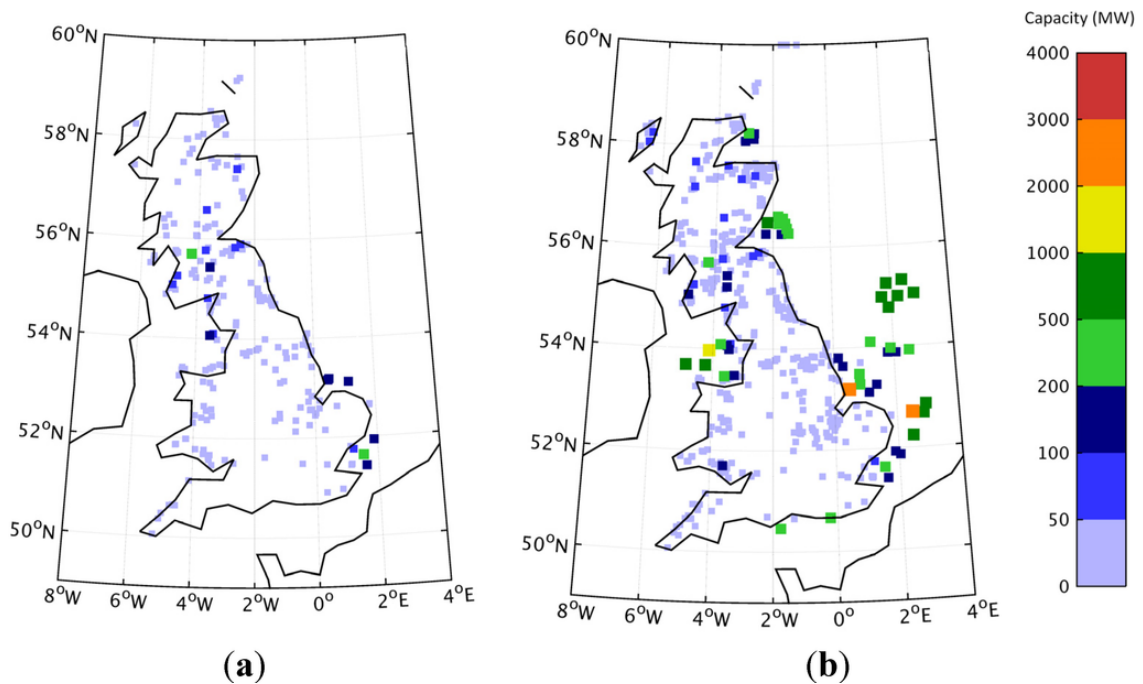
Figure 3.3 a: The 2012 GB wind farm distribution as used in Cannon et al. (2015). b: A potential future GB wind farm scenario, as used in Drew et al. (2015). Source:Drew et al. (2015)

wind power model, and the MERRA wind speed data itself. The validation of the wind speeds was completed in order to show that the variability present in the observed GB wind speeds is accurately represented in MERRA. It was shown that MERRA is able to successfully reproduce observed near-surface wind speeds over large spatial and temporal scales. However, MERRA's performance is weaker when there is complex terrain, or over short time spans.

Staffell and Pfenninger (2016) found that there is a positive bias in the MERRA wind speeds over GB, which if uncorrected would lead to an overestimation of wind power production. The correction of this bias is dealt with in the Cannon et al. (2015) model using the power curve, which is calibrated against observed wind power production. The merit of performing the correction at this stage means that any differences between modelled and observed generation which are not due to the MERRA wind speed bias (such as farms operating at reduced efficiency) are also included in the correction. The model was shown to perform well compared to observations, with a correlation coefficient of 0.96 between the hourly MERRA capacity factor time series and National Grid generation data for 2012 (see Cannon et al. (2015) for further details).

3.3.1 Future wind power scenarios

In order to study the impact of increasing installed wind power generation capacity on the GB power system a series of wind power scenarios are required. In this study four wind power installation scenarios are considered, with GB installed wind power capacity of 0GW, 15GW 30GW and 45GW (hereafter referred to as the NO-WIND, LOW, MED and HIGH scenarios, see Table 3.2).

Table 3.2 Installed wind power capacity scenarios used in this thesis.

Scenario	Installed Wind Power Capacity (GW)	Wind farm scenario
NO-WIND	0	Cannon et al. (2015)
LOW	15	Cannon et al. (2015)
MED	30	Cannon et al. (2015)
HIGH*	45	Cannon et al. (2015)
HIGH	45	Drew et al. (2015)

The LOW scenario is approximately equivalent to the current day power system of GB (2016), with the MED and HIGH scenarios based on the amount of installed wind power capacity in the National Grid Gone Green scenarios for 2025 and 2035 respectively (National Grid (2015)). The spatial distribution of wind farms is held constant in the LOW and MED scenarios (corresponding to the 2012 distribution in Cannon et al. (2015), Figure 3.3a). However, for the HIGH scenario the wind farm distribution is changed to include substantial increases in offshore wind (as used in Drew et al. (2015), Figure 3.3b). Within this thesis sensitivity tests have also been conducted in which the distribution of Cannon et al. (2015) is used to create a scenario including 45GW of wind power. This is referred to as the HIGH* scenario.

3.4 Load Duration Curves

To understand the combined demand-supply impact of weather and climate on the power system load duration curves (LDCs) are used. In the simplest case, load can be understood as the hourly demand for power (see grey lines in Figure 3.4). To form a LDC each year of demand is converted into a cumulative frequency curve, showing the percentage of the year that a given load threshold is exceeded. By convention these are displayed as in the bottom panel of Figure 3.4. Any point on the curve shows the percentage of the year (x-axis) for which the residual load (the hourly demand - wind power generation) required exceeds a threshold (y-axis).

In a more general sense, load can be thought of as the residual demand for power once the generation from variable renewable sources is removed. In a power system where wind power is the only renewable generation, this results in load being described as hourly demand-net-wind (hourly demand - wind power generation; DNW). A LDC can then be created from the DNW time series in the same way as for demand alone (see black line in the bottom panel of Figure 3.4).

An essential assumption in this thesis is that wind generation is given preference over other conventional generation types (such as coal or nuclear). This is a common approach within the analysis of power systems when seeking to explore the impact of increasing installed wind power capacity on the power system (De Jonghe et al. (2011), Ueckerdt et al. (2015), Buttler et al. (2016)). The LDCs created in this thesis assume that a perfect forecast is available for both electricity demand and wind power production. The transmission network is also assumed capable of utilising all available wind generation at a given time. Both of these assumptions are gross approximations of real world power system behaviour, but are used as this study is not focused on the operational power system dynamics.

This study is intended to demonstrate the impacts of inter-annual climate variability on a prescribed power system configuration. For simplicity this study therefore assumes that GB is an isolated system with no inter-connectors, and that the operational behaviour of each type of generation is constant throughout these scenarios.

3.4.1 Justification of the choice of method

LDCs are a commonly used tool within power system modelling to investigate the impacts of renewable energy integration on the grid (Thatcher (2007), De Jonghe et al. (2011)), George and Banerjee (2011), Ueckerdt et al. (2015), Buttler et al. (2016)) and the market price for power (Green and Vasilakos (2010)). Using LDCs means that many aspects of power system operation are neglected from the modelling (such as transmission network constraints, ramping requirements, part-loading of plant or energy storage). Neglecting these factors results in an idealised view of the GB power system, which is not directly comparable to reality. For example De Jonghe et al. (2011) compared power system simulations from LDC's and from a unit-commitment model including the constraints mentioned above, and showed that including the constraints leads to a reduced amount of (slow to respond) baseload plant and increased amount of (fast-response) peaking plant required for system operation.
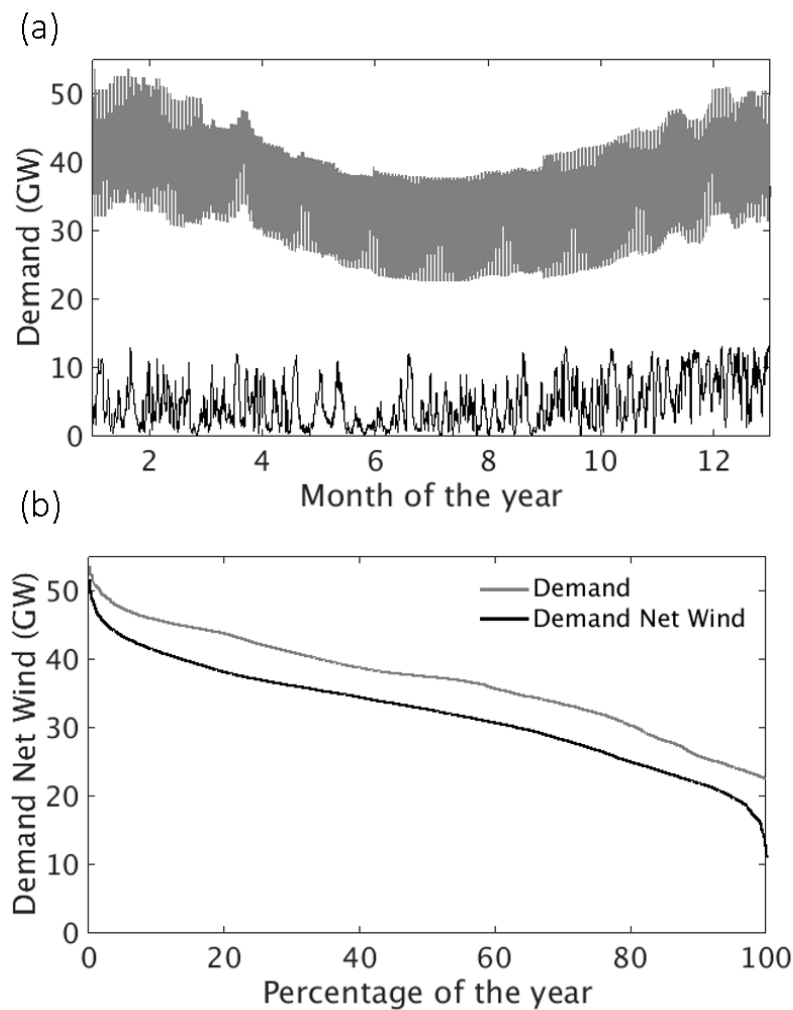
Figure 3.4 Top: Weather-dependent demand (grey) and wind power (black) time series Bottom: The corresponding demand only LDC (grey) and DNW-LDC (black). Data used is from the LOW scenario for the year 1980.

LDCs have been chosen for use in this study rather than a more sophisticated power system modelling tool (such as cost optimisation models used in De Jonghe et al. (2011). Deane et al. (2012) or Pfenninger and Keirstead (2015)) in order to allow multiple decades of data to be processed in a computationally efficient way. This modelling setup also allows for the quantification of the isolated impacts of weather and climate on the GB power system, which is one of the primary aims of this thesis.

3.4.2 Metrics for Load Duration Curve analysis

To explore the LDCs in detail a set of metrics are derived, to demonstrate how interannual climate variations influence different parts of a power system. The metrics discussed below are not exact descriptions of system operation. They are chosen in order to provide proxies from which the gross impact of inter-annual climate variability on the

components of the power system can be inferred. In reality the impacts of weather and climate on the power system would be much more complex (see section 2.4.4).

The metrics draw on the principle of *merit order* as an indication of the operating preference of electricity generation (Stoft (2002), Green (2005); see section 2.4). The variations in these metrics are of direct relevance to existing, or potential investors in generating plant and subsequently of strong relevance to policy makers with an interest in the cost effectiveness and security of the future power system.

The metrics for power system analysis are as follows:

1. Total Annual Energy Requirement (TAER): The sum of the annual load and is equivalent to the area under an LDC (see Figure 3.5a). TAER represents the total annual amount of energy required to be met by conventional generating plant (for GB this would be predominantly nuclear and gas; units GWh).

2. Peak load requirement: The 0% duration threshold on the LDC, i.e., it is the highest hourly load recorded on the system in any given year (Figure 3.5c point C, units GW).

3. Peaking plant: Operational data has shown that peaking plant (i.e. plants that only operate for a smaller percentage of the year and are extremely flexible) can be assumed to be economically efficient when operating for less than 7% of the year (DECC (2013), PB (2013)). Two distinct metrics for peaking-plant are identified: (a) the minimum load requirement at which peaking-plant is expected to be economically efficient (i.e., the y-axis load threshold corresponding to an x-axis duration of 7%; units GW; Figure 3.5b, point A), and (b) the total volume of energy (TVE) for which peaking-plant would be the most economically efficient generation type (i.e., the area integral between the LDC and the minimum load-level threshold for durations below 7%; units GWh; illustrated by the dark shading in Figure 3.5b).

4. Baseload plant: Operational data has shown that baseload plant (i.e. plants that only operate for a large percentage of the year and are generally in-flexible) is assumed to be economically efficient when it operates for more than 91% of the year (based on a general expectation for new GB nuclear build; DECC (2013), PB (2013)). Analogously to the peaking-plant metrics, the following metrics are defined: (a) the maximum load requirement at which baseload-plant is economically efficient to operate (Figure 3.5b point B), and (b) the TVE for which baseload-plant is the most economically efficient generation type (Figure 3.5b).

5. Operating hours of a mid-merit plant: A typical mid-merit plant in the

current GB power system might expect to operate when load exceeds 30GW (i.e., there are cheaper generators to call upon for 29GW of generation, but the 31GW of generation requires a more expensive generator to be used). This mid-merit plant is assumed to operate for the hours in the year when DNW exceeds 30GW (see Figure 3.5c point E).

6. Wind power curtailment: Wind power curtailment is assumed to occur when wind-power production exceeds the capacity of the power system to use it (more sophisticated definitions are possible based on local transmission and scheduling constraints; see Freris and Infield (2008)). Two definitions of curtailment are considered: (a) *demand driven curtailment*, defined as occurring in hours when wind-power is greater than demand (WP>D, shaded area in Figure 3.5c). In practice, however, wind-power is unlikely to be allowed to reach this instantaneous level (due to issues of system stability, as discussed for the Irish power system in McGarrigle et al. (2013)). A second definition is therefore used. (b) *stability driven curtailment* whereby curtailment occurs when wind-power is instantaneously greater than 70% of demand (WP>70%D). For both of the definitions, the TVE curtailed is calculated (i.e., units GWh).
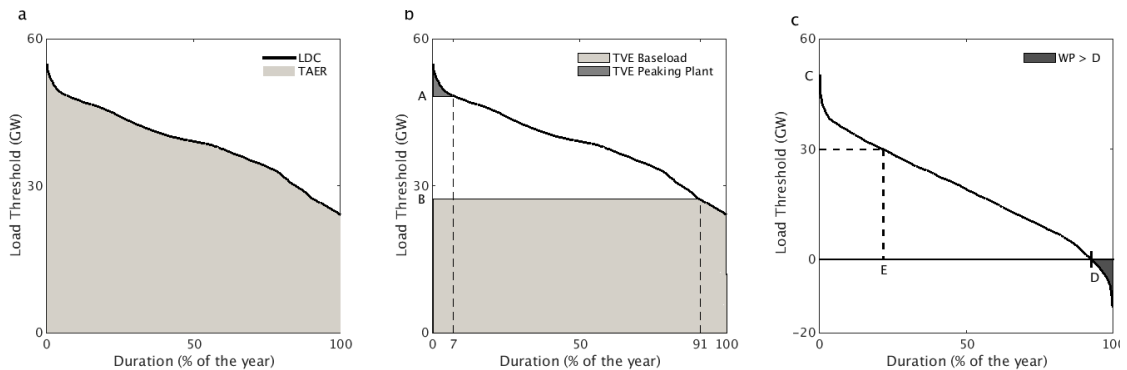
Figure 3.5 Power system metrics illustrated are: (a) TAER (shading); (b) peaking-plant and baseload TVE (dark and light shading respectively) with points A and B marking the minimum and maximum load requirement for peaking plant and baseload plant respectively; (c) curtailed energy due to excess supply (WP>D, dark shading to the right of point D) and the number of hours of operation for a mid-merit plant (point E). Note that the change in the y-axis scale in (c). In each subplot, the solid black line is a single year's LDC.

These metrics should not be interpreted as distinct operating thresholds for specific plant types. They are instead indicative values that relate to preferred operating levels for an economically optimal power system. For example, it would be expected that a power system containing large amounts of wind power generation as well as large amounts of nuclear generation would not operate in the way suggested by this analysis, as rapid variation of nuclear operation is best avoided for both technical (i.e. reliability) and economic reasons. Another important note is that power plants are planned and built

over multiple years. Once constructed an individual plant's operating hours may vary from one year to the next, which could impact plant revenues. The varying power and energy values presented in subsequent chapters represent a measure of investment uncertainty that should be considered by system planners.

3.5   Chapter Summary

In this chapter models of *weather-dependent* demand and wind power generation data are presented. From these, synthetic demand and wind power data can be created from the MERRA re-analysis (for use in chapters 4 and 5) and HiGEM (for use in chapter 6). Multiple wind power generation data-sets are created to account for the planned increases in installed wind power capacity in GB. These datasets are then used as inputs to create LDCs, which can then be analysed using a series of metrics.

The focus on only weather-dependent power system components allows for the removal of exogenous factors (such as human behaviour on weekdays, changes due to weekends and holidays, and long term economic growth). The use of LDCs allows for the focus on weather-dependent load, without complex system dynamics, such as network constraint, minimum plant loading, or ramping rates. The exclusion of these constraints makes the LDCs computationally efficient, and therefore the amount of climate model data that can be processed is not limited.

The power system metrics defined in this chapter allow for the investigation of the impacts of climate variability and climate change on a planned system. The metric values therefore represent investment uncertainty that should be considered by system planners. The metrics also can provide guidance on topical issues for system operation such as the amount of wind power generation that is present at times of peak load, and the amount of wind power curtailment.

Chapter 4:

The impact of inter-annual climate variability on the GB power system

Previous studies on the impact of inter-annual climate variability on the GB power system have shown substantial inter-annual variability in wind power production (Earl et al. (2013), Bett et al. (2013), Cannon et al. (2015), Drew et al. (2015)). When the GB power system is analysed as a whole (rather than as individual components) inter-annual climate variability is also shown to cause differences in electricity price (POYRY (2009), Green and Vasilakos (2010)) and the potential for energy storage (Grünewald et al. (2011)). These studies are limited to a maximum of 13 years of data. The objective of this chapter is therefore to quantify the impact of inter-annual climate variability on the GB power system (section 1.4, objective 2). To do this the MERRA re-analysis (Rienecker et al. (2011)) is used to create synthetic weather-dependent demand and wind power generation data, which is used as inputs to create LDCs. Idealised power system metrics (as described in section 3.4.2) are then used to quantify the inter-annual variability of the GB power system.

This chapter first discusses the impact of inter-annual climate variability on a GB power system with no wind power generation (section 4.1). Following this the impact of inter-annual climate variability on a system which is approximately equivalent to a present day GB power system is evaluated (section 4.2). This is to investigate how much the GB power system is already exposed to the influence of installed wind power generation. Plausible future power system scenarios are then investigated, with increased installed wind power capacity (section 4.3). The implications of increasing amounts of offshore wind generation within the GB power system are then quantified (section 4.4). Section 4.5 revisits a previous, influential study in order to investigate the amount of

extra information that can be gained through using a multi-decadal time series of data for analysis. Section 4.6 then goes on to quantify the potential uncertainty of using short data records in power system modelling studies (section 4.6). A summary of the key findings from this chapter is given in section 4.7.

Key results from this chapter have been published, Bloomfield et al. (2016) "Quantifying the sensitivity of power systems to climate variability". *Environmental Research Letters*

4.1 Impact of inter-annual climate variability on GB electricity demand

Figure 4.1 shows modelled demand-only LDCs (black) for years 1980-2015. When no wind power capacity is installed there is a 3% max-min range in the GB total annual energy requirement (TAER; see Table 4.1). This is equivalent to 10TWh of energy or ~10 days winter demand. The highest and lowest years of TAER are 2010 and 2007 respectively.

Inter-annual differences in the GB power system's total annual energy requirement are largest at high loads when no wind power capacity is installed (Figure 4.1). This indicates that inter-annual variations in climate have the greatest impact on the operating opportunity of peaking plant and peak load. This is quantified in Table 4.1; it can be seen that the max-min range of peaking plant total volume of energy (TVE) is large compared to the max-min range of baseload plant TVE. Table 4.2 shows the inter-annual max-min range of conventional plant operating opportunity is greatest at high load levels, with a ~3GW inter-annual max-min range for peaking plant operating opportunity compared to a 0.5GW inter-annual max-min range for baseload plant operating opportunity. A substantial inter-annual max-min range in peak load requirement is seen (~8GW; Table 4.2).

Table 4.3 shows that in the NO-WIND scenario a mid-merit plant, required to operate when load exceeds 30GW, would be called upon for ~7000 hours/year with an inter-annual max-min range of 250 hours/year (which is ~4% of the mean annual operation). The curtailment metrics are not applicable to the NO-WIND scenario as there is no wind power present. These results highlight that in a system without wind power there is weather-dependent inter-annual variability present, which is greatest for plants operating as peaking plant, as opposed to baseload plant.

4.2 Impact of inter-annual climate variability on a GB power system with present day wind power production

The focus of this section is the LOW scenario in which 15GW of wind power capacity is installed (this is approximately equivalent to the GB power system, which had a total capacity of 13.3GW at the end of 2015; DECC (2016)). Figure 4.1 shows LDCs from the LOW wind power scenario (grey) for 1980-2015. It is clear from Figure 4.1 that the addition of 15GW of installed wind power capacity causes a reduction in TAER, compared to the NO-WIND scenario. This reduction is due to wind power generation replacing conventional generation, such as coal and gas.

An increase in the inter-annual variability of TAER is seen when 15GW of wind power capacity is installed (doubling to ∼7% of the mean TAER for the NO-WIND scenario; Table 4.1). The highest and lowest years of TAER are now 2010 and 1990 (plotted in blue and red on Figure 4.1 respectively) as opposed to 2010 and 2007. This indicates that different climate conditions are now driving the inter-annual variability in TAER. This is discussed in detail in Chapter 5.

The reduction in mean TAER happens predominantly for plants operating as baseload (as seen in Buttler et al. (2016)). Table 4.1 shows that mean baseload TVE decreases by 37TWh when 15GW of wind power is installed, whereas the mean peaking plant TVE increases by 0.4TWh.

The inter-annual max-min range of baseload plant operating opportunity approximately triples when 15GW of wind power capacity is installed (Table 4.2). The inter-annual max-min range of peaking plant TVE does not increase as substantially (see Table 4.1). Similar increases are seen in potential operating opportunity for the respective plants (see Table 4.1). This shows that the inclusion of present day levels of wind power capacity has increased the investment uncertainty of baseload plant significantly more than peaking plants.

The mean peak load is decreased when 15GW of wind power capacity is installed (Table 4.2). The inter-annual max-min range in peak load also decreases, indicating a positive compensation between wind power availability and extreme peak demand events, as suggested in Brayshaw et al. (2012). The reduction in peak load suggests that wind power generation is able to provide some firm capacity at peak load. The comparison of results between the NO-WIND and LOW scenarios suggests that peak load may have become easier to manage when installed wind power capacity is present (due to the

reduction in max-min range of peak load; Table 4.2).

The number of operating hours of a mid-merit plant decreases to 5600 hours/year when 15GW of wind power capacity is installed. This is accompanied by a ∼3-fold increase in inter-annual variability of the plants operation (approximately 900 hours/year, see Table 4.3). No curtailment is seen for the LOW wind power scenario (see section 3.4.2 for definitions).
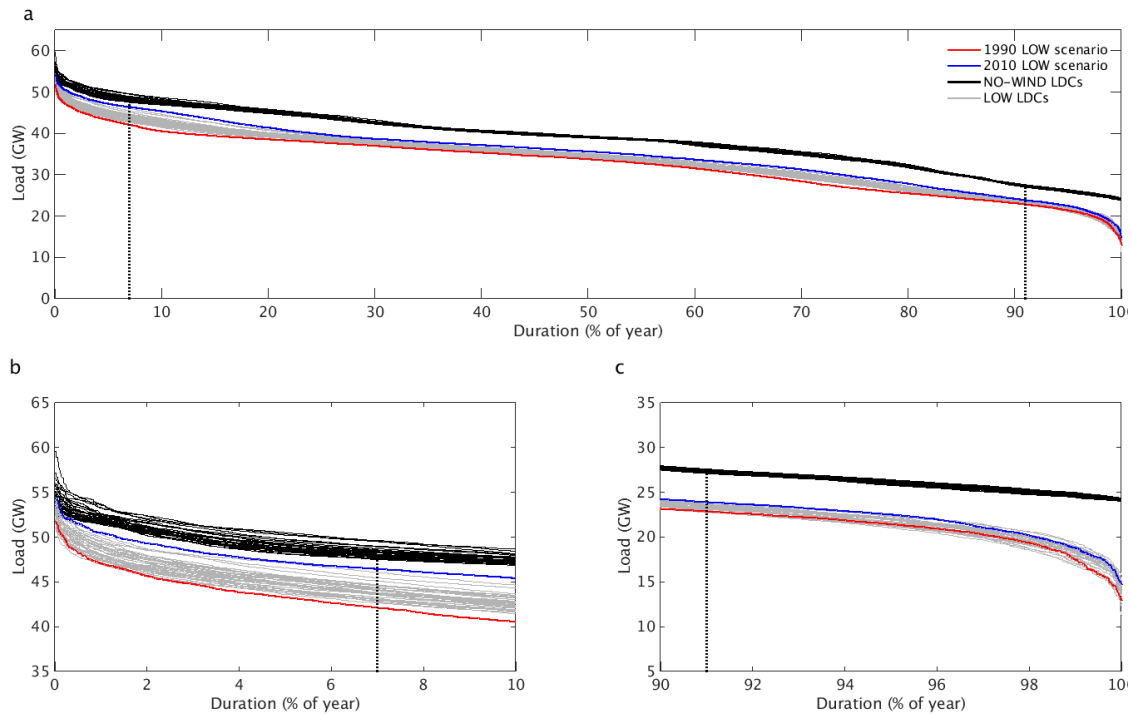
Figure 4.1 LDCs from $1980 - 2015$ for NO-WIND (black) and the LOW installed wind power capacity scenario (grey). The lowest and highest DNW years for the LOW scenario are plotted in red and blue respectively. (a) shows the full max-min range of operating durations. (b) and (c) are identical to (a) but highlight only the low- and high- duration parts of the curves respectively.

4.3 The impact of increasing wind power generation on the GB power system

In this section the impact of increasing the amount of wind power generation in the GB power system from current levels is investigated. To do this metrics are compared from the LOW, MED, and HIGH scenarios (see section 3.4.2 for definitions). Each metric is discussed in turn in the following subsections.

Table 4.1 Mean and inter-annual max-min range of TAER and TVE from Peaking and Baseload plant (in TWh) under four different wind-farm installation scenarios. The max-min range is the difference between the highest and lowest annual values of each metric. For convenience of comparison, the max-min range of values are also expressed as a percentage (normalised by the mean value from the NO-WIND scenario).

Scenario	TAER (TWh) Mean	max-min range		Peaking Plant TVE (TWh) Mean	max-min range		Baseload Plant TVE (TWh) Mean	max-min range	
NO-WIND	326	10.2	(3%)	1.3	0.7	(54%)	227	3.8	(2%)
LOW	283	23.8	(7%)	1.7	0.9	(69%)	190	11.8	(5%)
MED	240	39.8	(12%)	1.9	1.0	(77%)	128	45.9	(20%)
HIGH	170	48.7	(15%)	2.0	1.2	(92%)	18	55.0	(24%)

Table 4.2 The mean and inter-annual max-min range of Peak Load, Peaking plant operating opportunity and Baseload plant operating opportunity under the four different installed wind power scenarios. For convenience of comparison, the max-min range of values are also expressed as a percentage (normalised by the mean value from the NO-WIND scenario)

Scenario	Peak Load (GW) Mean	max-min range		Peaking Plant Opportunity (GW) Mean	max-min range		Baseload Plant Opportunity (GW) Mean	max-min range	
NO-WIND	55.0	8.4	(15%)	47.1	3.3	(7%)	26.0	0.4	(2%)
LOW	52.9	6.1	(11%)	42.6	5.3	(11%)	22.7	1.3	(5%)
MED	51.8	6.0	(11%)	39.9	5.5	(12%)	15.1	5.3	(20%)
HIGH	50.1	8.2	(15%)	36.2	4.2	(9%)	2.5	6.4	(25%)

Table 4.3 The mean and inter-annual max-min range of mid-merit plant operation (marginal at 30GW) under the four different installed wind power scenarios. For convenience of comparison, the max-min range of values are also expressed as a percentage (normalised by the mean value from the NO-WIND scenario)

Scenario	Marginal mid-merit plant operation (hours/year) Mean	max-min range	
NO-WIND	7100	250	(4%)
LOW	5600	880	(12%)
MED	3600	1600	(22%)
HIGH	2600	1600	(22%)

4.3.1 Total Annual Energy Requirement

Figure 4.2 shows LDCs for the NO-WIND, LOW, MED, and HIGH wind power scenarios. Increasing the amount of installed wind power capacity from 15GW to 45GW leads to a reduction in the mean TAER of $\sim 60\%$ (Table 4.1). A doubling in the max-min range of TAER is also seen.
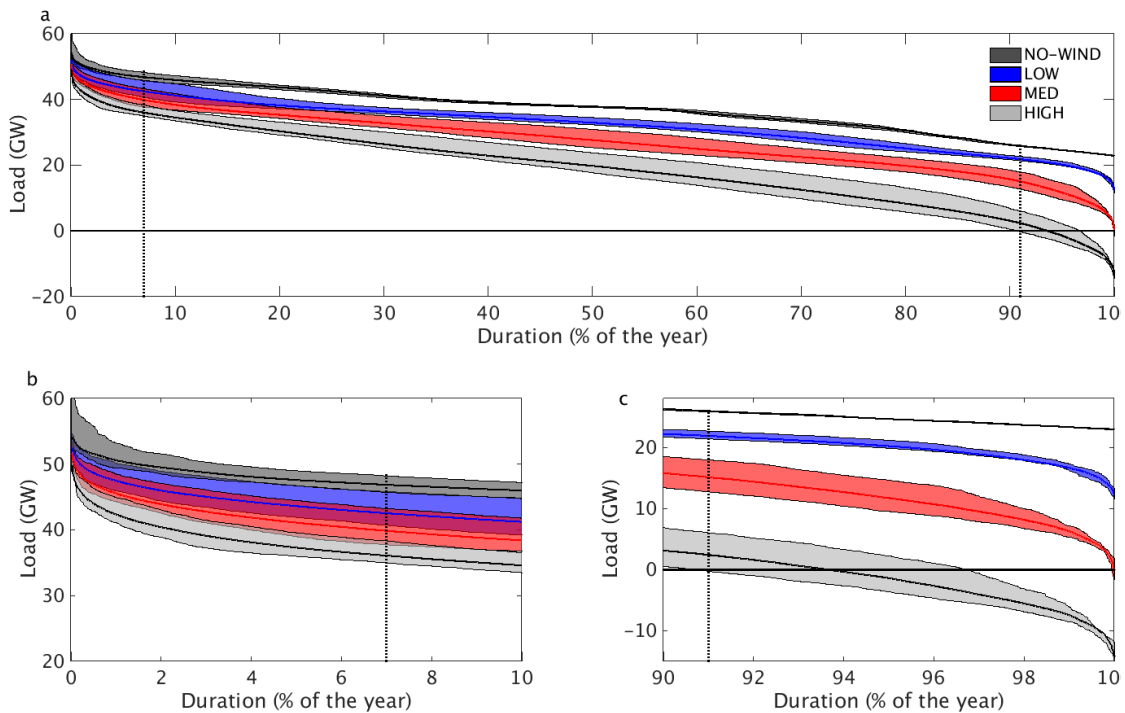

Figure 4.2 LDCs for NO-WIND LOW, MED and HIGH wind power scenarios (black, blue, red and grey respectively). The multi-year mean LDC in each scenario is a solid line, with the edges of the shaded area marking the two extreme years from the set of 36 LDCs within each scenario. Vertical dashed lines show the percentage of time that baseload-plant (91%) and peaking-plant (7%) are required to operate as defined in DECC (2013). (a) shows the full max-min range of operating durations. (b) and (c) are identical to (a) but highlight only the low- and high- duration parts of the curves respectively.

The increase in the max-min range of TAER is due to the increased volume of wind power capacity on the system, which has larger inter-annual variability than demand (see Figure 4.3). The max-min range of the annual average demand anomaly from the 1980-2014 mean (black line in Figure 4.3) is 2% with the two most extreme years being 2007 and 2010. The max-min range of the annual average capacity factor anomaly is 39%. (Capacity factor is the percentage of wind power generation over a year compared to potential maximum output; red line in Figure 4.3.) The annual average wind power capacity factor is $\sim$20 times as variable as demand. This explains why the addition of installed wind power capacity leads to increased variability in TAER.

The most extreme years of TAER are not changed as more wind power capacity is installed, between 15GW and 45GW. This suggests that the meteorological driver of TAER is not changed as more wind power capacity is installed. This is further discussed in chapter 5, as well as the causes of the extreme wind power generation in 1986, 1990 and 2010.
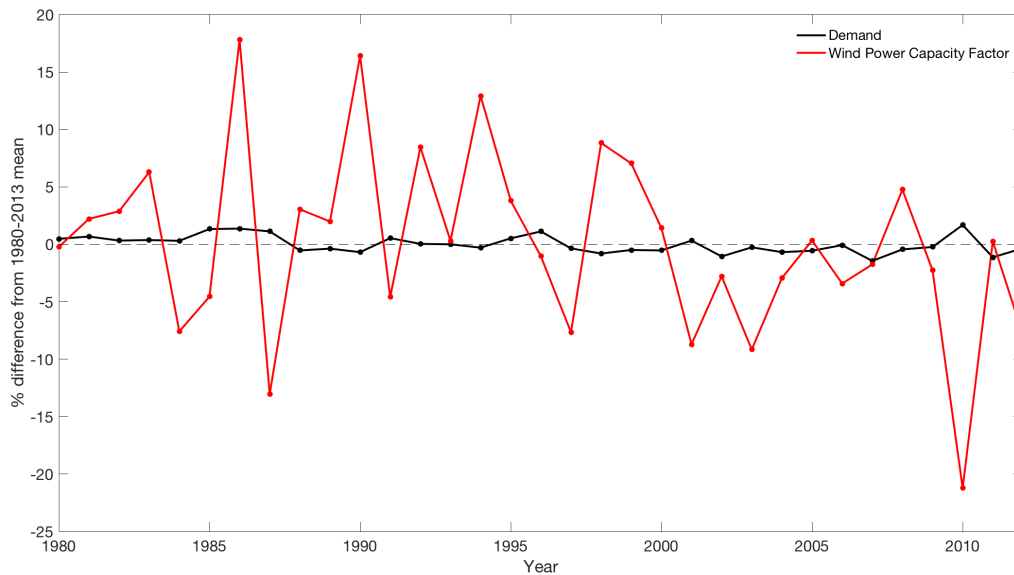
Figure 4.3   The percentage difference from the 1980-2013 mean value of both demand (black) and wind power generation (red) for years 1980-2013

4.3.2   Baseload Plant

The maximum baseload plant operating opportunity dramatically decreases from ∼22GW to ∼3GW with increasing installed wind power capacity (Table 4.2, Figure 4.2). The inter-annual max-min range in baseload plant operating opportunity also drastically increases across the scenarios (Table 4.2).

Table 4.1 shows that as the amount of installed wind power capacity is increased the mean baseload TVE reduces rapidly, with only small amounts of baseload generation required in a power system with 45GW of installed wind power capacity.

There is a large increase in the max-min range of baseload TVE as the amount of installed wind power capacity is increased to 30GW (Table 4.1) which is then followed by a smaller increase in max-min range as the installed wind power capacity is increased to 45GW. The differences in max-min range of baseload TVE between the MED and HIGH scenario are partially due to increasing installed wind power capacity and partially due to the changing geographical distribution of wind farms. These differences shall be examined

in section 4.4.

The large reductions suggest that in systems with large amounts of installed wind power capacity baseload plant may be required to operate for much shorter periods of the year than at present. This would require baseload plant to become significantly more flexible.

4.3.3 Peaking plant

Table 4.2 shows that as the amount of installed wind power capacity increases, the mean peaking plant operating opportunity decreases (from $\sim$43GW to $\sim$36GW by the time 45GW of wind power capacity is installed; Table 4.2). The inter-annual max-min range of peaking plant operating opportunity is approximately constant in the LOW and MED scenarios (Table 4.2) although the max-min range corresponds to an increasing fraction of total peaking plant operating opportunity. This shows that in a system with high levels of wind power generation, peaking plant may be required to start operating at lower load thresholds, but the inter-annual range around the value at which operation may begin could be larger.

45GW of installed wind power capacity results in a further reduction in peaking plant operating opportunity (with peaking plant now being called upon to operate for all loads above $\sim$36GW). However, there is a reduction in the max-min range of inter-annual peaking plant operation compared to the MED scenario. This is due to the changing wind farm distribution in the HIGH scenario, discussed in section 4.4.

The reason for the increase in peaking plant TVE with increasing installed wind power capacity is not immediately obvious, as the mean load at 7% of the LDC (i.e the peaking plant minimum load requirement) is decreasing with increasing installed wind power capacity (see Figure 4.2). The peaking plant TVE metric however, concerns the area integral between the minimum load requirement threshold and peak load (see Figure 3.4.2), which is increasing with increasing installed wind power capacity. If each set of curves is normalised by the value of load at the 7% threshold then the increase in peaking plant TVE is clearer (Figure 4.4). The gradients of the LDCs become steeper as more wind power capacity is installed on the system.

Large differences are seen in the potential operating opportunity for peaking plant and baseload plant as the amount of wind power capacity installed on the system is increased. The reduction in peaking plant operating opportunity ($\sim$6GW) is small compared to the $\sim$19GW reduction in baseload plant operating opportunity. This shows that as the
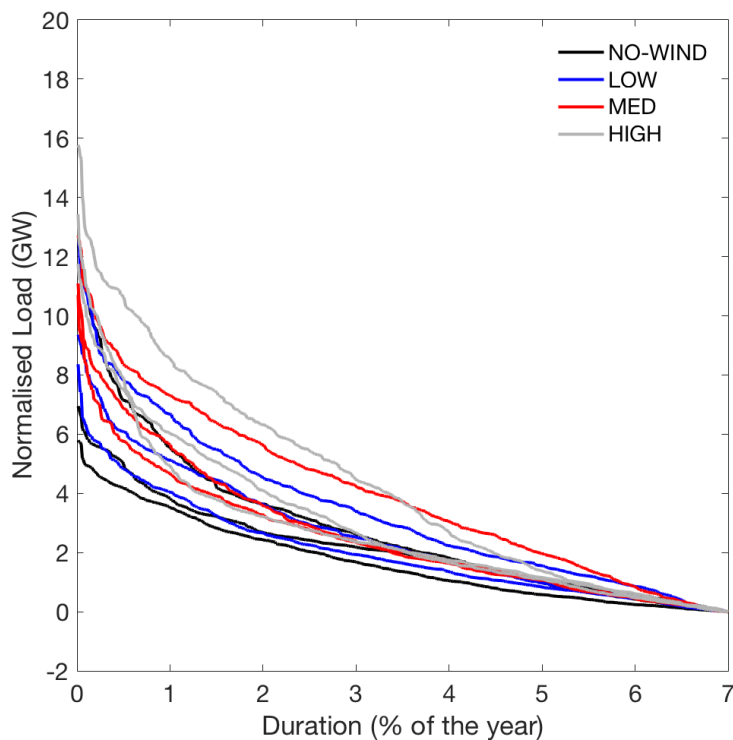
Figure 4.4 Normalised LDCs for the mean, maximum, and minimum years of peaking plant TVE for each wind power scenario (see Appendix 8.3 for details of the years). The curves are normalised against the value of load at the 7% threshold on the LDC (i.e. the peaking plant minimum load requirement).

amount of wind power capacity installed on the system is increased, baseload plant is impacted more strongly than peaking plant, resulting in larger investment uncertainty for baseload plants. Larger adaptation measures would also be required for baseload plants in systems with large amounts of installed wind power capacity.

4.3.4   Peak Load

Table 4.2 shows that the mean peak load reduces with increasing installed wind power capacity (∼53GW to ∼50GW from the LOW to HIGH scenarios). This suggests that as the amount of installed wind power capacity is increased, wind power generation is able to provide an increasing amount of firm capacity at times of peak load (Firm capacity is the amount of energy which can be guaranteed to be available; Freris and Infield (2008)). The reduction in mean peak load also suggests that some peaking plants which are currently marginal at very high load levels may not be required to operate every year in systems with large installations of wind power capacity.

The max-min range of peak load increases as the amount of installed wind power capacity is increased. However, even when 45GW of wind power capacity is installed the max-min range of peak load does not exceed the max-min range in a system with no installed wind power capacity. This suggests that the compensation between wind power production and peak load (as implied by Brayshaw et al. (2012)) is still present with large volumes of installed wind power capacity. This also implies that even with 45GW of installed wind power capacity securing enough generation for times of peak load is easier to plan for than in the NO-WIND scenario.

4.3.5 Mid-merit plant

The number of hours that a mid-merit plant would be expected to operate decreases substantially as the amount of wind power capacity installed on the system is increased (from an average of 5600h/year in the LOW scenario to 2600h/year in the HIGH scenario; Table 4.3). The inter-annual variability in the number of operating hours increases from 880 hours/year under the LOW scenario to 1600 hours/year in the HIGH scenario. This shows that mid-merit plant would be required to respond in a similar way to baseload in a system with increased installed wind power capacity.

4.3.6 Curtailment

Table 4.4 shows that no curtailment is seen in the GB power system until 30GW of wind power capacity is installed. Figure 4.2 shows that there are very few hours of curtailment in this scenario. It is noted that the current GB power system already experiences significant amounts of wind power curtailment due to network constraint. This analysis shows that if network constraint was not a reason for curtailment then 30GW of installed wind power capacity could easily be incorporated into the GB power system.

From the MED to HIGH scenarios the amount of demand driven curtailment (wind power > demand) and stability driven curtailment (wind power > 70% demand) increases dramatically. Focussing on the demand driven curtailment, the mean energy curtailed each year increases from 1GWh to ~2.4TWh as an extra 15GW of wind power capacity is installed. The inter-annual max-min range of curtailment also increases from 14GWh to 2.4TWh (note the change in units). A qualitatively similar result is seen for stability driven curtailment, but with more curtailment in each scenario (see Table 4.4).

The ratio between the amount of curtailment seen in the MED and HIGH scenarios

for demand driven and stability driven curtailment is not constant (i.e. the 40-fold increase from MED to HIGH for stability driven curtailment can be compared to the 12000-fold increased from MED to HIGH for demand driven curtailment). This shows that the impacts of curtailment are very sensitive to the metrics definition.

Table 4.4 The mean and inter-annual max-min range of energy curtailed per year. See section 3 for metric definitions.

Scenario	Energy curtailed: WP > D (TWh)		Energy curtailed: WP > 70%D (TWh)	
	Mean	max-min range	Mean	max-min range
NO-WIND	0	0	0	0
LOW	0	0	0	0
MED	0.001	0.014	0.3	0.4
HIGH	2.4	2.4	13	11

4.4 The impact of increasing offshore wind power generation on the GB power system

Tables 4.1 to 4.4 show differences in power system metrics between the MED and HIGH scenario which can not be explained solely by the increase in installed wind power capacity. In this study the LOW and MED wind power scenarios use a common spatial distribution of wind farms, with mostly onshore wind turbines (Figure 3.3a). In the HIGH scenario a spatial distribution including more offshore wind turbines is used (Figure 3.3b). The difference in these two distributions has been previously investigated by Drew et al. (2015) where it was found the distribution with more offshore wind farms has a higher average annual capacity factor (39.7%) compared to the distribution used in the LOW and MED scenarios (32.7%). The 25th 50th and 75th percentiles of the current wind farm distribution are capacity factors of 12% 25% and 48%. These percentiles are increased in the future wind farm distribution to 18% 36% and 60% respectively (Drew et al. (2015); see Figure 4.5). Drew et al. (2015) showed that the changes in capacity factor between the two wind farm distributions are almost entirely due to increasing the amount of installed offshore wind generation.

The impact of changing the spatial distribution of wind farms on the GB power system is investigated in the following subsections. Each of the previously described power system metrics is calculated using both of the wind farm distributions, including scaled wind power capacity from $0 - 45$GW in 1GW intervals. Demand remains as described in section 3.2. This is in order to understand how much of the change between the MED and
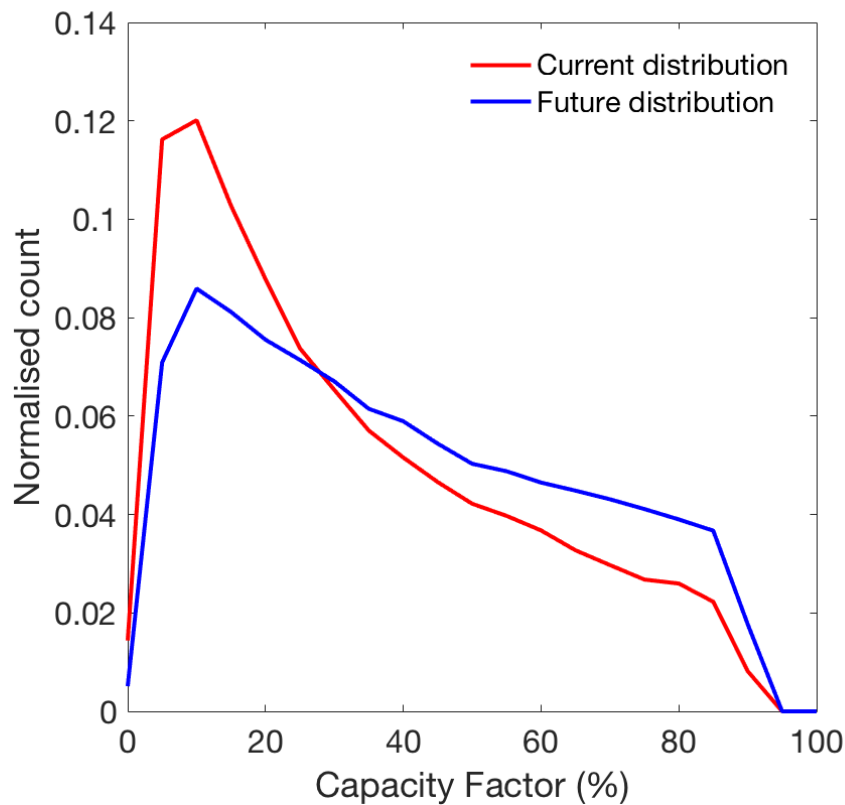
Figure 4.5 Relative frequency distribution of the hourly GB-aggregated capacity factor derived from the full (1980 to 2015) time series for the current wind farm distribution (from Cannon et al. (2015), red) and with the future distribution (from Drew et al. (2015), blue)

HIGH scenarios is due to the increase in installed wind power capacity (from 30GW in the MED scenario to 45GW in the HIGH scenario) and how much is due to the different spatial distribution of wind farms.

4.4.1   Total Annual Energy Requirement

Increasing the installed wind power capacity from 0-15GW and 15-30GW both result in a 43TWh reduction in TAER. However, a 70TWh reduction is seen when the installed wind power capacity is increased from 30-45GW. The construction of TAER, as an area integral under a LDC (see section 3.4) means that increasing the amount of installed wind power capacity in the power system using the same distribution of wind farms leads to a linear reduction in mean TAER (see Figure 4.6a).In the current wind farm distribution an increase in installed wind power capacity of 1GW leads to a 2.9TWh reduction in the mean TAER over the 36 year period. If this is compared to the future wind farm distribution an increase in installed wind power capacity of 1GW leads to a 3.5TWh

reduction in the mean TAER.

The larger reduction in TAER is due to increased number of hours with high capacity factor (due to higher offshore wind speeds; see Figure 4.5). Figure 4.6 shows 43TWh of the 70TWh reduction in TAER is due to the increase in wind power production from 30-45GW, whereas the remaining 27TWh are due to increasing offshore wind power capacity. This highlights that the placement of wind farms can have large impacts on the results from power system modelling studies, and should be given more attention within the literature.
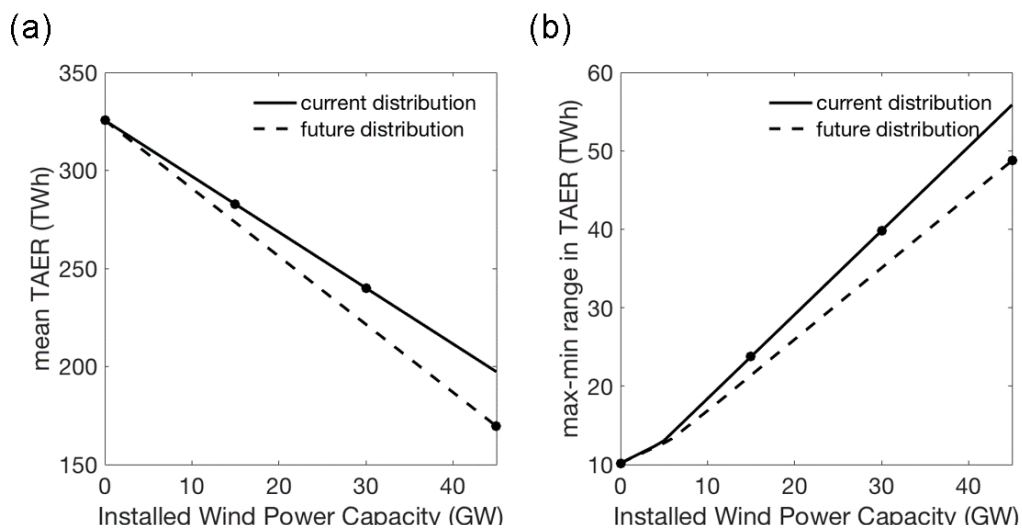

Figure 4.6 The impact of increasing installed wind farm capacity on TAER. The solid line indicates the "current-day" spatial wind-farm distribution (as used in the LOW and MED scenarios), whereas the dashed line indicates the "future" spatial wind farm distribution (as used in the HIGH scenario). (a) Mean TAER and (b) max-min range of TAER, The four main scenarios used (NO-WIND, LOW, MED and HIGH) are marked on the relevant curves as black dots for reference.

Figure 4.7b shows the max-min range of TAER for installed wind power capacity of 0-45GW using both the current and future wind farm distributions. The first point to note is that the max-min range of TAER is larger in the current wind farm distribution than the future distribution. The reduction in range from the MED-HIGH scenario compared to the LOW-MED scenario is explained by the capacity factors from the future wind farm distribution being less variable than the current distribution, due to the more constant nature of offshore wind (see Drew et al. (2015) for further details).

A change in gradient is seen in Figure 4.6 after the point where 5GW of wind power capacity is installed. From 5GW the max-min range of TAER increases more rapidly with increasing installed wind power capacity. This can be understood by referring to
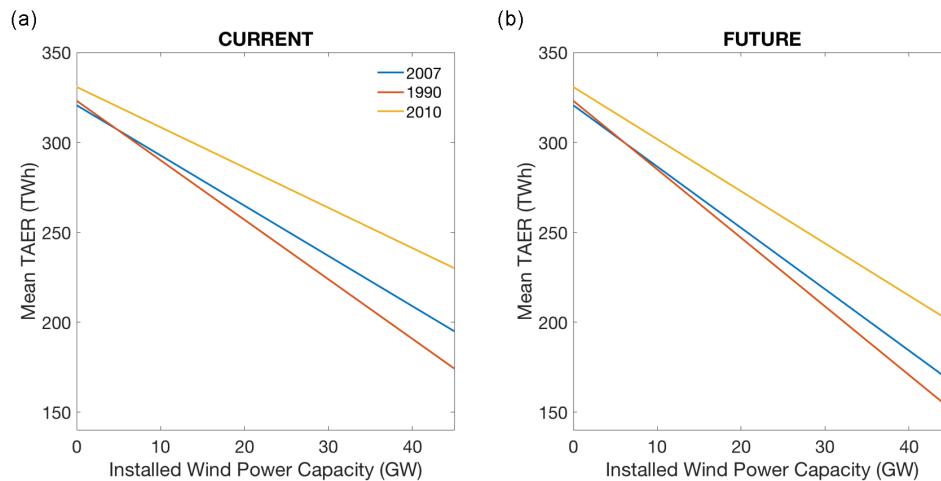
Figure 4.7 The impact of increasing installed wind farm capacity on TAER for the three most extreme years. (a) TAER for the current wind farm distribution (b) TAER for the future wind farm distribution.

Table 8.2 which shows for the NO-WIND scenario the most extreme years of TAER are 2010 and 2007, whereas in the LOW scenario the most extreme years of TAER are now 2010 and 1990. The reason for this change is shown in Figure 4.7, where the TAER for each of the extreme LDCs is given as the amount of installed wind power on the system is increased. The intercept of these curves shows TAER in the NO-WIND scenario, and the gradient shows the reduction in TAER per installed GW of wind power capacity. Once 5GW of installed wind power capacity is present 1990 becomes the most extreme curve for both the current and future wind farm distributions.

This shows that as the amount of installed wind power capacity is increased different years have the potential to control the max-min range of the power system metrics. This emphasises the importance of using a long time series of data for analysis to accurately evaluate the potential range of operating conditions.

4.4.2 Baseload plant

In this section the focus is on baseload plant operating opportunity, although the same qualitative result is seen for baseload TVE and mid-merit plant requirement (not shown). Figure 4.8a shows the mean baseload plant operating opportunity for both the current and future wind farm distributions, with installed wind power capacity ranging from $0 - 45$GW. Unlike TAER, the relationship between the amount of installed wind power capacity and mean baseload plant operating opportunity is not linear. This is because hours from the DNW time series used to create the baseload metric change as

the amount of wind power capacity installed on the system is increased.

The mean baseload plant operating opportunity is higher in the current wind farm distribution than the future wind farm distribution (Figure 4.8a). This is due to the higher capacity factors in the future wind farm distribution (therefore lower values of DNW; see Figure 4.5 and Drew et al. (2015)). The large drop off in baseload plant requirement between the MED and HIGH scenarios from 15.1GW to 2.5GW is shown here to be predominantly due to the increasing volume of wind power generation on the system, with only minor differences being due to the change in wind farm distribution.

The max-min range in baseload plant operating opportunity is relatively consistent between the two wind farm distributions until ~ 20GW of wind power capacity is installed. After this point a noticeable difference is seen between the max-min ranges, with the future wind farm distribution having a smaller max-min range of plant operation than the current wind farm distribution. This is attributable to the reduced variability of wind power generation in the HIGH scenario.

The sharp change in gradient at $\sim$15GW in the current wind farm distribution and $\sim$10GW in the future wind farm distribution is due to different years of data now representing the most extreme years, from which the max-min range is calculated, in the same way as described for Figure 4.7. Table 8.2 shows that there are multiple changes in the maximum and minimum years of baseload plant operating opportunity up until the MED scenario. From this point 2010 and 1990 are the maximum and minimum year respectively, as seen for TAER.

4.4.3   Peaking Plant

The response of mean peaking plant operating opportunity to increasing installed wind power capacity is similar to that seen for mean baseload plant metrics (see Figure 4.9a). As the amount of installed wind power capacity is increased, the mean peaking plant requirement is reduced. This reduction is larger in the future wind farm distribution than in the current distribution (Figure 4.9). The reduction in peaking plant operating opportunity between the MED and HIGH scenarios is shown as approximately half due to the increases in installed wind power capacity and half due to the change in wind farm distribution (Figure 4.9). This emphasises the importance of accurately describing the wind farm distribution used in power system modelling.

The changes in max-min range for peaking plant operating opportunity are complex. In the current wind farm distribution there is approximately linear growth in the max-min
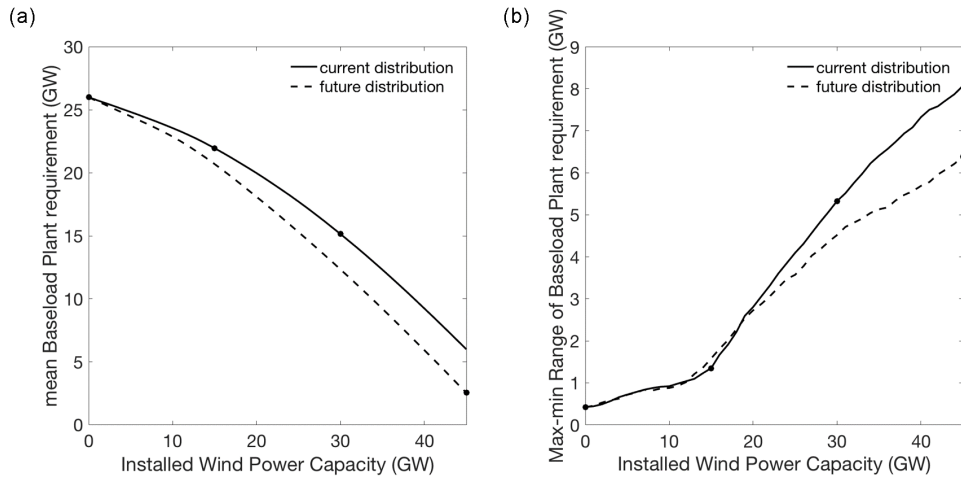
Figure 4.8   The impact of increasing installed wind power capacity on baseload plant operating opportunity (a) Mean baseload plant operating opportunity and (b) inter-annual max-min range of baseload plant operating opportunity, the solid line indicates the "current-day" spatial wind-farm distribution, whereas the dashed line indicates the "future" spatial wind farm distribution. The four main scenarios used (NO-WIND, LOW, MED and HIGH) are marked on the relevant curves as black dots for reference.
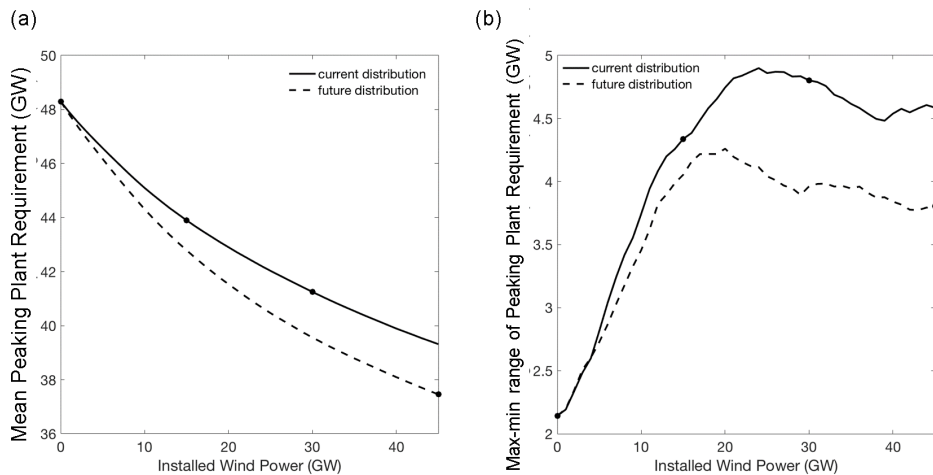
Figure 4.9   The impact of increasing installed wind power capacity on peaking plant operating opportunity (a) Mean peaking plant operating opportunity and (b) inter-annual max-min range of peaking plant operating opportunity, the solid line indicates the "current-day" spatial wind-farm distribution, whereas the dashed line indicates the "future" spatial wind farm distribution. The four main scenarios used (NO-WIND, LOW, MED and HIGH) are marked on the relevant curves as black dots for reference.

range of peaking plant operating opportunity from $0-25$GW, however after this point the growth plateaus. This is also seen in the future wind farm distribution, but the plateau begins at approximately 15GW.

4.4.4 Peak Load

The mean peak load shows a larger reduction in the future wind farm distribution than in the current wind farm distribution as the amount of wind power capacity installed on the system is increased (Figure 4.10a). This shows that at times of mean peak load there is at least moderate wind power production in both distributions. It should be noted that this discussion is related to the mean peak load, therefore there may still be years with no wind power production at peak load, which is of critical importance to system operation.

In the current wind farm distribution the addition of installed wind power capacity leads to a reduction in the max-min range of peak load until ∼20GW of wind power capacity is installed (Figure 4.10b). The installation of additional wind power capacity above 20GW does very little to the max-min range of peak load, but reduces the mean peak load. This shows that large increases in installed onshore wind capacity could potentially aid the ability of the power system to meet with extreme peak loads.
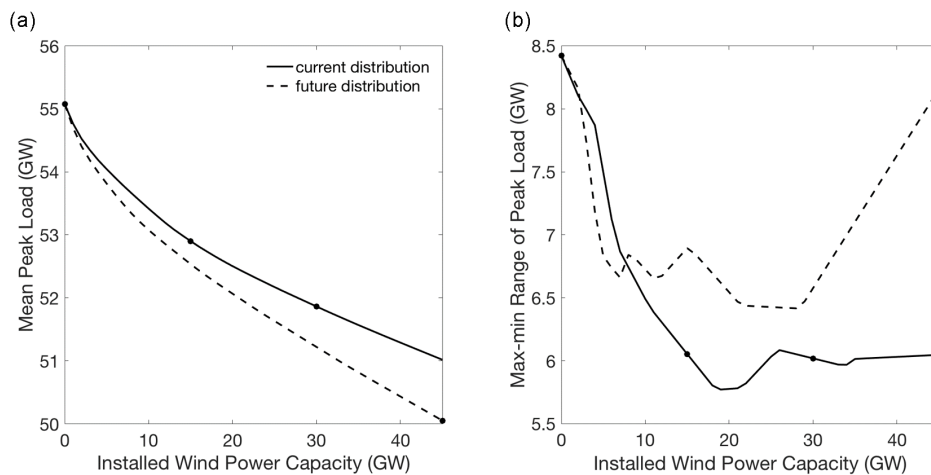
Figure 4.10 The impact of increasing installed wind power capacity on peak load (a) Mean peak load and (b) inter-annual max-min range of peaking load, the solid line indicates the "current-day" spatial wind-farm distribution, whereas the dashed line indicates the "future" spatial wind farm distribution. The four main scenarios used (NO-WIND, LOW, MED and HIGH) are marked on the relevant curves as black dots for reference.

In the future wind farm distribution a reduction in the max-min range of peak load

is seen until approximately 6GW of installed wind power capacity. The max-min range of peak load then stays approximately constant until 30GW of wind power capacity is installed. This suggests that large increases in offshore wind power would not impact the range of peak loads that the GB power system may experience. Once 30GW of installed wind power capacity is exceeded then the max-min range of peak load begins to rise again, however even with 45GW of wind power installed on the system the range of peak load is still less than in a power system with no installed wind power capacity.

4.4.5   Curtailment

Figure 4.11 shows the mean hours and the max-min range of energy curtailed under the demand-driven curtailment scenario (wind power > demand). A similar result is seen for the stability-driven curtailment scenario, however, much larger volumes of energy are curtailed (not shown). Until 30GW of wind power capacity is present then the mean energy curtailed is less than 1GWh (Figure 4.11 therefore starts at 30GW for visual clarity).

There is rapid growth in the mean amount of energy curtailed between 30GW and 45GW of installed wind power capacity. Figure 4.11 shows that this growth is larger if a high percentage of offshore wind generation is present (i.e. with 45GW of installed wind power capacity the future distribution has a mean value of 2.4TWh of curtailment, the current distribution only has a mean value of 1.3TWh of curtailment). The max-min range of energy curtailed is comparable to the mean amount of curtailment for all levels of installed wind power capacity. This shows that curtailment is an extremely variable metric which could be poorly estimated with a small volume of data, or an incorrect distribution of wind farms.

4.5   Limitations of modelling studies using short records of demand and wind power data

The results presented in sections 4.1 to 4.4 add to a growing body of literature that demonstrate the need for power system modelling to take a more robust approach to its treatment of weather and climate data, including the use of multi-decadal data, and an accurate representation of wind farm distributions.

To emphasise the importance of long meteorological datasets to power system modelling an example case is selected from a technical report from POYRY (2009). The
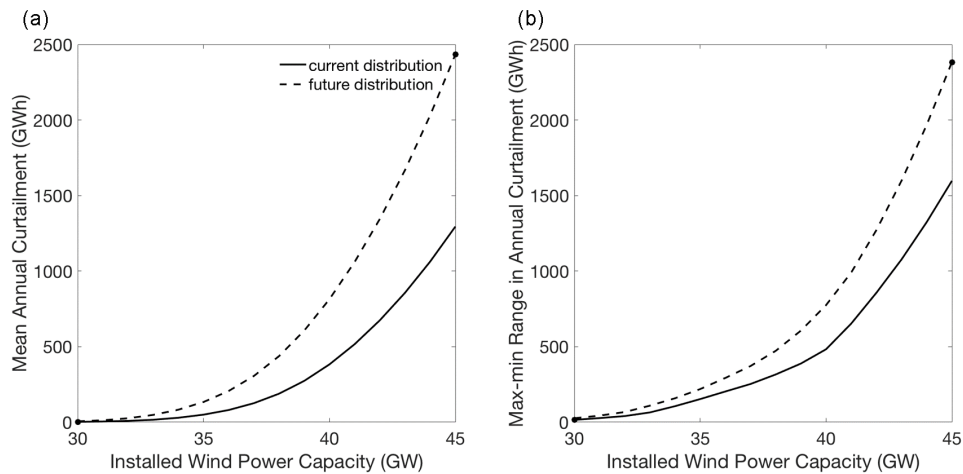
Figure 4.11 The impact of increasing installed wind power capacity on wind power curtailment (a) Mean wind power curtailment and (b) inter-annual max-min range of wind power curtailment. The solid line indicates the "current-day" spatial wind-farm distribution, whereas the dashed line indicates the "future" spatial wind farm distribution. The four main scenarios used (NO-WIND, LOW, MED and HIGH) are marked on the relevant curves as black dots for reference.

example bases their findings on wind power data generated using 10m wind speeds over multiple locations across GB from 2000-2007. This wind power data is used as an input to a complex simulation of the GB electricity market in order to understand the potential impacts of intermittency. POYRY (2009) found a ∼13% difference in the total wind power generated between highest and lowest years in this period.

Evaluating the study period of POYRY (2009) using the re-analysis based methodology described in section 3.3 leads to a 11% inter-annual max-min range of wind power generation. Extending the study period to 1980-2015 results in the inter-annual max-min range of wind power generation increasing to 32%. i.e. an almost 3 fold increase on the original study. The years from 2000-2007 have a below average capacity factor when compared to 1980-2015 (see Figure 4.12 and Earl et al. (2013), Bett et al. (2013), Cannon et al. (2015)). The inter-annual swings between annual capacity factors are also relatively small compared to the large swings between 1986-1987 and 2009-2010-2011 (Figure 4.12). The impact of inter-annual climate variability is therefore likely to be substantially underestimated by POYRY (2009), and again emphasises the importance of understanding the meteorological context of the years of data which are used within modelling simulations of power systems with high levels of wind power generation.
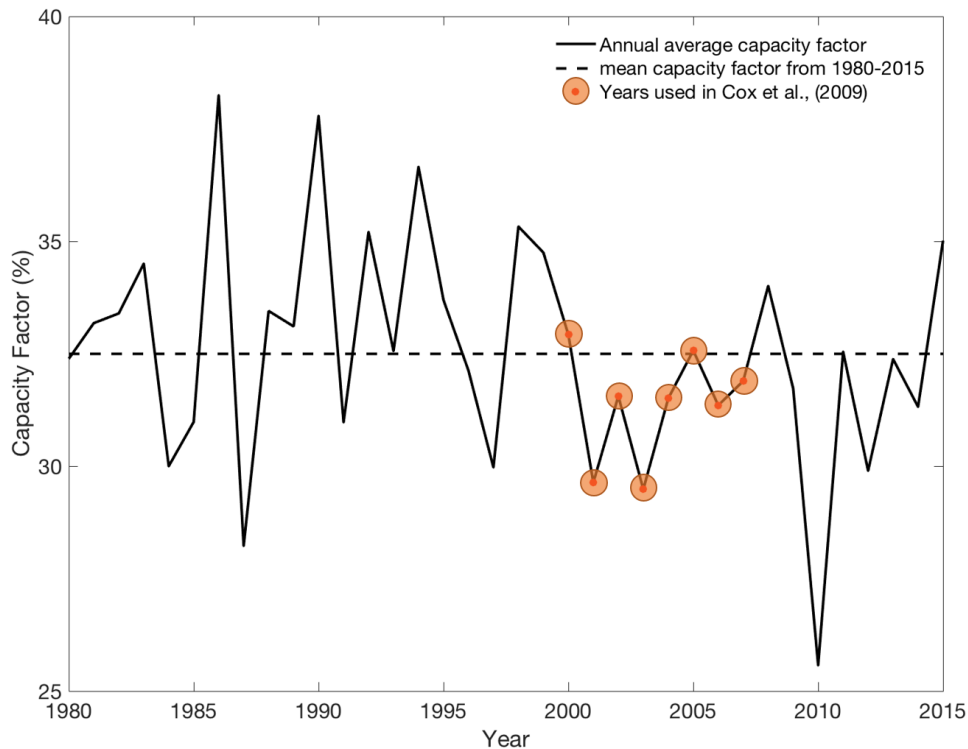
Figure 4.12 Annual Average GB capacity factor (%) for the years 1980-2015. The mean over the study period is plotted as a dashed line. Red points include years from the POYRY (2009) study.

4.6 The importance of a multi-decadal time series of data for investment problems

Previous studies investigating future changes in installed plant capacity base their results on short data records, with it being common for only a single year of data to be used for analysis (George and Banerjee (2011), De Jonghe et al. (2011), Ueckerdt et al. (2015), Pfenninger and Keirstead (2015), Buttler et al. (2016)). In this section the uncertainty that relying on a single year of weather data introduces into these modelling studies is quantified.

To do this changes in the operating opportunity of baseload plant when the amount of installed wind power capacity is increased from 15GW to 30GW are investigated (i.e. from the LOW to MED scenarios). These changes are of interest to plant owners wishing to understand uncertainty in future operating hours. Baseload plant has been chosen as this was the type of plant which was shown to be most susceptible to the impacts of increasing installed wind power capacity in section 4.3.

The period from 1980 to 2015 is used for analysis. Five different sampling period

experiments are performed. For each experiment n years of data are randomly selected from the 36 year record, where $n = 1, 2, 5, 10$ or 36. Each year of data is treated as serially independent, therefore allowing consecutive years of extreme demand or wind power generation to occur (which have not been seen in the 36 year meteorological record).

Figure 4.13 shows the changes in baseload plant operating opportunity from the LOW to MED scenarios, calculated using different lengths of sampling data. The *truth* is treated as the change in baseload plant operating opportunity from the LOW to MED scenario from Table 4.2 (6.7GW; calculated using data from 1980-2015) and is represented by the grey dotted line. The changes in baseload operating opportunity are represented by two standard deviations of the change from the LOW to MED scenario, calculated from all samples with the same sampling period. The dashed lines show the results from the random sampling experiment and the solid lines show the amount of variability if only consecutive sets of years are allowed to be used in the analysis (i.e. for $n = 2$ 1980,1981 and 1981,1982 etc. are chosen). The results using consecutive years of data are plotted for comparison to show the extra variability which is present through considering the possibility of different pairings of years of data. Two standard deviations is used to include 95% of the data within the analysis and therefore does not include extreme events which may be less physical (i.e. the extreme low wind year of 2010 could be picked consecutively many times in the bootstrap analysis).
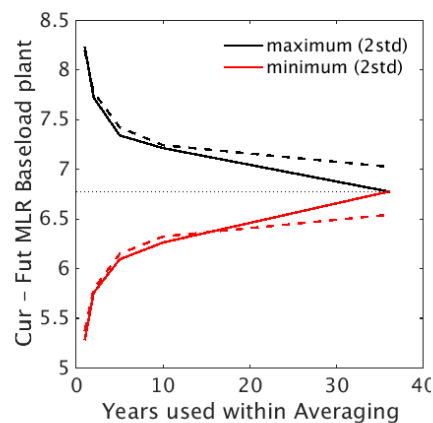
Figure 4.13 Simulated reduction in baseload plant operating opportunity between MED and LOW wind power scenarios as a function of climate-data sample length. Solid lines represent results using consecutive years from 1980-2015. Dashed lines represent results of random sampling experiments including 1000 samples in order to calculate the maximum change in GW (+2 standard deviations from the mean, black dashed lines) and the minimum change in GW (-2 standard deviations from the mean, red dashed lines). For reference the mean value over the continuous period from 1980-2015 is plotted as a grey dotted line.

When a single year sampling period is used to calculate the change in baseload plant operating opportunity differences in the projected change of ∼3GW are seen (which is ∼ 40% of the value calculated from the 36 year sampling experiment). These differences rapidly reduce as the sample size is increased, with the difference in baseload plant operating opportunity being ∼0.5GW for sampling periods greater than 10 years. The ∼3GW scope for error using one year of data is potentially significant, as it is comparable to the size of the projected change in nuclear power capacity in the *Gone Green* scenario from National Grid (2015) where a 2.3GW increase is projected from 2020 to 2030.

This section has shown that using a short sampling period for analysis of the difference between present day and future power systems can introduce potentially significant levels of uncertainty into power system planning projections. The sampling uncertainties identified here are likely to be underestimates of the full climate uncertainty: 36-years is a relatively "short" observing window for climate extremes, Moreover the role of anthropogenic climate change has not been considered.

4.7   Chapter Summary

The results from this chapter emphasise the importance of the role of inter-annual climate variability in the GB power system as an integrated whole, both now and under near-future installed wind power capacity scenarios. These results add to a growing body of evidence that demonstrate that power system modellers should begin to take a more robust approach to their treatment of weather and climate data, including the use of multi-decadal data. The danger of over-reliance on a short dataset has been clearly demonstrated by revisiting the influential study of POYRY (2009) using these new tools, where it is shown that the max-min range of inter-annual variation in GB wind power generation is underestimated by at least a factor of three. It is noted that the results of the max-min range analysis conducted in this thesis are dependent on the time period selected for analysis and using a re-analysis product spanning a different period could lead to qualitatively different results.

Key results from this chapter are given below:

- As the amount of installed wind power capacity increases, the total amount of energy required from conventional generators is reduced. In this sense, wind is contributing to the goal of decarbonising the power system. Consistent with De Jonghe et al. (2011) and Buttler et al. (2016), the addition of more installed wind power capacity

is particularly disruptive for plants operating as baseload rather than peaking plant. This could mean that current plant operating regimes may need to be adapted, or wind power generation may have to be curtailed.

- Despite the reduction in the average energy required, the introduction of additional installed wind capacity acts to exacerbate the impact of year-to-year variability on the power system. The increasing impact of year-to-year variability is particularly pronounced for baseload type plants and the number of hours of wind power curtailment. This adds to the previously described disruption for baseload plant, as increased inter-annual operating range means that there may be significant variability in annual cash-flow.

- Both the magnitude and max-min range of peak load is reduced in a system including installed wind power capacity up to 45GW, compared to a demand-only system. This shows a positive compensation between demand and wind power generation at peak demand, and suggests wind power generation may be able to provide firm capacity at times of peak load.

- The results have highlighted the changes in GB power system operation which may occur under different wind farm distributions. The mean value of all power system metrics (except curtailment) is reduced in a system with large amount of offshore generation compared to a system with mostly onshore generation. This highlights the need for power system modellers to represent the location of installed wind power generation accurately.

- The amount of error that may be introduced by using only a single year of data has also been assessed with results suggesting that interannual climate variations could cause up to 100% changes in the operating opportunity of baseload plant from 2015 to 2030.

It is concluded that recent experience of the GB power systems' year to year variability should not be viewed as providing a robust guide to its future variability. Inter-annual variability in particular will have an increasing impact as larger quantities of wind power capacity are installed. This suggests that the role of long term climate variability on the GB power system should be revisited thoroughly using more advanced power system models (which have typically relied on much shorter data records).

Chapter 5:

The Meteorological drivers of GB power system variability

Chapter 4 has shown that inter-annual climate variability causes substantial impacts to the operation of the GB power system. However, the chapter did not address the meteorological causes of the inter-annual variability. Previous studies have investigated the meteorological drivers of peak demand (e.g. Brayshaw et al. (2012), Leah and Foley (2012), Thornton et al. (In review)) and renewable energy generation (e.g. Brayshaw et al. (2011b), Ely et al. (2013), Colantuono et al. (2014)). The meteorological drivers of other power system components have, however, received relatively little attention.

The objective of this chapter is to identify the meteorological drivers of the observed GB power system variability for the previously described wind power scenarios (section 1.4, objective 3). This chapter highlights key meteorological phenomena relevant to power system operation using the LDC approach from chapter 3.

The chapter begins by briefly describing the methods of analysis used for each metric (section 5.0.1). Sections 5.1 and 5.2 show the relationships between meteorological variables with weather-dependent demand and wind power generation respectively. Section 5.3 then investigates the co-variability between seasonal demand and wind power generation. This is in order to understand the behaviour of the weather-dependent power system components individually, before analysing them as power system metrics. Five power system metrics are examined in this chapter. The meteorological drivers of Total Annual Energy Requirement (TAER) are investigated in section 5.4, followed by the meteorological drivers of baseload Total Volume of Energy (TVE; section 5.5), peaking plant TVE (section 5.6) peak load (section 5.8) and wind power curtailment (section 5.7). A summary of the key results from this chapter are given in section 5.9.

5.0.1 Chapter methodology

This chapter focusses on finding the meteorological drivers of power system metrics (discussed in chapter 4) using the MERRA re-analysis Rienecker et al. (2011). The demand data used for analysis is the weather-dependent demand described in section 3.2.2 and wind power generation is from the Cannon et al. (2015) model (section 3.3).

A similar method of analysis is conducted in sections 5.4 to 5.6. Initially the time of year that the metrics are weather-sensitive is identified. Following this, correlation maps are created between annual-mean (and seasonal-mean) 2m temperature and the chosen power system metric, for each wind power scenario. This is followed by correlation maps between annual-mean (and seasonal-mean) 10m wind speed and the chosen power system metric. The large scale meteorological drivers of the metrics inter-annual variability are then investigated.

Correlation coefficients presented in this chapter are calculated by averaging meteorological variables over GB from 11.3^oW-2.7^oE and 50^oN-59^oN (the area which land-only temperatures are averaged over to create electricity demand data). Correlation coefficients are only discussed if they have a p-value less than 0.05, and are therefore deemed statistically significant. Grid boxes with a p-value less than 0.05 are represented by the hashed areas on the correlation maps.

A different method of analysis is used in sections 5.7 and 5.8 to identify the synoptic conditions present during wind power curtailment and peak load events respectively. Rather than performing correlation analysis, the focus in these sections is on the synoptic conditions occurring during extreme power system events. This will contribute to existing literature on peak demand (Brayshaw et al. (2012), Leah and Foley (2012)) and wind power curtailment (Quest (2013)). Sections 5.7 and 5.8 examine the meteorological conditions associated with the top 10 most extreme events for each metric. The top 25, and top 50 events have also been examined, but show similar results so are not presented in this thesis.

5.1 The meteorological drivers of GB electricity demand

The weather-dependent GB electricity demand (hereafter referred to as demand) is strongly linked to 2m temperature by construction (see section 3.2). The correlation coefficient (r) between annual-mean GB-averaged 2m temperature and annual-mean GB demand is -0.76 (p value (p) = 0.01), however, this correlation changes significantly over

the course of the year. Figure 5.1 shows the monthly breakdown of these correlations. An extremely high correlation coefficient (r varying from -0.96 to -0.98, both with $p <$ 0.05)) is seen between monthly-mean demand and monthly-mean temperature in winter (December, January and February). This correlation remains high at the start of spring (March and April) but is significantly reduced by the end of the season. The correlation in winter and spring is negative due to energy being required for heating (Bessec and Fouquau (2008), Psiloglou et al. (2009)). A large change is seen in the relationship between temperature and demand from May to June, with a transition from heating-induced demand, to cooling-induced demand. Positive correlation is seen between temperature and demand in June, July, August, and September. No significant correlation is seen between autumn-mean temperature and autumn-mean demand (September, October, and November). This can be explained by Figure 5.1 as these months show the transition from cooling-induced demand back to heating induced demand. This transition is slower than the change from heating-induced demand to cooling induced demand seen from May to June.

5.2 The meteorological drivers of GB wind power generation

Figure 5.2 shows the correlation between GB-averaged 10m wind speed and GB aggregate wind power capacity factor at both annual and seasonal timescales. The capacity factors are calculated following the method described in section 3.3 using the wind farm distribution of Cannon et al. (2015), and are insensitive to changes in wind farm distribution (e.g., Drew et al. (2015)).

High correlation is seen throughout the year between monthly-mean 10m wind speed and monthly mean GB aggregate wind power capacity factor (consistent with the wind power capacity factor being calculated using 2m, 10m, and 50m wind speeds). The correlation in winter, spring and autumn is marginally higher than seen in summer (Figure 5.2). The reduced correlation in the transition seasons which was seen between monthly-mean 2m temperature and monthly-mean GB demand is not seen in the correlation between monthly-mean GB-average 10m wind speed and monthly-mean GB aggregate capacity factor.
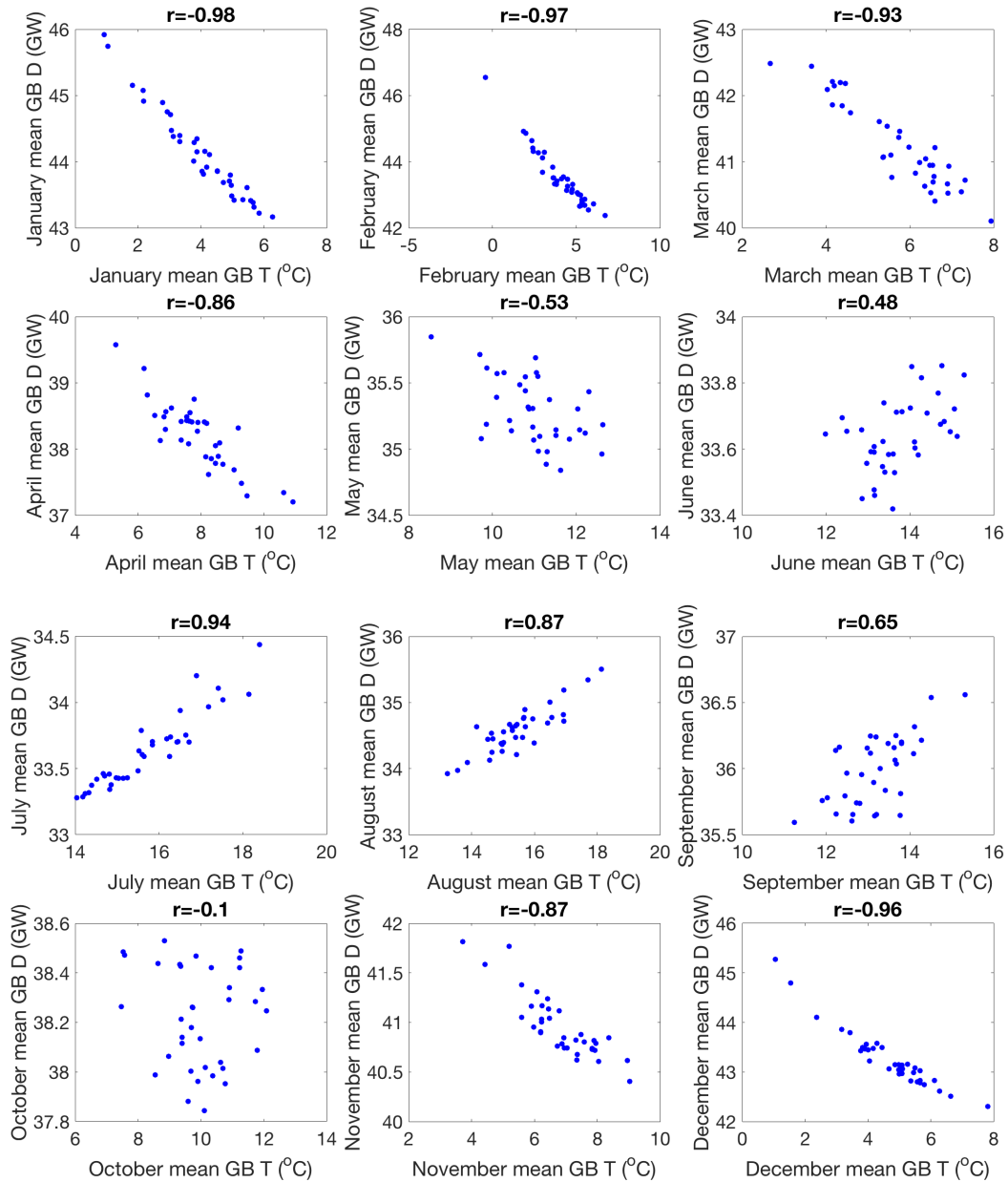
Figure 5.1 Scatter plots of monthly-mean 2m temperature (T) vs monthly-mean GB demand (D) for 1980-2015. Correlation coefficient (r) is given in the titles for each month. All correlations are statistically significant (p value less than 0.05) except for October where p=0.2.

5.3 The relationship between demand and wind power generation

Monthly-mean GB demand also shows strong correlation with monthly-mean GB-averaged 10m wind speed. The correlation coefficient is negative in all months, however only the winter and summer months show significant correlation between monthly-mean wind speed and monthly-mean demand (r ranges from -0.48 to -0.61 from December to February and r=-0.43 in July and August; p values < 0.05). This shows that the

Figure 5.2   Scatter plot of mean 10m wind speed (u) vs mean GB wind power capacity factor (CF) for 1980-2015. annual-mean and seasonal-mean plots are shown. Correlation coefficient (r) is given in the titles for each month All correlations are significant (p value < 0.05).

months which have relatively lower wind speeds have higher demands (reasons for this are discussed in subsequent sections).

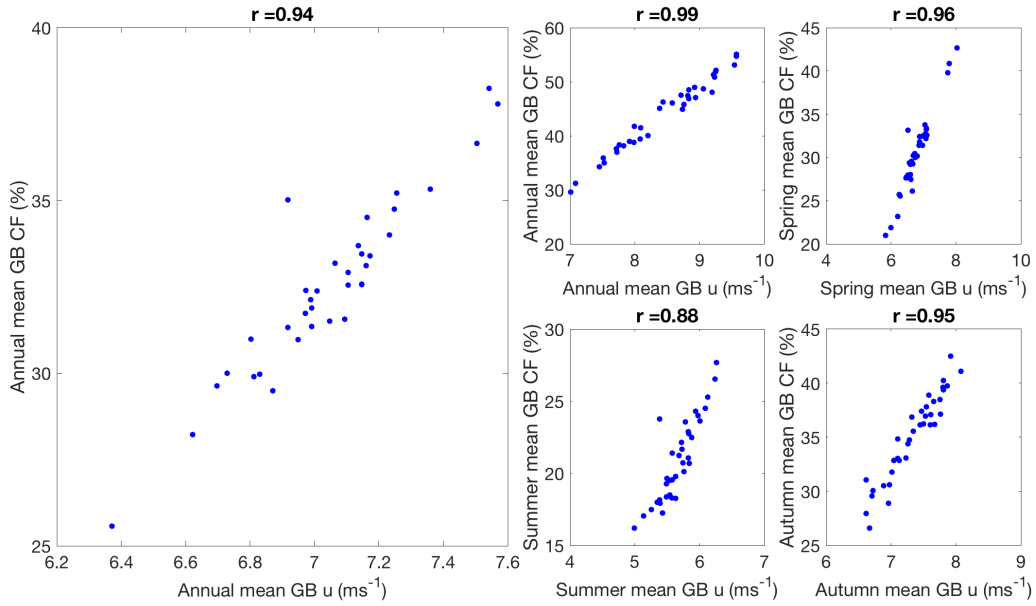Significant correlation is also found between GB aggregate wind power capacity factor and GB mean 2m temperature. Significant positive correlation is seen between monthly-mean 2m temperature and GB aggregate capacity factor from December to February (ranging from r =0.54 to r=0.7; p values < 0.05). This shows that relatively milder winter months tend to have higher capacity factors. Significant negative correlation is seen from June to August (ranging from r=-0.5 to r=-0.56; p values < 0.05), showing that relatively cooler summer months have higher wind power generation. No significant correlation is seen in the transition seasons.

As no wind speed data is used in the construction of the demand data, and no temperature data is used in the construction of the wind power capacity factor data this suggests that the correlation is due to the underlying relationship between temperature and wind speed. This is shown in Figure 5.3a and c for winter and summer respectively (no significant correlation is found in spring and autumn). In months with high wind speeds, warm air masses from the North Atlantic are advected over GB. In winter the temperatures are milder than present over the cold land surface, whereas, in summer the advected temperatures are milder than the warm land surface.

The evidence of the relationship between seasonal-mean temperatures and wind

speeds over GB suggests that there may be a similar relationship present between seasonal-mean demand and seasonal-mean wind power generation. This relationship is shown in Figure 5.3b and e for winter and summer respectively (no significant correlation is found in spring and autumn). Winters experiencing higher seasonal-mean demand (due to colder seasonal-mean temperatures) also experience lower seasonal-mean wind power capacity factors (due to lower seasonal-mean wind speeds). Summers experiencing increased demand (due to warmer seasonal-mean temperatures) also have lower mean capacity factors (due to lower seasonal-mean wind speeds).

Figure 5.3c shows the mean sea-level pressure anomaly between the five years of highest winter-mean temperature, and the five years of lowest winter-mean temperature (a similar pattern is seen for the years of highest - lowest demand, not shown). A dipole in pressure is seen over the Azores/Mediterranean and Iceland/Northern Europe, somewhat resembling the North Atlantic Oscillation (NAO) although with an eastward extension. When GB winter-mean temperatures and GB winter-mean wind speeds are above average, this is associated with a negative pressure anomaly to the north of GB, suggesting more storms are passing over GB (similar to the positive phase of the NAO). This pattern leads to reduced demands and increased wind power generation. The situation is reversed for low GB winter-mean temperatures, suggesting a southward shift of the North Atlantic storm track and the potential for increased atmospheric blocking over Europe. This results in increased demands and reduced wind power generation.

Figure 5.3f shows the mean sea level pressure anomaly between the five years of highest summer-mean 2m temperature and the five years of lowest summer-mean temperature. A positive pressure anomaly is seen over GB. This pattern is indicative of blocking, which would result in high temperatures over GB and low wind speeds (and therefore high demand and low wind power generation).

This section has shown that there is a relationship between seasonal, near surface temperatures and wind speeds over GB, in winter and summer. This results in a relationship between seasonal demand and wind power generation. The large scale mechanism responsible for the relationship is different for both seasons. Winters with anomalously high seasonal-mean demand and low seasonal-mean wind power generation are associated with anomalously weak flow over GB, due to a southward shift of the storm track. Summers with anomalously high seasonal-mean demand and low seasonal-mean wind power generation are associated with an area of high pressure over GB, which is likely the conditions needed for a heatwave.
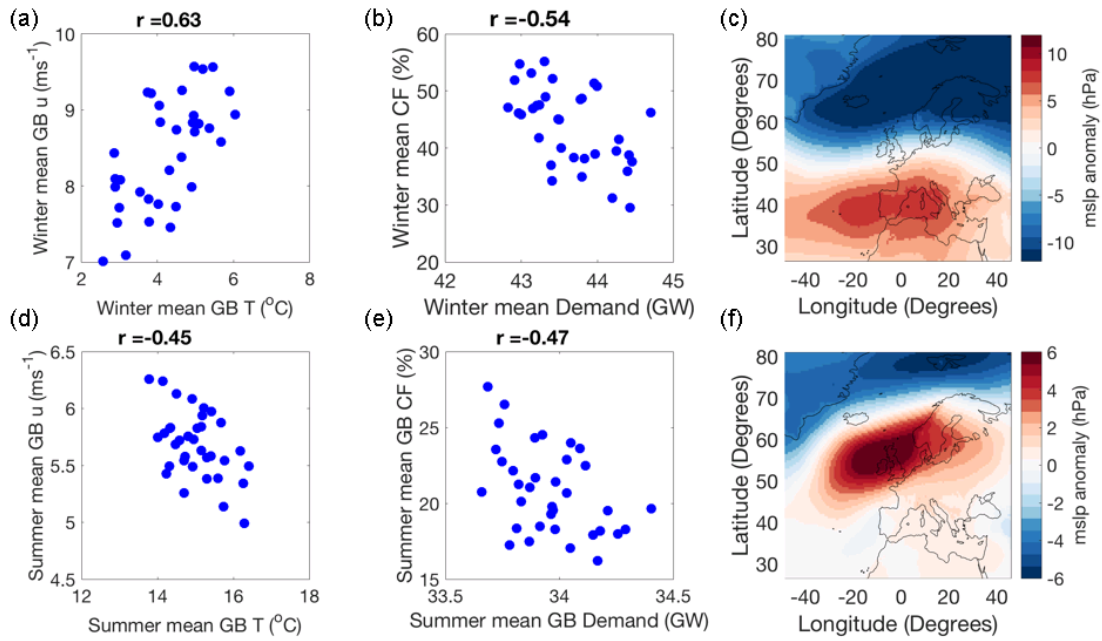
Figure 5.3 Seasonal-mean relationships between (a) winter temperature vs. winter wind speed (b) winter demand and winter capacity factor and, (c) composite sea-level pressure anomalies for the five highest - five lowest years temperature. (d), (e) and (f) as above but for summer-mean. Correlation coefficients (r) are given in the titles for each month. All correlations are statitistically significant (p values < 0.05)

The quantity used for analysis in this thesis is demand-net-wind (DNW; i.e., hourly demand - wind power generation), therefore the seasonal correlation between demand and capacity factor shown in Figure 5.3 could have substantial impacts on the inter-annual variability of power system metrics calculated in the following sections.

5.4 Total Annual Energy Requirement

As discussed in section 3.4.2 Total Annual Energy Requirement (TAER) represents the total amount of conventional power generation required to meet annual power system load. TAER is calculated as an annual sum of a years DNW, which is equivalent to the area under a LDC (see section 3.4.2 for more details). The meteorological drivers of TAER are analysed in the four wind power capacity scenarios given in section 3.3.1, which are NO-WIND, LOW, MED and HIGH (referring to the level of installed wind power capacity). For details of how the correlation maps within this section are created see section 5.0.1.

5.4.1 2m Temperature

Significant negative correlation is seen over GB between annual-mean 2m temperature and TAER for the NO-WIND scenario (Figure 5.4a; r=−0.76). This strong correlation with temperature is consistent with the analysis in section 5.1 as in the NO-WIND scenario TAER is simply the total annual demand. Figure 5.4a shows that for the NO-WIND scenario, when GB TAER is high there are also low temperatures over a large proportion of Europe.

The inclusion of 15GW of installed wind power capacity (i.e., the LOW scenario) leads to a large change in both the magnitude and spatial extent of the correlation between TAER and annual-mean 2m temperature (compare Figure 5.4a and b). In the LOW scenario the correlation between annual-mean 2m temperature and TAER falls to −0.19 over GB (see Figure 5.4b; p=0.05). There is still statistically significant correlation between annual-mean 2m temperature and TAER over the majority of central and northern Europe (p< 0.05), however, the magnitude of the correlation is much weaker than in the NO-WIND scenario.
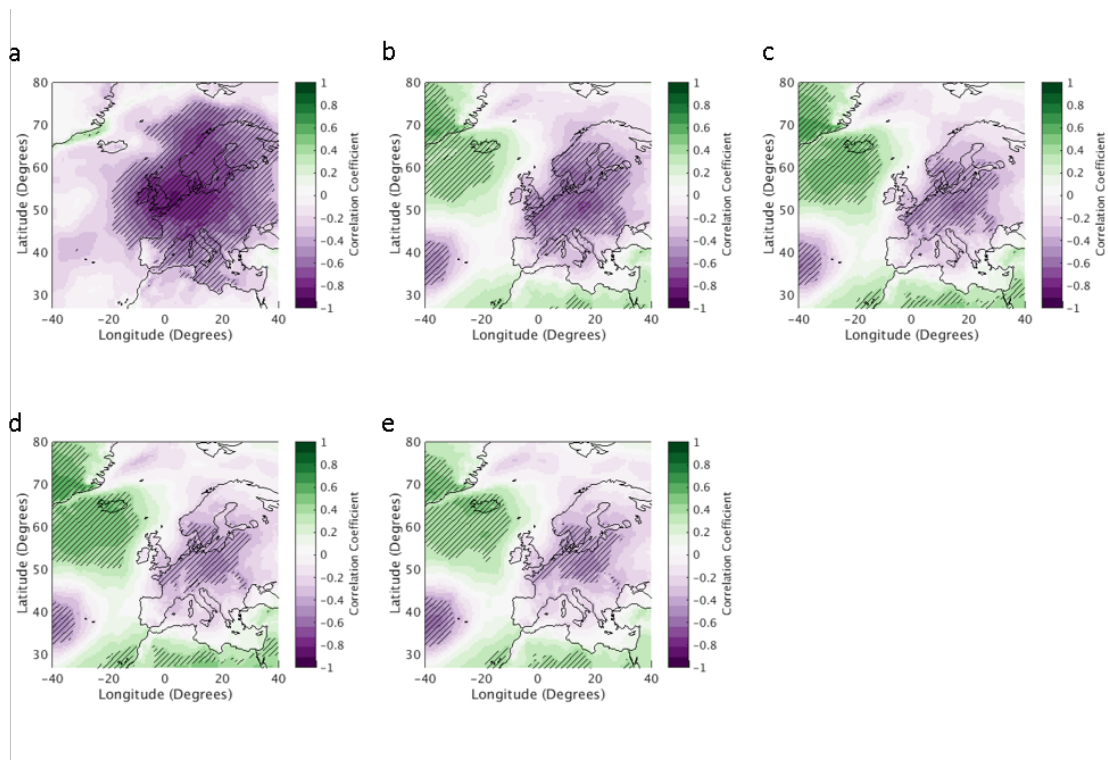

Figure 5.4 Correlation maps between annual-mean 2m temperature and TAER for the (a) NO-WIND (b) LOW (c) MED (d) HIGH and (e) HIGH* scenario, for years 1980-2015. Significant correlation (p-value < 0.05) is hatched.

Increasing the amount of installed wind power capacity (ie. in the MED and HIGH scenarios), results in a further decrease in the correlation between annual-mean 2m tem-

perature and TAER (see Figure 5.4c and 5.4d respectively).

Figure 5.4d and 5.4e show that changing the distribution of wind farms used to provide 45GW of wind power generation from one with mostly onshore generation (the HIGH* scenario) to one with a larger reliance on offshore wind, (the HIGH scenario) does not qualitatively change the pattern of correlation between annual-mean 2m temperature and TAER over GB.

The relationship between TAER and 2m temperature for the NO-WIND scenario is examined seasonally in Figure 5.5 to see if the annual correlations are strongly influenced by the correlations present in particular seasons. Strong negative correlation over central and northern Europe is seen in winter and spring in Figure 5.5a and Figure 5.5b respectively. This is the same as seen in Figure 5.4a for the whole year. Summer (Figure 5.5c) shows no significant correlation over GB.

This shows that in the NO-WIND scenario the correlation between annual-mean 2m temperature and TAER is dominated by the winter and spring temperature response. This is consistent with section 5.1 which showed that the strongest correlation between GB seasonally-averaged temperature and GB seasonally-averaged demand is present during these months. It is interesting that significant correlation is not found between summer-mean temperature and TAER given the positive correlation in section 5.1. This is due to the relationship between winter and spring temperatures and TAER dominating the annual responses.

Figure 5.6 shows seasonal correlation maps for the LOW scenario. The spatial patterns of negative correlation present in winter and spring (Figure 5.6a and 5.6b) are similar to that seen in the NO-WIND scenario, with an area of significant correlation present over central and northern Europe. Summer and Autumn have very low correlation between seasonal-mean 2m temperature and TAER in the LOW scenario. This shows that winter and spring 2m temperatures are still important to describe the behaviour of TAER in a system including 15GW of installed wind power capacity. The spatial pattern of correlation shown in Figure 5.6 is also present in the MED and HIGH scenarios (not shown). A weakening of the negative correlation between average winter 2m temperature and TAER is seen over central and northern Europe as more wind power is included on the system. The reason for the reduction in correlation is discussed in section 5.4.3.

Figure 5.5 Correlation maps of seasonally-averaged 2m temperature and TAER from the NO-WIND scenario for (a) winter (DJF) (b) spring (MAM) (c) summer (JJA) and (d) autumn (SON), for the years 1980-2015. Significant correlation (p-value < 0.05) is hatched.

5.4.2 10m Wind Speed

Figure 5.7 shows correlation maps of annual-mean 10m wind speed and TAER for each of the wind power capacity scenarios. In the NO-WIND scenario, the correlation between TAER and annual-mean 10m wind speed is low and not statistically significant when averaged over the whole of GB (Figure 5.7a).

A change is seen in the magnitude and the spatial extent of the correlation present between annual-mean 10m wind speed and TAER from the NO-WIND to the LOW scenario (compare Figure 5.7a and b). The correlation becomes increasingly negative, to -0.73 over GB (Figure 5.7b). This is consistent with results from section 5.2 which showed that monthly-mean wind power generation is strongly negatively correlated with monthly-mean wind speed throughout the year. The area of strong negative correlation is centred over GB and extends across the whole region from $50N - 60$N and $-40E - 40$E
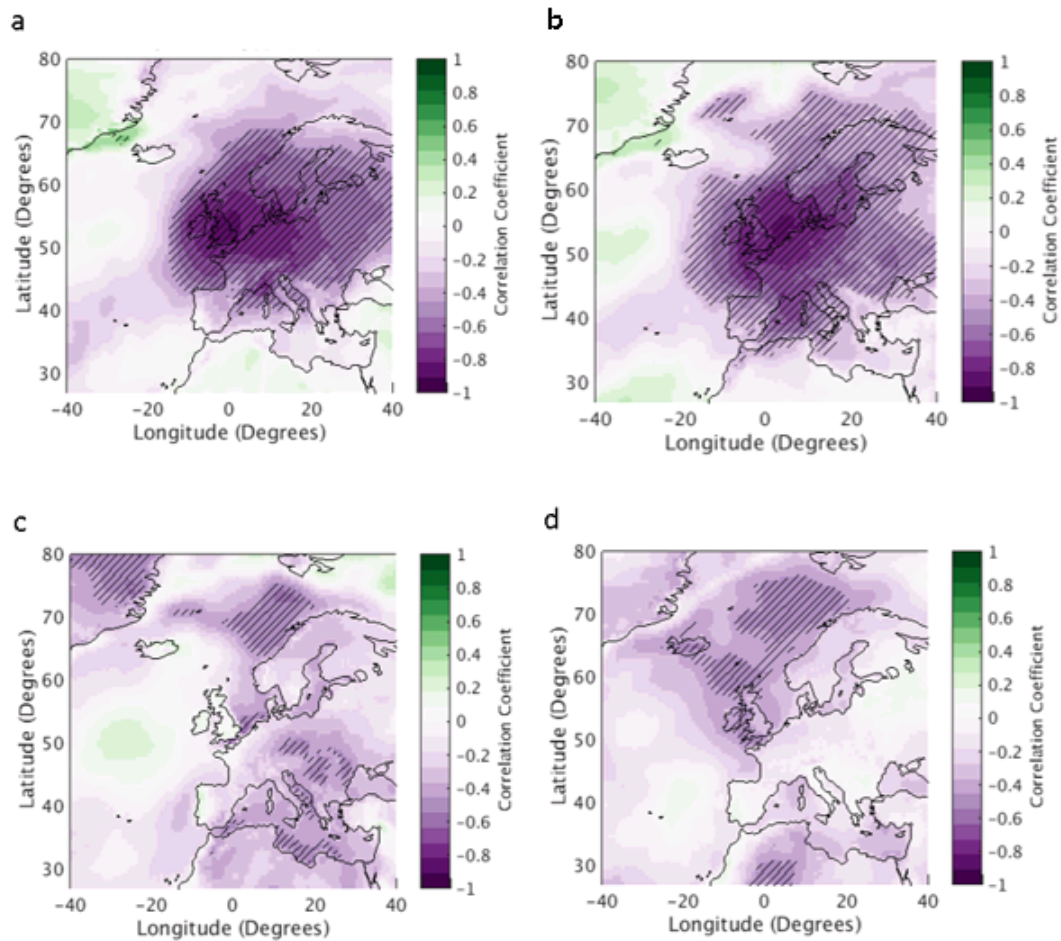
Figure 5.6 Correlation of seasonally-averaged 2m temperature and TAER from the LOW scenario,for (a) winter (DJF) (b) spring (MAM) (c) summer (JJA) and (d) autumn (SON), for the years 1980-2015. Significant correlation (p-value < 0.05) is hatched.

(Figure 5.7b). This suggests that years with high TAER, have low 10m wind speeds over GB, but high 10m wind speeds over southern Europe and the Mediterranean.

As the amount of wind power capacity installed on the system is increased (i.e., the MED and HIGH scenarios) changes in the correlation maps are small compared to the change seen between the NO-WIND and LOW scenario. The strength of the correlation between annual-mean 10m wind speed and TAER is moderately increased as increasing amounts of wind power are installed on the system, but the structural pattern of the correlation remains the same. Changes in wind farm distribution from the HIGH to HIGH* scenario, do not qualitatively effect the correlation between annual-mean 10m wind speed and TAER (Figure 5.7d and 5.7e respectively).

A seasonal breakdown of the relationship between annual-mean 10m wind speed and TAER is shown in Figure 5.8 for the NO-WIND scenario and Figure 5.9 for the LOW
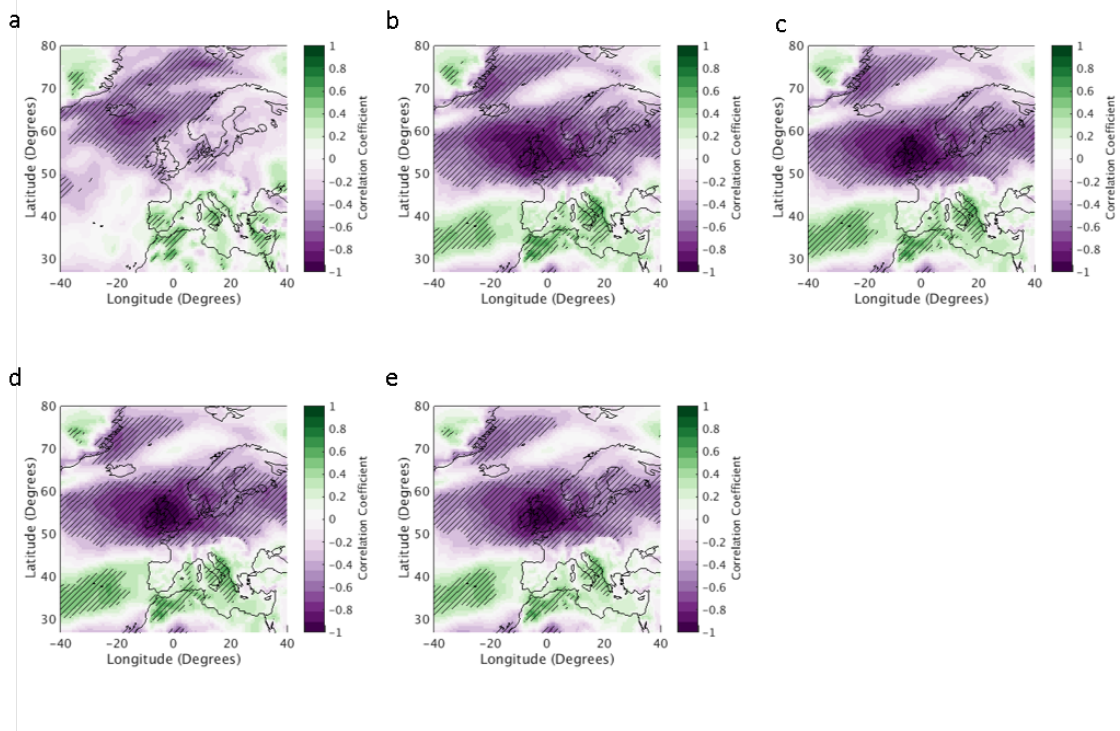
Figure 5.7 Correlation between annual-mean 10m wind speed and TAER for the (a) NO-WIND (b) LOW (c) MED (d) HIGH* and (e) HIGH scenario, for years 1980-2015. Significant correlation (p-value < 0.05) is hatched.

scenario (results for the MED and HIGH scenario are qualitatively similar to that found in the LOW scenario, and are not shown). Significant negative correlation is seen in the NO-WIND scenario between winter-mean 10m wind speed and TAER, (r=−0.46; Figure 5.8a) and spring-mean wind speed and TAER (r=-0.38; Figure 5.8b). This correlation must however, be due to meteorological correlations between wind and temperature discussed in section 5.3, as there is no direct effect of wind power on the system.

Seasonal correlation maps between average 10m wind speed and TAER are plotted in Figure 5.9 for the LOW scenario. The correlation between winter-mean wind speed and TAER is increased over GB (r=-0.71) compared to the NO-WIND scenario. The strength of the correlation between spring-mean wind speed and TAER is also increased (r=-0.45). Including wind power generation does not change the seasonal relationships between summer and autumn wind speeds and TAER, with low correlation still seen in both seasons.

5.4.3 Temperature driven vs wind speed driven power system

A comparison of Figures 5.4 to 5.9 shows that in the NO-WIND scenario the inter-annual variability of TAER can be predominantly explained by the inter-annual variability
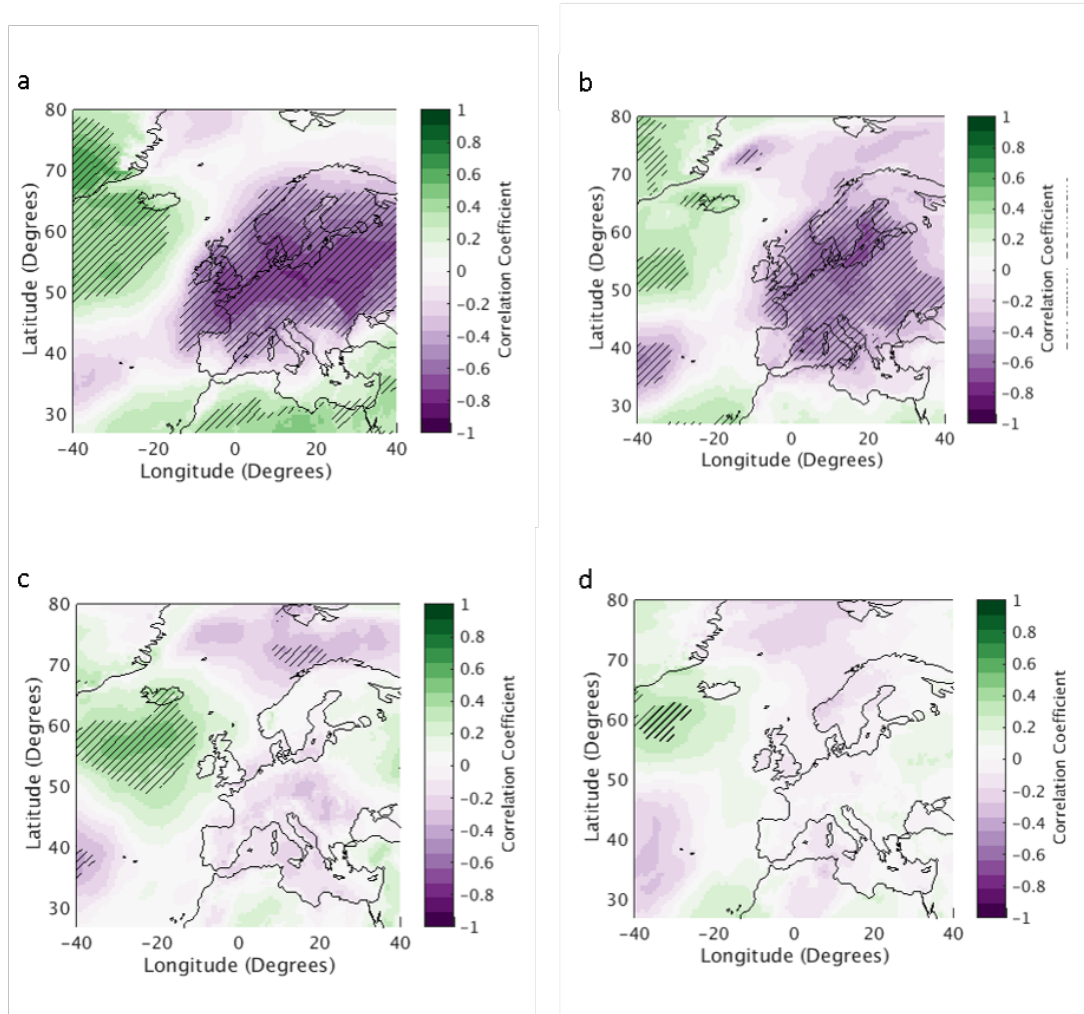
Figure 5.8 Correlation of seasonally-averaged 10m wind speed and TAER for the NO-WIND scenario (a) winter (DJF) (b) spring (MAM) (c) summer (JJA) and (d) autumn (SON), for years 1980-2015. Significant correlation (p-value < 0.05) is hatched.

of winter 2m temperatures, whereas in the LOW scenario the inter-annual variability of TAER is closely linked to both the inter-annual variability of winter-mean 2m temperatures and the inter-annual variability of winter-mean (and to some extent spring-mean) 10m wind speeds. This suggests that there is a relatively modest level of installed wind power capacity between these two scenarios (i.e., a lower wind power capacity than that currently installed) where the dominant meteorological driver of the inter-annual variability of TAER changed from being 2m temperature to 10m wind speed.

Figure 5.10 shows the correlation coefficients averaged over GB for both annual-mean 2m temperature and TAER and annual-mean 10m wind speed and TAER plotted against varying levels of installed wind power capacity from 0 to 45GW. Once 6GW of wind power capacity is installed the correlation between annual-mean 2m temperature and TAER drops below that of annual-mean 10m wind speed and TAER. This shows the point at which the dominant meteorological driver of the GB power system is changed.

Figure 5.10 shows that once ∼20GW of wind power is installed on the system then
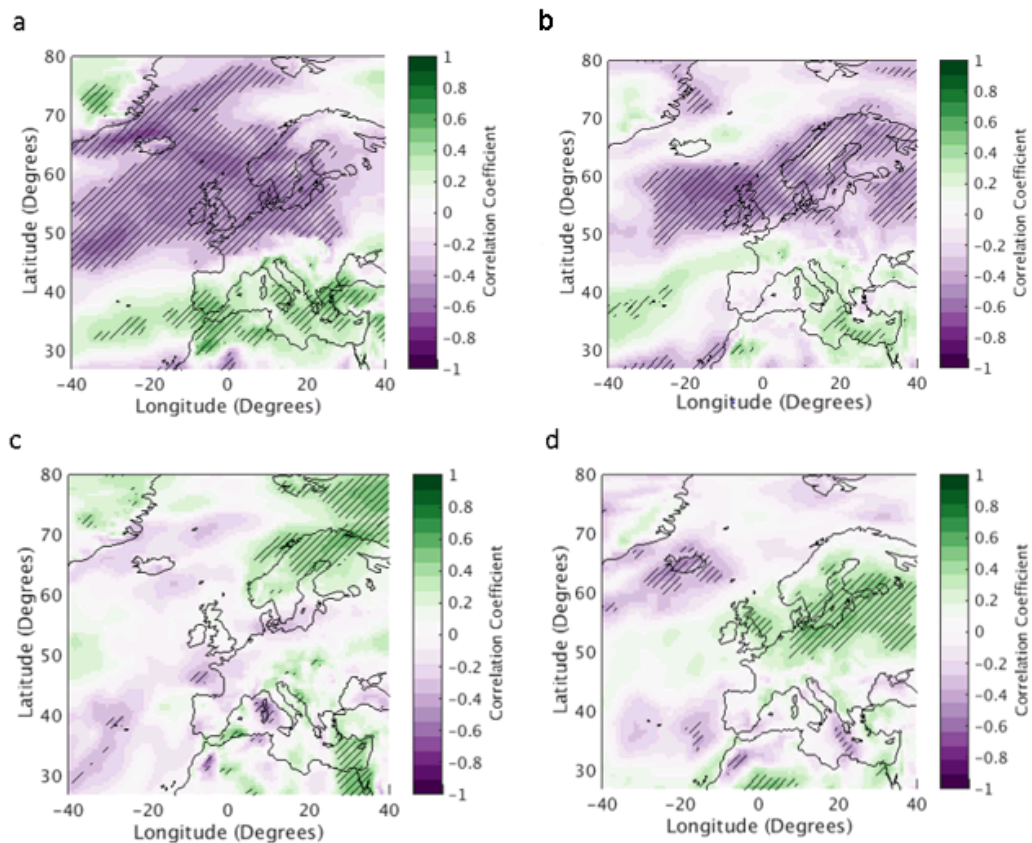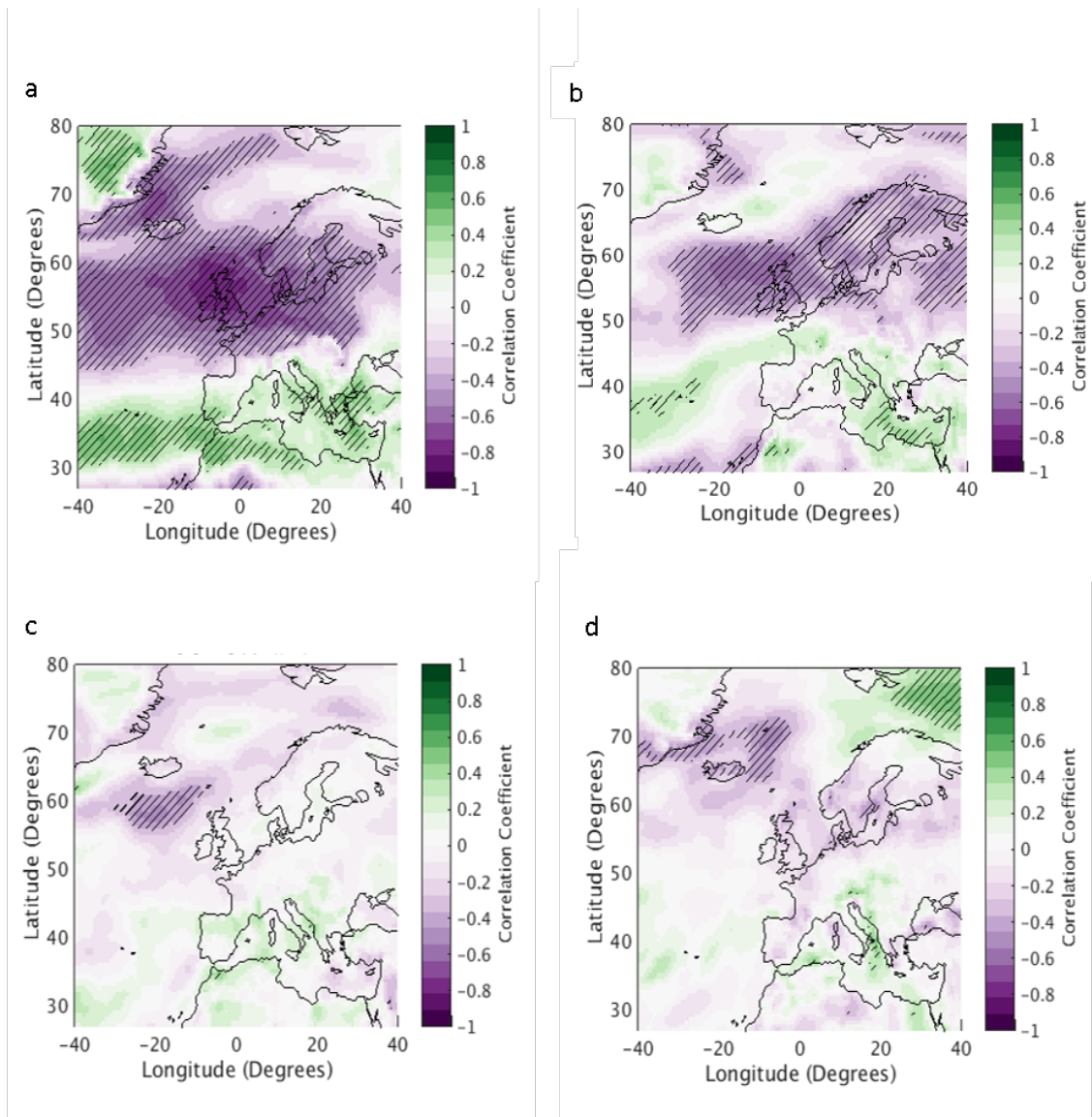
Figure 5.9   Correlation of seasonally-averaged 10m wind speed and TAER from the LOW scenario, for (a) winter (DJF) (b) spring (MAM) (c) summer (JJA) and (d) autumn (SON), for years 1980-2015. Significant correlation (p-value < 0.05) is hatched.

there are only very moderate changes in the correlation between annual-mean 10m wind speed and TAER over GB. This shows that installing more wind power capacity won't significantly change the main meteorological drivers of power system behaviour, however, the relative sensitivity to temperature continues to reduce.

5.4.4   Large scale drivers of TAER variability

TAER has been shown to correlate highly with annual-mean 2m temperatures in the NO-WIND scenario and annual-mean 10m wind speed in the LOW scenario, with the majority of this sensitivity resulting from winter. This section investigates the meteorological drivers of the inter-annual near-surface temperature and wind speed variability
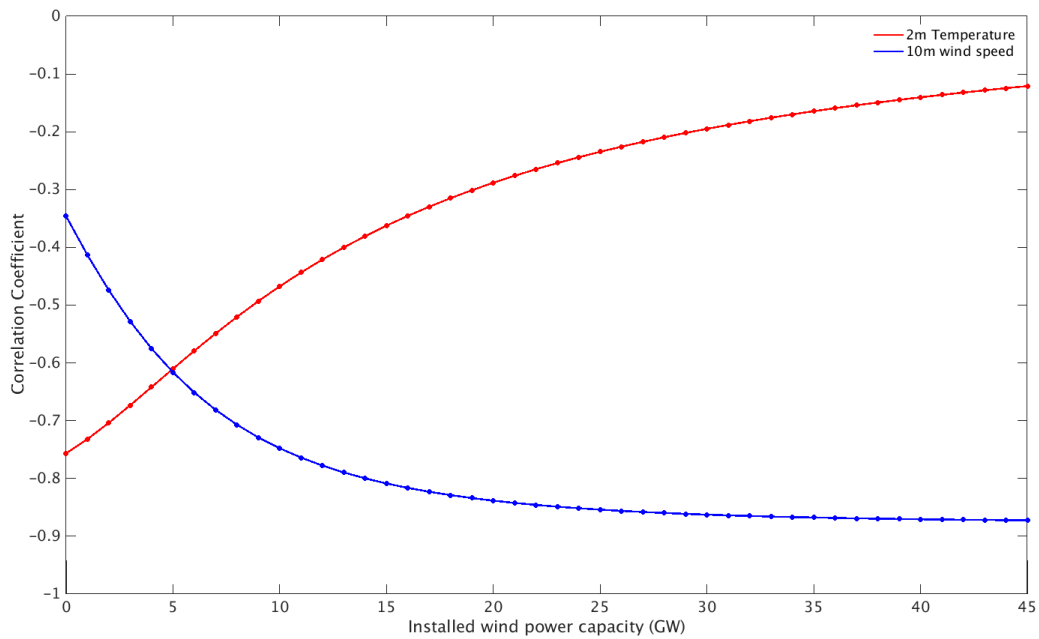
Figure 5.10 Correlation between annual-mean 2m temperature and TAER (red) and annual-mean 10m wind speed and TAER (blue) with varying levels of installed wind power generation from 0GW-45GW. Note the negative y-axis. Correlations between 10m wind speed and TAER are statistically significant at all levels of installed wind power generation ($p< 0.05$) However correlations between 2m temperature and TAER are only significant until 20GW of wind power generation are installed.

influencing TAER, for varying levels of installed wind power generation.

To gain a broad understanding of potential large-scale drivers of the inter-annual variability of TAER annual mean sea-level pressure anomalies have been plotted for the NO-WIND and LOW scenarios (Figure 5.11). Years of high TAER in the NO-WIND scenario are associated with high pressure over Iceland and the Norwegian sea. This is again seen for the years of TAER in the LOW scenario, but the associated mean sea-level pressure anomalies are larger. This dipole in pressure is similar to the structure seen between the years of highest - lowest winter-mean temperature in Figure 5.3, a similar dipole structure is seen if the years of highest - lowest winter-mean wind speed, winter-mean demand or winter-mean wind power generation are plotted, with much weaker dipole structures in other seasons (not shown). This shows that winter weather dominates the annual picture of the TAER mean sea-level pressure anomalies.

The areas of largest mean sea-level pressure anomaly in Figure 5.11 align well with the centres of action of the NAO. The phase of the NAO is associated with changes in the intensity and location of the North Atlantic jet stream and storm track (Woollings et al. (2010)). Changes in these phenomena would cause changes to the near surface
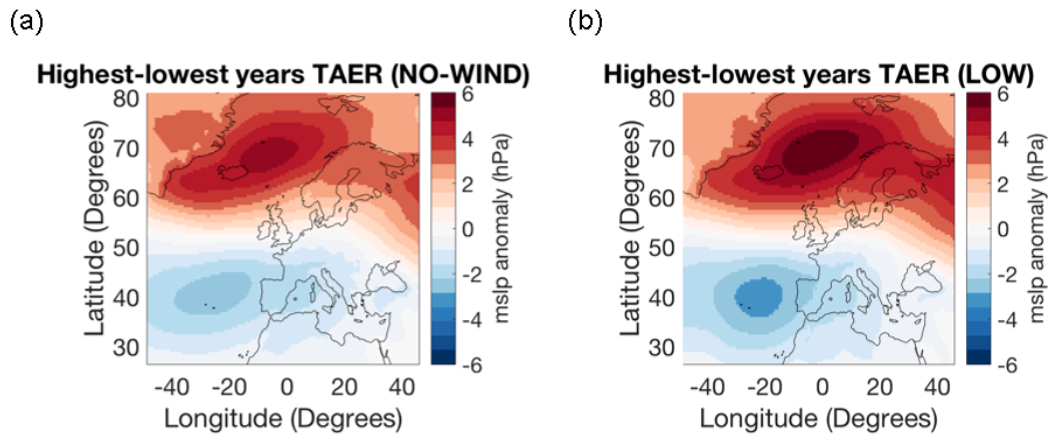
Figure 5.11 Annual mean sea-level pressure (mslp) anomaly plots for the five highest - five lowest years of (a) TAER for the NO-WIND scenario (b) TAER for the LOW scenario.

temperatures and wind speeds over GB, and therefore changes to demand and wind power generation. This is investigated further in the following section

5.4.4.1 The North Atlantic Oscillation

A station-based, daily NAO index has been calculated from the MERRA data, by calculating the normalised mean sea-level pressure difference between Lisbon and Reykjavik as in Hurrell et al. (2003) (the closest grid boxes from MERRA to each city are chosen). Figure 5.12 shows the correlation between various annual-mean indices and the NAO index. The values of the NAO index may be sensitive to the chosen method. However, in this section the focus of the analysis is on the ability of an index that conflates the impacts of temperature and wind speed to significantly correlate with GB power system metrics.

Significant correlation is seen between GB annual-mean 2m temperature, annual-mean demand, TAER (NO-WIND) and the annual-mean NAO index (Figure 5.12a-c). This shows that in a power system with no wind power generation the annual-mean NAO index is able to provide an indication of the TAER experienced by the system. The correlation between winter-mean temperature and winter-mean NAO index is 0.69, with a correlation between GB winter-mean demand and winter-mean NAO index of -0.64. These correlations are higher than those seen through the whole year in Figure 5.12 due to this being the time of year where demand is most sensitive to temperature. The correlation between TAER (NO-WIND) and winter-mean NAO index is -0.33. This is lower than seen in Figure 5.12 due to TAER including data-points from the whole year
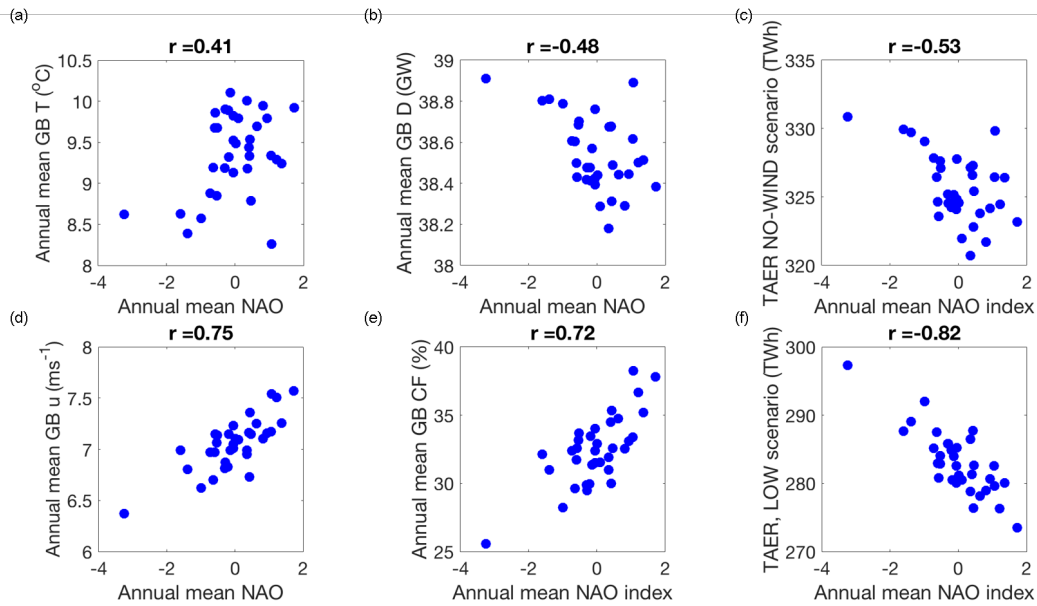
Figure 5.12 Correlation coefficient (r) between the NAO-index and (a) annual-mean 2m temperature (b) annual-mean demand (c) annual mean TAER (NO-WIND scenario) (d) annual-mean 10m wind speed (e) annual-mean GB aggregate capacity factor (f) annual-mean TAER (LOW scenario). All correlations are significant (p-value < 0.05)

and it has previously been noted that the dominant driver of 2m temperature and 10m wind speeds in summer is different to the NAO-like pattern seen in winter (i.e., associated with an area of high pressure; see Figure 5.3f)

The correlation between annual-mean wind speed and annual-mean NAO index is 0.75, with similarly high correlation seen between annual-mean GB aggregated wind power capacity factor, TAER (for the LOW scenario), and annual-mean NAO index. These correlations are stronger than those seen between annual-mean temperature and annual-mean NAO index (compare Figure 5.12d-f to Figure 5.12a-c). The correlation coefficient of -0.82 between TAER for the LOW scenario and annual-mean NAO index shows that the NAO index is a good indicator of the TAER experienced by a power system including 15GW of installed wind power capacity. Comparing Figure 5.12c to Figure 5.12f shows that as the amount of wind power generation installed on the system is increased the effect of the NAO as a predictor of TAER gets stronger.

Although the NAO index is able to give an indication of years of high or low TAER it is not able to separate out the temperature-dependence or wind-speed dependence of the power system. (e.g. Figure 5.3 showed that the years of most extreme seasonal-mean temperature are not always the years of most extreme seasonal mean wind speed.) It is common practise to correlate the NAO with power system metrics in the literature (Brayshaw et al. (2011b), Ely et al. (2013), Curtis et al. (2016)) however, this analysis has

suggested seasonal-mean, near surface temperatures/wind speeds may be able to provide more useful information on power system operation.

The NAO has previously shown to be related to the location and strength of the eddy-driven jet (Woollings et al. (2010)). Therefore, in the following section the relationship between TAER and the Eddy-driven jet is investigated.

5.4.4.2 The Eddy-driven Jet

This sections investigates if there is a relationship between GB 2m temperatures,10m wind speeds and the eddy-driven jet, and if this relationship impacts the inter-annual variability of TAER. Figure 5.7 showed that in the LOW scenario there was a dipole structure over Europe when the annual-mean 10m wind speed is correlated with TAER. This suggests that the behaviour of TAER in the LOW scenario may be related to the location of the eddy-driven jet. This is further suggested by the dipole structure being present in the correlation plots between annual-mean 850hPa wind speeds and TAER for the LOW scenario (r=-0.48 over GB, not shown) and for the correlation between annual-mean 250hPa wind speeds and TAER (r=-0.61 over GB, not shown) for the LOW scenario. The dipole structure is strongest in winter at all heights in the troposphere.

To investigate the relationship between the eddy-driven jet and the GB power system daily eddy-driven-jet latitude index is calculated from MERRA following the method of Woollings et al. (2010). The 850hPa zonal wind component is longitudinally averaged in the region from 0-60W. The resulting field is then 10-day low pass filtered in order to remove the effect of synoptic events. The jet latitude is then calculated for each day for the winters from 1980-2015. The jet latitude is defined as the latitude at which the maximum daily zonal wind speed is reached in the region of 15N-75N.

The eddy-driven jet latitude exhibits a tri-modal structure, with peaks at 35N, 45N and 50N associated with a southern jet, central jet and northern jet respectively (Woollings et al. (2010)). When the eddy-driven jet is in the southern location (35N) GB would experience conditions similar to the negative phase of the NAO, with low near-surface wind speeds and a higher potential for blocking to be present over GB. The central and northern jet stream locations closely resemble the positive and negative phase of the East Atlantic (EA) pattern respectively (see Figure 2.7). The central location (and positive phase of the EA pattern) is associated with above average near-surface temperatures over Europe. Conversely when the eddy-driven jet is in the northern location (and negative phase of the EA pattern) then Europe experiences below average temperatures.

Figure 5.13a shows the daily eddy-driven-jet latitude index plotted for the six winters with lowest seasonal-mean temperature and highest seasonal-mean temperature. The red and blue shading highlight the locations of the southern and northern jet, which are co-located with the latitude bands of highest correlation when the annual-mean 10m wind speed is correlated with TAER (Figure 5.7). The location of the eddy-driven jet is different between the highest and lowest winter-mean temperature years. In the years with lower mean temperature the eddy-driven jet is predominantly located in the southern and central locations. In the years of highest mean temperature the eddy-driven jet is predominantly in the central location (Figure 5.13a).

Similar behaviour is seen for the winters of highest and lowest demand. In the years of lowest demand (therefore highest temperatures) the eddy-driven jet is mostly located in the central and northern positions, whereas the years of highest demand (therefore lowest temperatures) see the eddy-driven-jet located over central and southern Europe (Figure 5.13b).

Figure 5.13c shows that this relationship is also seen for TAER in the NO-WIND scenario. This result is in agreement with the relationship between TAER in the NO-WIND scenario and annual-mean NAO index in section 5.4.4.1. The years of highest TAER spend more days in the southern jet location (associated with a negative phase of the NAO) than the years of low TAER.

Figures 5.13d and e show that during winters with the highest GB mean 10m wind speeds (and therefore highest mean wind power generation) the eddy-driven jet is predominantly in the central or northern locations. In the LOW scenario TAER is both temperature dependent and wind speed dependent (see section 5.4.3. Therefore years of lowest TAER require above average wind speeds and above average temperatures (resulting in reduced demands). Figure 5.13f shows that in the LOW scenario years of lowest TAER the eddy-driven jet is located in the central and northern locations. This is consistent with more cyclonic weather systems passing over GB and can provide the increased wind speeds needed for high wind power generation, and reduced TAER. When the jet is located in the central location GB experiences above average temperatures (therefore below average demands). The relationship between eddy-driven jet location and TAER is very similar to that seen in Figure 5.13d-f for the MED and HIGH scenarios (not shown).

The results found in this section are consistent with those found in section 5.4.4.1, years with high TAER spend have more days where the jet stream is located in the southern location (which is associated with the negative phase of the NAO). The eddy-
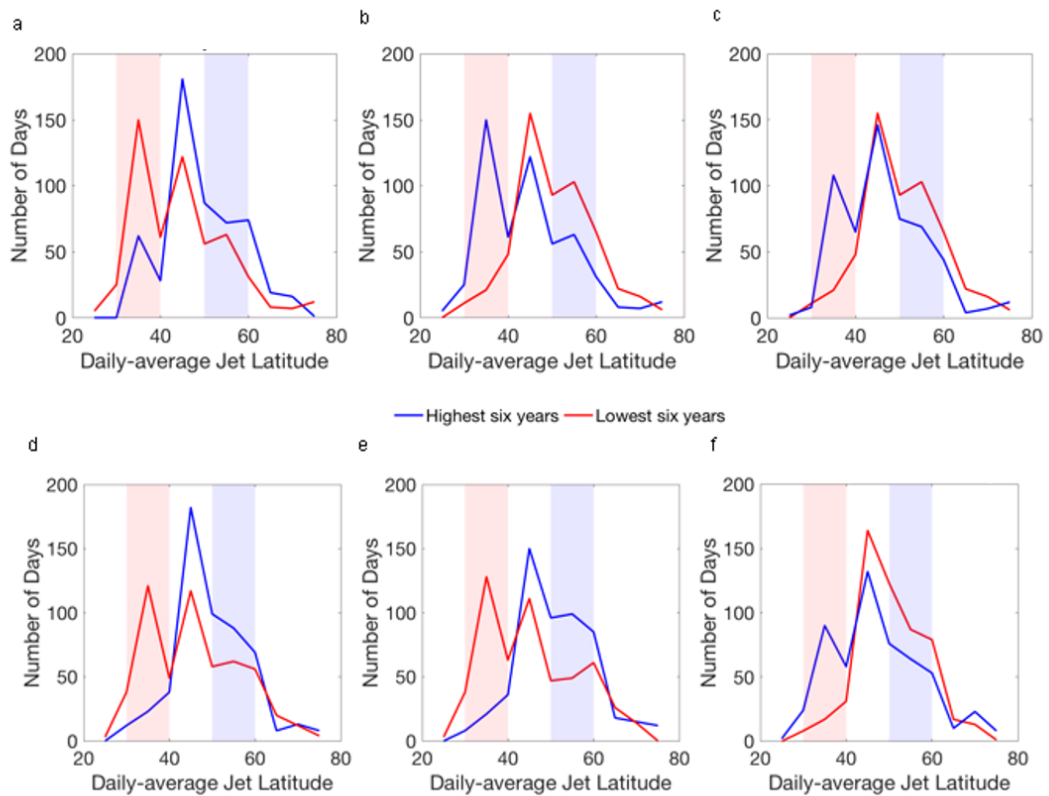
Figure 5.13 Daily eddy-driven-jet latitude for the 6 highest and 6 lowest winters of (a) winter-mean 2m temperature (b) winter-mean demand (c) TAER (NO-WIND scenario) (d) winter-mean 10m wind speed (e) winter-mean GB aggregate capacity factor (f) TAER (LOW scenario). Shaded areas indicate the areas of maximum correlation between 10m wind speed and TAER in Figure 5.7

driven jet location is extremely variable throughout the winters, therefore the relationships are not as well defined as seen in section 5.4.4.1. Once again it is hard to tell if the differences between histograms of eddy-driven jet latitude for high and low TAER years are due to anomalous GB temperatures or wind speeds. This further highlights the value of using simple metrics (i.e., the correlation between 2m temperatures or 10m wind speeds and TAER) to provide justifications of exactly why a given year had high/low TAER.

5.4.5 Summary

In a power system with no installed wind power capacity (NO-WIND scenario) TAER correlates highly with annual-mean 2m temperature, with highest correlation seen in winter and spring. As the amount of installed wind power capacity is increased to 15GW (LOW scenario) the strength of the correlation between TAER and annual-mean 2m temperature is reduced, with increased correlation present between TAER and annual-mean 10 wind speed (again with the majority of this correlation present in winter and spring). A

transition from a temperature dependent power system to a wind speed dependent power system was found at 6GW. As the amount of installed wind power capacity is increased to 45 GW (HIGH scenario) minimal changes are seen in the correlation between annual-mean 10m wind speed and TAER, suggesting the meteorological driver of inter-annual TAER variability is unchanged.

The NAO index has been shown to correlate highly with TAER, with increasing predictive power as the amount of installed wind power capacity is increased. A relationship between TAER and the location of the eddy-driven jet has also been found, with years where the jet is predominantly in its southern location (associated with negative NAO index) having increased TAER due to below average temperatures and below average wind speeds being present over GB.

5.5   Baseload Plant

The focus of this section is the generation opportunity for baseload type power plant, i.e., the total volume of energy (TVE) for which baseload-type generators are economically efficient (see Section 3.4.2 for full discussion). Before examining the meteorological drivers of baseload TVE, the impact of diurnal and annual cycles on baseload TVE is shown for each wind power scenario. As baseload operates for large percentages of a year, it is convenient to consider the hours for which baseload generation is most economically marginal (i.e., the hours corresponding to the lowest 9% of residual load or, equivalently, the 91-100% duration range on a LDC). Figure 5.14 shows the timing and distribution and characteristics of these hours.

Figure 5.14a shows that the marginal baseload hours occur from 0:00-07:00 in the NO-WIND scenario, consistent with the minimum of the diurnal cycle of demand (see Figure 3.2). The period in which baseload plant is marginal is from May to October in the NO-WIND scenario (Figure 5.14b). This is the lower half of the annual cycle of demand, and the warmest half of the year. The theoretical wind power capacity factor at times when baseload plant is marginal is positively skewed, with predominantly low potential for wind power generation (note this is the NO-WIND scenario, so this is a theoretical rather than operational capacity factor; Figure 5.14c).

The range of times when baseload plant is marginal increases when 15GW of wind power capacity is installed on the system (i.e., the LOW scenario). The hours of the day when baseload is not required extends to include a wider range of low demand (22:00-
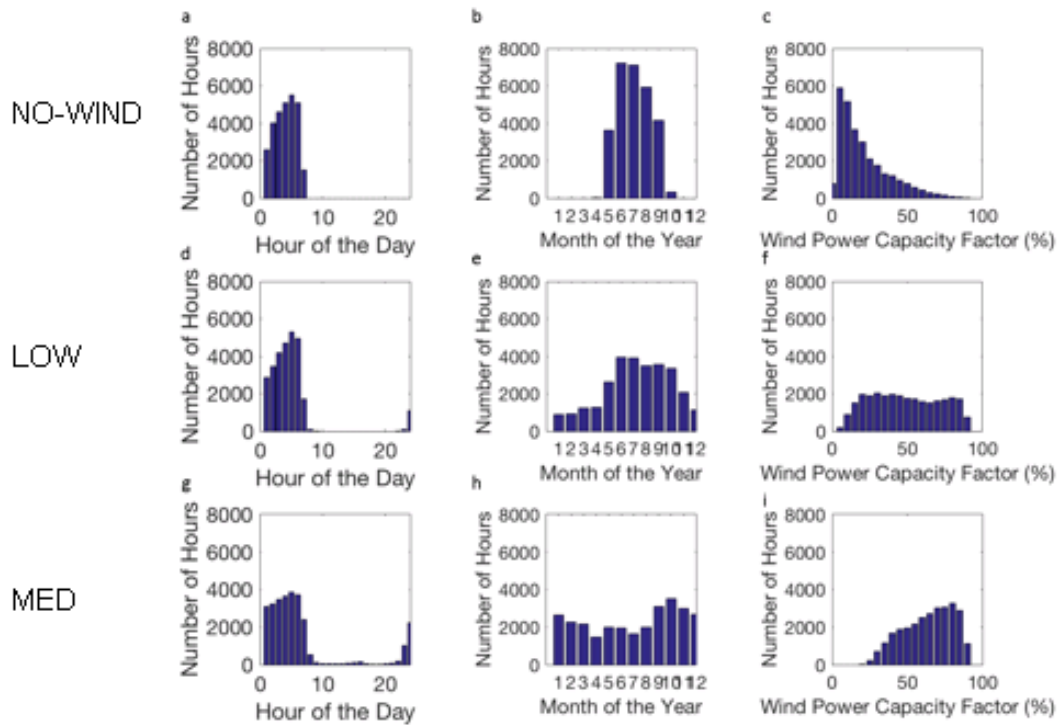
Figure 5.14 Hours where not all installed baseload plant is able to operate (i.e., hours from 91-100% of all LDCs from 1980-2015) for the NO-WIND scenario (top), the LOW scenario (middle) and the MED scenario (bottom) for. (a,d,g) the hour of the day (b,e,h) the month of the year, (c,f,i) wind power capacity factor.

07:00, Figure 5.14d.) There are times when baseload plant is marginal in all months of the year in the LOW scenario (Figure 5.14e). These changes are due to DNW becoming more variable once wind power capacity is installed on the system.

A broader range of wind power capacity factors are present in the LOW scenario than seen during the NO-WIND scenario for times when baseload plant is marginal (compare Figure 5.14f with Figure 5.14c). It becomes increasingly common for it to be windy during times when baseload plant is marginal. Installing further wind power capacity on the system in the MED scenario results in baseload plant becoming marginal in all hours of the day (Figure 5.14c), although it is still much more frequent for baseload plant to not be required at night. There are significantly more hours when baseload plant is marginal in winter in the MED scenario, with it being common for baseload plant to be marginal in all months of the year (Figure 5.14g). There is a negative skew to the distribution of capacity factors experienced when baseload plant is not required in the MED scenario (Figure 5.14h i.e., baseload plant tends to be restricted on windy days). Similar results to this are seen in the HIGH scenario (not shown). The meteorological conditions present during times when baseload plant is marginal are further investigated below.

5.5.1 2m Temperature

It was not possible to detect significant correlation between annual-mean 2m temperature and baseload TVE in the NO-WIND scenario. This is due to a cancellation of seasonal correlations (see Figure 5.15 which shows correlation maps between seasonal-mean temperature and baseload TVE). High correlation is seen between summer-mean GB temperature and baseload TVE due to these being the months when baseload plant is most often marginal (Figure 5.14b). Significant negative correlation is seen over GB in spring. These correlations are opposite sign due to the changing relationship between temperature and demand throughout the year. In years of higher summer temperature (and therefore higher summer demand; see Figure 5.1) there is a higher value of baseload TVE. This can be interpreted as fewer hours where baseload plant is marginal in summer. In spring, years with lower annual-mean temperature have higher baseload plant TVE, due to the negative relationship between temperature and demand in spring.
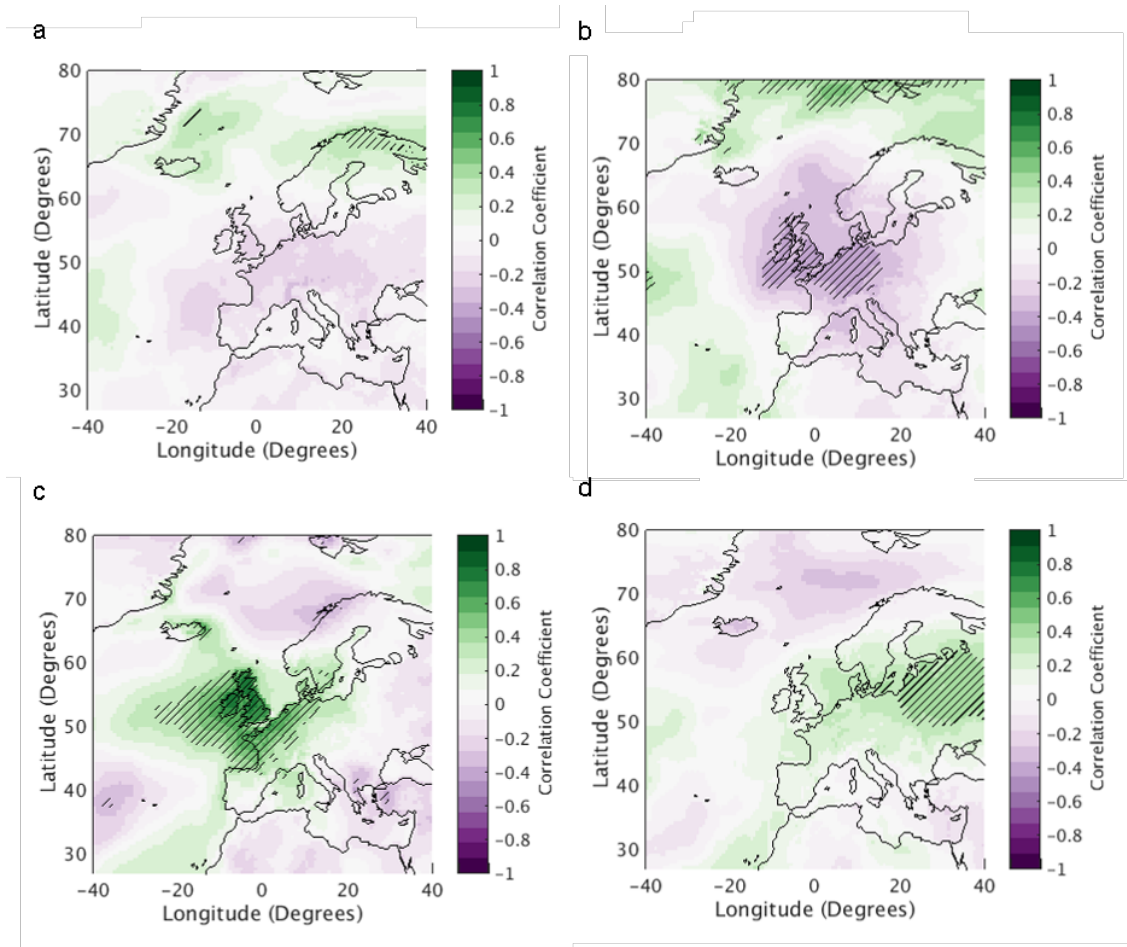

Figure 5.15 Correlation between seasonal-mean 2m temperature and baseload TVE from the NO-WIND scenario (a) winter (DJF) (b) spring (MAM) (c) summer (JJA) (d) autumn (SON), for years 1980-2015. Significant correlation (p-value < 0.05) is hatched.

Figure 5.16 shows the correlation maps between seasonal-average 2m temperatures and baseload TVE for the LOW scenario. Significant negative correlation is seen between winter-mean 2m temperatures and baseload TVE (Figure 5.16a). The winter-mean seasonal correlation maps look similar to those observed for TAER (Figure 5.6), although, the magnitude of the negative correlation is weaker. Comparing Figure 5.15 and Figure 5.16 shows that from the NO-WIND to the LOW scenario there is a change in the strongest correlations, from a positive relationship between summer-mean 2m temperatures and baseload TVE in the NO-WIND scenario to a negative relationship between winter-mean temperatures and baseload TVE in the LOW scenario. This is due to the u-shaped relationship between temperature and demand (see Figure 5.1 and section 2.1 for details). The correlation is present in winter due to it being possible for baseload plant to be marginal in the LOW scenario, when wind power generation is high. The reduced significance of the correlation between summer-mean 2m temperature and baseload TVE is due to the hours when baseload in marginal being changed from low demand (in the NO-WIND scenario) to low demand and high wind power generation (see Figure 5.14).

Correlation maps between seasonal-average 2m temperature and baseload TVE for the MED and HIGH scenarios show the strength of the negative correlation during winter is increased (not shown). This is due to an increasing number of hours being present where the residual load (i.e., the DNW) drops very low due to high wind power generation. This therefore means that the temperature effect on demand (i.e., warm winter days having lower demands) becomes increasingly important for the baseload TVE metric (see Figure 5.14h).

5.5.2   10m Wind Speed

It was not possible to detect statistically significant correlation between annual-mean or seasonal-mean 10m wind speed and baseload plant TVE over GB in the NO-WIND scenario (Figure 5.17a). This suggests that the number of hours in which baseload plant is marginal is insensitive to 10m wind speeds when no wind power capacity is installed.

As an increasing amount of wind power capacity is installed on the system, significant and increasingly strong correlation is found over GB between annual-average 10m wind speed and baseload TVE (Figure 5.17b and c). The spatial pattern of correlation present in power systems including installed wind power capacity is similar to Figure 5.7 for the correlation between annual-mean 10m wind speed and TAER, with a dipole structure present between northern and southern Europe.
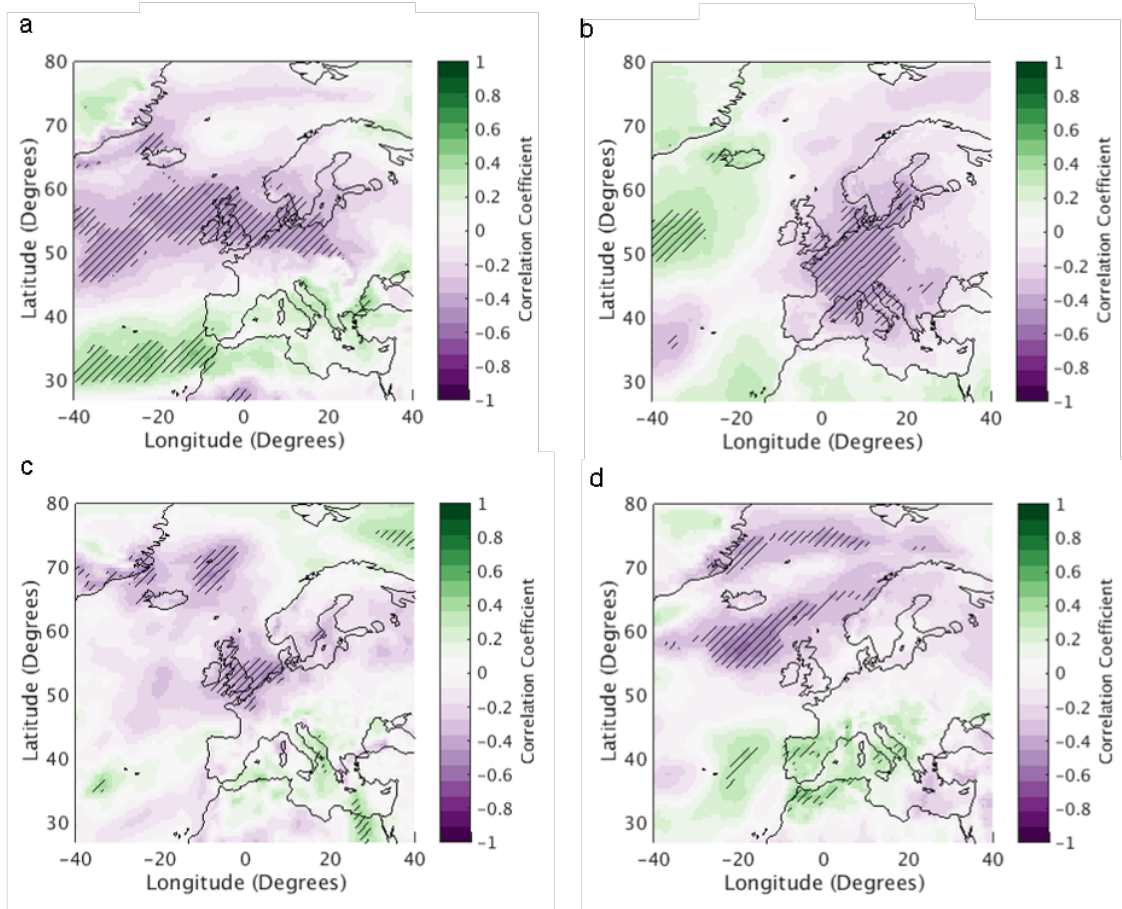
Figure 5.16 Correlation of seasonally-averaged 2m temperature and baseload TVE from the LOW scenario, for (a) winter (DJF) (b) spring (MAM) (c) summer (JJA) and (d) autumn (SON), for years 1980-2015. Significant correlation (p-value < 0.05) is hatched.
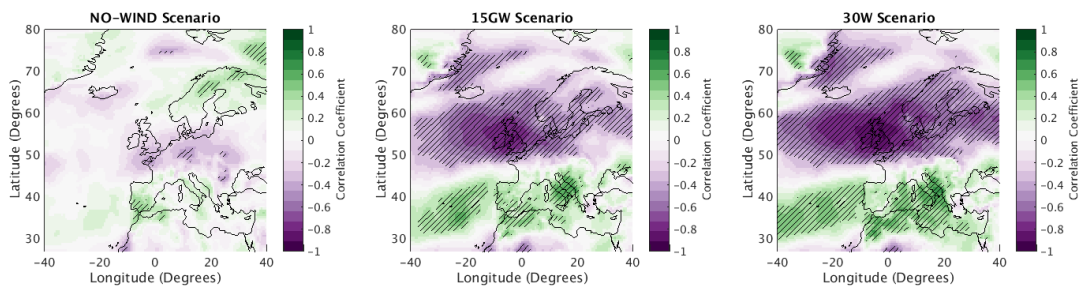
Figure 5.17 Correlation between annual-mean 10m wind speed and Baseload plant TVE for the (left) NO-WIND (middle) LOW and (right) MED scenario, for years 1980-2015. Significant correlation (p-value < 0.05) is hatched.

Significant correlation is found over GB in winter (r=-0.38) and spring (r=-0.52) in the LOW scenario (not shown). In the MED and HIGH scenarios the correlation between seasonal-average 10m wind speeds becomes most strongly negative in winter (r= -0.61 in the MED scenario and r=-0.64 in the HIGH scenario). This shows that in power systems with large amounts of wind power capacity, there are more hours in which baseload plant is marginal in winter. This is due to DNW being used as the variable for analysis. The seasonal cycle of wind power generation means that some of the hours of highest wind power generation are present in winter, if these are combined with an hour of low demand (i.e., during the night) then this can lead to very low loads. It is interesting that with large amounts of installed wind power generation these loads are sometimes lower than seen in summer.

5.5.3 Temperature driven vs. wind speed driven power system

A comparison of Figures 5.15 to Figure 5.17 shows that from the NO-WIND to the LOW scenario the hours in which baseload plant is marginal transfer from being temperature dependent to wind speed dependent. To investigate this change further, the correlation coefficients over GB have been calculated between summer-mean 2m temperature and baseload TVE, and winter-mean wind speed and baseload TVE, assuming a power system where there were varying levels of wind power capacity from 0GW to 45GW in 1GW intervals. These seasons are chosen due to them containing the strongest correlations between 2m temperature and 10m wind speed for 0GW and 45GW of installed wind power capacity respectively. Figure 5.18 shows the result of this. A turning point is seen at 8GW of installed wind power capacity, where the correlation with GB annual-mean 2m temperature starts to rapidly fall, until becoming relatively constant at ~20GW. The correlation between GB annual-mean 10m wind speed and baseload TVE becomes increasingly negative from 8GW, also plateauing at 20GW.

The point at which increasing the amount of installed wind power no longer impacts the correlation between winter-mean 10m wind speed and baseload TVE is similar to that seen for TAER (6GW). However, for baseload TVE a much larger amount of installed wind power is required for the metric to become strongly wind speed dependent (~10GW for baseload TVE vs. ~6GW for TAER). This is due to baseload TVE initially having a weak dependence on winter weather (see Figure 5.14), which increases as more wind power capacity is installed in the system.

Although baseload TVE correlates highly with summer temperatures the range of
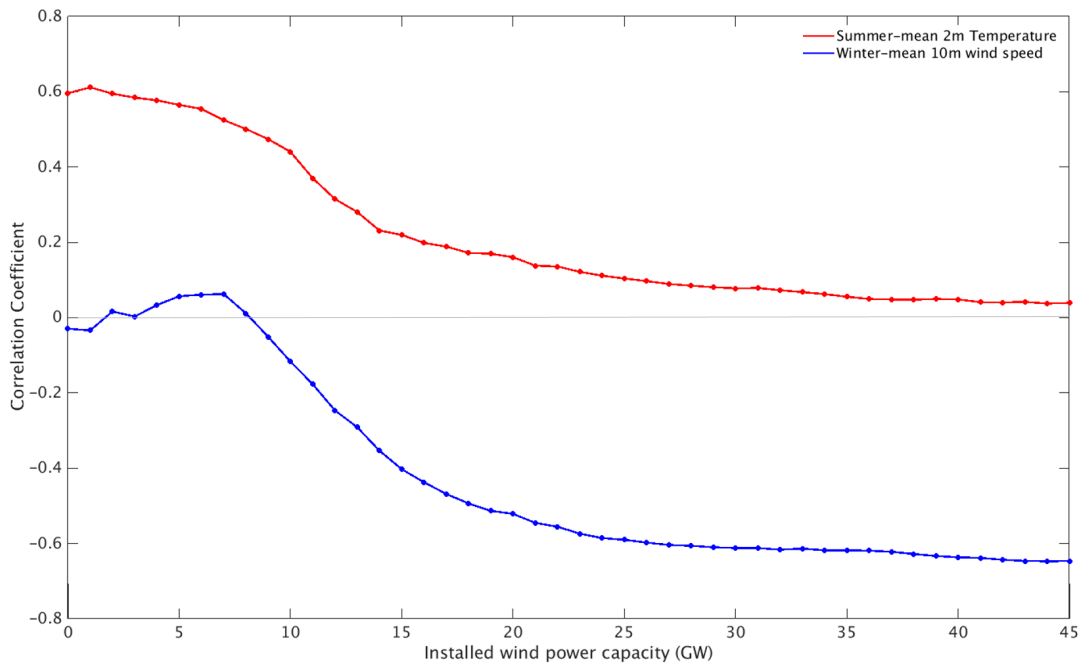
Figure 5.18 Correlation coefficient over GB is calculated between (a) summer-mean 2m temperature box averaged over GB and baseload TVE (red line) and winter-mean 10m wind speed box averaged over GB and baseload TVE (blue line) with a changing level of installed wind power from 0GW-45GW. Correlation between summer-mean 2m temperature and baseload TVE are statistically significant until 10GW of wind power generation is installed. Correlation between winter-mean 10m wind speed and baseload TVE are statistically significant once 10GW of wind power generation are installed.

summer demands is relatively small. The max-min range of winter demands is 2.5 times larger than the max-min range of summer demand, over approximately the same temperature range (due to the asymmetric u-shaped relationship between temperature and demand; see section 2.1). Therefore although it is important to understand the temperature sensitivity of baseload TVE, changes in summer temperature would not cause substantial changes to the amount of time baseload plant is marginal (with chapter 3 showing that there is very little variability in baseload TVE in the NO-WIND scenario).

Significantly more variability in the amount of time baseload plant is marginal is seen in the LOW scenario, which could cause problems for power system operation. Therefore the meteorological causes of the variability in baseload TVE in a system with present-day levels of installed wind power capacity are investigated in the next section.

5.5.4 Large scale drivers of baseload plant operation variability

The similarity in the spatial patterns of correlation between annual-mean 10m wind speeds and baseload TVE seen in Figure 5.17b and 5.17c and those seen for TAER suggest

that the meteorological drivers of the power system behaviour are similar for both metrics. This is investigated in the following subsections.

5.5.4.1 The North Atlantic Oscillation

Figure 5.19 shows the correlation between annual-mean NAO index and baseload TVE for the NO-WIND, LOW, and MED scenarios (the NAO index is calculated as described in section 5.4.4.1). No significant correlation is seen between annual-mean NAO and baseload TVE in the NO-WIND scenario (with no significant correlation seen between seasonal-mean NAO and baseload TVE; not shown). In the NO-WIND scenario baseload TVE has been shown to correlate highly with summer temperatures. Figure 5.3 showed that the years of most extreme summer temperatures are explained by an anticyclonic pressure pattern over GB, it is therefore not surprising that no significant correlation is seen between baseload TVE and the NAO index.

Figure 5.19 shows significant negative correlation between annual-mean NAO and baseload TVE in the LOW scenario. If the correlation between NAO and baseload TVE is examined seasonally then the highest correlation is seen in spring (r =-0.53). This is also the season with highest correlation between seasonal-mean 10m wind speed and baseload TVE.

As seen with TAER, increasing the amount of installed wind power capacity increases the predictive power of the NAO for baseload TVE (Figure 5.19c). This shows that in a power system including large amounts of installed wind power capacity the inter-annual variability of baseload TVE can be explained by variability in the annual-mean NAO-index.

5.5.4.2 The Eddy-driven Jet

The focus of this section is on the relationship between baseload TVE and the location of the winter eddy-driven jet in the LOW scenario, as previous sections have shown that in the NO-WIND scenario baseload TVE is associated with summer temperatures. The eddy-driven jet latitude is calculated as described in section 5.4.4.2.

For completeness the eddy-driven jet latitude at years of most extreme baseload TVE was examined for NO-WIND scenario and no relationship was found. Figure 5.20 shows the relationship between eddy-driven jet latitude and baseload TVE for the LOW scenario. In winters with low baseload TVE the eddy-driven jet is predominantly located in the central and northern locations. This results in windier and milder conditions over
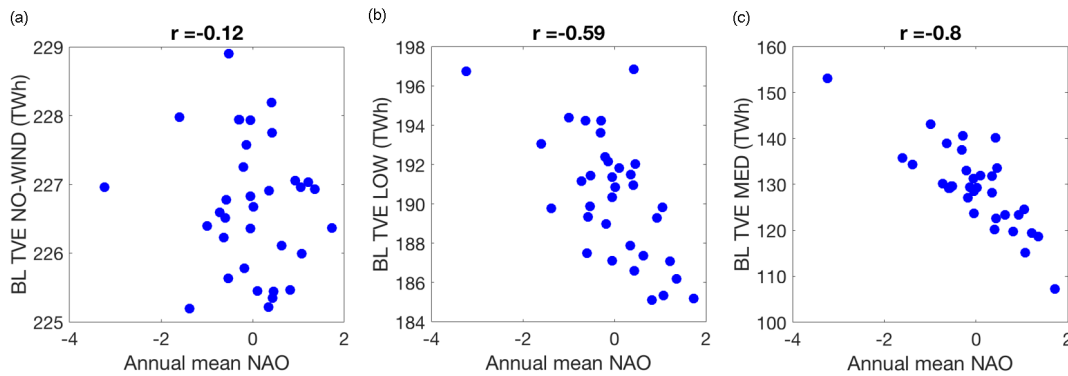
Figure 5.19   Correlation between annual-mean NAO index and baseload (BL) TVE for the (a) NO-WIND scenario (b) LOW scenario (c) MED scenario. Correlation coefficient (r) is given. Correlation is significant ($p < 0.05$) for the LOW and MED scenarios.

GB, therefore above average wind power generation. The above average wind power production results in low values of DNW, which result in days where baseload plant may become marginal.

In years of high baseload TVE the eddy-driven jet is much more likely to be located over southern Europe. During these winters there are lower wind speeds over GB and therefore lower wind power production. Winters of a southward located jet therefore lead to less hours in winter when baseload plant is marginal.

Figure 5.20 only shows the eddy-driven jet locations for the LOW scenario as the extreme years of baseload TVE are similar for the MED and HIGH scenario. This suggests that increasing the amount of installed wind power capacity does not change the meteorological driver of the number of hours that baseload plant could be required not to operate. The main difference in the relationship between baseload TVE and the eddy-driven jet to what was seen in section 5.4.4.2 for TAER is that for baseload TVE significantly more wind power is required on the system before a dependence on winter weather develops, and therefore a relationship with eddy-driven jet latitude.

This analysis has shown that increasing the amount of installed wind power capacity to present day levels has had a large impact of the meteorological drivers of baseload plant operation. However, increasing the amount of installed wind power capacity further results in minimal changes to the meteorological drivers of baseload plant operation.
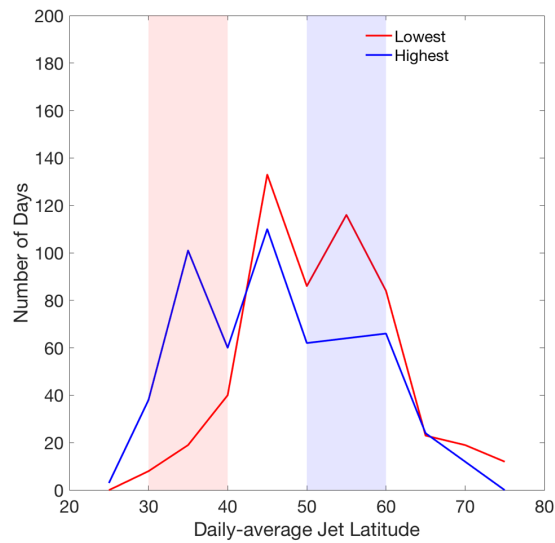
Figure 5.20 Daily winter eddy-driven-jet latitude for the lowest six years of base load TVE (blue) and highest six years of baseload TVE (red) for the LOW scenario. Shaded areas indicate the areas of maximum correlation between 10m wind speed and TAER in Figure 5.17.

5.5.5 Summary

In a power system with no installed wind power capacity baseload TVE is related to mean summer temperatures. This is due to summer being the time in which demand is lowest, therefore it is most likely for baseload plant to become marginal. A transition from a temperature-driven to wind speed-driven power system is seen as wind power capacity is installed (with the transition completing at ~10GW). Times of lowest DNW (i.e. when baseload plant may become marginal) are now often present in winter, when high wind power production is present at night (i.e. times of reduced demand). Winter-mean wind speed has the strongest correlation with baseload plant TVE by the MED scenario, showing a baseload plant operation is controlled by winter weather in a power system including large amounts of installed wind power capacity. The large scale drivers of baseload TVE are similar to those seen for TAER once 15GW of wind power generation is installed on the system, with a relationship present between NAO index, eddy-driven jet latitude and baseload TVE.

5.6 Peaking Plant TVE

In this section the meteorological drivers of peaking plant TVE are discussed. Peaking plant TVE describes the amount of energy for which peaking plant would be the most economically efficient generation type. This corresponds to the first 7% of each LDC (i.e.,

the hours with the highest 7% residual demand).

The hours contributing to peaking plant TVE (hereafter denoted "peaking plant hours") are during the day (from 9:00-21:00) and from October to March in the NO-WIND scenario (see Figure 5.21a and 5.21b respectively). These are times when both the diurnal and seasonal cycles of demand are greatest. The wind power capacity factor during the hours that peaking plant is required in the NO-WIND scenario is extremely varied (i.e., hours corresponding to peaking plant TVE may include a wide range of wind conditions, Figure 5.21c). This is a theoretical capacity factor as there is no wind power capacity installed on the system in this scenario).

The hour of the day in which peaking plant hours occur stays relatively constant when 15 GW of wind power is installed on the system (i.e., the LOW scenario; Figure 5.21d). There is a slight increase in the annual range of operation for the LOW scenario, with peaking plant now operating from September to April (Figure 5.21e). The largest difference between the NO-WIND and LOW scenario is in the range of wind power capacity factors that are present during hours of economically efficient peaking plant operation. In the LOW scenario it is common for wind power capacity factor to be low during peaking plant hours, with hourly wind power capacity factors rarely exceeding 40% (Figure 5.21f). The change in the capacity factor distributions is due to the peaking plant hours being the hours of highest DNW (i.e., demand minus wind power generation). In a system with no wind power generation peaking plant hours must occur at times of highest demand, whereas in a system including wind power generation peaking plant hours occur at times of the highest DNW, therefore a mixture of high demand and low wind power generation.

These changes are accentuated as the amount of wind power capacity installed on the system is increased in the MED scenario (Figure 5.21g-i) and HIGH scenario (not shown). This shows that as the amount of wind power generation installed on the system is increased the timing of peaking plant hours becomes more strongly dependent on wind power capacity factor (rather than peak demand), but otherwise there is little change seen in the distribution of peaking plant hours in terms of months the of the year or hours of the day.

5.6.0.1   2m Temperature

Seasonal analysis has shown that in the NO-WIND scenario an area of negative correlation is found over parts of GB in winter (Figure 5.22). This is similar to the result seen in Figure 5.5 for TAER. However, for peaking plant TVE the area of significant correla-
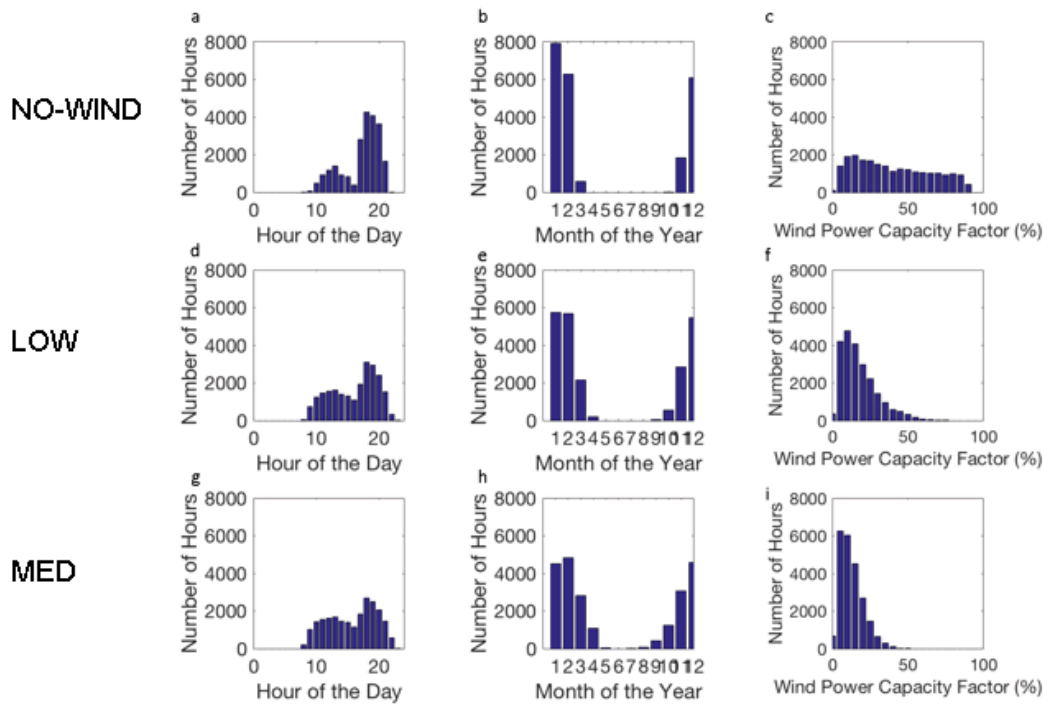
Figure 5.21 The hours of operation of peaking plant from 1980-2015 (i.e., the hours from 0-7% of all 36 LDC's) for the NO-WIND scenario (top), the LOW scenario (middle) and the MED scenario (bottom) for. (a,d,g) the hour of the day (b,e,h) the month of the year, (c,f,i) wind power capacity factor (%).
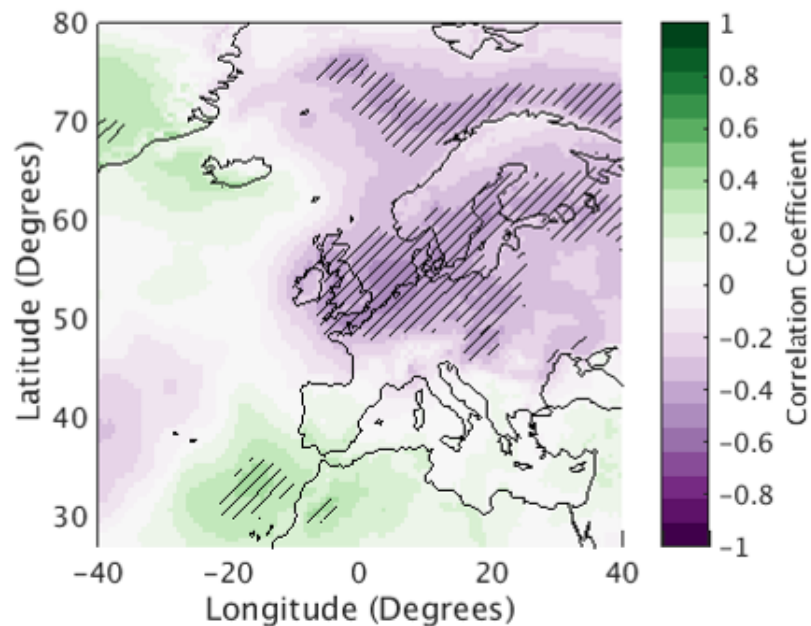
Figure 5.22 Correlation between winter-mean 2m temperature and Peaking Plant TVE for the NO-WIND scenario. Significant correlation (p-value < 0.05) is hatched.

tion is restricted to parts of GB and central Europe, and is much weaker in magnitude. In the NO-WIND scenario peaking plant is rarely used outside winter (as demand is typically lower), therefore it is not surprising that significant correlation is not found between peaking plant TVE and mean 2m temperature in other seasons (see Figure 5.21). The negative correlation between winter-mean 2m temperature and peaking plant TVE is due to the negative relationship between winter temperatures and demand (see Figure 5.1). Winter months experiencing below average temperatures also experience above average demands, therefore this leads to increased values of peaking plant TVE.

Installing wind power capacity on the system leads to a reduction in the strength of the correlation between winter 2m temperature and peaking plant TVE over GB (r = -0.10 for the LOW scenario and r =0.06 for the MED scenario, compared to r=-0.31 in the NO-WIND scenario). This suggests that in a system containing significant amounts of wind power capacity, peaking plant TVE becomes less dependent on winter-mean 2m temperature.

5.6.0.2 10m Wind Speed

It was not possible to identify significant correlation between peaking plant TVE and GB annual-mean or seasonal-mean 10m wind speeds in any of the wind power capacity scenarios. This suggests that the relationship between peaking plant TVE and meteorological variables is not as straightforward as previously seen for TAER and baseload TVE. The following subsection examines the timing of events more carefully, to try and understand why there is no significant annual or seasonal correlations present.

5.6.1 Hourly Analysis of Peaking Plant TVE

In this section the hourly data from the peaking plant TVE metric has been examined. Figure 5.23a shows hourly 2m temperature vs hourly peaking plant TVE for all winter data-points (as this is the season in which the majority of peaking plant is required; Figure 5.21) in the NO-WIND scenario. There is a large range of temperatures and loads in which peaking plant hours occur. Significant correlation is seen between the two variables (r=-0.46) showing that in warmer temperatures the amount of peaking plant that is required is lower.

Weak, but significant correlation is also seen between the hourly 10m wind speeds and peaking plant TVE for the NO-WIND scenario (Figure 5.23b; r=-0.10). The range of 10m wind speeds in which peaking plant hours occur is large, but is most commonly

around 5-8ms^{-1}.
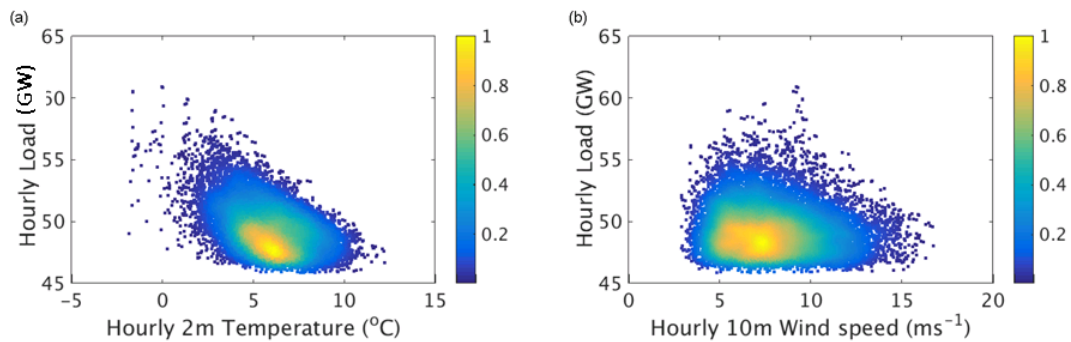
Figure 5.23 Frequency density plots of load during peaking plant hours in winter for the NOWIND scenario, showing the relationship with:: (a) hourly 2m temperatures vs. 10m wind speeds (b) hourly demand vs. hourly wind power capacity factor.

When wind power capacity is included on the system very little change is seen between the correlation of hourly 2m temperature and peaking plant TVE (compare r=-0.50 in the MED scenario with r = -0.46 in the NO-WIND scenario) or in the correlation between 10m wind speeds and peaking plant TVE (compare r=-0.08 in MED vs r=-0.10 in NOWIND). This suggests that in systems including large amounts of wind power generation the hourly temperature impacts the value of peaking plant TVE more than the hourly wind speed.

This analysis suggests that in any given peaking plant TVE hour, the temperature and wind speed at the time play a roll in determining the value of DNW. However, the total peaking plant TVE in a season has only a weak connection to the seasonal-mean temperatures and wind speeds.

5.6.2 Summary

Peaking plant TVE can be related to winter-mean temperatures in a system with no installed wind power capacity. However, once wind power capacity is included on the system the relationship between peaking plant TVE and meteorological variables becomes complex, with each hourly value being dependent on the temperature and wind speed conditions present. This metric behaves very differently to TAER and baseload TVE, showing that there is not one meteorological phenomena which can explain all the behaviour of all plant types.

5.7 Wind Power Curtailment

This section examines the time of day and the meteorological conditions associated with wind power curtailment events. The focus of this section is on the stability driven curtailment for the MED and HIGH scenarios, when wind power curtailment becomes frequent (i.e., hours where wind power generation is greater than 70% of demand; see section 3.4.2 for full definition). The MED scenario is the first scenario when any hours of curtailment are seen with this definition. Figure 5.24 shows histograms of hours of stability driven curtailment for the MED scenario. Both seasonal and annual histograms have been plotted to show the timing of the curtailment events throughout the year.

Figure 5.24 Conditions during hours of stability driven curtailment for the MED scenario for the whole re-analysis period (black) winters (blue) summers (red) springs (green) and autumns (yellow) for: (a) amount of curtailment (GW) (b) the wind power capacity factor (c) 10m wind speed (d) 2m temperature (e) Demand (f) hour of the day (g) wind speed anomaly from seasonal-mean (h) the temperature anomaly from the seasonal-mean.

Figure 5.24a shows the amount wind power generation curtailed over all curtailment hours in the MED scenario. The largest hourly values of curtailment reach ~10GW. Winter and autumn curtailment hours are more common than spring and summer curtailment hours. Figure 5.24f shows that for each season, curtailment happens exclusively at night, when the diurnal cycle of demand is at its minimum. The timing of curtailment hours is consistent throughout seasons, however the magnitude of demand which must be exceeded for a curtailment event to take place is varied across seasons. For example in winter, wind power must be greater than ~30GW for curtailment to occur whereas in

summer this threshold is reduced to ~ 22GW (see Figure 5.24e) due to the seasonal cycle of demand.

Wind power capacity factors are always greater than 40% during curtailment hours (Figure 5.24b), with the highest capacity factors seen in winter. In summer capacity factors rarely exceed 80% during curtailment events. The range of capacity factors seen during curtailment hours for each season can be explained by looking at the 10m wind speeds (Figure 5.24c). The wind speeds associated with curtailment hours are higher in winter than summer. This is both due to the higher demand exceedance threshold being required in winter (see Figure 5.24e) and the increased probability of high wind speeds in winter (due to the seasonal cycle of wind speeds). If the wind speeds are viewed as a seasonal anomaly from the 36 year record (Figure 5.24g) curtailment hours are then present during anomalously high wind speed events in all seasons.

The GB mean 2m temperature during curtailment hours is shown in Figure 5.24d. In all seasons curtailment hours happen at times of low demand. In summer low demand requires anomalously cool temperatures whereas in winter anomalously warm temperatures are required (Figure 5.24h).

Figure 5.25 shows the same set of subplots as Figure 5.24 but for stability driven curtailment in the HIGH scenario. The number of curtailment hours is significantly increased in each season (note the change in y-axis in Figure 5.25 compared to 5.24). The magnitude of each curtailment hour can be as much as 20GW (Figure 5.25a). Curtailment hours are present throughout the day, although there is still a preference for night-time curtailment (Figure 5.25f).

The histogram of demand for each season's curtailment hours has a bi-modal structure (Figure 5.25e). The lower peak of this is located in the same position as for the MED scenario (Figure 5.24e). A second peak has developed due to the occurrence of day-time curtailment. This is consistent with the stationary points in the diurnal cycle of demand at 00:00-05:00 and 10:00-15:00 (see Figure 3.2).

The subplots showing wind power capacity factor, 10m wind speed, 10m wind speed anomaly, 2m temperature and 2m temperature anomaly during curtailment hours look very similar between the MED and HIGH scenarios (compare Figure 5.24 and 5.25). The range of wind speeds and temperatures experienced during hours of curtailment is, however, slightly larger in the HIGH scenario. This shows that the range of meteorological conditions experienced during a curtailment event does not change considerably as the amount of wind power installed on the system is increased beyond the MED scenario
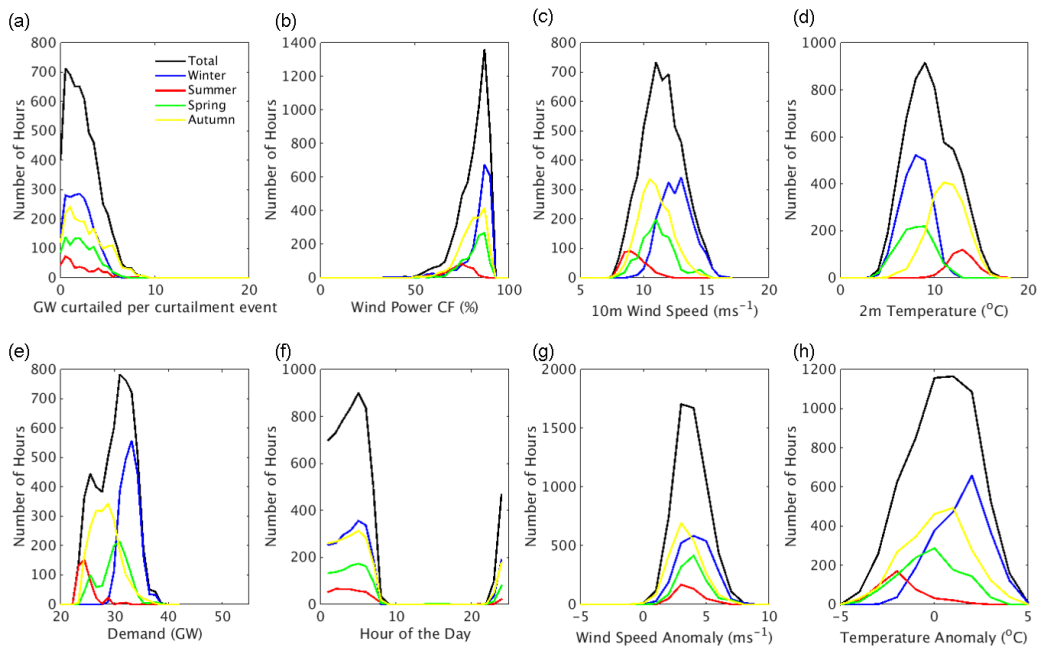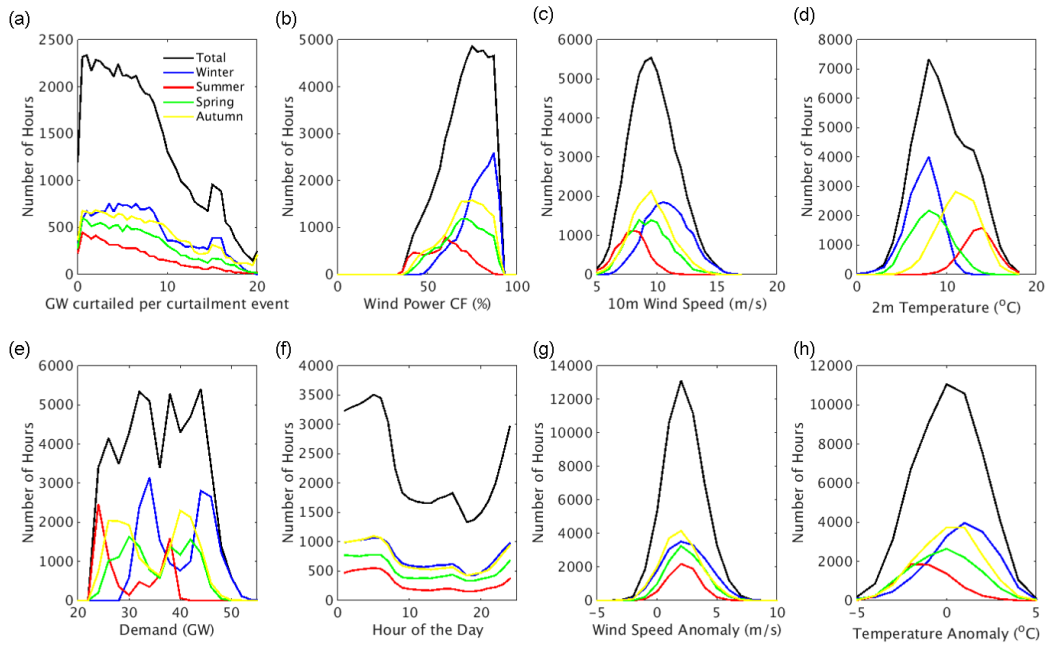
Figure 5.25 Conditions during hours of stability driven curtailment for the HIGH scenario for the whole re-analysis period (black) winters (blue) summers (red) springs (green) and autumns (yellow) for: (a) amount of curtailment (GW) (b) the wind power capacity factor (c) 10m wind speed (d) 2m temperature (e) Demand (f) hour of the day (g) wind speed anomaly from seasonal-mean (h) the temperature anomaly from the seasonal-mean.

(equivalent to $\sim$2035). Increasing the amount of wind power on the system reduces the constraints on the timing of curtailment events. In the MED scenario curtailment is only possible during night, however in the HIGH scenario curtailment is possible throughout the day.

5.7.1 Extreme Curtailment Events

In reality the amount of curtailment seen in section 5.7 may not be realistic due to the definition of curtailment neglecting any system transmission constraints. The meteorological conditions present during the most extreme curtailment events are however of interest to power system operators, as these times of extreme wind power generation would definitely require system action. Details of the meteorological conditions associated with the most extreme curtailment events seen in the study period are therefore examined in closer detail in this subsection.

Extreme wind power curtailment events have been categorised in terms of the amount of curtailment (GW) and duration of curtailment (number of hours) per event. The results shown in this section are only for the extreme-duration-events as they are qualitatively similar to the extreme-amount-events. The focus is on the MED scenario although the

same results are seen qualitatively for the HIGH scenario.

Figure 5.26 shows composites of temperature, wind speed and mean sea-level pressure for the top-ten most extreme curtailment events (the top-25 and top-50 events have also been investigated and show qualitatively similar results). The top-ten curtailment events happen between May and October (i.e., mostly during summer). Eight out of the ten events commence at 22:00, ending at 16:00 the following day. The top-ten events vary in duration from 18 to 34 hours (with 201 hours of data in total over all 10 events). This is the only incidence of curtailment in the 36 year period which is greater than 24 hours long. This shows that it is extremely rare for there to be curtailment at the peak of the diurnal cycle of demand in the MED scenario.

Figure 5.26a shows that during the top-ten curtailment events the temperature over GB is in the range of 10-20°C. This is anomalously cold for the summer and autumn events (see Figure 5.24d and h). These conditions are conducive for low summer demands over GB.

High wind speeds are experienced surrounding GB during extreme curtailment events (Figure 5.26b). This allows for the high wind power production that is needed for curtailment. Figure 5.26c shows that the high wind speeds and cool summer temperatures over GB are associated with a low pressure system centred to the North of GB, which brings strong westerly flow from the North Atlantic.
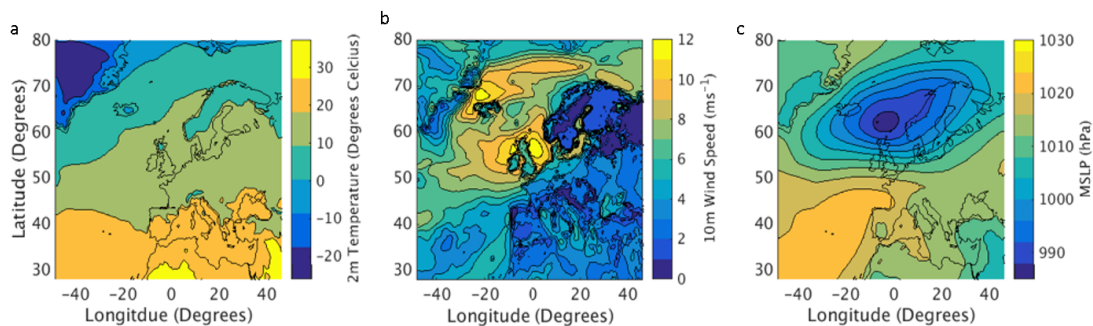
Figure 5.26 Composites of the top 10 stability driven curtailment events from 1980-2015, classified by event duration. (201 hours of data) for (a): 2m Temperature (Degrees Celsius) (b) 10m Wind Speed (m/s) (c) Mean sea-level pressure (MSLP; hPa).

Further examination of the low pressure system to the North of GB has been conducted for each hour of the curtailment events. Figure 5.27 shows composites of mean sea-level pressure for the first 6 hours of the curtailment events, hours 6-12 and hours 12-18 (lengths greater than this have not been investigated as the shortest of the top 10 events is 18 hours). The location of the low pressure system is consistent for all 18

hours of the curtailment events. A strong pressure gradient is still present over GB at the end of the curtailment events, therefore there is still high wind power generation when curtailment ceases. The curtailment events cease to exist when demand increases to a level above the wind power production. This is usually at 16:00, when the diurnal cycle of demand is approaching its peak (see Figure 3.2).
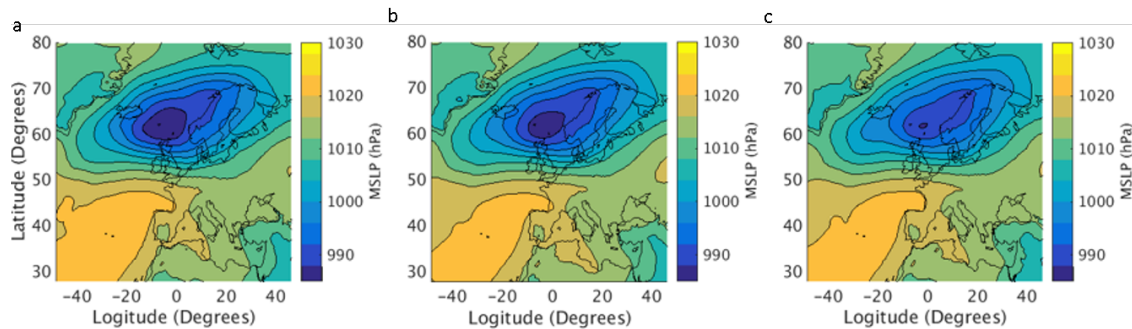
Figure 5.27   Composites of the top 10 curtailment events classified by event duration (201 hours of data) showing the mean sea-level pressure (MSLP; hPa) from (a) the first six hours of the events. (b) Hours six to twelve of the events. (c) Hours twelve to eighteen of the events.

5.7.2   Summary

Wind power curtailment events are associated with times of high wind power generation, therefore anomalously high GB-mean wind speed. Curtailment events also require low demand, which require anomalously cold summer temperatures or anomalously warm winter temperatures. As the amount of wind power generation installed on the system is increased the timing of curtailment events becomes less restricted, with curtailment events becoming possible in all hours of the day by the HIGH scenario.

The top-ten most extreme curtailment events from the 1980-2015 period all occur between May and October and are all at least 18 hours long. These events had anomalously warm temperatures and anomalously high wind speeds. These conditions were reached due to the presence of a low pressure centre located to the North of GB. The stationary location of the low pressure centre resulted in high wind power generation over GB for a prolonged period, therefore a large amount of curtailment.

5.8   Peak Load

This section investigates the synoptic conditions associated with extreme peak load events (see section 3.4.2 for a definition) and how they are changed from the NO-WIND

to HIGH scenarios. To do this the top-ten most extreme peak load events from the whole 36-years of data are isolated (the top-25 and top-50 events have also been investigated and show qualitatively similar results). In order to isolate the top-ten extreme events, a thresholding approach is applied, where a peak load hour is discarded if found to be within five days either side of an existing peak load hour. This is in order to have 10 meteorologically distinct peak load events. A five day threshold is applied due to the knowledge from previous work that GB peak load can be associated with persistent blocking events, known to last for a number of days (see section 2.5 and Brayshaw et al. (2012)). If the thresholding was not applied then the following composites would contain multiple hours of data from the same meteorological event.

Following the isolation of the top-ten peak load events for each wind power scenario, composites of wind speed anomaly (Figure 5.28) temperature anomaly (Figure 5.29) and mean sea-level pressure (Figure 5.30) have been created. The wind speed and temperature anomalies are calculated as anomalies from the 36-year winter-mean values of the variable in question (all peak load events happen in December, January or February).

Figure 5.28a shows that in the NO-WIND scenario there are anomalously low wind speeds to the North of GB during peak load. Wind speed anomalies of ~-0.5ms^{-1} are seen over Southern England, whereas wind speed anomalies can reach -4ms^{-1} in the North of GB (Figure 5.28e). In the LOW scenario peak load events are associated with anomalously low wind speeds centred over GB of at least -4ms^{-1} (Figure 5.28b and 5.28f). The magnitude of the wind speed anomaly over GB is therefore much more negative in the LOW scenario than in the NO-WIND scenario (see Figure 5.28f), with large low wind speed anomalies off the coast of Northern Scotland. The same pattern of wind speed anomaly is seen in the MED scenario (Figure 5.28c and 5.28g) and HIGH scenario (not shown), with the magnitude of the negative wind speed anomaly over GB increasing as more wind power capacity is installed on the system.

Figure 5.29 shows the temperature anomalies during peak load events for the NO-WIND, LOW, MED and HIGH* scenario. In the NO-WIND scenario peak load events are associated with anomalously cold temperatures over GB, Central Europe and parts of Northern Europe. Temperature anomalies can be up to -7°C over GB (Figure 5.29e). The magnitude of the temperature anomalies are reduced over GB, Central and Northern Europe in the LOW scenario (Figure 5.29b and f). The magnitude of the temperature anomaly over GB slightly decreases as the amount of wind power capacity installed on the system is increased in the MED scenario (Figure 5.29c and g) and the HIGH scenario
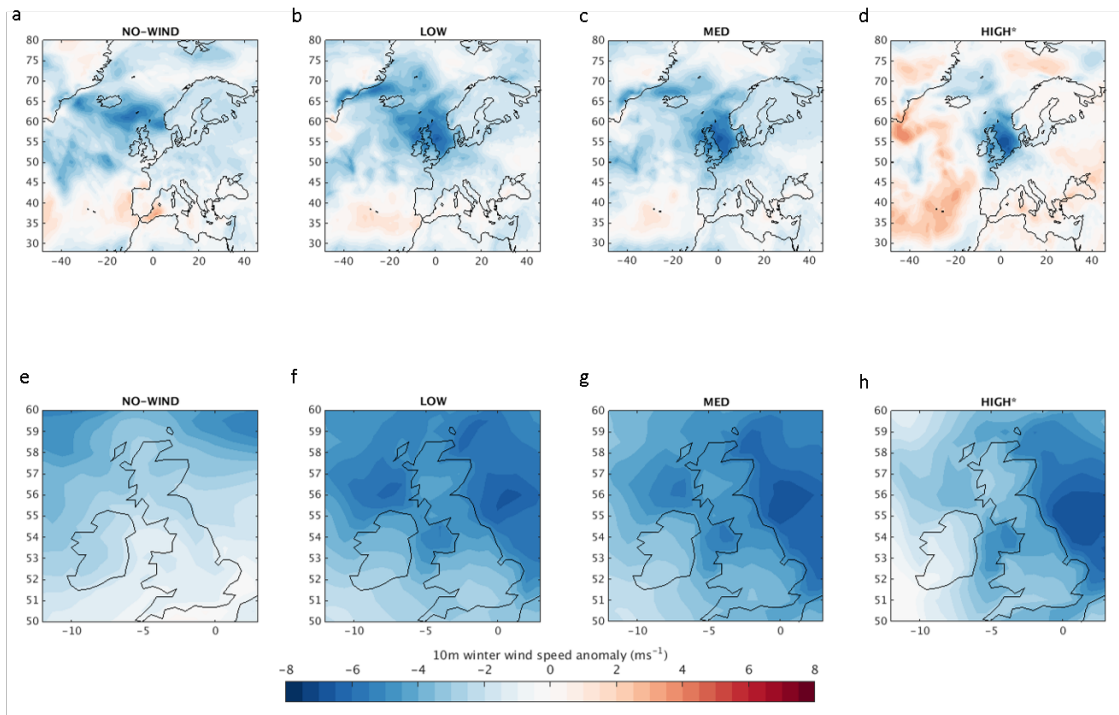
Figure 5.28 Composites of 10m wind speed anomaly over Europe (a-d) and GB (e-h) during the top-ten extreme peak load events for (a and e) NO-WIND, (b and f) LOW (c and g) MED and (d and g) HIGH scenarios. **make text bigger**

(Figure 5.29d and h). However, the spatial pattern of temperature anomalies over Europe remains constant.

To further understand the wind speed and temperature anomalies, composites of the mean sea-level pressure at times of peak load have been created for the NO-WIND, LOW, MED and HIGH* scenarios (Figure 5.30). An area of high pressure to the North of GB is present in the NO-WIND scenario (Figure 5.30a). The location of this high pressure during winter causes there to be a reversal of pressure gradient over GB, and therefore a reversal of the zonal flow. The advection of easterly air from the cold European continent results in the strong negative temperature anomalies over GB. This synoptic situation is consistent with the pressure patterns seen in Brayshaw et al. (2012) linked to GB peak demand events.

If the NO-WIND and LOW scenarios are compared a change in the synoptic pattern present over GB is seen. The high pressure is now centred over GB (Figure 5.30b). This results in extremely low winds over GB due to the low pressure gradient. The lack of advection of cold air over GB results in a reduced temperature anomaly compared to the NO-WIND scenario. The stagnant air results in low wind speeds (therefore low wind power generation) and moderately low temperatures.

The composites from the MED and HIGH scenarios show that a similar synoptic
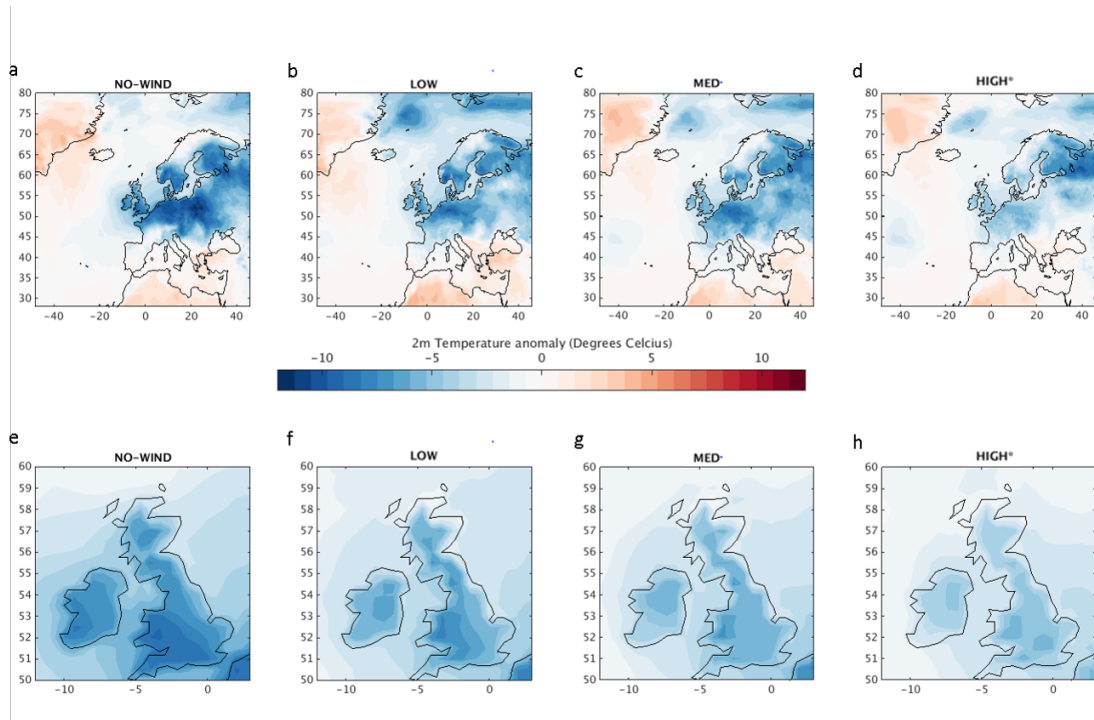
Figure 5.29 Composites of 2m temperature anomaly over Europe (a-d) and focussing on GB (e-h) during the top-ten extreme peak load events for (a and e) NO-WIND, (b and f) LOW (c and g) MED and (d and g) HIGH scenarios.
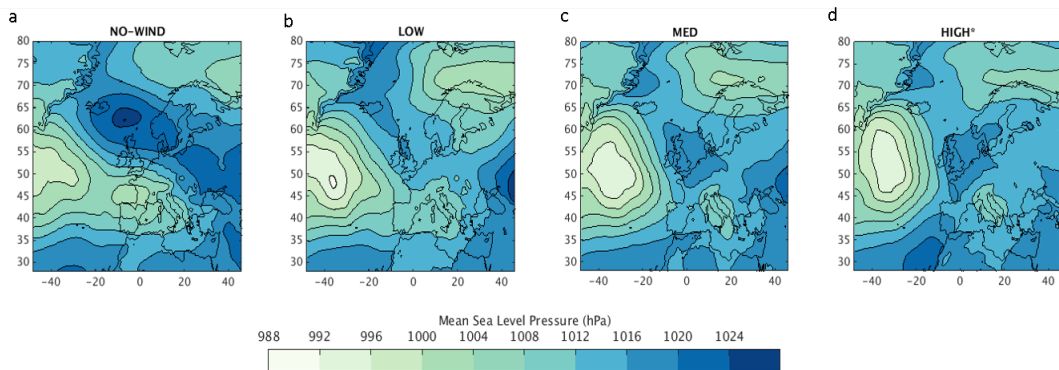
Figure 5.30 Composites of mean sea-level pressure over Europe during the top-ten extreme peak load events for (a) the NO-WIND, (b) LOW, (c) MED and (d) HIGH scenarios.

situation to the LOW scenario is seen (Figure 5.30c and d), with the magnitude of the high pressure over GB being somewhat stronger in scenarios where more wind power capacity is installed on the system.

5.8.1 Summary

This analysis has shown that in a power system with no installed wind power capacity peak load events are associated with the presence of an anticyclone to the North of GB, causing a reversal of the zonal winds over GB, This results in anomalously low

temperatures over GB and average wind speeds.

As the amount of installed wind power capacity is increased the synoptic situation associated with peak load is changed. An anticyclone is located directly over GB, resulting in anomalously low wind speeds, but more moderate temperatures. This suggests that depending on the level of installed wind power capacity different synoptic conditions are present at times of peak load.

5.9 Chapter Summary

This chapter has shown that a wide range of meteorological drivers are relevant to power system operation. In order to understand the meteorological drivers of the GB power system a range of analysis tools were used which varied depending on the characteristics of the power system metric in question.

The inter-annual variability experienced by the GB power system metrics is predominantly controlled by winter weather. In a system without installed wind power capacity the variability of the GB power system is associated with variability in temperatures, whereas in systems with installed wind power capacity the variability is driven by variations in wind speeds. The dependence on wind speeds rather than temperature becomes stronger as more wind power generation is installed on the system.

Key results from this chapter are summarised below:

- TAER shows significant correlation with GB winter-mean and spring-mean 2m temperatures when no wind power capacity is installed. Installing 15GW of wind power capacity causes TAER to become strongly dependent on GB winter-mean 10m wind speeds. In the years of anomalously low winter-mean, 10m wind speed (and therefore high TAER) the eddy-driven jet is predominately located in the southern position, and a negative annual-mean NAO index is found.

- Baseload TVE is strongly controlled by summer temperatures when little installed wind power capacity is present, due to this being the time of year when demand is lowest. As the amount of wind power capacity installed on the system is increased, the hours of lowest DNW (comprising the period in which baseload plant is marginal) change to include a larger proportion of winter hours. This then causes baseload TVE to strongly correlate with winter-mean wind speeds.

- Strong correlation between winter-mean temperature and peaking plant TVE is

found in the NO-WIND scenario. In systems including wind power generation the relationship between peaking plant TVE and meteorological variables becomes more complex, with little correlation seen between seasonal-mean weather variables and peaking plant TVE. There is however correlation between the hourly load during times of peaking plant TVE and hourly 2m temperatures, showing that meteorological variability is still impacting peaking plant TVE.

- Extreme wind power curtailment events are caused by a stationary, or slow-moving low pressure system, located to the north of GB. Even in scenarios with relatively high levels of installed wind power capacity, extreme wind power curtailment events tend to last less than 24 hours. This upper limit to the duration is associated with the evening peak in the diurnal cycle of demand (i.e., controlled by human behaviour rather than weather conditions).

- In a system with no installed wind power capacity, peak load events are associated with anomalously low temperatures over Europe. These conditions are caused by a high pressure centred to the north of GB, causing a reversal in the zonal flow. As the amount of wind power installed on the system is increased then peak load events are also associated with anomalously low wind speeds over GB, due to high pressure now being centred over GB.

In highlighting the synoptic conditions present during extreme power system events this chapter has provided useful information for system operators wishing to understand which meteorological conditions a weather-dependent power system is most susceptible to.

As the amount of wind capacity installed on the GB power system is increased, the inter-annual weather-sensitivity of, both TAER and baseload TVE shifts from being dependent on temperature (for systems with no wind power capacity) to being dependent on 10m wind speeds. This change suggests that power system stakeholders could be exposed to weather risk across a much wider spectrum of meteorological phenomena in power systems including high levels of installed wind power capacity.

The chapter has also highlighted that climate models must have a good representation of the eddy-driven jet stream, with small biases in near-surface temperatures and wind speeds over GB if they are to be used to robustly model the impact of climate change on the GB power system. These points are discussed further in section 7.3

Chapter 6:

The impact of climate change on the GB power system in the HiGEM model

Chapter 4 has shown that the GB power system is significantly impacted by present day inter-annual climate variability. With increasing atmospheric green-house gas concentrations scientists are confident that the atmosphere will warm (Kirtman et al. (2013)), which may lead to changes in the global circulation. Climate change may therefore impact weather-dependent power system operation, with potential reductions in GB heating-induced demand (Isaac and van Vuuren (2009),Golombek et al. (2011)) and annual-mean wind power generation (Cradden et al. (2012) Hueging et al. (2013)). The previously cited studies did not, however, account for any bias present in the climate models used to gain their findings.

This chapter investigates the potential for the climate model HiGEM to be used to study the impacts of climate change on the GB power system (section 1.4, objective 4). To do this, the relevant meteorological fields used to model demand and wind power generation are evaluated, then bias corrected (sections 6.1 and 6.2). This chapter then investigates if climate model data is able to represent the important meteorological phenomena highlighted in chapter 5 which are needed for the accurate modelling of the GB power system, such as the co-variability of temperatures and wind speeds (section 6.3).

Once there is confidence in the ability of HiGEM to be used for power system modelling then the methods used in chapter 4 are adapted to cope with the reduced resolution of climate model data (section 6.4). Following this the impact of climate change on GB

demand (section 6.5), wind power generation (section 6.6) and the power system as a whole (section 6.7) are investigated (section 1.4, objective 5). A summary of the chapter's findings is given in section 6.9.

6.1 Modelling demand with HiGEM

In order to generate hourly demand from HiGEM the method used in section 3.2 is followed. An overview of the method is given below:

- GB daily-mean land-only near surface, effective temperatures are calculated from HiGEM

- A multiple linear regression model (see Equation 3.3) calculates daily-mean demand (the seasonal cycle of temperature is prescribed).

- daily-mean demand is interpolated to hourly demand using diurnal cycle anomaly curves (the characteristics of these diurnal curves evolve slowly with season, see section 3.2)

The only weather-dependent input to this demand model is daily-mean, land-only 2m temperature. 2m air temperature and the land fraction of each grid box are outputs from the HiGEM control run and future climate simulations, therefore, no changes to the methodology in section 3.2 are required. Section 6.1.1 evaluates the daily-mean, land-only, 2m temperatures and resultant demand from HiGEM. Section 6.1.2 attempts to correct for the bias present in the HiGEM 2m temperature data, and shows the improvement in fit when comparing the daily-mean demand data.

6.1.1 Evaluation of HiGEM temperatures

In order to model GB demand using HiGEM, any bias present in the daily-mean, land-only, 2m temperatures must be understood, and if necessary bias corrected (hereafter land-only 2m temperature is simply referred to as *surface air temperature* or SAT for convenience). Figure 6.1a shows a quantile-quantile plot of daily-mean SAT from MERRA and daily-mean, SAT from years 21-70 of the HiGEM control run HiGEM (see section 3.1.2 for more details). A similar range of GB SAT's are seen in HiGEM compared to MERRA. This suggests HiGEM can be used to model GB demand. However, temperatures in the lower 50 percentiles of SAT are warmer in HiGEM than MERRA and the top 10 percentiles of SAT are moderately colder in HiGEM than MERRA.
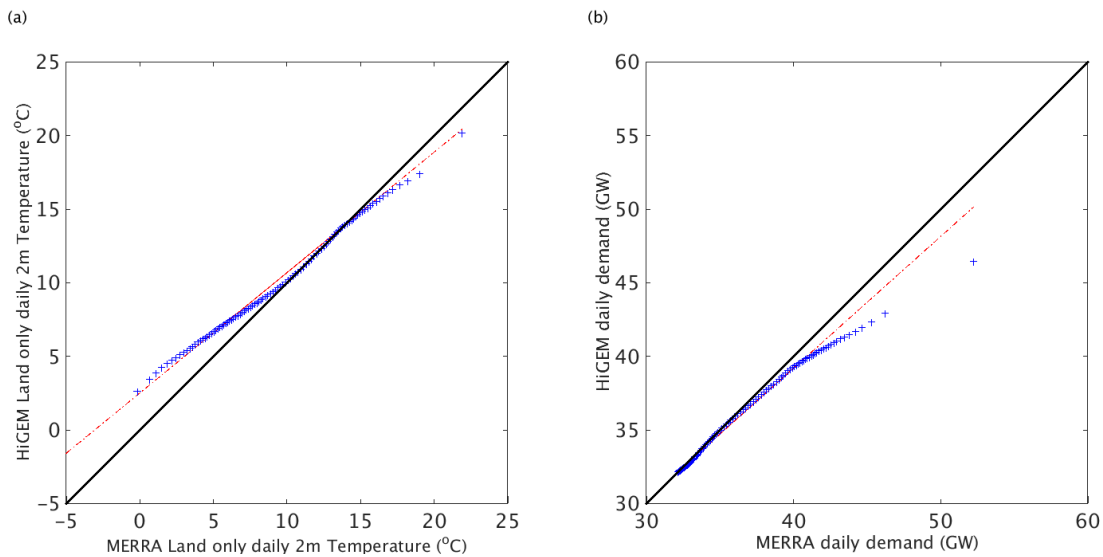
Figure 6.1 Quantile-quantile plots for 36 years of MERRA data (1980:2015) vs. 50 years of HiGEM data for (a) daily-mean, land-only, 2m temperatures (box-averaged over GB from −11.3E: 2.7E and 50N−59N) (b) daily-mean GB demand. The black line shows a 1:1 line and red dashed line shows the line of best fit through the quantiles.

The difference in spatial resolution between HiGEM and MERRA result in differences in the number of grid boxes used to create the daily-mean SAT (see Appendix 8.1 for a comparison of the two model grids). In both datasets a grid box is considered as land if it has a land fraction of 50% or more. Both MERRA and HiGEM have shown to be insensitive to moderate changes in this parameter (see Appendix 8.1).

Daily demands from both MERRA and HiGEM created using the method in section 3.2 are compared in the quantile-quantile plot in Figure 6.1b. Differences in the daily-mean, SAT between MERRA and HiGEM seen in Figure 6.1a lead to differences in daily-mean demand. The warmer winter temperatures in HiGEM lead to reduced demand (due to the negative relationship between temperature and demand).

Figure 6.2 shows seasonal histograms of daily-mean, SAT for MERRA and HiGEM. HiGEM reproduces the seasonal distributions of MERRA daily-mean, SAT reasonably well in spring, summer and autumn (although the MERRA distribution is somewhat wider in spring and summer) but larger differences are seen in winter. During winter the mean daily-mean, SAT in HiGEM are warmer than MERRA, with a 2.2^oC difference in mean-winter temperature (Figure 6.2c). The seasonal variability of daily-mean, SAT in MERRA and HiGEM is comparable, with HiGEM being ∼25% less variable than MERRA in all seasons (Figure 6.2; see Table 6.1).

It is common for climate models from the CMIP5 archive to have a strong summer warm bias in the mid latitudes (Cheruy et al. (2014), Christensen and Boberg (2012)).
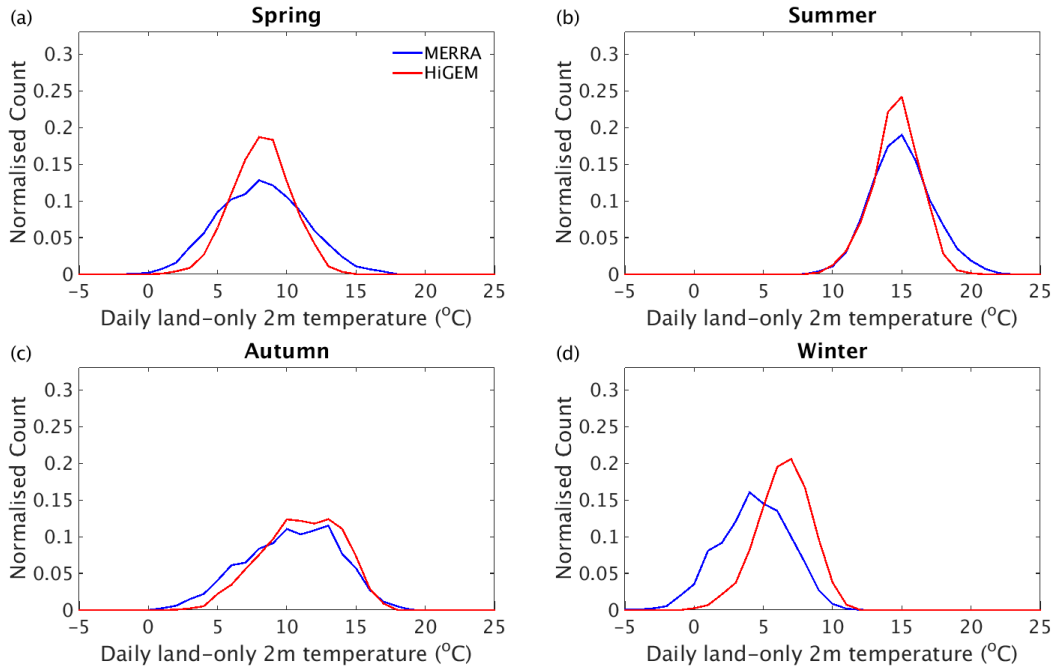
Figure 6.2 Seasonal histograms of daily-mean, land-only, 2m temperatures from 36 years of MERRA data (blue) and 50 years of HiGEM data (red).

Models with the strongest bias will generally overestimate the amount of incoming solar radiation and underestimate the amount of cloud (Cheruy et al. (2014)). This is not seen in HiGEM, with summer temperatures being moderately lower than in MERRA (Figure 6.2).

6.1.2 Bias correction of HiGEM temperatures

In order to correct for the bias in the mean and the variance in the HiGEM daily-mean SAT a seasonal cycle correction and a variance correction is implemented. Equations 6.1 to 6.3 show the bias correction applied to the HiGEM data.

$$H_{anom} = HiGEM - HiGEM_{SC} \tag{6.1}$$

$$M_{anom} = MERRA - MERRA_{SC} \tag{6.2}$$

$$H_{corrected} = \frac{\sigma_{M_{anom}}(H_{anom} + MERRA_{SC})}{\sigma_{H_{anom}}} \tag{6.3}$$

Here H and M represent HiGEM and MERRA respectively, SC represents the seasonal cycle, anom, the anomaly from the seasonal cycle, σM_{anom} and σH_{anom}, are the standard deviations of the anomaly time series of MERRA and HiGEM respectively.

Fitted seasonal cycles for MERRA ($MERRA_{SC}$) and HiGEM ($HiGEM_{SC}$) data are shown in Figure 6.3. These are constructed by fitting a sine and cosine curve to the data. The seasonal cycles shown in Figure 6.3 are close to the monthly mean temperatures, confirming that the seasonal cycles fit is a reasonable approximation. Figure 6.3 shows that the seasonal cycle in HiGEM has a smaller amplitude than seen in MERRA. This is consistent with the cooler summer temperatures (Figure 6.2b) and warmer winter temperatures (Figure 6.2d).
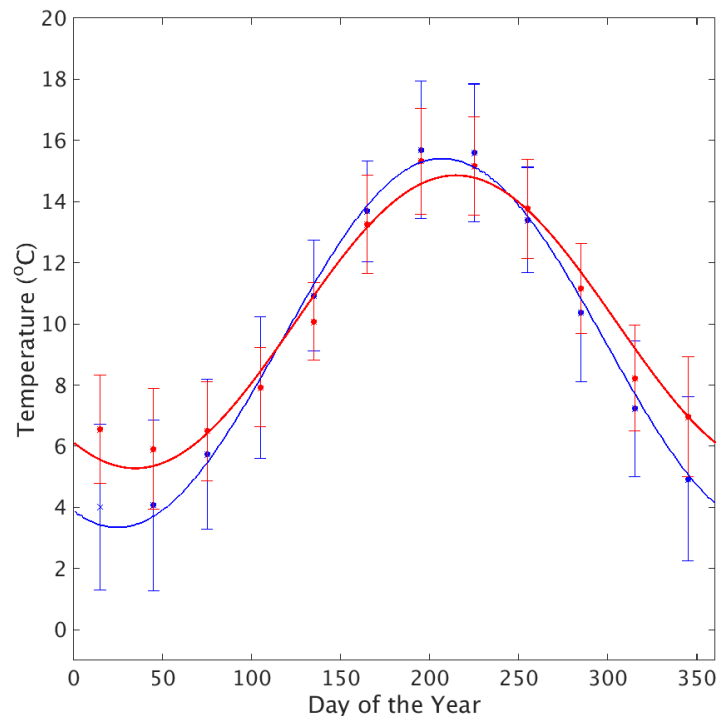
Figure 6.3 Fitted seasonal cycles for 36 years of MERRA data (blue) and 50 years of HiGEM data (red) for daily-mean, land-only, 2m temperatures. Scatter points represent the monthly mean temperatures and error bars show 2 standard deviations of the monthly mean temperature.

Table 6.1 shows the mean and standard deviations of MERRA and HiGEM SAT. The standard deviation of the MERRA daily-mean SAT's is larger than seen in HiGEM in all seasons, however, the difference varies throughout the year. The largest difference in in spring (where the standard deviation of MERRA is 35% larger than in HiGEM) and smallest difference in autumn (where the standard deviation of MERRA is 15% larger than in HiGEM).

A seasonal variance correction is applied to HiGEM to correct for these biases. This is implemented by multiplying the anomaly from the mean seasonal cycle (H_{anom}) by the ratio of the standard deviations of the anomaly series (i.e., $\frac{\sigma_{Manom}}{\sigma_{Hanom}}$; see Equation 6.3). The correction is applied at daily resolution. To do this a linear blending is applied to

the seasonal values of $\frac{\sigma_{Manom}}{\sigma_{Hanom}}$ to smoothly transition between the seasons which require less variance correction (autumn) to those which require a large correction (spring).

Table 6.1 also shows the bias corrected HiGEM data. In summer, autumn and winter the magnitude of the mean temperature bias is decreased compared to the original HiGEM data. In spring the mean bias is marginally increased, however, the bias in the standard deviation of the data is reduced. The bias corrected daily-mean SAT's compare well to the MERRA data (Figure 6.4a). Differences associated with the coldest days (i.e. the winter temperatures) are reduced considerably compared to those seen in Figure 6.1a.

Table 6.1 daily-mean, land-only, 2m temperature seasonal-mean(represented by an over-bar) and standard deviation (σ) values for 36 years of MERRA data (M), 50 years of HiGEM data (H), and 50 years of bias corrected HiGEM data (H_{BC}).

Season	$\overline{M}$	$\overline{H}$	$\overline{H_{BC}}$	σM	σH	σH$_{BC}$
Spring	8.2	8.2	7.7	3.1	2.1	2.8
Summer	15.0	14.6	15.3	2.2	1.7	2.0
Autumn	10.3	11.1	10.1	3.3	2.8	3.5
Winter	4.3	6.5	4.7	2.5	1.9	2.4
Annual	9.4	10.1	9.5	4.8	3.8	4.7

The demand calculated from the bias corrected temperatures is seen to qualitatively fit much better with the MERRA data than the original HiGEM data (compare Figure 6.1b and Figure 6.4b). All quantiles sit close to the 1:1 line in Figure 6.4b therefore the bias correction has been successful. There is still a slight under-estimation of demand in HiGEM in the top 5 percentiles, due to small remaining winter temperature biases. The bias is amplified due to this being the time where demand is most sensitive to temperature.

6.2 Modelling wind power with HiGEM

Section 3.3 described the method for calculating hourly wind power capacity factor from the MERRA re-analysis (following Cannon et al. (2015)). In this section the methodology is adapted to calculate wind power capacity factor from HiGEM, using the limited near-surface wind data available from the model.

The only near-surface wind speed data available from the HiGEM control run, $2xCO_2$ and $4xCO_2$ simulations is daily-mean 10m wind speed. This is significantly lower temporal resolution than is available in MERRA, so within this analysis bias correction will be applied based on the daily-mean 10m wind speeds from MERRA.

An overview of the method is given below:
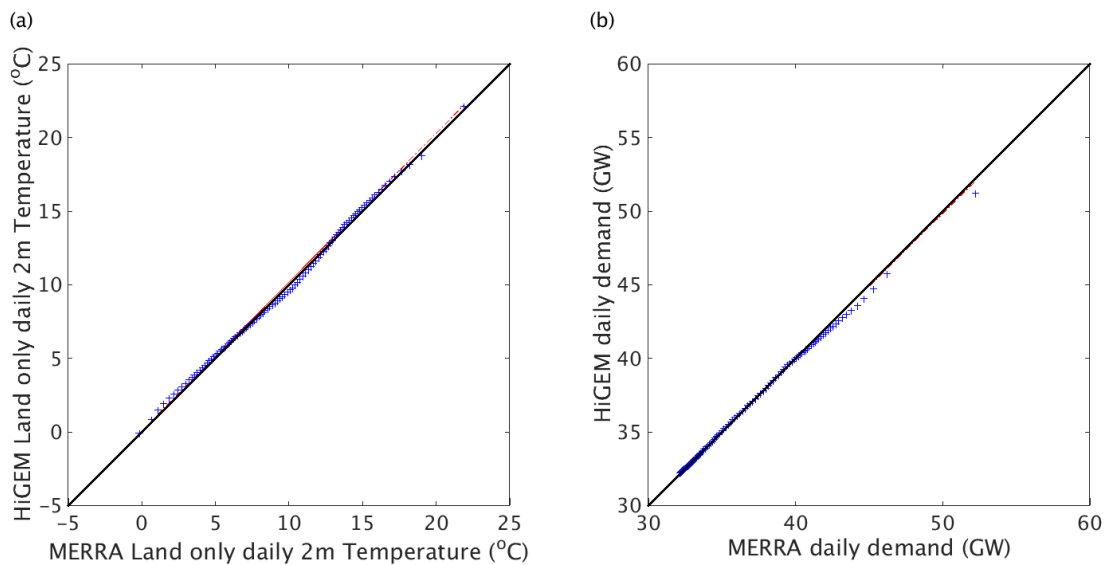
Figure 6.4 Quantile-quantile plots for MERRA vs. bias corrected HiGEM data for (a) daily-mean, land-only, 2m GB temperature (box-averaged over GB from $-11.3E$: $2.7E$ and $50N-59N$) (b) daily-mean GB demand. The black line shows a 1:1 line and red dashed line shows the line of best fit through the quantiles.

- Wind farm locations, wind farm hub-heights, the modelled wind power curve, and the 10m wind speeds are identified.

- The 10m wind speeds are interpolated onto the locations of the wind farms.

- The 10m wind speeds are extrapolated to hub-height using a logarithmic scaling law.

- The power output at each wind farm is calculated using the power curve.

- The power output is converted into a nationally-aggregated capacity factor.

The same wind farm locations, hub-heights, and power curve are used in the model of HiGEM wind power as used for the MERRA data in section 3.3. The focus of this modelling will be on the future wind farm distribution of Drew et al. (2015).

Cannon et al. (2015) used 2m, 10m, and 50m wind speeds to create a logarithmic wind speed profile at each farm location, and used these profiles to extrapolate near-surface wind speeds to hub-height wind speeds. The method of generating capacity factor using HiGEM data is different to this, as only 10m wind speeds are available. Instead a logarithmic law is used (see Equation 2.7) with a constant value of the roughness length ($z_0 = 0.05$m). This is equivalent to farmland terrain, and is commonly used in wind power

modelling (Kubik et al. (2013)). Bias correction is then applied to the hub-height wind speeds, following this the method of Cannon et al. (2015) can be completed in order to get daily-mean nationally-aggregated capacity factor. Before discussing the bias corrections applied to the hub-height wind speeds some insight into why the bias correction is required is given in section 6.2.1, and reasons for choosing to apply the correction at hub-height rather than on the raw HiGEM output are given in section 6.2.2.

6.2.1 Evaluation of HiGEM wind speeds

Quantile-quantile plots of both the daily-mean hub-height wind speed data from all farms over GB, and daily-mean aggregate capacity factor (following the method described above) from MERRA and HiGEM are compared in Figure 6.5. HiGEM's derived daily-mean, hub-height wind speeds are on average 10% lower than MERRA, for all except the top 10 percentiles, where HiGEM overestimates MERRA (Figure 6.5a). This results in HiGEM's wind power estimate producing too many incidences of low daily-mean capacity factor (Figure 6.5b). Figure 6.5a suggests that there is either a bias in:

- The daily-mean 10m wind speeds from HiGEM (hereafter in this section the daily-mean is assumed).

- The value of z_0 used to extrapolate wind speeds to hub-height.

- Both of the above.

Figures 6.6 and 6.7 shows seasonal histograms of land-only and ocean-only 10m wind speeds respectively. Land-only grid boxes are defined as boxes with a land fraction greater or equal to 50% (see Appendix 8.1). HiGEM over-estimates land-only 10m wind speeds, with the largest differences in winter (1.1ms^{-1}) and smallest in summer (0.2ms^{-1}). HiGEM is also more variable than MERRA in all seasons over land. The largest difference is seen in spring where there is a $\sim$35% difference in the standard deviation between MERRA and HiGEM data. In ocean-only regions HiGEM underestimates the 10m wind speeds, with the largest difference seen in autumn (1.9ms^{-1}). The standard deviation of the ocean-only, 10m wind speeds are comparable between MERRA and HiGEM in all seasons except summer, where the MERRA 10m wind speeds are $\sim$20% more variable.
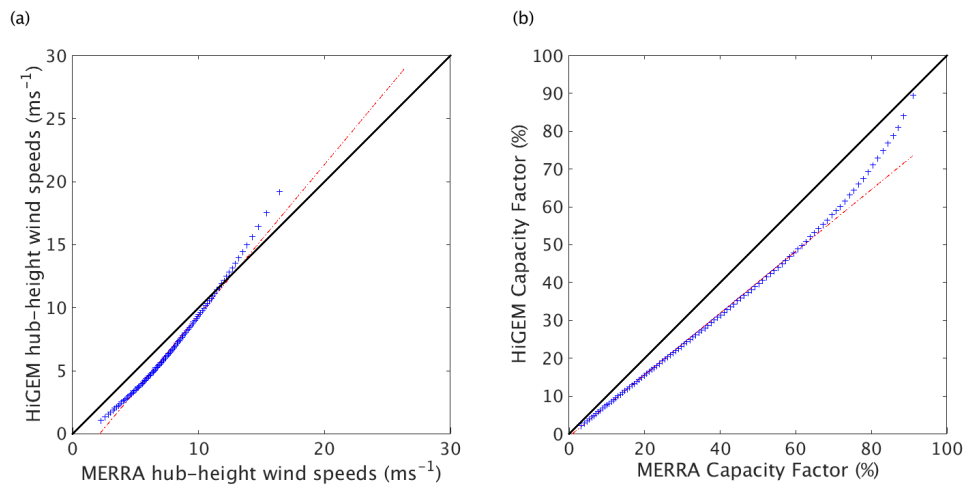
Figure 6.5   Quantile-quantile plots for MERRA vs. HiGEM showing (a) daily-mean hub-height wind speeds for all sites over GB (b) daily-mean GB aggregate capacity factor. The black line shows a 1:1 line and red dashed line shows the line of best fit through the quantiles.
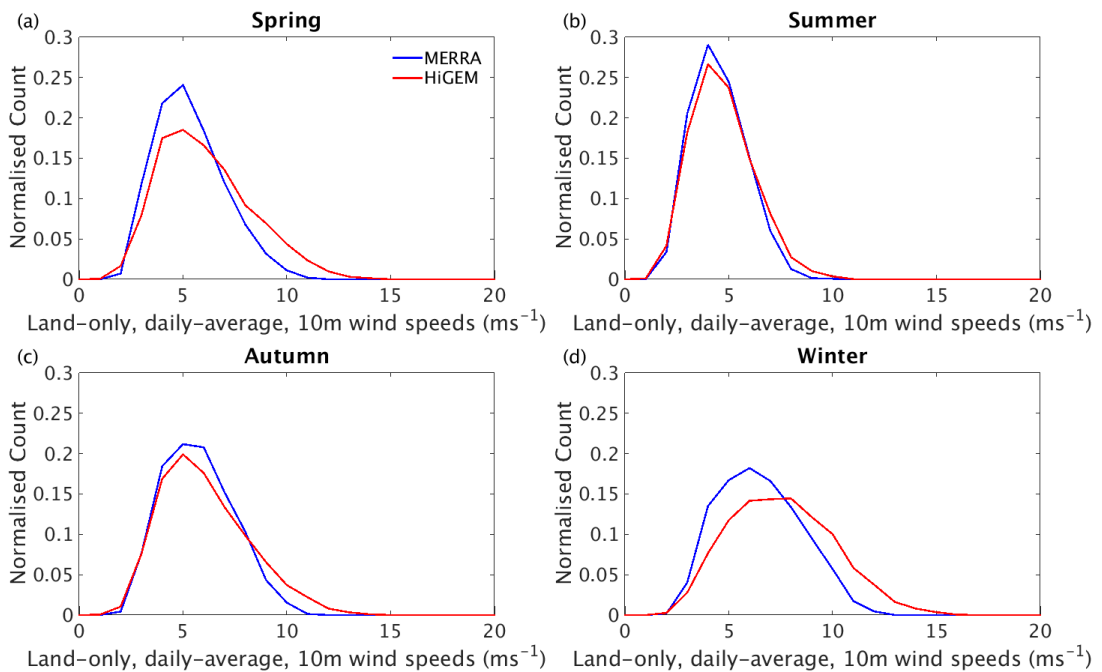
Figure 6.6   Relative frequency histograms of daily-mean, land-only, 10m wind speeds for 36 years of MERRA data (blue) and 50 years of HiGEM data (red) for (a) spring (b) summer (c) autumn (d) winter.
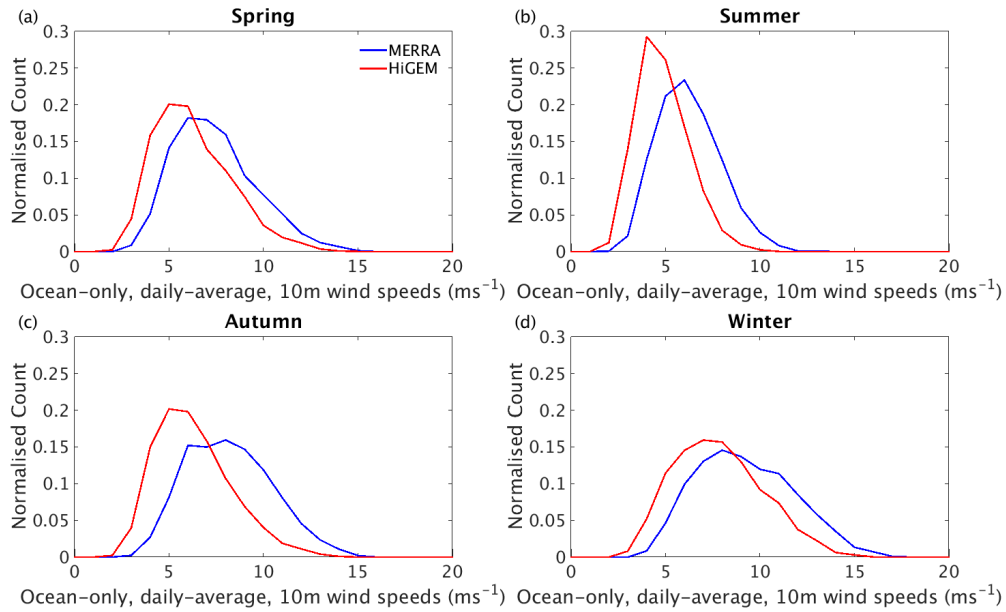
Figure 6.7 Relative frequency histograms of daily-mean, ocean-only, 10m wind speeds for 36 years of MERRA data (blue) and 50 years of HiGEM data (red) for (a) spring (b) summer (c) autumn (d) winter.

6.2.2 Evaluation of model roughness length

The wind farms of GB are located in multiple terrains. The largest distinction is between onshore and offshore wind farms. Onshore wind farms can be located in multiple environments such as farmland ($z_0 \approx 0.05$m), urban areas ($z_0 = 0.3$m-1m) or mountain regions ($z_0 > 1$m). Offshore wind farms can either be in coastal seas ($z_0 \approx 10^{-3}$) or in calm ocean ($z_0 \approx 10^{-4}$m; Freris and Infield (2008)). The HiGEM wind power model has been tested with multiple values of z_0, held constant over the whole domain, all of which could be appropriate for different individual wind farms (see Figure 3.3). Figure 6.8 shows that changing the value of z_0 leads to large changes in the daily-mean capacity factor. A z_0 of ~ 0.5m provides the best fit to the MERRA data. This value of z_0 is equivalent to the centre of a small town (Freris and Infield (2008)), which would not be appropriate for nearly all of the wind farms in the distributions.

This analysis has shown that bias correction is required to the 10m wind speed data. It has also shown that a single correction for the whole year is not appropriate. A spatial correction is also required due to the large differences in bias between the MERRA and HiGEM data in land-only and ocean-only grid boxes, and differences in z_0 at each farm location.
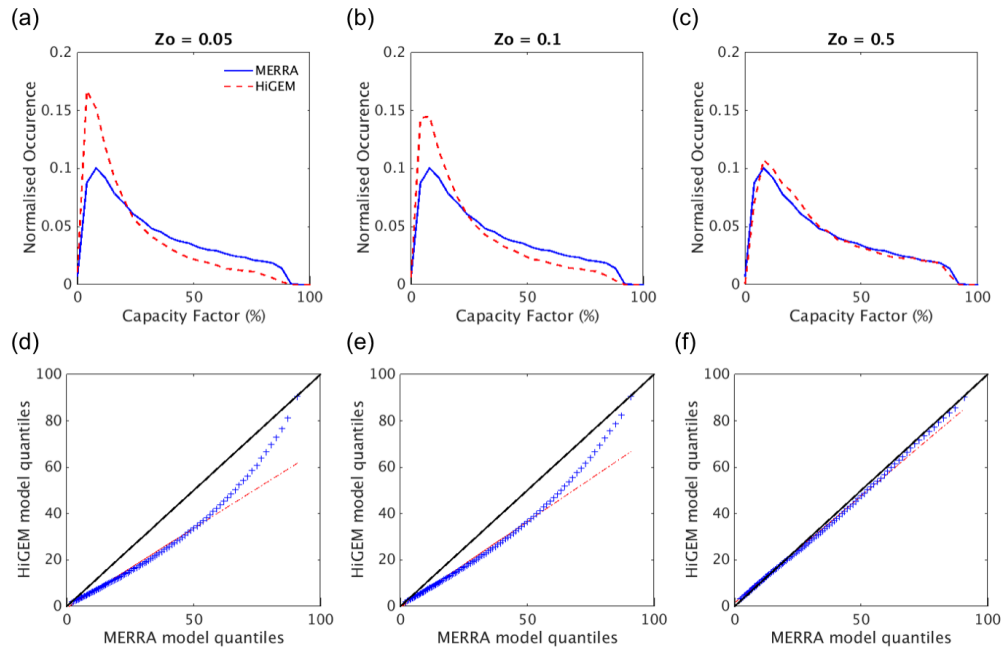
Figure 6.8 Comparison of the MERRA and HiGEM capacity factor data created using different values of z_0. (a and d) $z_0 = 0.05$ (b and e) $z_0 = 0.1$ (c and f) $z_0 = 0.5$. In subplots (d)-(f) The black line shows a 1:1 line and red dashed line shows the line of best fit through the quantiles.

6.2.3   Bias correction of HiGEM wind speeds

To correct for the bias in the HiGEM, the hub-height wind speeds from each farm in MERRA are compared to equivalent values estimated from HiGEM. A seasonal quantile correction is then applied as the wind speed bias is not constant throughout the year (see Figures 6.6 and 6.7).

Figure 6.9 shows histograms at six wind farms, from diverse locations across GB for MERRA, HiGEM and bias corrected HiGEM data. Depending on the wind farm location the size of the initial bias in HiGEM is considerably different (i.e. compare farms b and c). This suggests that bias correction at each farm location is more appropriate than a single bias correction for all farms. The bias in hub-height wind speeds at all of the wind farms (including those in Figure 6.9) is substantially reduced once the bias correction has been applied.

Figure 6.10a shows the quantile-quantile plot of the hub-height wind speeds from MERRA and the bias corrected HiGEM data. The bias corrected data no longer under-estimates the hub-height wind speeds as seen in Figure 6.5a. There is still a small bias in the bias corrected hub-height, wind speeds. However, the bias corrected data is a vast

Figure 6.9 Relative frequency histograms of 36 years of MERRA data (blue) 50 years of HiGEM data (red) and 50 years of bias corrected HiGEM data (red dotted) at 6 wind farm locations across GB which are shown on the map.

improvement compared to the original HiGEM data. The corrected wind speeds result in a much more accurate distribution of daily-mean capacity factors (compare Figure 6.10b with Figure 6.5b).
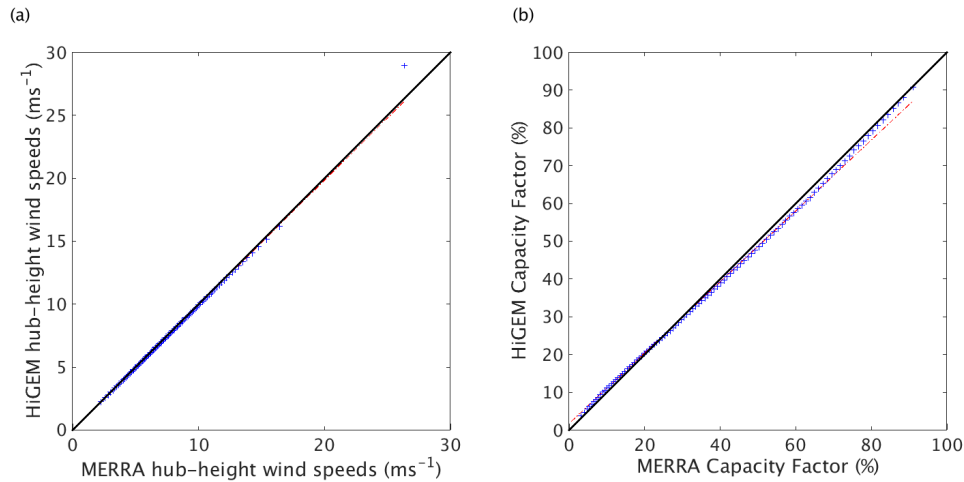
Figure 6.10 Quantile-quantile plots of MERRA data vs bias corrected HiGEM data for (a) daily-mean, hub-height wind speeds for all farms over GB (b) daily-mean aggregate capacity factor. The black line shows a 1:1 line and red dashed line shows the line of best fit through the quantiles.

6.3 Evaluating key characteristics of bias corrected HiGEM

6.3.1 Inter-annual variability of wind power

Chapter 4 showed that a large proportion of the inter-annual variability present in the GB power system is due to inter-annual variability in wind power generation, therefore it is important that the inter-annual variability of the HiGEM wind power capacity factor data are examined in detail.

Figure 6.11a shows a histogram of the annual average GB aggregate capacity factors from the MERRA and bias corrected HiGEM wind power models. A good agreement is seen between the distributions of annual aggregate capacity factor between MERRA and bias corrected HiGEM, with only 0.7% difference in mean annual aggregate capacity factor. However, there is less variability in the bias corrected HiGEM capacity factors (with 33% more variability seen in annual aggregate capacity factor in MERRA). This could be due to sampling uncertainty between the 50 years of data and 36 years of MERRA data, or due to moderate amounts of bias remaining in the corrected HiGEM capacity factor data (Figure 6.10).

Figure 6.11b shows the absolute differences between adjacent years annual aggregate capacity factor. HiGEM captures the general behaviour seen in MERRA, however, it

does not have many large year-year differences. It would be particularly important for these differences to be captured if HiGEM was to be used for wind farm site assessment, as large year-year swings in wind power output could result in wind farms not being able to make loan repayments.

The similarity between the properties of the GB aggregate capacity factor data for MERRA and bias corrected HiGEM suggest that the bias corrected HiGEM data can be used to model GB wind power generation. However, the HiGEM data should be treated with caution as although more years of data are used, there is still not as much inter-annual variability in capacity factor as seen in MERRA. This has the potential to impact the inter-annual variability of power system operation discussed in later sections.
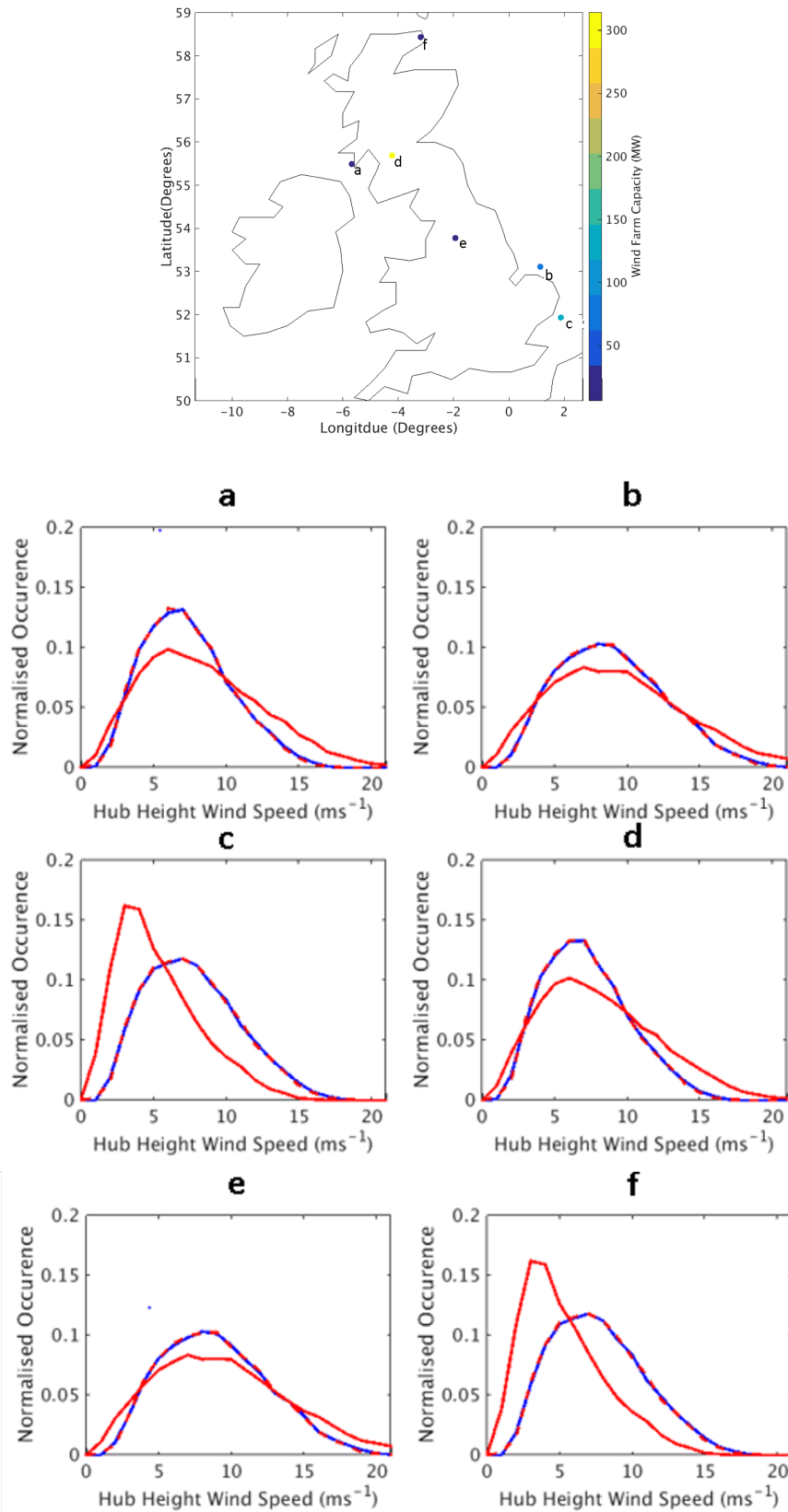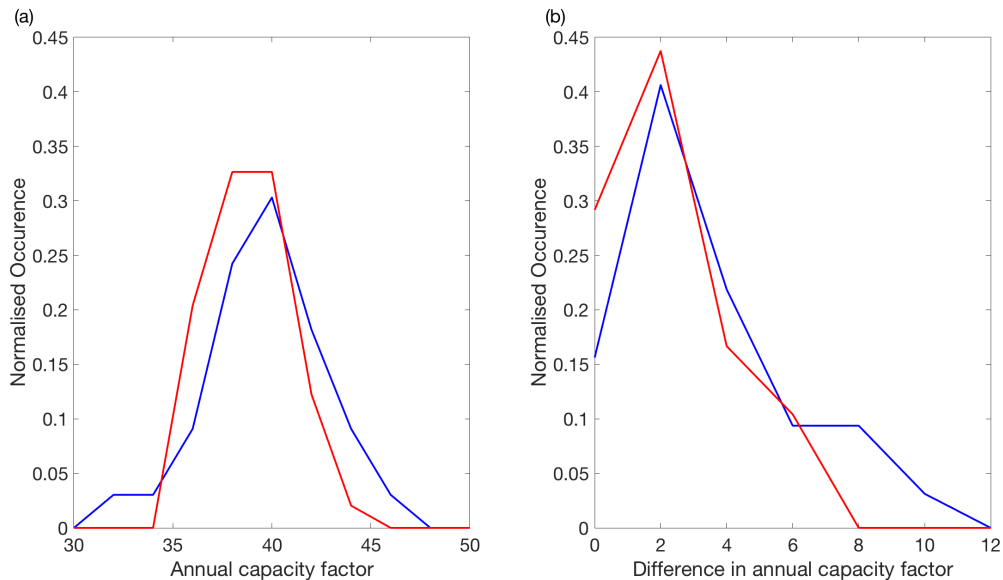

Figure 6.11 Relative frequency histograms of 36 years of MERRA data (blue) 50 years of HiGEM data (red) and 50 years of bias corrected (BC) HiGEM data (red dashed) for (a) Annual average capacity factors (b) the difference between adjacent years annual capacity factor (%).

6.3.2 Daily co-variability of wind speed and temperature in HiGEM

In this chapter so far little regard has been given to the daily co-variability of the temperature and wind speed data, and how bias correction may impact this. Maintaining the co-variability between temperature and wind speed is important as the quantity impacting the GB power system in this study is demand-net-wind (DNW; i.e. hourly demand - hourly wind power generation). If HiGEM does not initially have accurate co-variability between temperatures and wind speeds, or if the bias correction has altered the co-variability of the temperature and wind speed time series compared to that seen in MERRA, this may have consequences for DNW, which could impact values of the power

system metrics used for later analysis.

Figure 6.12 shows bi-variate histograms of daily-mean SAT and hub height wind speeds from 30 years of MERRA (1980-2009) and the first 30 years of the HiGEM control run. Figure 6.12d shows that before the bias correction the biases in both temperature and wind speed impacted the co-variability of the series when compared to MERRA. These biases are present in all seasons (not shown). After bias correction there is an overall reduction in the differences in co-variability between MERRA and HiGEM, with only small biases remaining (see Figure 6.12e). Tests with other analysis periods of HiGEM (including resampling with replacement) confirm that the choice of period for analysis does not impact the results shown in Figure 6.12.
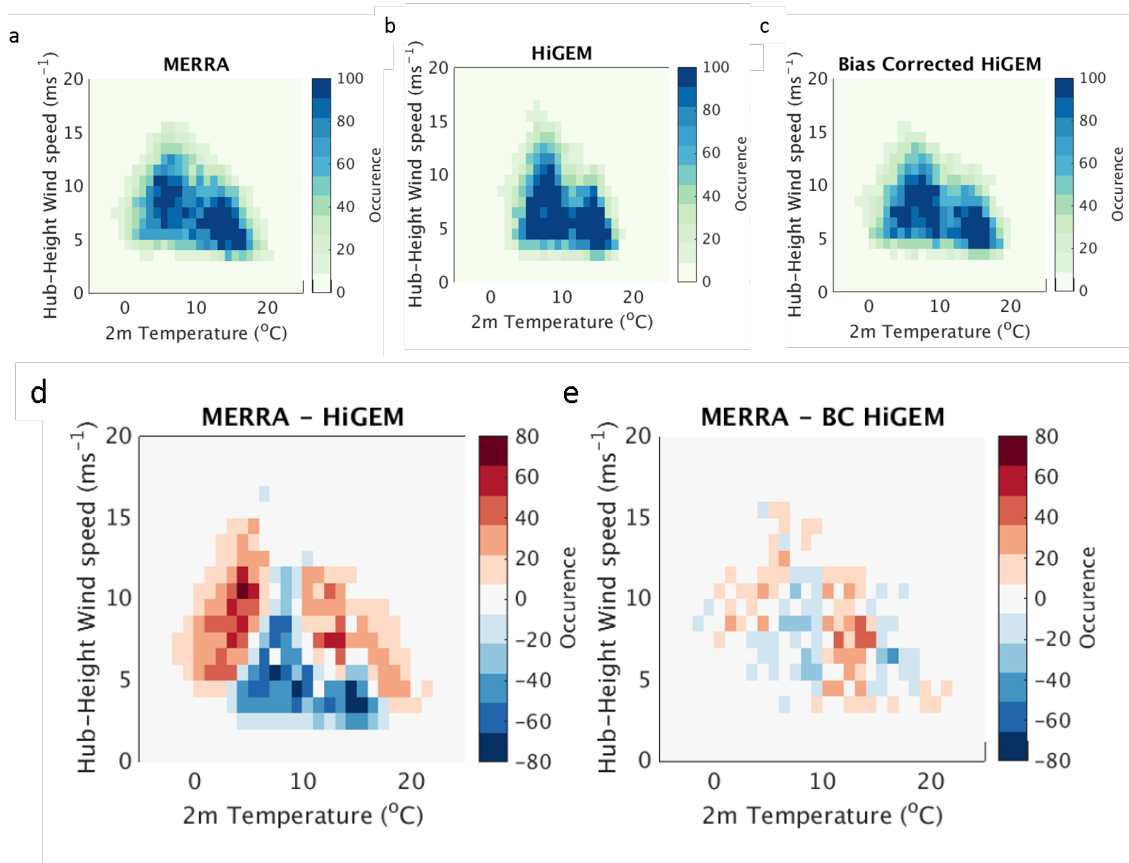
Figure 6.12   Bi-variate histograms of daily-mean temperature vs daily-mean hub-height wind speed for (a) MERRA (b) HiGEM (c) Bias corrected HiGEM (d) MERRA - HiGEM (e) MERRA - Bias corrected HiGEM. 30 years of MERRA data (1980-2009) are used with the first 30 years of the HiGEM control run simulation.

This section has shown that following bias correction the daily co-variability between HiGEM's wind speed and temperature is in good agreement with MERRA. This analysis has given confidence that HiGEM can provide useful information for power system modelling, and has highlighted that climate models which reproduce the co-variability of near-surface temperature and wind speed can be an important tool to generate consistent

time-series of demand and wind power generation. The consistency that can be provided from climate model data is more suitable for power system modelling studies than using purely statistical techniques (such as used in Curtis et al. (2016)) as maintaining the co-variability of wind power generation and demand, results in the improved simulation of the impacts of wind power generation on power systems.

6.4 The impact of present-day climate variability on the GB power system using HiGEM

This section explores whether bias-corrected climate model output can be used to investigate the impact of climate variability on power systems. HiGEM is used for this analysis (see section 3.1.2 and Shaffrey et al. (2009) for details). The impact of temporal resolution of the available HiGEM data on power system operation is discussed in section 6.4.1. Following this a selection of the metrics from chapter 4 are analysed for the NO-WIND and HIGH scenarios using HiGEM (sections 6.4.2 and 6.4.3 respectively). This is in order to determine the affect that using the lower resolution HiGEM data could have on the analysis of the impact of climate change on the GB power system.

6.4.1 The impact of temporal resolution on wind power capacity factor variability

The only common wind speed outputs from HiGEM's control, and future climate simulations that can be used to generate wind power capacity factor data are daily-mean 10m wind speeds. This section investigates how the reduction of temporal resolution (from hourly to daily) impacts the power system metrics calculated using HiGEM. To do this the MERRA data is analysed at multiple time resolutions, degrading its temporal resolution from hourly to daily.

Figure 6.13a shows the first 7 days of MERRA-derived capacity factors from the year 1980 for three methods of creating hourly capacity factor (similar results are seen for all time periods in all years). The hourly capacity factor (orange line) fluctuates throughout each day. The blue line shows the daily-mean capacity factor (note that the sum of the orange and blue lines over a 24 hour period are not equal due to the non-linear relationship between wind speed and capacity factor). The daily-mean capacity factor in Figure 6.13a shows much less variability than the hourly capacity factor. The yellow line in Figure 6.13a shows an hourly interpolation between the daily-mean capacity factor values, which

generally follows the trend of the hourly capacity factor time series. However, there are large fluctuations in capacity factor over small time periods which are not captured by the interpolated capacity factor time series. These periods might be problematic for power system modelling as maintainting the co-variability of wind power generation and demand has been shown to be important for accurate power system modelling results (see section 6.3).
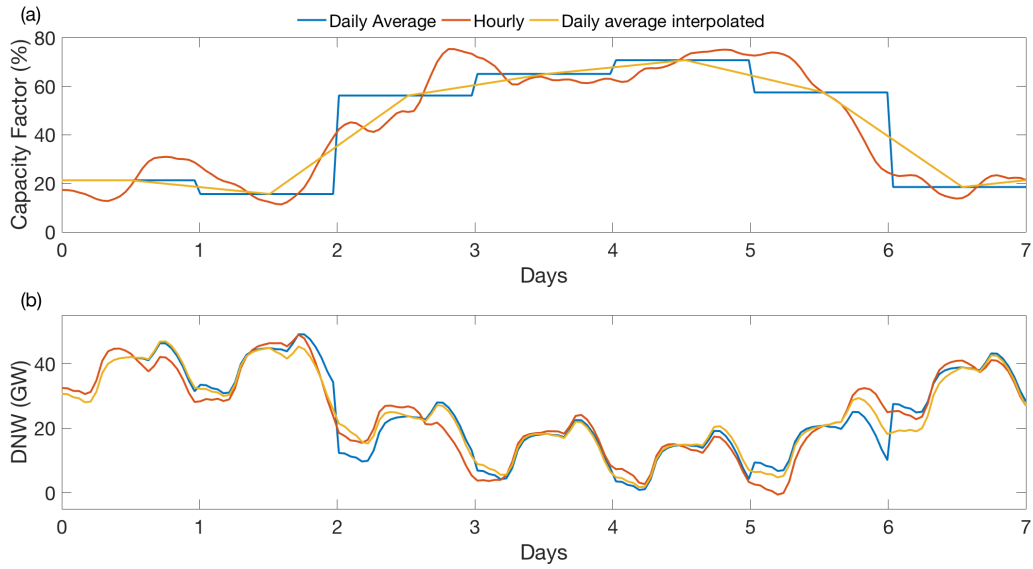
Figure 6.13 The first 7 days from 1980 of (a) of MERRA-derived wind power capacity factor using the method of Cannon et al. (2015) (b) Demand-net-wind (DNW) for: hourly data (orange) daily-mean data (blue) and an hourly interpolation between daily-mean data (yellow).

Figure 6.14 shows annual and seasonal histograms of hourly wind power capacity factor for the three temporal resolutions of MERRA data from Figure 6.13. A general result seen in all seasons is that the interpolated time series has less hours with capacity factor between 0-20% and 80-100%, and more hours with capacity factor of 20-40%, resulting in the daily-mean capacity factors being more comparable to the hourly capacity factors. However, these differences are small and generally the temporal resolution of the data has had a small impact on the distribution of capacity factors.

The hourly variability of power system metrics created using each series may still be significantly different. Selected power system metrics for the HIGH scenario (the focus of the analysis in following sections) are given for all three data resolutions in Table 6.2.

The magnitude of the mean TAER, mean peaking plant TVE and mean peak load are very similar between the hourly, hourly interpolated and daily-mean datasets. There are larger differences in the mean baseload TVE between the three datasets. This is due to hours of baseload plant operation being associated with both low demand and high wind
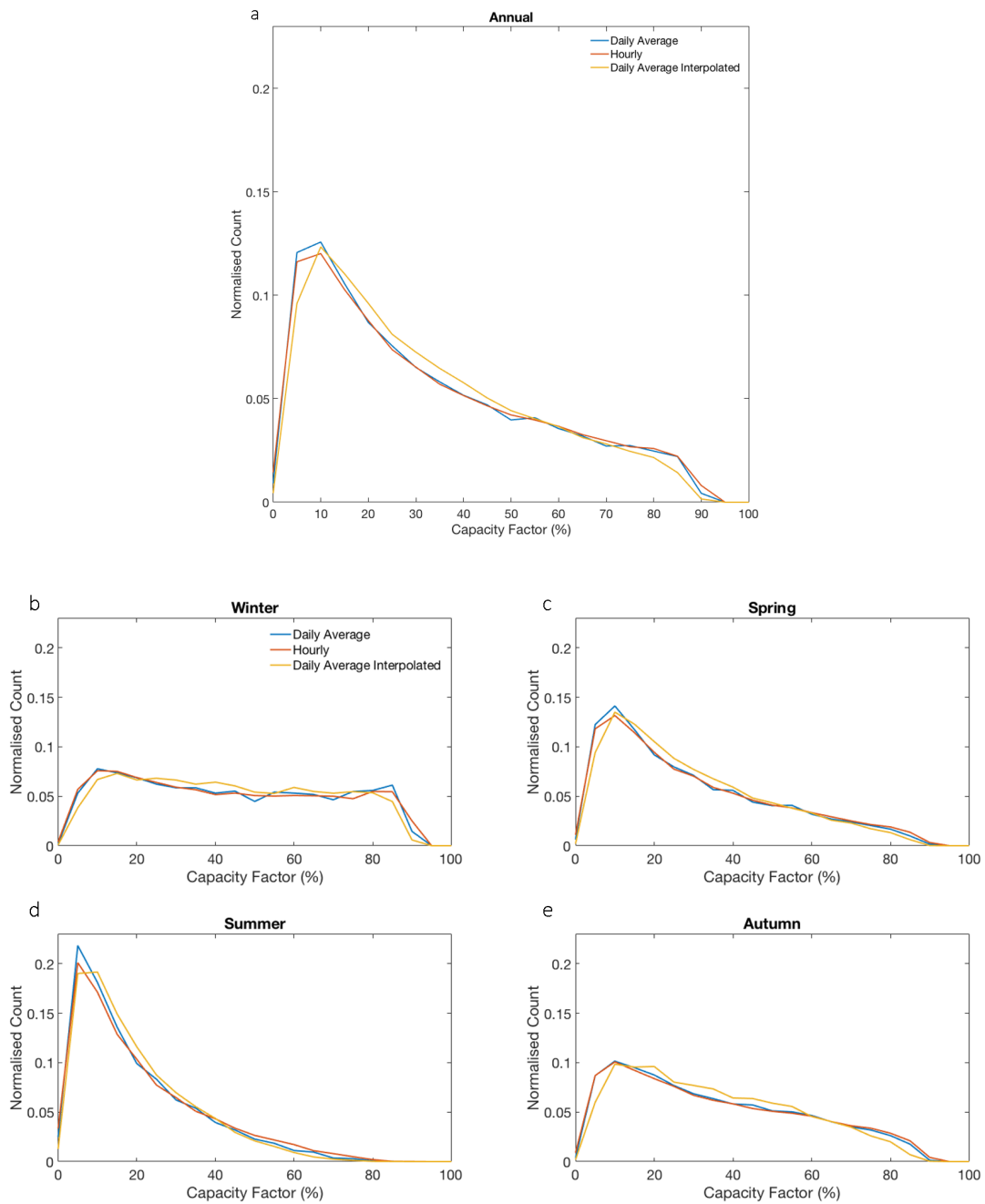
Figure 6.14 Relative frequency histograms of hourly wind power capacity factor data using the method of Cannon et al. (2015) on 36 years of MERRA data for hourly data (orange) daily-mean data (blue) and an hourly interpolation between daily-mean data (yellow) for (a) annually (b) winter (c) spring (d) summer (e) autumn

power production. The hours of low demand are well represented due to the inclusion of the diurnal cycle in the demand model. The hours of highest night-time wind power production in the hourly MERRA data are not present in the daily-mean, or interpolated time series.

Table 6.2 Mean and inter-annual max-min range of TAER, Peaking plant TVE, Baseload plant TVE and Peak load in the HIGH wind power scenario using multiple temporal resolutions of MERRA.

Scenario	Data	TAER (TWh)		Peaking Plant energy (TWh)		Baseload Plant energy (TWh)		Peak Load (GW)	
		Mean	Range	Mean	Range	Mean	Range	Mean	Range
HIGH	MERRA hourly	170	48.7	2.0	1.2	18.0	55.0	50.1	8.2
HIGH	MERRA interpolated	170	53.8	2.0	1.5	24.0	69.0	49.4	9.2
HIGH	MERRA daily-mean	170	54.3	2.0	1.2	16.2	65.0	50.1	8.4

The peak load and peaking plant TVE metrics are reproduced well with lower resolution data. This is thought to be due to these metrics being generally associated with times of low wind power generation and high demand. The demand is unchanged in all of the simulations, therefore this suggests that low wind power generation events are reproduced better by the daily-mean and interpolated data than high wind power generation events.

The results in Table 6.2 suggest that using lower resolution wind power generation data can have some small consequences for the potential operating opportunity and inter-annual max-min range of baseload plan operation. A 10% difference in the inter-annual max-min range of TAER is also seen between the hourly and interpolated data. Overall, the lower resolution data is able to reproduce the operating characteristics of the GB power system well and should not have large consequences for the interpretation of results in the remainder of this chapter.

In this study the daily-mean data has been chosen for analysis as it captures the behaviour of baseload TVE and peak load better than the interpolated data series. This is an interesting result which shows that care needs to be taken when creating hourly data from lower resolution data as different methods lead to significantly different results.

6.4.2 Impact of climate variability on a power system with no installed wind power capacity

In this section the values of the power system metrics under the NO-WIND scenario are compared using MERRA and bias corrected HiGEM derived inputs. This is in order to evaluate the ability of HiGEM to reproduce the power system behaviour seen in chapter

4. The only input for the NO-WIND scenario is demand, which is calculated in the same way for MERRA and HiGEM. The metrics discussed in this section therefore explore the demand-driven-variability present within the power system.

Table 6.3 shows the selected power system metrics created with 36 years of MERRA and 50 years of HiGEM data. The mean values of the metrics are comparable between MERRA and HiGEM, with the largest difference (8%) seen for peaking plant TVE. HiGEM's reduced mean peak load and peaking plant TVE are due to the moderate warm bias remaining in winter temperatures after bias correction (resulting in reduced winter demands; see section 6.1.2).

The inter-annual max-min range of all power system metrics are also comparable between MERRA and HiGEM, with the largest differences seen for TAER and peak load. A comparable number of cold years (resulting in high TAER) are seen between MERRA and HiGEM, however an extreme warm year (therefore low TAER) analogous to 2007 is not seen in the fifty year HiGEM record (Figure 6.15) leading to the reduced inter-annual range. A similar result is seen for peak load (not shown). The question of whether HiGEM is able to simulate warm years (such as 2007) would require further investigation with a longer time series of HiGEM data or an ensemble simulation (which is beyond the scope of this thesis).

The implication of using HiGEM rather than MERRA for analysis is that the moderate remaining bias in winter temperatures is leading to small deviations in peaking plant operation to those observed in MERRA. Sampling uncertainty between the years of MERRA and HiGEM used result in a different set of extreme conditions in MERRA and HiGEM, therefore moderately influencing the max-min range of power system metrics. Overall the differences between MERRA and HiGEM derived power system metrics for the NO-WIND scenario are small. This shows HiGEM can be used to model GB power system operation well in systems with no installed wind power capacity.

Table 6.3 Mean and inter-annual max-min range of TAER, the total energy required from Peaking and Baseload plant (in TWh) and peak load (GW) using two different climate inputs. All conducted using the NO-WIND wind power scenario.

	TAER (TWh)		Peaking Plant energy (TWh)		Baseload Plant energy (TWh)		Peak Load (GW)	
Dataset	Mean	Range	Mean	Range	Mean	Range	Mean	Range
MERRA	320	9.1	1.3	0.7	227	3.8	55.0	9.1
HiGEM control	321	8.2	1.2	0.7	224	4.1	54.7	8.6
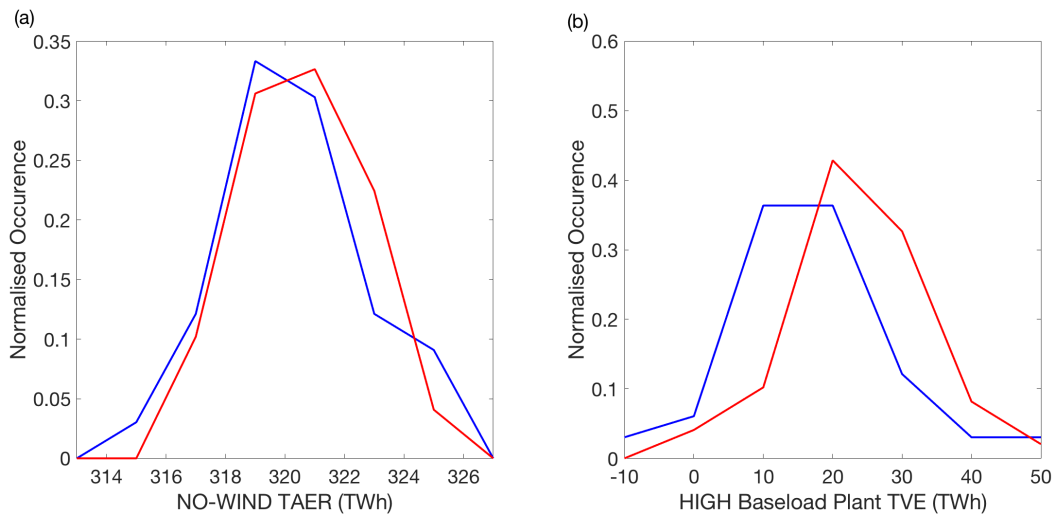
Figure 6.15 Relative frequency histograms using MERRA (blue) and HiGEM (red) to create (a) TAER from the NO-WIND scenario. (b) Baseload TVE from the HIGH scenario

6.4.3 The impact of climate variability on a power system with a high installed wind power capacity

Examining demand in isolation is useful for understanding, but is not relevant for the current GB power system as there is already ∼15GW of wind power capacity installed and significant investments are planned in the near future (National Grid (2015)). In this section metrics are calculated from HiGEM and MERRA data for the HIGH scenario. HiGEM wind power generation is calculated using the daily-mean method described in section 6.4.1. The HiGEM derived metrics are then compared to the metrics from chapter 4 calculated from hourly MERRA data.

Table 6.4 Mean and inter-annual max-min range of TAER, the total energy required from Peaking and Baseload plant using two different climate inputs and the HIGH wind power scenario.

	TAER (TWh)		Peaking Plant energy (TWh)		Baseload Plant energy (TWh)		Peak Load (TWh)	
Dataset	Mean	Range	Mean	Range	Mean	Range	Mean	Range
MERRA	170	48.7	2.0	1.2	18.0	55.0	50.1	8.2
HiGEM control	169	37.8	1.9	1.4	23.1	50.4	49.0	10.2

The mean value of TAER, peaking plant TVE, and peak load compare well between HiGEM and MERA (Table 6.4). The mean value of Baseload TVE is ∼20% larger when calculated using HiGEM data, compared to MERRA (see Table 6.4). Table 6.2 shows that using daily-mean wind speed data leads to a 15% *reduction* in the mean baseload TVE. The increase seen in Table 6.4 is therefore not due to the method of using daily-

mean wind speed data, but due to differences between the MERRA and HiGEM wind speeds. Figure 6.11 showed that the mean annual average capacity factor in HiGEM is lower than MERRA by 0.7%, with MERRA containing a larger range of capacity factors. The increased mean capacity factor in MERRA results in reduced DNW, which has lead to the reduced mean baseload TVE (see Figure 6.15).

The max-min range of peaking plant TVE, and peak load are moderately larger in the HiGEM than in MERRA and the max-min range of TAER and Baseload TVE are reduced in HiGEM compared to MERRA (Table 6.4). These differences are due to the reduced inter-annual variability of the capacity factors calculated using the fifty years of HiGEM data compared to MERRA (Figure 6.11). HiGEM also has a moderate low bias in capacity factor remaining after bias correction (Figure 6.10) which could exacerbate this problem.

This section has shown that in a system that includes a large amount of wind power generation the differences in power system metrics are larger than those seen in section 6.4.2 for the NO-WIND scenario. However, HiGEM is still able to produce the power system metrics calculated from MERRA well, and there is confidence that it can be used in the following sections to investigate the impact of climate change on the GB power system.

6.5   The impact of climate change on GB electricity demand in HiGEM

This section discusses how a changing climate could impact daily-mean electricity demand using the HiGEM control run, idealised $2xCO_2$, and $4xCO_2$ simulations. The $2xCO_2$ scenario occurs at ~2070 in Relative Concentration Pathway scenario 8.5 (RCP8.5) from the Intergovernmental panel on climate change (IPCC) 5th assessment report, whereas $4xCO_2$ occurs at ~2100 (Kirtman et al. (2013)). The bias correction determined in section 6.1 for the control run data is performed on the $2xCO_2$ and $4xCO_2$ simulations. It is assumed that model bias remains constant in a future climate. The focus of this section is daily-mean demand, although qualitatively the same results are seen if the hourly demand is used (i.e. by including the seasonal diurnal cycle anomaly curves).

Figure 6.16 shows normalised histograms of daily-mean, SAT for the HiGEM control run, $2xCO_2$, and $4xCO_2$ simulations. Figure 6.16a shows there is an annual-mean increase in temperature from the control run to the $2xCO_2$ simulation of 1.2^oC. This is further

increased in the 4xCO$_2$ simulation (with a difference of 3.4^{o}C between the control run and 4xCO$_2$ simulation). Figure 6.16b-e shows that this increase in mean temperature is present in every season, however, the largest seasonal-mean increase is seen in summer (4.9^oC between the control run and 4xCO$_2$ simulation), and smallest increases in winter (1.9^oC between the control run and 4xCO$_2$ simulation).

The inter-annual max-min range of 2m temperatures is greater in the 2xCO$_2$ simulation than the control run by 0.3^{o}C, with a larger difference seen between the 4xCO$_2$ simulation and control run (1.2^{o}C). The large difference between the 4xCO$_2$ simulation and the control run is due to a large warming trend being present in the 4xCO$_2$ simulation over GB. The inter-seasonal variability of daily-mean, SAT also increases from the control run to the future climate simulations, with the largest increases in autumn.
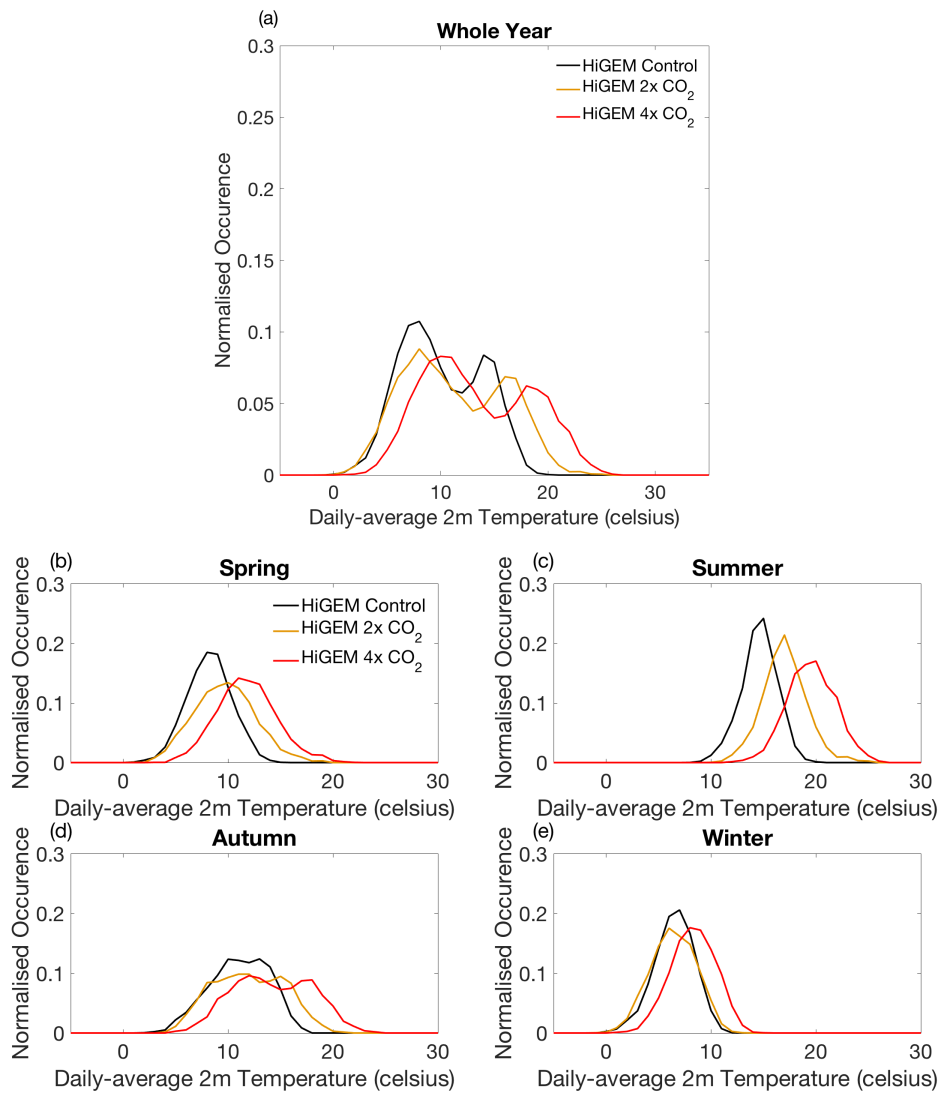
Figure 6.16   Relative frequency histograms of daily-mean 2m temperatures from the HiGEM control run (black) HiGEM 2xCO$_2$ scenario (orange) and HiGEM 4xCO$_2$ scenario (red) for (a) the whole year (b) spring (c) summer (d) autumn (e) winter.

Histograms of daily-mean demand for the whole year and individual seasons are shown in Figure 6.17a-e. Analysing the whole year shows that there is a reduction in the intra-annual variability of daily-mean demand in both the future climate scenarios (with a 15% reduction seen by the 4xCO$_2$ simulation; Figure 6.17a). There is a reduction in days with a daily demand of over 45GW and in days with daily demand less than 33GW. The largest reduction is seen for winter, where the inter-annual max-min range of winter demands reduces by 11% between the control run and 4xCO$_2$ simulation.
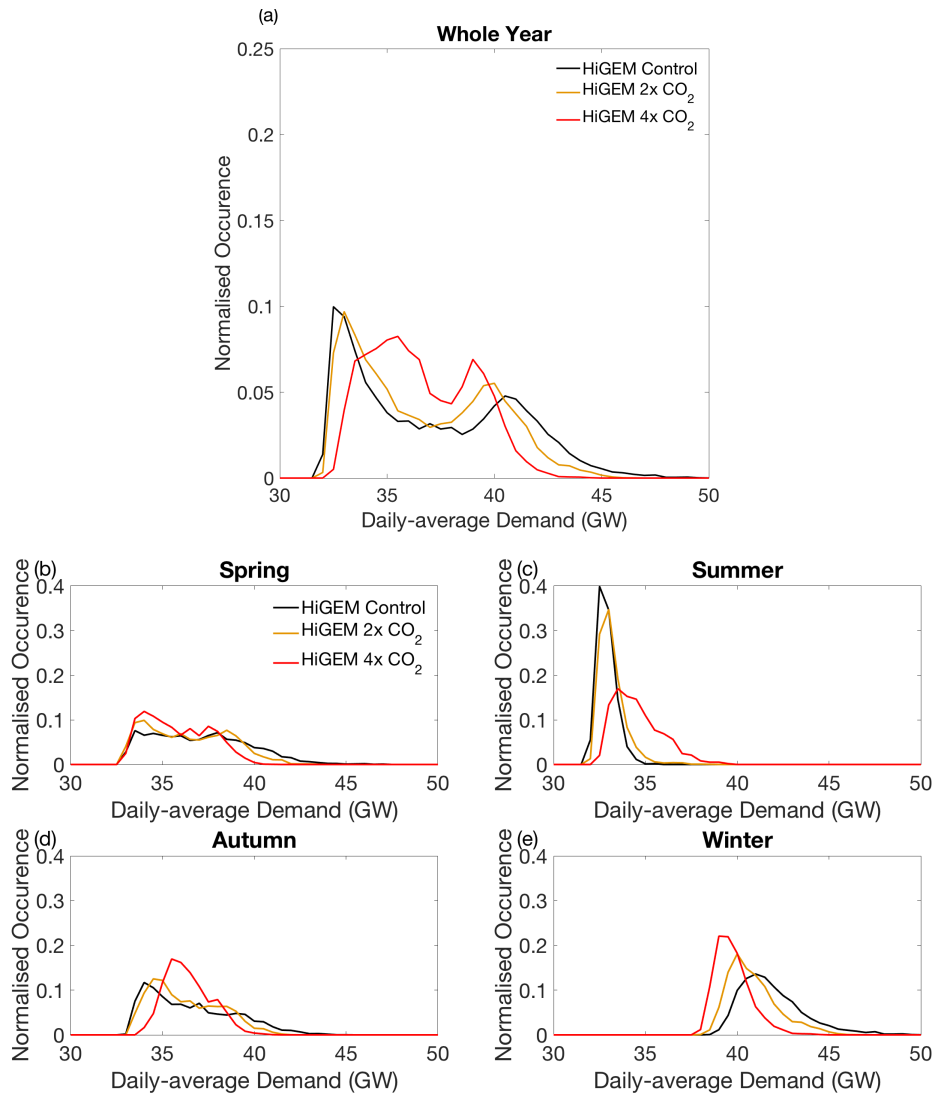
Figure 6.17 Relative frequency histograms of daily-mean demand calculated from the HiGEM climate model control run (black) 2xCO$_2$ simulation (orange) and 4xCO$_2$ simulation (red) for (a) the whole year (b) spring (c) summer (d) autumn (e) winter.

The reduction in the number of days with demand greater than 45GW is due to the reduction in winter and spring daily demands in a warmer climate (see Figure 6.17). This reduction is due to the temperature increase in these seasons being located in the most sensitive region of the u-shaped demand function, with warmer temperatures meaning a

reduced heating demand (see Figure 6.18). In winter the 3.2^oC increase in temperature between the control run and $4xCO_2$ simulation results in a 2.1GW reduction in mean demand ($\sim$-5%), with a mean temperature increase of 1.5^oC in spring associated with a 1.3GW reduction in mean demand ($\sim$-5%; see Figure 6.18). In summer the mean demand increases in a future climate (by 1.7GW between the control run and $4xCO_2$ simulation; $\sim$+5%). This is due to summer temperatures beginning to be present in the uptick of the u-shaped temperature response, with warmer temperatures leading to increased cooling demand.

The change in the mean demand is less obvious than the changes in intra-annual demand. A 0.5GW reduction in the mean demand is seen between the control run and $2xCO_2$ simulation, associated with a 1.2^oC increase in annual-mean temperature. A similar magnitude of reduction in mean demand is also seen between the control run and the $4xCO_2$ simulation ($\sim$0.5GW), but in this case associated with a much larger increase in annual-mean temperature ($\sim3.5^oC$; see Figure 6.18). The similarity in mean demand between the $2xCO_2$ and $4xCO_2$ simulations is due to the trade-off present between warmer winters and springs requiring less heating-induced demand, and warmer summers requiring increased cooling-induced demand (see Figure 6.18).
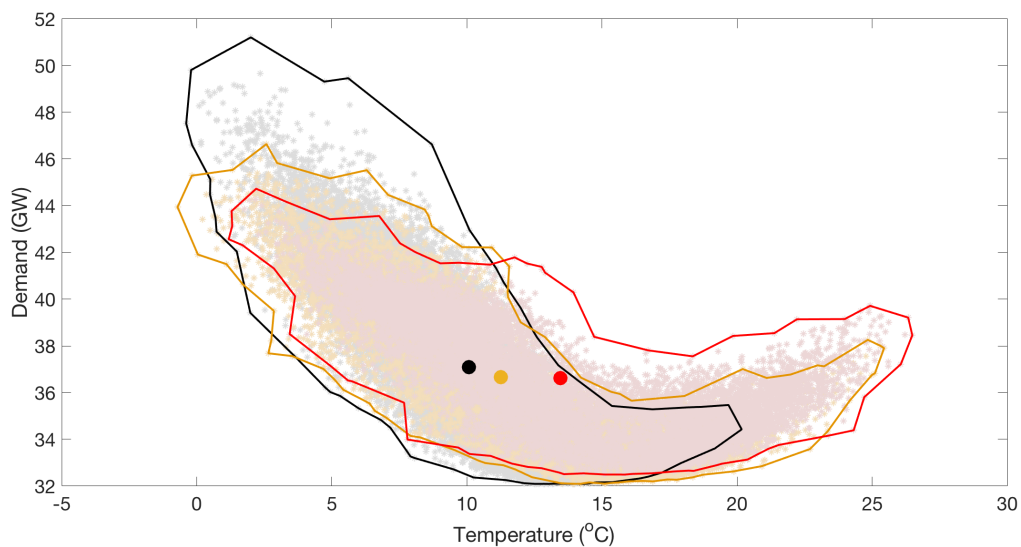
Figure 6.18 Daily-mean temperature vs. daily-mean demand for the HiGEM control run (grey scatter points with the boundary marked in black) $2xCO_2$ simulation (orange scatter points and boundary) and $4xCO_2$ simulation (red scatter points and boundary). The mean temperature vs. demand from each simulation is given as large scatter points.

The change in the seasonal behaviour of demand with increasing temperature can be seen clearly in Figure 6.19. An increase in the mean seasonal cycle of temperature is seen in both the $2xCO_2$ and $4xCO_2$ simulations (Figure 6.19a) with the largest increase

seen in summer. These increases in temperature lead to a reduction in the seasonal cycle of demand (Figure 6.19b). In the $2xCO_2$ simulation the reduction in the seasonal cycle is confined to winter and spring. This is due to small changes in spring and winter temperature resulting in a large change in demand (see u−shaped relationship in Figure 6.18). In the $4xCO_2$ simulation the winter and spring demands see further reductions due to increasing temperatures. This is accompanied by increases in mean seasonal cycle during summer, due to more temperatures being present in the up-tick of the u-shaped relationship (see Figure 6.18). The implications of increasing temperatures on demand and total power system operation are discussed in section 6.8.
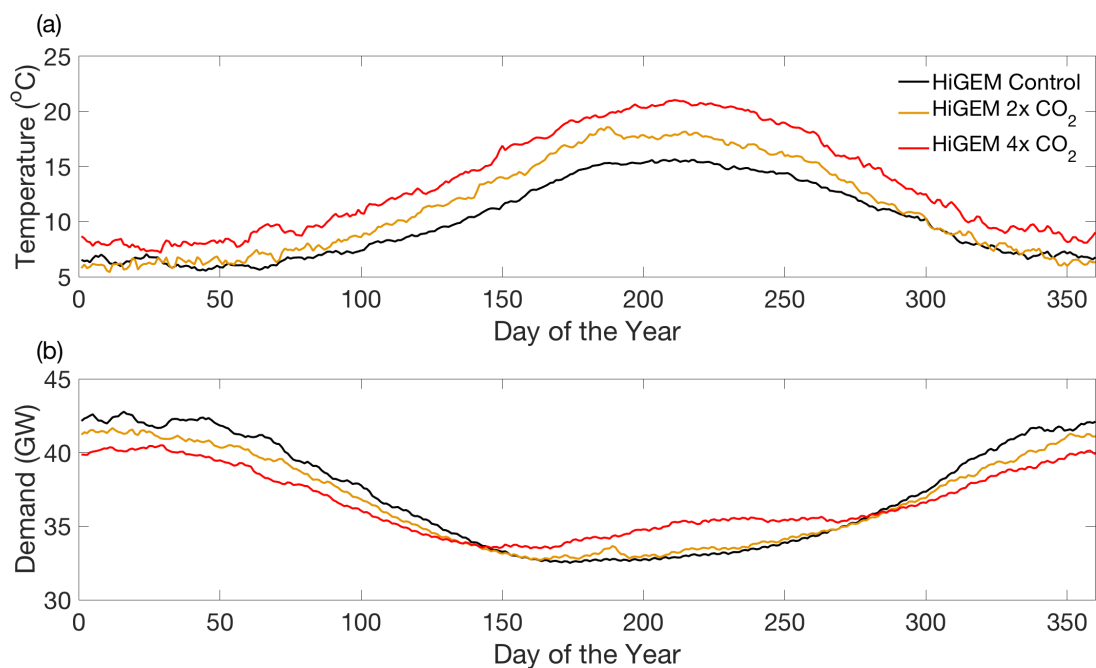
Figure 6.19 Mean seasonal cycle comparison for 60 years of the HiGEM control run (black) 30 years of the $2xCO_2$ run (orange) and 30 years of the $4xCO_2$ run (red) for (a) daily-mean, land-only, 2m temperature (b) daily-mean GB demand.

The results discussed in this section are strongly influenced by the design of the demand model (see Section 3.2 for details of its construction). The model includes a quadratic relationship between temperature and demand, which results in the increased demand for cooling in summer and heating in winter. This relationship is kept constant in the future climate scenarios. Previous studies have shown that the shape of the quadratic relationship between temperature and demand differs significantly between countries (see Figure 2.3, Bessec and Fouquau (2008), Psiloglou et al. (2009)). This could mean that the assumed quadratic structure used in this thesis is not appropriate in a future climate. This would be an interesting point for future research, but is beyond the scope of the current project.

6.6 The impact of climate change on GB wind power production in HiGEM

This section shows how the amount of wind power produced by a set wind turbine distribution may be impacted by climate change. To do this wind power generation is calculated for the HIGH scenario, across the three HiGEM simulations (control, $2xCO_2$, and $4xCO_2$). It is assumed that the model's wind speed bias is constant in a changing climate.

Normalised histograms of GB aggregate, daily-mean, wind power capacity factor are plotted in Figure 6.20 for all three HiGEM simulations. Only small differences are present between the annual and seasonal histograms, suggesting there may only be small changes in wind power generation over GB in a future climate. The largest statistically significant, seasonal-mean change in GB aggregate, daily-mean, wind power capacity factor between the control run and $2xCO_2$ simulation is seen in winter, with a 1% increase. This agrees with Cradden et al. (2012), Nolan et al. (2012), Hueging et al. (2013) and Tobin et al. (2015), however, these studies also found a reduction in summer-mean capacity factor, which is not seen in the $2xCO_2$ simulation (negligible change is seen).

Comparing the control run and $4xCO_2$ simulation shows a 2% reduction in summer-mean and a 4% reduction in spring-mean wind power capacity factor (shown to be statistically significant using a 2-sample test) as seen in Cradden et al. (2012), Nolan et al. (2012), Hueging et al. (2013) and Tobin et al. (2015). However, this is accompanied by a negligible change in winter-mean capacity factor and 2% increase in autumn-mean capacity factor. This suggests that the response of wind power generation to climate change is complex, and requires a multi-model assessment for a more robust determination of future changes.

Figure 6.21 shows the long-term-mean zonal wind and wind speed anomalies at 10m above the surface for the HiGEM future simulations and control run. Figure 6.21 shows that there are visible differences in long-term daily-mean 10m wind speed over the North Atlantic, but these differences are very small over GB, consistent with only small changes seen in the capacity factor distributions. Figure 6.21 agrees with the findings of Catto (2009) which showed minimal changes in 920hPa wind speed over GB in the $2xCO_2$ simulation.

Figure 6.21 shows that the changes in wind *speed* over GB from HiGEM are much smaller than the changes in zonal wind over GB. The changes in zonal mean 10m wind
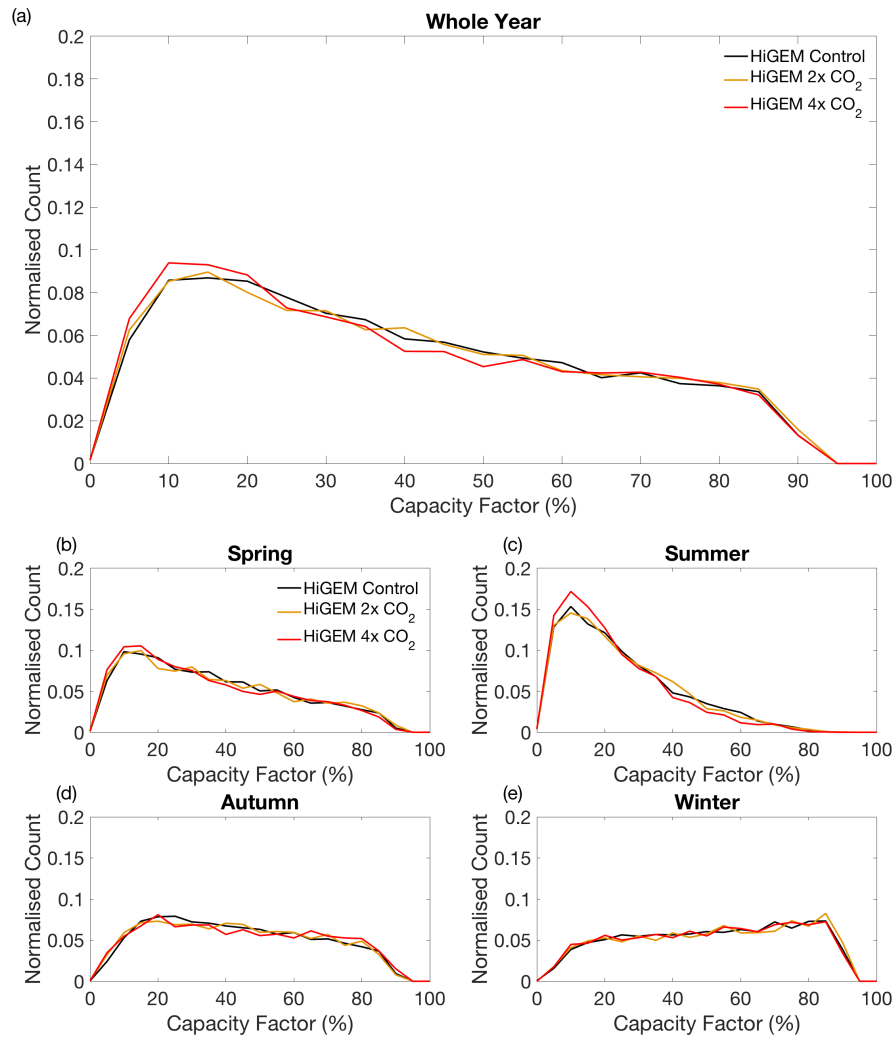
Figure 6.20 Relative frequency distributions of hourly GB aggregate capacity factor from the HiGEM control run (black) $2xCO_2$ simulation (orange) and $4xCO_2$ simulation (red) for (a) the whole year (b) spring (c) summer (d) autumn (e) winter.

speed in HiGEM look similar to the mean change in storm track density found by Zappa et al. (2013b) when using the full CMIP5 model distribution. This shows that HiGEM behaves similarly to the CMIP5 multi-model mean, however, it is noted that there is a large spread within the CMIP5 models responses to climate change. The implications of the changes in wind power generation in a future climate are discussed in section 6.8.

6.7 The impact of climate change on the GB power system

Table 6.5 shows the mean and max-min range of a selection of power system metrics calculated using the HiGEM control run, $2xCO_2$, and $4xCO_2$ simulations for the HIGH wind power scenario (i.e., 45GW of installed wind power capacity). A reduction in the mean, and max-min range of all of the metrics is seen in the $2xCO_2$ simulation compared
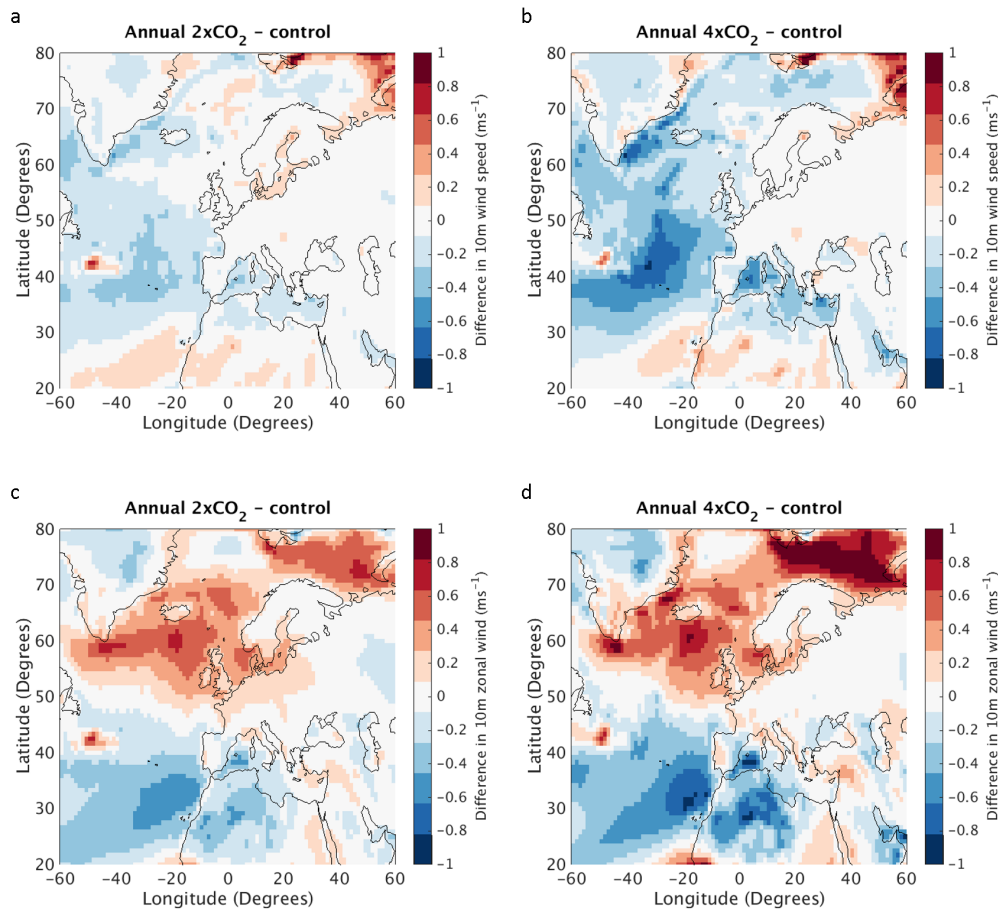
Figure 6.21 Changes in long-term mean wind for (a) 10m wind speed HiGEMs $2xCO_2$ - control run (b) 10m wind speed $4xCO_2$ - control run (c) 10m zonal wind HiGEMs $2xCO_2$ - control run (b) 10m zonal wind $4xCO_2$ - control run.

to the control run. The changes in metric values between the control run and $2xCO_2$ simulation are generally larger than the changes in metric values between the $2xCO_2$ and $4xCO_2$ simulations (Table 6.5). The impact of climate change on each of the metrics from Table 6.5 are described in more detail in the following subsections.

6.7.1   Total Annual Energy Requirement

The mean value of TAER is reduced by 3% from the control run to the $2xCO_2$ simulation. Figure 6.22a shows that between the control run and $2xCO_2$ simulation there is a moderate reduction in high hourly loads and a moderate increase in low hourly loads. The largest seasonal changes between the control run and $2xCO_2$ simulation is seen in winter (Figure 6.22b). This is due to the combined effects of reduced heating-induced demand (due to warmer temperatures) and a 1% increase in winter capacity factor.

Section 6.5 showes how summer demand may increase due to increased requirement

for cooling (Figure 6.17). However, Figure 6.22b shows that in the $2xCO_2$ simulation there are no noticeable differences in summer hourly load. This suggests that hours of increased demand are also hours of increased wind power generation in the $2xCO_2$ simulation.

A similar, small reduction in mean TAER is seen when the control run and $4xCO_2$ simulation are compared (Table 6.5). Figure 6.17 shows that the seasonal changes in load are larger than previously seen in the $2xCO_2$ simulation. A larger reduction in the highest winter loads is seen, with it also being more common to have hours of very low load in winter (Figure 6.22b). The largest seasonal changes in load are present in summer, where more hours of high load are seen compared to the control run and $2xCO_2$ simulation, and less hours of low load. These changes are due to the increase in temperature causing large increases in summer demands (Figure 6.17) and reductions in wind power generation (Figure 6.20). The mean reduction in TAER is less than seen in the $2xCO_2$ simulation as cooling-induced demand is increasing more than heating-induced demand is reducing (Figure 6.18).

Table 6.5   Mean and inter-annual max-min range of TAER, the total energy required from Peaking and Baseload plant, and peak load using three different HiGEM simulations. All conducted using the HIGH wind power scenario. Percentages show the difference between the control run and future simulation value.

	TAER (TWh)		Peaking Plant energy (TWh)		Baseload Plant energy (TWh)		Peak Load (GW)	
Simulation	Mean	Range	Mean	Range	Mean	Range	Mean	Range
HiGEM control	169	37.8	1.9	1.4	23.1	50.4	49.0	10.2
HiGEM $2xCO_2$	164 (-3%)	34.1 (-10%)	1.6 (-16%)	0.9 (-36%)	18.6 (-20%)	42.1 (-17%)	47.4 (-4%)	5.9 (-43%)
HiGEM $4xCO_2$	166 (-2%)	42.7 (+12%)	1.4 (-27%)	1.0 (-30%)	15.9 (-32%)	48.0 (-5%)	46.1 (-6%)	6.4 (-38%)

Chapter 4 showed that when large amounts of installed wind power capacity are present then the behaviour of the wind power generation controls the power system metrics more than the behaviour of demand (which varies over much smaller ranges). The changes in mean TAER between the control run, $2xCO_2$ and $4xCO_2$ simulations are only small due to the similarity of the DNW time series between the three simulations (see Figure 6.22a) This is due to the similarities in the wind power generation between the three simulations (see Figure 6.20).

The inter-annual max-min range of TAER is reduced by 10% in the $2xCO_2$ simulation compared to the control run. The distributions of hourly load look similar between the control run and $2xCO_2$ simulation (Figure 6.22a). This therefore suggests the range of loads experienced in all years in the $2xCO_2$ simulation is more similar than in the control run. This could potentially aid system balancing (see section 6.8 for further discussion).

In contrast, an increase in the max-min range of TAER is seen between the control

run and $4xCO_2$ simulations. This suggests that the range of annual conventional operating conditions is increased. This is due to the inter-annual max-min range of summer temperatures increasing by 50% from the control run to the $4xCO_2$ simulation, therefore in some years the high hourly loads from Figure 6.22d are seen.
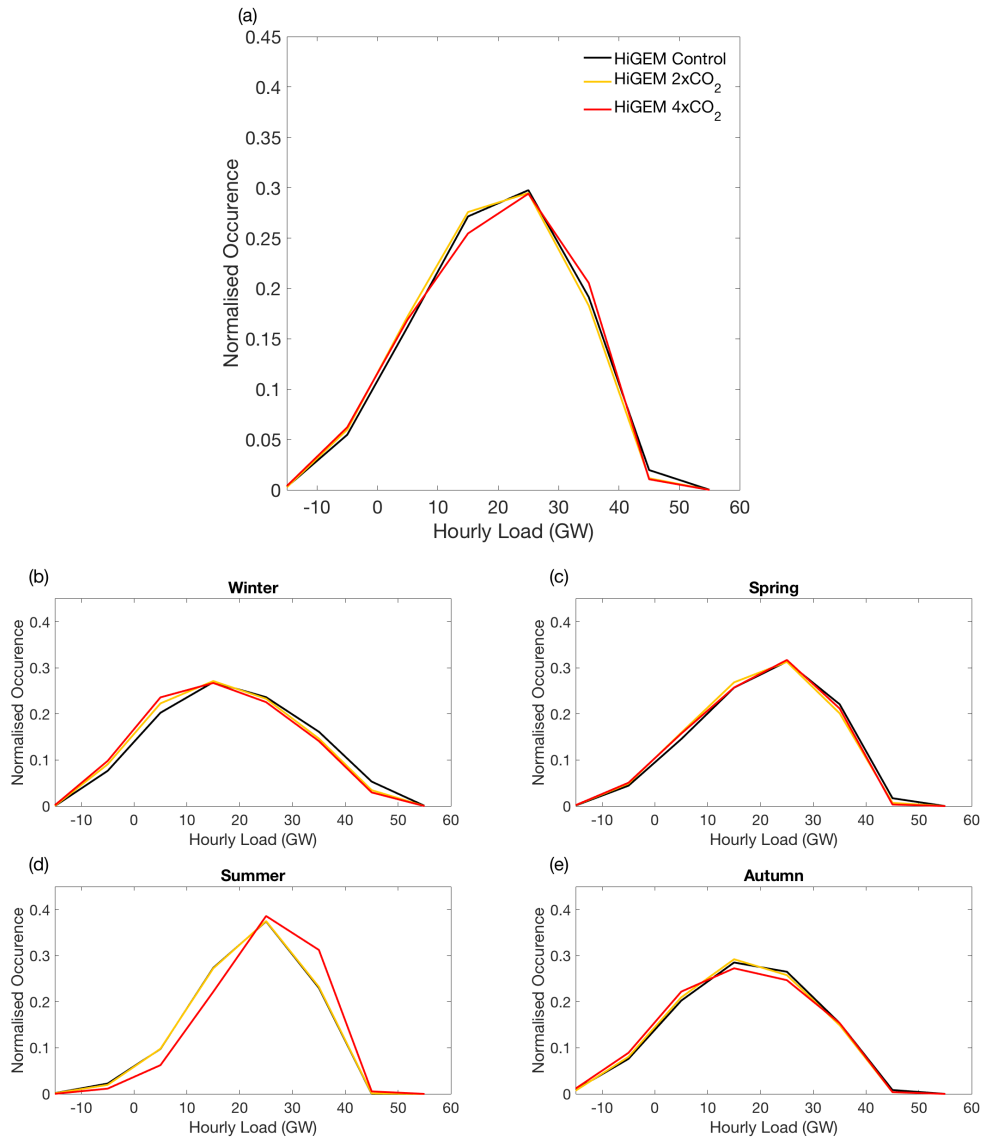
Figure 6.22 Relatively frequency histograms of hourly load from the HIGH scenario calculated from the HiGEM climate model control run (black) $2xCO_2$ simulation (orange) and $4xCO_2$ simulation (red) for (a) the whole year (b) spring (c) summer (d) autumn (e) winter.

6.7.2 Peaking Plant TVE

The mean value of peaking plant TVE reduces by 16% from the control run to the $2xCO_2$ simulation (Table 6.22). The hours in the LDC that contribute towards the peaking plant TVE metric are associated with hours of low wind power generation in the extended winter season (see section 5.6). The mean winter demand reduces by 1GW

between the control run and $2xCO_2$ simulations, as well as this the mean winter capacity factor is increased by 0.5%, resulting in a reduction in winter load (Figure 6.22b) and therefore a reduction in mean peaking plant TVE.

The further reduction in peaking plant TVE from the control run to the $4xCO_2$ simulation is predominantly due to a larger reduction in mean winter demand (a mean winter temperature increase of 1.9^oC results in a mean winter demand reduction of 2.1GW in the $2xCO_2$ simulation). This results in a reduction in hourly load (Figure 6.22b) and therefore a reduction in mean peaking plant TVE.

The 36% reduction in the max-min range of peaking plant TVE from the control run to the $2xCO_2$ simulation is due to daily winter demand becoming less variable. This is due to increasing temperatures resulting in winter demands existing in the base of the u-shaped relationship between temperature and demand (see Figure 6.18). This results in a reduction in the max-min range of mean winter load of 20% from the control run to the $2xCO_2$ simulation, leading to a reduction in the max-min range of peaking plant TVE.

A smaller reduction in the max-min range of peaking plant TVE is seen from the control run to the $4xCO_2$ simulation (30%; Table 6.22). The reduction is less because the reduction in the max-min range of mean winter load is only 11% (compared to the 20% reduction seen from the control run to the $2xCO_2$ simulation).

The changes in peaking plant TVE between the control run and future simulations are large compared to the changes seen for TAER. This is due to peaking plant TVE's dependency on winter, where a clear reduction in the mean and max-min range of mean winter load are seen, whereas, TAER is dependent on all seasons weather. Increases in summer load counteract reductions in winter load, leading to smaller changes in TAER (Figure 6.18).

6.7.3 Baseload TVE

Chapter 5 showed that in the HIGH scenario hours from all months of the year are used to create the baseload TVE metric, therefore the changes in load in all seasons are examined below.

The mean baseload TVE reduces by 20% from the control run to the $2xCO_2$ simulation. This is due to the reduction in seasonal-mean load in winter (-8%) spring (-5%) and autumn (-3%). The further reduction in mean baseload TVE in the $4xCO_2$ simulation is due to the further reductions in mean demand in, autumn (-5%) and winter (-15%) when

compared to the control run, with both seasons having more hours of low load in Figure 6.22.

The reduction in max-min range of baseload TVE in the $2xCO_2$ simulation is due to all seasons (except summer) experiencing a $\sim$20% reduction in the max-min range of seasonal loads compared to the control run. The reduction in Baseload TVE is only 5% between the control run and $4xCO_2$ simulation. Mean summer load increases by 12% in the $4xCO_2$ simulation (see Figure 6.22d), accompanied by a 10% increase in the max-min range. This counteracts the reductions in inter-annual variability of baseload TVE seen in the $2xCO_2$ simulation (due to the reduced variability seen in winter, spring, and autumn).

6.7.4 Peak Load

In the HIGH scenario peak load is associated with hours of high winter demand and low wind power generation. This section therefore focusses on the upper percentiles of winter load. The reduction in the mean peak load in the $2xCO_2$ simulation is associated with the 8% reduction in winter-mean load (predominantly due to the 1GW reduction in winter-mean demand). The reduction in peak load shows it is increasingly uncommon for the extreme cold temperatures required for present day peak load to be reached in a warmer climate. A further reduction in mean peak load occurs in the $4xCO_2$ simulation due to the 12% reduction in mean winter load (mostly due to the 2.1GW reduction in mean demand).

A large reduction in the max-min range of peak load is seen when the control run is compared to the $2xCO_2$ simulation. This is due to the daily demands being less variable in the $2xCO_2$ simulation, with it being increasingly unlikely for demands to be present in the up-tick of the u-shaped temperature-demand relationship (see the boundary in Figure 6.18).

The max-min range of peak load in the $4xCO_2$ simulation is larger than seen in the $2xCO_2$ simulation (Table 6.22). This is due to the $4xCO_2$ simulation having a larger max-min range of winter-mean demands than the $2xCO_2$ simulation (a max-min range of 11.3GW is seen in the $4xCO_2$ simulation compared to 10.1GW in the $2xCO_2$ simulation).

6.8 Implications of climate change for GB power system operation

A quadrupling of CO_2 concentrations has been shown to result in a 5% reduction in mean winter demand, due to a reduced requirement for heating in a warmer climate. This reduction in mean winter demand is accompanied by a 5% increase in summer demand due to an increased requirement for cooling. These seasonal changes lead to a reduction in the seasonal cycle of demand, which could lead to changes in the operating opportunity of conventional power stations. The potential reduction in the seasonal cycle of demand in a future climate is beneficial to system operators, as the type of generation operating throughout the year could become more uniform. Increases in summer demand could also mean that there is less renewable energy curtailment (which was shown to happen in chapter 5 at times of low summer demand).

Small changes in potential future wind power generation are seen compared to demand. A quadrupling of CO_2 concentrations results in a ~0.5% reduction in mean winter wind power capacity, and a 2% increase in summer capacity factor. Potential changes in the location of areas of high wind power generation are important for wind farm developers, who are building wind farms that could be operational towards the end of the century. The consistency of the capacity factors seen in Figure 6.20 between the control run and future climate simulations suggests that wind farms built over GB now could still be able to provide similar amounts of wind power generation in a future climate.

The potential changes in the demand and wind power generation in a future climate have important consequences for GB power system operation. The combination of a reduction in mean demand but only small changes in mean wind power capacity factor result in only small changes to the total annual energy requirement of the GB power system under climate change. However, less generation is required from peaking plant and baseload plant to meet system load (see Table 6.5). This is useful information for potential plant investors.

Chapter 4 showed that including large amounts of installed wind power capacity had the largest impacts on baseload plant operation. Climate change is shown here to also have a large potential impact on mean baseload plant operating opportunity (Table 6.5). However, the max-min range of baseload plant operating opportunity is reduced in both of the future climate simulations. This suggests that potential increases in inter-annual variability of the baseload plant operation due to increased wind power generation may

be counter-acted by climate change.

The reduction in mean peak load in a future climate could mean that there is the potential for less conventional generation to be required to meet the most extreme demands. This would be beneficial for system operators who would have to pay less generation to be present in case a high demand event occurs. The potential reduction in max-min range of peak load is also beneficial for system operation as it would mean that there is more confidence in the amount of generation needed to be on standby in case of an extreme event.

HiGEM has provided useful insight to the potential changes in mean and inter-annual variability of the GB power system, however, this is a single model. Substantial spread is present within the CMIP5 ensemble of models, which should be incorporated into this analysis as future work if it is to provide more meaningful results to power system modellers. This is further discussed in chapter 7.

A key assumption within this chapter is that the future GB power system will look very similar to the current system, with the inclusion of large amounts of wind power generation. This is one of many possible pathways which the GB power system could take, and further work could investigate other options for power system operation.

6.9   Chapter Summary

This section has shown that HiGEM can be used to create weather-dependent inputs for power system modelling, with the use of bias correction. Through bias correction, the co-variability of near surface temperatures and wind speeds was improved (compared to re-analysis). It is important for this to be retained for modelling of power systems including temperature dependent demand, and wind power generation, and highlights that power system modelling techniques relying on weather-generators, may create unrealistic co-variability between demand and wind power generation.

Key results on the impact of climate change on the GB power system are given below:

- The impact of climate change on the GB power system was analysed using two future climate simulations from HiGEM ($2xCO_2$ and $4xCO_2$). In the $2xCO_2$ simulation an increase in temperature is found in every season when compared to the control run. This results in a reduction in the heating-demand for GB during spring, autumn, and winter and an increase in the cooling-demand in summer (as suggested by Isaac and van Vuuren (2009)). This response is further pronounced in the $4xCO_2$

simulation.

- The inter-annual and inter-seasonal variability of demand decreases in winter, spring and autumn in the future climate simulations but increases in summer. The seasonal cycle of demand is also reduced in both future climate simulations.

- Minimal changes in both the mean and inter-annual variability of potential future wind power generation are seen in a future climate. This suggests that changes in mean and inter-annual variability of wind power generation due to climate change are small compared to the changes which are seen when the distribution of wind farms over GB is changed.

- When analysing the GB power system as a whole, the mean value of all of the power system metrics is reduced when compared to the control run, predominantly due to a reduction in mean winter demand. This suggests that less conventional generation could be required in a future climate, particularly in winter.

- The inter-annual max-min range of all power system metrics is reduced in a future climate when compared to the control run. This is predominantly due to the reduction in both the mean and max-min range of winter demand, which causes the majority of weather-dependent inter-annual variability in a present climate.

This chapter has highlighted that climate models can be used to provide useful information for power system modelling studies. Synoptic timescale co-variability of near-surface temperatures and wind speeds has been shown as important to accurately reconstruct the power system metrics (and is therefore important for power system planning). HiGEM reproduces the co-variability between temperatures and wind speeds seen in MERRA well. However, if HiGEM was used without validation, there could be significant errors in the demand and wind power generation, resulting in large errors in the co-variability between the two series.

The results from this section should not be taken as definitive conclusions on the future response of the GB power system to climate change. Within the literature there is a large spread results concerning the potential change in wind power generation over GB in a future climate (e.g., Hueging et al. (2013), Tobin et al. (2015)). As well as this Mirasgedis et al. (2007) have shown that the impact of climate change on demand is extremely sensitive to the magnitude of the warming experienced. A more rigorous assessment of the impact of climate change on the GB power system is therefore needed. This would require the comparison of multiple climate models, encompassing a wide range

of climate projections. Further discussion on the implications of this work are given in chapter 7.

Chapter 7:

Discussion and Conclusions

The impact of inter-annual climate variability on power system operation is commonly overlooked by power system modellers due the difficulties of using appropriate climate model data, and the high computational cost of repeating multiple years of simulations (Mideksa and Kallbekken (2010), Pfenninger and Keirstead (2015)). The impact of climate change on power system operation has also received little detailed examination in the literature due to the low spatial resolution of climate model data and the issues associated with model bias (Dowling (2013)). This thesis has aimed to estimate the impact of inter-annual climate variability and climate change on the GB power system and understand its meteorological drivers. To do this an idealised modelling framework has been constructed based on LDCs.

LDCs allow for the use of multi-decadal records of demand and wind power generation data. This is often missing from energy system modelling studies, which may be limited to the use of either a *typical meteorological year* or even to a series of time slices of representative system operation days within a season. The use of single years of data is not appropriate when modelling systems including renewable generation due to the low-frequency variability that is present in the climate system. However, using single years of data is common practise within the literature (George and Banerjee (2011), De Jonghe et al. (2011), Ueckerdt et al. (2015), Pfenninger and Keirstead (2015), Buttler et al. (2016)).

The LDC approach treats GB as an aggregate zone, with no spatial constraints on the generation and transmission of energy to localised areas of demand. This means that this study is not able to provide information about temporal phenomena such as plant ramping rates, or on spatial phenomena such as network constraint. Rapid technological development in the coming decades (such as increased demand-side management, or

energy storage) is also not accounted for in the current modelling framework.

In order to analyse the LDCs a series of metrics were constructed as proxies for power system operation. Similar metrics have been used in other studies in the field to understand the behaviour of conventional generation in a system including wind power (e.g. George and Banerjee (2011) and Buttler et al. (2016)) but in these studies the focus is again limited to the analysis of one year of meteorological data. These metrics provide an idealised description of power system operation, as their construction does not account for the temporal behaviour of the power system such as power plant ramping rates or part loading of plant. The metrics are instead intended to give an indication of the impact of inter-annual climate variability on different aspects of a potential power system.

The modelling framework used in this thesis is readily adaptable to any country in which a large amount of renewable generation is planned, and which therefore wishes to understand the potential impacts of climate variability. A good example of this would be developing countries looking to develop energy infrastructure along a low-emissions pathway.

The remainder of this chapter provides a summary of the key results from this thesis and their implications. Sections 7.1 to 7.4 are structured around the primary science objectives that were presented in chapter 1. The chapter ends by highlighting some avenues for future work (section 7.5) and with the key conclusions (7.6).

7.1 Quantification of inter-annual climate variability in the GB power system under recent observed climate

In this thesis, inter-annual climate variability has been shown to impact the operation of the GB power system at all levels of installed wind power capacity, including a system with no installed wind power capacity. Previous studies have acknowledged that variability in GB demand is related to temperature (e.g. Taylor and Buizza (2003), Bessec and Fouquau (2008), Psiloglou et al. (2009), Thornton et al. (2016)). However, the impact of increasing installing renewable generation capacity on this underlying level of variability has not been investigated (Pfenninger and Keirstead (2015), Ueckerdt et al. (2015)).

Increasing the amount of installed wind power capacity results in a reduction the amount of conventional generation required to meet system load. This reduction is not however felt uniformly throughout the system with a ~90% reduction in baseload plant operating opportunity compared to a ~20% increase in peaking plant operating opportu-

nity. The greater relative reduction of baseload plant operating opportunity compared to peaking plant has been previously observed by George and Banerjee (2011), De Jonghe et al. (2011) and Buttler et al. (2016). However, these studies were all conducted using a single year of data, therefore they are not able to provide any information on the impact of inter-annual climate variability on power system operation.

In this study the impact of inter-annual climate variability on all aspects of the GB power system was found to increase with installed wind power capacity. Again, these impacts are not felt uniformly throughout the GB power system. A 5-fold increase in the inter-annual variability of baseload plant operation is seen when the amount of installed wind power capacity on the GB power system is increased from 15 to 45GW. This is large compared to the 0.25-fold increase in the inter-annual variability of peaking plant operation. This is likely to be useful for informing the expected generation opportunities for power plant.

Peak load is reduced in a system including 15GW of installed wind power capacity compared to a system with no installed wind power capacity. This shows that on average, wind power generation is able to provide a contribution at times of peak demand. This is consistent with Buttler et al. (2016) who used only one year of data. Even in a system with 45GW of installed wind power generation, both the mean and inter-annual variability of peak load is reduced compared to a power system with no installed wind power capacity.

A notable result found in this thesis is that the observed changes in GB power system operation are dependent on both the amount and the location of the installed wind power capacity. Previously, Drew et al. (2015) found that including more offshore wind generation leads to an increase in mean capacity factor compared to a distribution with only onshore turbines. The changing capacity factor distribution has been shown here to have important consequences for power system operation. Taking one example, there is a 70TWh reduction of TAER (Total annual energy requirement) between the MED and HIGH wind capacity scenarios (section 3.3). 43TWh of this reduction can be attributed to increasing the volume of wind power installed on the system and 27TWh is due to changing the wind farm distribution. This shows that if power system modelling studies do not accurately represent the distribution of wind farms then there could be large errors in the resultant wind power generation output, and resultant power system impacts. The impacts of changing the distribution show that the recent past experience of the power system cannot be used as a robust guide for future power system operation.

Within this chapter significant increases in installed wind power generation are ap-

plied to the GB power system, with total amounts reaching those predicted for 2035 by National Grid (2015). It is noted here that National Grid (2015) (on which the wind power scenarios for this thesis are based on) also suggest that by 2035 there would be significant changes in consumers demand for power. A roll out of smart meter technology, combined with the electrification of the heat and transport sectors would result in significantly increased GB electricity demand, with the potential for large changes in the diurnal cycle. These changes are not reflected in this modelling work as the demand data is kept at the present day levels throughout the study. This should be noted when interpreting some of the results within the chapter. For example, with 45GW of installed wind power generation, wind power curtailment may be less frequent than suggested by this study due to increased GB demand.

7.2 Characterisation of the meteorological drivers of inter-annual variability in the GB power system

Chapter 5 has shown that winter weather predominantly explains the inter-annual variability of the power system metrics analysed in chapter 4. The GB power system metrics studied did not all have the same meteorological drivers; however, a general theme was that with the addition of installed wind power generation the metrics transitioned from being temperature dependent to wind speed dependent. This was due to the power system metrics being controlled by the behaviour of wind power rather than demand. The amount of installed wind power capacity required for this transition to occur variable depending on the metrics (e.g. for TAER the transition happened at 6GW whereas for baseload plant the transition occurred at ∼10GW).

TAER and baseload plant TVE were both related to the latitude of the eddy-driven jet and phase of the NAO. This builds upon previous studies which relate the phase of the NAO to regional wind power production (Brayshaw et al. (2011b), Jerez et al. (2013)). The correlations of eddy-driven jet latitude and NAO index with power system metrics contain the conflation of temperature dependent and wind speed dependent variability. This suggests that the these phenomena might not be the best way of characterising the meteorological drivers of the power system (as is common practise in the literature; Brayshaw et al. (2011b), Ely et al. (2013), Curtis et al. (2016)) and the relationships between seasonal-mean, near-surface temperatures/wind speeds and power system metrics can provide more useful information on system operation. The focus of this analysis was on

the NAO. Other modes of climate variability such as the EA pattern, or EAWR (discussed in the background chapter) may also be important, this would be an interesting avenue for further work.

Extreme power system events (such as peak load and wind power curtailment) can be related to particular synoptic conditions occurring on timescales of days. The specific synoptic conditions associated with these events are dependent on the amount of wind power capacity that is installed on the power system at a given time. In a power system with no installed wind power capacity peak load events are present when there is high pressure to the north of GB. This is associated with anomalously high winds which bring anomalously cold air over GB and result in high demand events. This synoptic situation is similar to one of the three found during peak demand events in Brayshaw et al. (2012) and Leah and Foley (2012). In contrast, when wind power capacity is installed, the synoptic situation present at times of peak load is a high pressure centred over GB. This results in low wind speeds over GB and moderately cold air. This was another synoptic condition found to be present during times of peak demand in Brayshaw et al. (2012). This analysis demonstrates that, as the amount of wind generation is increased over GB, the synoptic situation which results in peak load events is likely to change.

The synoptic conditions associated with extreme curtailment events in a power system with 30GW of installed wind power capacity agree with the synoptic situation found by Quest (2013). The days of most extreme curtailment are associated with a low pressure centre to the north of GB. This thesis has extended the work of Quest (2013) by analysing the synoptic conditions present throughout the duration of extreme curtailment events in a power system including 30GW of wind power generation, The largest duration curtailment events are due to the low pressure centre remaining stationary for the duration of the event. It is noted that in reality curtailment would be seen with lower levels of installed wind power capacity than in this study, due to network constraint issues.

This work has highlighted the importance of accounting for climate variability when making decisions relevant to power system operation. In terms of peak load and curtailment events, the presence of specific synoptic situations should act as a warning for power system operators to evaluate the rest of the system to determine if the weather conditions will cause an extreme event. This work has also highlighted phenomena that must be well represented in climate models for them to provide useful information when used as an input for power system simulations. In highlighting the meteorological drivers of power system variability this study has allowed for the improved use of seasonal forecasts

of near-surface temperature, near-surface wind speed, and the NAO, within the energy sector.

7.3 Implications of climate model biases for power system simulations

This study rigorously assesses the bias in climate model data used for power system modelling, and the potential errors from leaving this bias uncorrected. HiGEM was chosen to investigate the impact of climate change on the GB power system due to its accurate representation of the storm track location compared to most models from the CMIP5 archive (Woollings et al. (2010), Catto (2009)).

HiGEM represents the magnitude and seasonal variability of 2m temperatures over GB well, however, there is a bias in the magnitude of the seasonal cycle. The analysis in this thesis highlighted that climate models with a warm bias in winter temperatures could produce winter demands which are too low. Conversely if summer temperatures are too cold then demand could also be too low. Both these relationships are consistent with expectation, due to the u-shaped relationship between temperature and demand. Bias correction techniques are not commonly used when looking at the impact of climate change on demand (Thatcher (2007), Mirasgedis et al. (2007), Isaac and van Vuuren (2009)), however, there are circumstances when climate model bias has been examined and deemed small (Mirasgedis et al. (2007)) or corrected (Franco and Stanstad (2007)).

An evaluation of the 10m wind speeds in HiGEM highlighted that the bias present in HiGEM was not constant throughout the year. The bias was also different depending on whether onshore or offshore grid boxes were examined. This analysis highlighted that near surface wind speed biases in climate models can be complex, and that a single correction for all wind farms (such as in as in Barstad et al. (2012) and Tobin et al. (2015)) may not be appropriate. If the bias in HiGEM wind speed was not corrected, the magnitude of wind power generation would be significantly reduced compared to observations. This highlights the importance of evaluating the climate model output for use in power system modelling studies, a process which is not always done within the literature (Cradden et al. (2012), Tobin et al. (2016), Hdidouan and Staffell (2017)).

The results from chapter 4 and 5 have shown the accurate representation of the synoptic timescale co-variability between temperature and wind speed is important if the co-variability of demand and wind power generation is to be captured (and therefore the

correct behaviour of power system metrics). HiGEM is able to reproduce the co-variability between near-surface temperatures and wind speeds well, even when the initial variables are biased. The bias corrections applied to the surface temperatures and wind speeds have not impacted the co-variability of the temperature and wind speed time series in HiGEM, and therefore do not reduced the amount of useful meteorological information that the climate model can provide for power system assessment. The assessment of the co-variability of near surface temperatures and wind speeds within climate models is highlighted as an important process that researchers should evaluate within climate model development if they are to be used for power system modelling. It could be speculated that HiGEM accurately represents the co-variability of near-surface temperatures and wind speeds well due to HiGEM representing the underlying physical weather phenomena responsible for the co-variability (e.g. extra-tropical cyclones (Catto et al. (2011)). This therefore suggests that GCM's are able to provide useful information for power system modelling at synoptic timescales.

7.4 The impact of climate change on the GB power system

The analysis in chapter 6 involving idealised future climate scenarios is a sensitivity experiment to investigate how increasing anthropogenic climate forcing may impact the weather-dependent power system components. This study quantified how climate change may impact the mean state and amount of inter-annual variability experienced by GB power system components.

The quadratic relationship between temperature and demand means that a $\sim3.5^{o}$C increase in mean GB land-only 2m temperature results in a mean decrease in demand of ~0.5GW ($\sim1\%$). The seasonal cycle of demand is much less pronounced in a future climate (as suggested by Thatcher (2007) for Australia). This is because the potential response of demand to climate change is not uniform across the seasons with a mean increase in summer demands ($+5\%$), a reduction in mean winter and mean spring demand ($- \sim5\%$) and no change in mean autumn demand.

A quadrupling of CO_2 concentrations results in a 15% reduction in the inter-annual variability of demand. This is predominantly due to a large reduction in the seasonal variability of winter demands (which see an 11% reduction in the inter-annual max-min range).

The changing relationship between temperature and demand in a future climate has

been observed before in Isaac and van Vuuren (2009) and Golombek et al. (2011) who have shown that GB has a significantly reduced heating requirement in a future climate scenario. These studies did not however analyse any changes in inter-annual variability of demand in a future climate. A $\sim16\%$ reduction is seen in the inter-annual variability of demand between the control run and the 4xCO$_2$ scenario. This reduction in variability is important to power plant owners who may have to adapt to changes in the number of hours per year (and time of year) in which they are required to operate.

A 2% reduction in summer wind power capacity factor is seen in a future climate, accompanied by a 0.5% increase in mean winter capacity factor. These results agree with Cradden et al. (2012), Hueging et al. (2013) and Tobin et al. (2015) who show that the mean summer wind speeds reduce for a range of future climate scenarios. Both Hueging et al. (2013) and Tobin et al. (2015) show an increase in inter-annual variability in GB wind power production in a future climate, which is not seen in this study. The results shown here, however, motivate the need for a multi-model assessment of changes in wind power generation using a variety of methods and climate models to robustly quantify potential future changes.

The changes in demand and wind power generation result in a reduction in the mean value and inter-annual variability of all of the power system metrics. These metrics have been shown in chapter 4 to be dominated by the variability of wind power rather than demand; however, in a future climate these changes in variability are due to changes in demand. For example a quadrupling of CO$_2$ results in a $\sim30\%$ reduction in peaking plant operation, and a 6% reduction in peak load. The reduction in mean demand could result in less conventional generation being required to meet system load, which could cause some currently operational peaking plant to shut down.

Power system modelling studies tend not to focus as far into the future as this work due to the uncertainty in power system configuration, and future demand towards the end of the century (Mideksa and Kallbekken (2010)). The results from chapter 6 can, however, be used in conjunction with other studies to understand how changes in climate may compare to the magnitude of changes that the GB power system may experience due to electrification of transport and heating, or energy efficiency improvements. For example, in this thesis we show that a 3TWh reduction in total annual energy requirement is seen between the control run and 4xCO$_2$ scenarios. This can be compared to the potential 26TWh increase in annual demand due to the electrification of transport (NERC (2016)). This comparison suggests that changes in annual mean temperature may not be the most

important factor in future demand patterns. Quantifying this contribution is important for policy makers considering future demand reduction or adaptation strategies.

7.5   Future Work

This thesis has highlighted a number of interesting avenues for further research which are discussed below:

- The framework for analysis used in this thesis does not incorporate spatial or temporal power system constraints, such as restrictions on plant ramping rates, or network constraint. Incorporating these constraints may lead to changes in the magnitude of the impacts of inter-annual climate variability on the GB power system observed in this study. This could be analysed by using the multi-decadal demand and wind power generation series created as part of this thesis as inputs for a high resolution power system model.

- Incorporating solar power within the current modelling framework would allow for understanding of how solar power impacts the inter-annual variability of the GB power system observed in this study. This would be an important development if the framework were to be used to accurately model countries such as GB with rapidly growing installed solar capacity or developing countries with high solar generation potential. Methods of modelling solar generation using re-analysis data are present in the literature (Jurus et al. (2013), Bett and Thornton (2016)) and could be adapted for use over GB.

- In this thesis the GB power system has been analysed extensively, however, the framework is easily adaptable for analysis in other countries. This framework could be particularly useful for developing countries who may plan to install large quantities of renewable generation to meet climate mitigation targets.

- This thesis has highlighted that GCM's can be used to provide useful information on power system operation. Therefore an avenue for future work could be to use multi-century records of HiGEM data to investigate the return periods of meteorological events associated with extreme power system risk (such as the meteorological conditions accounted with peak demand or extreme curtailment; discussed in chapter 5).

- A limitation of the analysis on the impact of climate change on the GB power system is that the $2xCO_2$ and $4xCO_2$ scenarios are simulations from one model. There is large uncertainty in climate model response to climate change, so it is important to note that this work shows only two possible future realisations. A thorough assessment of the impacts of future climate on the weather-dependent component of the GB power system would require a multi-model assessment.

7.6 Conclusions

Overall, the modelling techniques used in this thesis have been effective in assessing the impact of inter-annual climate variability and climate change on an idealised GB power system. The modelling tools used in this thesis complement previous literature, and highlight the need for existing power system planning studies to adapt to using increasing amounts of weather and climate data. In completing the over-arching thesis aim of exploring the impact of climate variability and climate change on the GB power system, a number of key conclusions have been found. The five key messages from this thesis are summarised in the bullet points below:

- Inter-annual climate variability impacts the GB power system for a system with no installed wind power capacity. The impacts become larger as the amount of installed wind power capacity is increased. Using a LDC approach a 60% reduction in mean TAER is seen between a present day power system and one with 45GW of installed wind power capacity. This reduction in mean is accompanied by a 50% increase in the inter-annual max-min range of TAER. The impacts of inter-annual climate variability are not uniform throughout the system, with the largest impacts seen for baseload plant. This shows that power system modelling studies should start taking a more robust approach to their use of weather and climate data, not relying on single-years of data to represent inter-annual fluctuations in weather-dependent power system components.

- Changes in the GB wind farm distribution from mostly onshore to mostly offshore results in a reduction in the impact of inter-annual climate variability on the GB power system. For example, the 70TWh reduction in mean TAER between the MED and HIGH wind power scenarios was 60% due to increasing the volume of installed wind power generation and 40% due to the increase in offshore generation. This shows that accurately representing the configuration of wind farms within a

power system modelling study is key to providing representative results.

- The inter-annual variability of the GB power system is predominantly controlled by winter weather, however the detailed meteorological drivers of power system behaviour differ depending on the power system metric which is analysed. A transition from a temperature dependent power system, to wind speed dependent power system is seen as more wind power generation is installed. This transition does not happen at the same level of installed wind power generation for all plant types, for example 6GW of installed wind power generation is required for TAER to become wind speed dependent and $\sim$10GW is required for baseload TVE. Near surface temperatures, wind speeds, and their co-variability are highlighted as important phenomena for climate models to accurately represent if they are to be used for power system modelling.

- Extreme power system events are controlled by specific synoptic conditions, the precise nature of which depend on the amount of wind power generation installed on the system. This highlights that the synoptic conditions associated with extreme power system events are not constant in time and will evolve with the installation of renewable generation capacity. For example, in a system with no installed wind power generation peak load events occur when high pressure is located to the North of GB, whereas when wind power capacity is installed peak load events are associated with high pressure centred over GB.

- Analysis using idealised future climate simulations from HiGEM has shown that a quadrupling of CO_2 concentrations could result in mean baseload TVE and peaking plant TVE both reducing by $\sim$30%. This is due to a reduction in heating-induced demand ($\sim$5%) and negligible changes in wind power generation. The inter-annual variability experienced by the total GB power system and its components is also be reduced if CO_2 concentrations are quadrupled (the inter-annual max-min range of peaking plant operation reduces by 30%, with baseload plan reducing by 5%). This reduction in inter-annual power system variability therefore somewhat counteracts increases in power system variability caused by installing more wind power generation.

It is however noted that the quantitive conclusions mentioned above are impacted by the idealised methodology of the thesis. The lack of temporal and spatial constraints within the LDC modelling result in increased amounts of baseload plant operation com-

pared to in reality (where ramping constraints would reduce operation). The static demand profile used in this thesis (with a fixed diurnal cycle in all scenarios) does not allow for changes in system operation due to the electrification of heat and transport. The combination of these factors may impact the results seen in Chapter 4. Finally, the fixed relationship between temperature and demand over time also may not be representative of the future uptake of air-conditioning in a warmer climate, which could impact the results in Chapter 6.

This thesis has highlighted some of the key meteorological phenomena which climate models must be able to reproduce accurately to be used in power system modelling studies, and emphasised the importance of assessing climate model bias. It is therefore hoped that this work will prove useful to power system modellers who are not aware of the potential biases in climate models, or of the impact climate model bias could have on power system modelling results. Furthermore, this work has provided a step towards the robust assessment of the impact of climate variability and climate change on the GB power system, emphasising the importance of the use of multi-decadal records of data for accurate impact assessment. Future collaboration between climate scientists and power system modellers should allow high resolution meteorological data to be combined with complex power system models, to provide useful information to policy makers and future power system investors.

Chapter 8:

Appendices

8.1 Appendix 1: Land Fraction Comparisons of MERRA and HiGEM

Table 8.1 MERRA GB annual-mean and standard deviation of daily-mean 2m temperatures, spatially averaged over GB with varying land fractions.

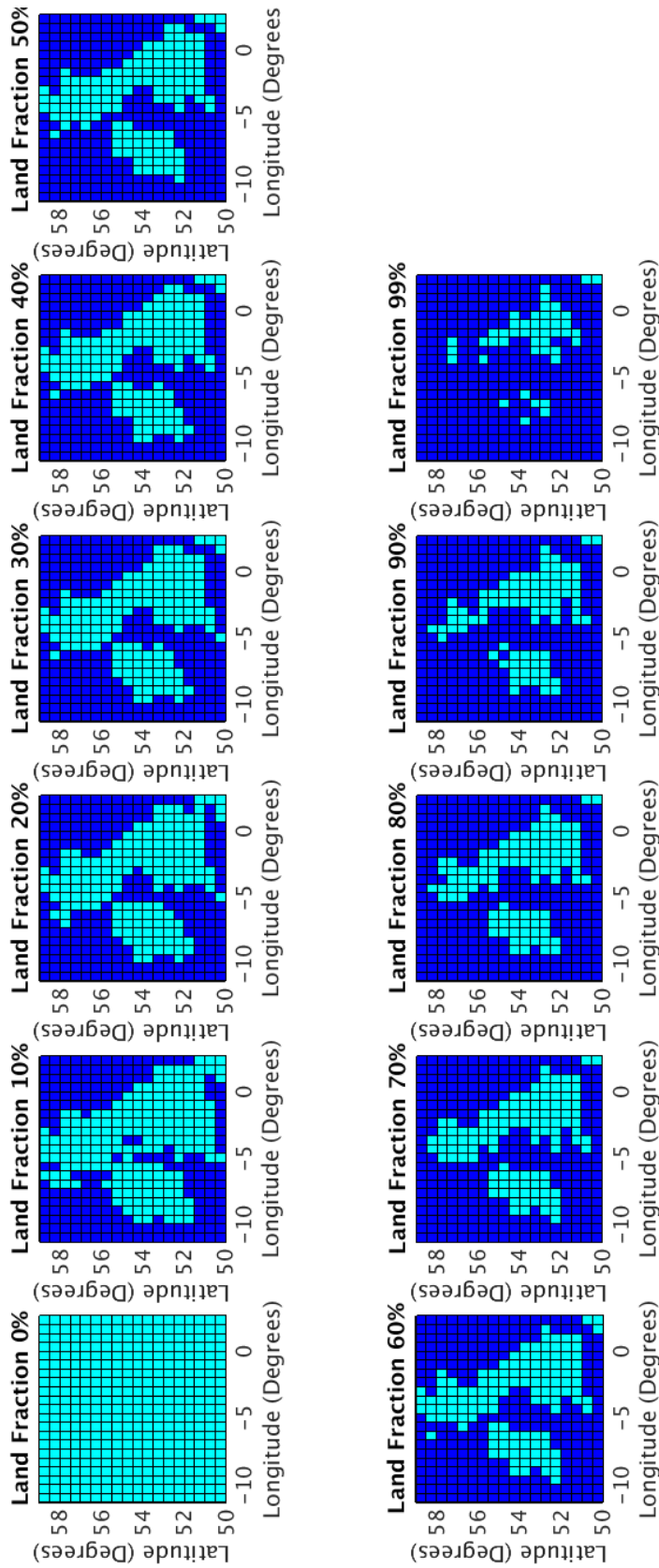|	MERRA		HiGEM	
Land Fraction (%)	GB annual mean temperature (K)	GB temperature standard deviation	GB annual mean temperature (K)	GB temperature standard deviation
0	10.36	3.71	9.75	4.00
10	10.22	4.62	9.57	4.73
20	10.05	4.83	9.50	4.97
30	9.96	4.90	9.41	5.09
40	9.90	5.08	9.34	5.15
50	9.87	5.15	9.33	5.28
60	9.83	5.18	9.09	5.37
70	9.75	5.35	8.92	5.51
80	9.55	5.41	8.91	5.66
90	9.46	5.48	8.64	5.68
100	9.41	5.83	8.70	5.76

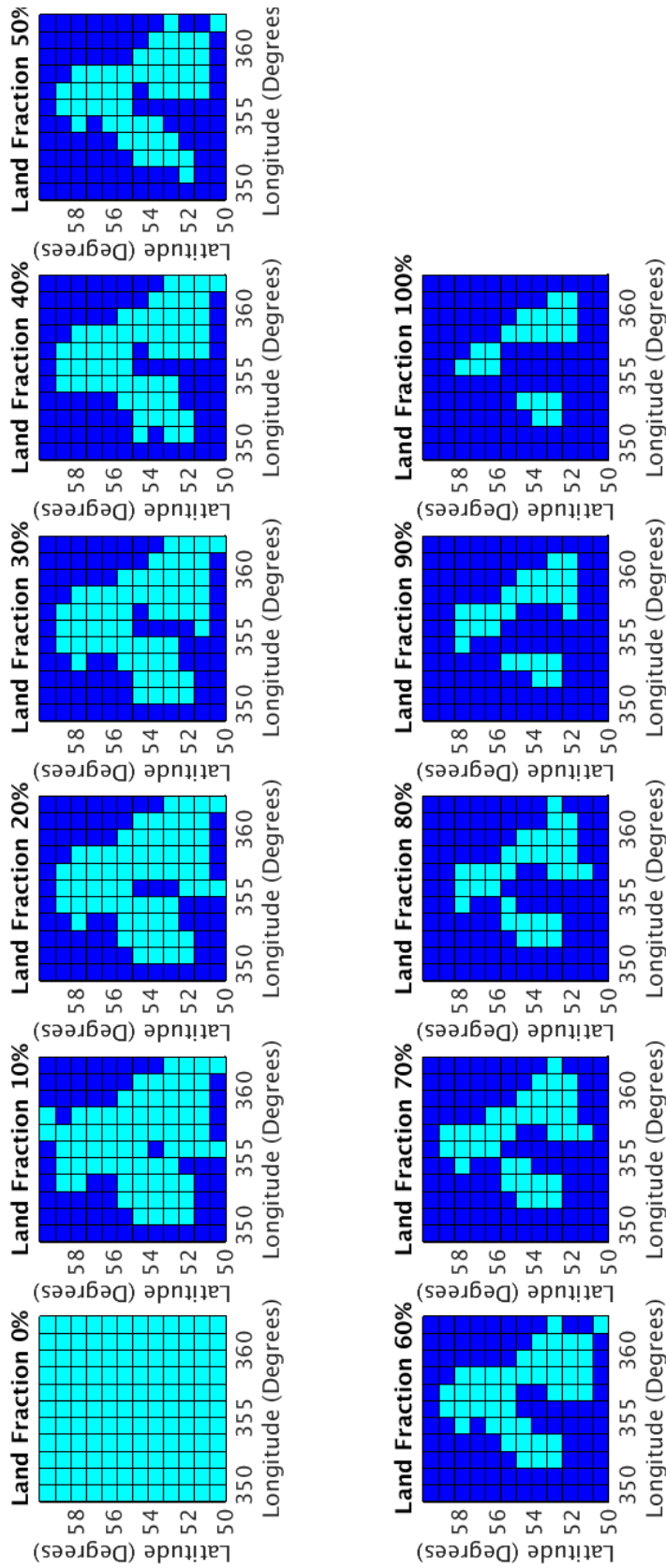**Figure 8.1** MERRA land fractions

Figure 8.2 HiGEM land fractions

8.2 Appendix 2: A comparison of 10m wind speeds between MERRA, ERA-interim, MERRA2 and HiGEM

Figure 8.3 shows seasonal histograms of the land-only and ocean-only winds from the data inputs used in this study, the MERRA re-analysis (Rienecker et al. (2011)) and HiGEM (Shaffrey et al. (2009)) in blue and red solid lines respectively. The ERA-interim (Dee et al. (2011)) and MERRA2 (available at: $https$: $//gmao.gsfc.nasa.gov/reanalysis/MERRA-2/$) re-analysis products are included for comparison.

Bias correction of meteorological fields in this thesis is performed assuming MERRA is the *truth*. In Figure 8.3 it is acknowledged that there are differences between re-analysis products (especially over the land) which means this assumption of truth is not strictly valid. The differences between re-analysis products in the land-only histograms are small compared to the differences between the re-analysis products and HiGEM, therefore the assumption is deemed valid.

The design of the Cannon et al. (2015) wind power model means that the wind power curve acts as a transfer function to correct differences between the re-analysis derived capacity factor and the observed capacity factor. These differences could be due to a bias in the re-analysis product, but also due to other factors such as reduced efficiency of wind turbine operation. If another re-analysis product was to be used then the power curve would have to be re-calibrated in order to provide the best fit between the new re-analysis and results. The differences between MERRA, MERRA2 and ERA-interim (Dee et al. (2011) are acknowledged in this appendix, however it is beyond the scope of this project to understand if any re-analysis is *most appropriate* for use in power system modelling.
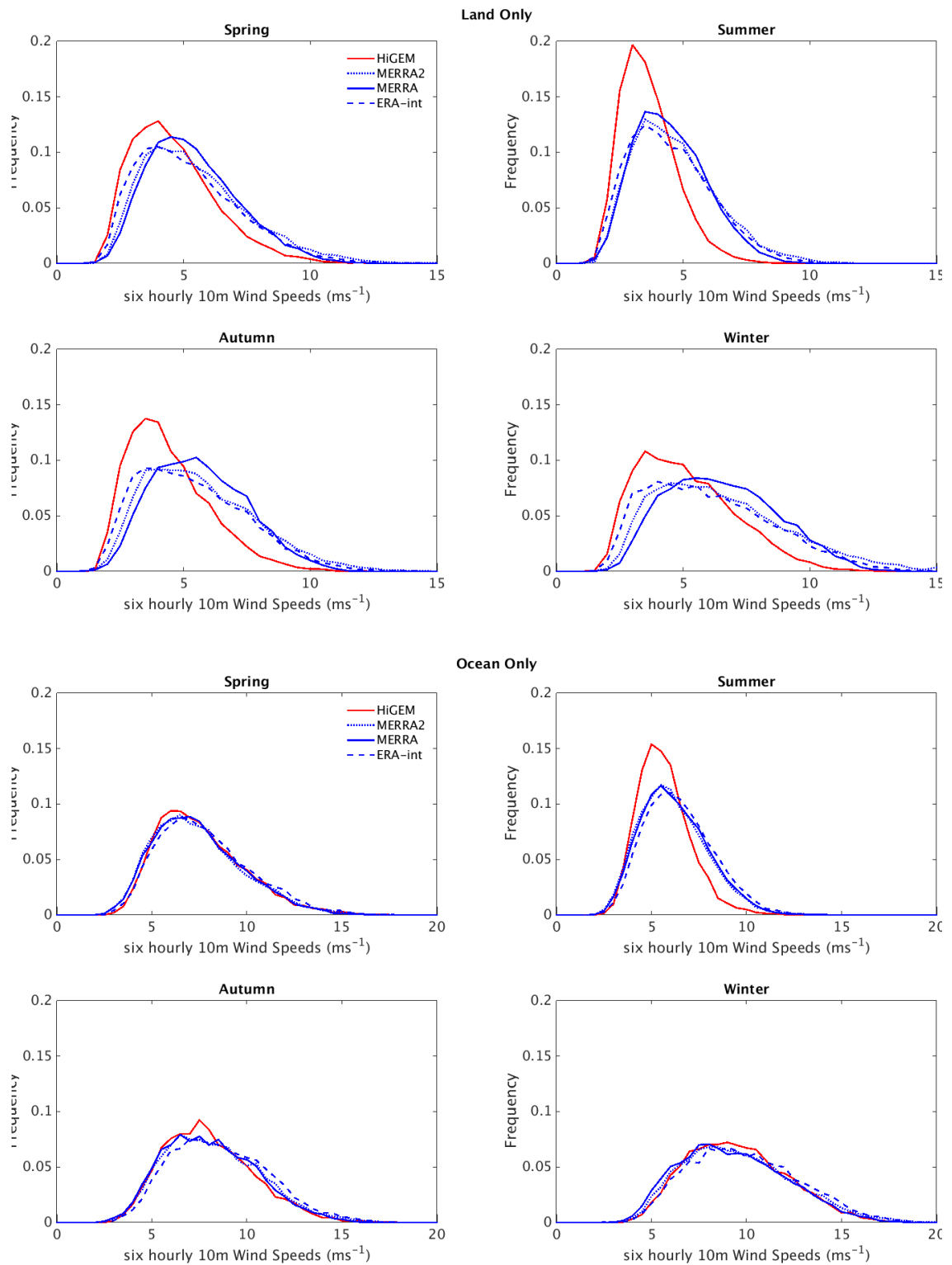
Figure 8.3 Seasonal histograms of land-only and ocean-only wind speeds from MERRA (blue solid) MERRA2 (blue dotted) ERA-interim (blue dashed) and HiGEM (red).

8.3 Appendix 3: Extreme years for power system metrics with variable levels of installed wind power generation

Table 8.2 The year of maximum and minimum values of each metric under the four different installed wind-power scenarios. See section 3.4 for definition of the scenarios and metrics.

Metric	NO-WIND max year	min year	LOW max year	min year	MED max year	min year	HIGH max year	min year
TAER	2010	2007	2010	1990	2010	1990	2010	1990
Peak Load	1987	1988	1982	1988	1995	2004	1995	1988
Peaking TVE	1982	1988	1997	2004	2006	1984	2006	1983
Peaking MLR	2010	2008	2010	1990	2010	1990	2010	1998
Mid Merit Plant	1996	2011	2010	1990	2010	1990	2010	1998
Baseload TVE	1985	1995	1984	2011	2010	1990	2010	1990
Baseload MLR	1995	2007	1984	2011	2010	1990	2010	1990

References

Antonanzas, J., N. Osorio, R. Escobar, R. Urraca, F. Martinex-de Pison, and F. Antonanzas-Torres, 2016: Review of photovoltaic power forecasting. *Solar Energy*, **136**, 78–111.

Apadula, F., A. Bassini, A. Elli, and S. Scapin, 2012: Relationships between meteorological variables and monthly electricity demand. *Applied Energy*, **98**, 346–356.

Baker, A., D. Bunn, and E. Farmer, 1985: *Load forecasting for scheduling generation on a large interconnected system*. Wiley, 57-67 pp.

Barnston, A. and R. Livezey, 1986: Classification, seasonality and persistence of low-frequency atmospheric circulation patterns. *Monthly Weather Review*, **115**, 1083–1126.

Barstad, I., A. Sorteberg, and M. Masquita, 2012: Present and future offshore wind power potential in northern Europe based on downscaled global climate runs with adjusted SST and sea ice cover. *Renewable Energy*, **44**, 398–405.

Beenstock, M., E. Goldin, and D. Nabot, 1999: The demand for electricity in Israel. *Energy Economics*, **21**, 168–183.

Bengtsson, L., S. Hagemann, and K. Hodges, 2004: Can climate trends be calculated from reanalysis data? *Journal of Geophysical Research*, **109**, 1–8.

Bengtsson, L., K. Hodges, and N. Keenlyside, 2009: Will extratropical storms intensify in a warmer climate? *Journal of Climate*, **22**, 2276–2301.

Bessec, M. and J. Fouquau, 2008: The non-linear link between electricity consumption and temperature in europe: A threshold panel approach. *Energy Economics*, **30 (5)**, 2705–2721.

Bett, P. and H. Thornton, 2016: The climatological relationships between wind and solar energy supply in Britain. *Renewable Energy*, **87 (1)**, 96–110.

Bett, P., H. Thornton, and R. Clark, 2013: European wind variability over 140 yr. *Advances in Science and Research*, **10 (1)**, 51–58.

References

Blackmon, M., 1976: A climatological Spectral Study of the 500mb Geopotential Height of the Northern Hemisphere. *Journal of Atmospheric Sciences*, **33**, 1607–1624.

Bloom, S., A. Takacs, A. DaSilva, and D. :edvina, 1996: Data assimilation using incremental analysis updates. *Monthly Weather Review*, **124**, 1256–1271.

Bloomfield, H., D. Brayshaw, L. Shaffrey, P. Coker, and H. Thornton, 2016: Quantifying the increasing senstivity of power systems to climate variability. *Environmental Research Letters*, **11 (124025)**.

Boilley, A. and L. Wald, 2015: Comparison between meteorological re-analyses from ERA-Interim and MERRA and measurements of daily solar irradiation at surface. *Renewable Energy*, **75**, 135–143.

Bossmann, T. and I. Staffell, 2015: The shape of future electricity demand: Exploring load curves in 2050s germany and britain. *Energy*, **90**, 1317–1333.

Brayshaw, D., C. Dent, and S. Zachary, 2012: Wind generation's contribution to supporting peak electricity demand: meteorological insights. *Journal of Risk and Reliability*, **226 (1)**, 44–50.

Brayshaw, D., B. Hoskins, and M. Blackburn, 2009: The basic ingredients of the North Atlantic storm track. Part 1: Land-sea contrast and orography. *Journal of Atmospheric Sciences*, **66**, 2539–2588.

Brayshaw, D., B. Hoskins, and M. Blackburn, 2011a: The basic ingredients of the north atlantic storm track. part 2: Sea surface temperatures. *Journal of Atmospheric Sciences*, **68**, 1784–1805.

Brayshaw, D., A. Troccoli, R. Fordham, and J. Methven, 2011b: The impact of large scale atmospheric circulation patterns on wind power generation and its potential predictability: A case study over the UK. *Renewable Energy*, **36 (8)**, 2087–2096, doi: 10.1016/j.renene.2011.01.025.

Buttler, A., F. Dinkel, S. Franz, and H. Spliethoff, 2016: Variability of wind and solar power: An assessment of the current situation in the European Union based on the year 2014. *Energy*, **106**, 147–161.

Cannon, D., D. Brayshaw, J. Methven, P. Coker, and D. Lenaghan, 2015: Using reanalysis data to quantify extreme wind power generation statistics: A 33 year case study in Great Britain. *Renewable Energy*, **75**, 767–778.

Cassou, C., L. Terray, J. Hurrell, and C. Deser, 2004: North atlantic winter climate regimes: Spatial asymmetry, stationarity with time and oceanic forcing. *Journal of Climate*, **17**, 1055–1068.

Cattiaux, J., R. Vautard, C. Cassou, P. Yiou, V. V. Masson-Delmotte, and V. Codron, 2010: Winter 2010: A cold extreme in a warming climate. *Geophysical Research Letters*, **37**, 1–5.

Catto, J., 2009: Extratropical cyclones in HiGEM: Climatology, structure and Future predicitions. Ph.D. thesis, University of Reading.

Catto, J., L. Shaffrey, and K. Hodges, 2010: Can climate models capture the structure of extratropical cyclones? *Journal of Climate*, **23**, 1621–1635.

Catto, J., L. Shaffrey, and K. Hodges, 2011: Northern Hemisphere Extratropical Cyclones in a Warming Climate in the HiGEM High-Resolution Climate Model. *Journal of Climate*, **24**, 5336–5352.

CCC, 2008: Building a low-carbon economy the UK's contribution to tackling climate change. Tech. rep., Committee on Climate Change, 1-12 pp., London.

CCC, 2017: Uk climate change risk assessment 2017 synthesis report: prioirities for the next five years. Tech. rep., Committee on Climate Change, 1-30 pp. URL https://www.theccc.org.uk/wp-content/uploads/2016/07/UK-CCRA-2017-Synthesis-Report-Committee-on-Climate-Change.pdf.

Chang, E., Y. Guo, and X. Xia, 2012: CMIP5 multimodel ensemble projection of storm track change under global warming. *Journal of Geophysical Research: Atmospheres*, **117 (D23118)**.

Cheruy, F., J. Dufrensne, F. Hourdin, and A. Ducharne, 2014: Role of clouds and land-atmosphere coupling in midlatitude continental summer warm biases and climate change amplification in cmip5 simulations. *Geohysical Research Letters*, **41**, 64936500.

Christensen, J. and F. Boberg, 2012: Temperature dependent climate projection deficiencies in CMIP5 models. *Geohysical Research Letters*, **39**, 1–5.

Colantuono, G., Y. Wang, E. Hannah, and R. Erdelyi, 2014: Signature of the North Atlantic Oscillation on British solar radiation availability and PV potential: The winter zonal seesaw. *Solar Energy*, **107**, 210–219.

Comas-Bru, L. and F. McDermott, 2014: Impacts of the EA and SCA patterns on the European twentieth century NAO-winter climate relationship. *Quarterly Journal of the Royal Meteorolgical Society*, **140**, 354–363.

Compo, G., et al., 2011: Review article the twentieth century reanalysis project. *Quarterly Journal of the Royal Meteorological Society*, **137**, 1–28.

Connolly, D., H. Lund, B. Mathiesen, and M. Leahy, 2010: A review of computer tools for analysing the integration of renewable energy into various energy systems. *Applied Energy*, **87**, 1059–1082.

Cradden, L., G. Harrison, and J. Chick, 2012: Will climate change impact on wind power development in the UK? *Climatic Change*, **115**, 837–852.

Curtis, J., M. Lynch, and Z. L, 2016: The impact of the North Atlantic Oscillation on electricity markets: A case study on Ireland. *Energy Economics*, **58**, 186–198.

Dacre, H., M. Hawcroft, M. Stringer, and K. Hodges, 2012: An extratropical cyclone atlas: A tool for illustrating cyclone structure and evolution characteristics. *BAMS*, **93**, 1497–1502.

Davies, T., M. Cullen, A. Malcolm, M. Mawson, A. Staniforth, A. White, and N. Wood, 2005: A new dynamical core for the met offices global and regional modelling of the atmosphere. *Quarterly Journal of the Royal Meteorological Society*, **131**, 1759–1782.

De Jonghe, C., E. Delarue, R. Belmans, and W. D'haeseleer, 2011: Determining optimal electricity technology mix with high level of wind power penetration. *Applied Energy*, **88 (6)**, 2231–2238.

Deane, P., A. Chiodi, M. Gargiulo, and B. Gallachoir, 2012: Soft-linking of a power systems model to an energy systems model. *Energy*, **42**, 303–312.

DECC, 2013: Electricity Generation Costs, UK. Tech. rep., Department of Energy and Climate Change, 1-30 pp. URL `http://www.decc.gov.uk/assets/decc/statistics/projections/71-uk-electricity-generation-costs-update-.pdf`.

DECC, 2016: Energy trends march 2016. Tech. rep., Department of Energy and Climate Change, 49 pp. URL `https://www.gov.uk/government/uploads/system/uploads/attachment_data/file/524695/Energy_Trends_March_2016.pdf`.

Dee, D., et al., 2011: The ERA-Interim reanalysis: configuration and performance of the data assimilation system. *Quarterly Journal of the Royal Meteorological Society*, **137**, 553–597.

Dong, B., R. Sutton, T. Woollings, and K. Hodges, 1998: The arctic oscillation signature in the wintertime geopotential height and temperature fields. *Environmental Research Letters*, **25**, 1297–1300.

Dowling, P., 2013: The impact of climate change on the European energy system. *Energy Policy*, **60**, 406–417.

Drew, D., D. Cannon, D. Brayshaw, J. Barlow, and P. Coker, 2015: The Impact of Future Offshore Wind Farms on Wind Power Generation in Great Britain. *Resources*, **4 (1)**, 155–171.

Earl, N., S. Dorling, R. Hewston, and R. von Glasow, 2013: 1980 - 2010 Variability in U.K. Surface Wind Climate. *Journal of Climate*, **26 (4)**, 1172–1191.

Ely, C., D. Brayshaw, J. Methven, J. Cox, and O. Pearce, 2013: Implications of the North Atlantic Oscillation for a UK-Norway Renewable Power System. *Energy Policy*, **62**, 1420–1427.

Emeis, S. and M. Turk, 2007: Comparison of logarithmic wind profiles and power law wind profiles and their applicability for offshore wind profiles. *Wind Energy*, 61–64.

ENTSOE, 2016: European network of transmission system operators for electricity data platform: `http://www.entsor.eu/data/Pages/default.aspx`. Accessed: 2016-01-05, accessed: 2016-01-05.

Felice, M. D., A. Allesandri, and F. Catalano, 2009: Seasonal climate forecasts for medium-term electricity demand forecasting. *Applied Energy*, **137**, 435–444.

Felice, M. D., A. Allesandri, and P. Ruti, 2013: Electricity demand forecasting over Italy: Potential benefits using numerical weather prediction models. *Electric Power Systems Research*, **104**, 71–79.

Filik, U., O. Gerek, and M. Kurban, 2011: A novel modeling approach for hourly forecasting of long-term electricity demand. *Energy Conversion and Management*, **52**, 199–211.

Franco, G. and A. Stanstad, 2007: Climate change and electricity demand in California. *Climatic Change*, **87**, 139–151.

Freris, L. and D. Infield, 2008: *Renewable Energy in Power Systems.* Wiley, 1-30 pp.

Fruh, W., 2013: Long-term wind resource and uncertainty estimation using wind records from Scotland as example. *Renewable Energy*, **50**, 1014–1026.

George, M. and R. Banerjee, 2011: A methodology for analysis of impacts of grid integration of renewable energy. *Energy Policy*, **39**, 1265–1276.

Gillett, N., H. Graf, and T. Osborn, 2008: *The North Atlantic Oscillation: Climatic Significance and Environmental Impact.* American Geophysical Union, Washington D.C., 193-208 pp.

Golding, E. and J. Stodhart, 1949: The generation of electricity by wind power. *I.E.E.E*, 1–23.

Golombek, R., A. Sverre, and I. Haddeland, 2011: Climate change: impacts on electricity markets in Western Europe. *Climatic Change*, **113**, 357–370.

Gordon, H., et al., 2002: The csiro mk3 climate system model. Tech. rep., CSIRO Atmospheric Research, 1-135 pp.

Green, R., 2005: Electricity and Markets. *Oxford Review of Economic Policy*, **21 (1)**, 67–87.

Green, R. and N. Vasilakos, 2010: Market behaviour with large amounts of intermittent generation. *Energy Policy*, **38 (7)**, 3211–3220.

Grünewald, P., T. Cockerill, M. Contestabile, and P. Pearson, 2011: The role of large scale storage in a GB low carbon energy future: Issues and policy challenges. *Energy Policy*, **39 (9)**, 4807–4815.

Gulev, S., O. Zonlina, and S. Grigoriev, 2001: Extratropical cyclone variability in the northern hemisphere winter from the necp/ncar reanalysis. *Climate Dynamics*, **17**, 795–809.

Harvey, B., L. Shaffrey, and T. Woollings, 2015: Deconstructing the climate change response of the Northern Hemisphere wintertime storm tracks. *Climate Dynamics*, **45**, 2847–2860.

Hawkins, S., S. Pryor, D. Eager, and G. Harrison, 2011: Characterising the reliability of production from future british offshore wind fleets. *Renewable Power Generation*, **1**, 212–218.

Hdidouan, D. and I. Staffell, 2017: The impact of climate change on the levelised cost of wind energy. *Renewable Energy*, **101**, 575–592.

Heaps, C., 2012: Long-range energy alternatives planning (leap) system. [software version 2015.0.16]. access at: `http://www.energycommunity.org/default.asp?action=47`.

Heide, D., L. von Bremen, M. Greiner, C. Hoffmann, M. Speckmann, and S. Bofinger, 2010: Seasonal optimal mix of wind and solar power in a future, highly renewable europe. *Renewable Energy*, **35**, 2493–2489.

Hekkenberg, M., R. Benders, H. Moll, and A. S. Uiterkamp, 2009: Indications for a changing electricity demand pattern: The temperature dependence of electricity demand in the Netherlands. *Energy Policy*, **37**, 1542–1551.

Held, I. and A. Hou, 1980: Nonlinear axially symmetric circulations in a nearly inviscid atmosphere. *Journal of Atmospheric Sciences*, **37**, 515–533.

Hippert, H., C. Pedreira, and R. Souza, 2002: Neural networks for short-term load forecasting: a review and evaluation. *IEEE Transactions of power systems*, **16**, 44–55.

Holton, J., 2004: *An introduction of dynamical meteorology.* Elsevier Academic Press, 314-330 pp.

Hor, C., S. Watson, and S. Majithia, 2005: Analyzing the impact of weather variables on monthly electricity demand. *IEEE Transactions on Power systems*, **20**, 2078–2085.

Howden, S. and S. Crimp, 2001: The effect of climate change on electricity demand. *Modsim 2001 international congress on modelling and simulation*, **1**, 565–600.

Hu, Z. and Z. Wu, 2004: The intensification and shift of the annual North Atlantic Oscillation in a global warming scenario simulation. *Tellus: Series A Dynamic Meteorology and Oceanography*, **56**, 112–124.

Hueging, H., R. Haas, K. Born, D. Jacob, and J. Pinto, 2013: Regional changes in wind energy potential over europe using regional climate model ensemble projections. *Journal of Applied Meteorology and Climatology*, **52**, 903–917.

Hurrell, J., Y. Kushnir, G. Otterson, and M. Visbeck, 2003: An Overview of the North Atlantic Oscillation. *Journal of Climate*, **134**, 263–273.

IEA, 2013: World energy outlook special report: Redrawing the energy-climate map. Tech. rep., International Energy Association, 1-134 pp. URL `www.worldenergyoutlook.org/energyclimatemap`.

References

Isaac, M. and D. P. van Vuuren, 2009: Modeling global residential sector energy demand for heating and air conditioning in the context of climate change. *Energy Policy*, **37 (2)**, 507–521.

Jerez, S., R. Trigo, E. Apergis, C. Bhattacharyya, H. Bierkens, and M. Bilgin, 2013: Time-scale and extent at which large-scale circulation modes determine the wind and solar potential in the Iberian Peninsula. *Environmental Research Letters*, **8 (004035)**.

Jurus, P., K. Eben, J. Resler, P. Krc, I. Kasanicky, E. Pelikan, M. Brabec, and J. Hosek, 2013: Estimating climatological variability of solar energy production. *Solar Energy*.

Keeley, S., R. Sutton, and L. Shaffrey, 2009: Does the North Atlantic Oscillation show unusual persistence on intraseasonal timescales? *Geophyiscal Research Letters*, **36**, L22 706.

Kennedy, D., T. Parker, T. Woollings, B. Harvey, and L. Shaffrey, 2016: The response of high-impact blocking weather systems to climate change. *Geophysical Research Letters*, **43**, 7250–7258.

Kirtman, B., et al., 2013: *Near-term Climate Change: Projections and Predictability.* Cambridge University Press, Cambridge, United Kingdom and New York, NY, USA, 9531028 pp.

Kubik, M., D. Brayshaw, P. Coker, and J. Barlow, 2013: Exploring the role of reanalysis data in simulating regional wind generation variability over Northern Ireland. *Renewable Energy*, **57 (1)**, 558–561.

Lam, J., 1998: Climatic and economic influences on residential electricity consumption. *Energy Conversion and Management*, **39 (7)**, 623–629.

Lam, J., H. Tang, and D. H. Li, 2008: Seasonal variations in residential and commercial sector electricity consumption in Hong Kong. *Energy*, **33 (3)**, 513–523.

Leah, P. and A. Foley, 2012: Wind generation output during cold weather-driven electricity demand peaks in Ireland. *Energy*, **39**, 48–53.

Lehmann, J., D. Coumou, K. Frieler, A. Eliseev, and A. Levermann, 2014: Future changes in extratropical storm tracks and baroclinicity under climate change. *Environmental Research Letters*, **8 (084002)**.

Li, M., T. Woolings, K. Hodges, and G. Masato, 2014: Extratropical cyclones in a warmer, moister climate: A recent atlantic analogue. *Geophysical Research Letters*, **41**, 8594–8601.

Li, X. and D. Sailor, 1995: Electricity use sensitivity to climate and climate change. *World Res. Reviews*, **7**, 334–346.

Liu, K., S. Subbarayan, R. Shoults, M. Manry, C. Kwan, F. Lewis, and J. Naccarino, 2002: Comparison of very short-term load forecasting techniques. *IEEE Transactions of power systems*, **11**, 877–882.

Lu, J., G. Vecchi, and T. Reichler, 2007: Expansion of the Hadley Cell under Global Warming. *Geophysical Research Letters*, **36**, 1–5.

Luo, D., Y. Yao, and A. Dai, 2015: Decadal Relationship between European Blocking and the North Atlantic Oscillation during 19782011. Part I: Atlantic Conditions. *Journal of Atmospheric Science*, **72**, 1152–1173.

MacDonald, A. E., C. M. Clack, A. Alexander, A. Dunbar, J. Wilczak, and Y. Xie, 2016: Future cost-competitive electricity systems and their impact on US CO2 emissions. *Nature Climate Change*.

MacGill, I., 2010: Electricity market design for facilitating the integration of wind energy: Experience and prospects with the Australian National Electricity Market. *Energy Policy*, **38 (7)**, 3180–3191.

MARKAL, 2008: Energy technology systems analysis programme: Markal energy system model. access at: `http://www.iea-etsap.org/web/Markal.asp`.

Martin, G. M., M. A. Ringer, V. D. Pope, A. Jones, C. Dearden, and T. J. Hinton, 2006: The physical properties of the atmosphere in the new Hadley Centre Global Environmental Model (HadGEM1). Part I: Model description and global climatology. *Journal of Climate*, **19**, 1274–1301.

Masato, G., B. Hoskins, and T. Woollings, 2012: Wave-breaking characteristics of midlatitude blocking. *Quarterly Journal of the Royal Meteorolgocial Society*, **138**, 1285–1296.

McColl, M., E. Palin, H. Thornton, D. Sexton, R. Betts, and K. Mylne, 2012: Assessing the potential impact of climate change on the UKs electricity network. *Climatic Change*, **115**, 821–835.

McGarrigle, E., J. Deane, and P. Leahy, 2013: How much wind energy will be curtailed on the 2020 Irish power system? *Renewable Energy*, **55 (1)**, 544–553.

McGregor, J., 2004: C-cam: geometric aspects and dynamical formula- tion. csiro marine and atmospheric research. *Technical Paper*, 1–40.

Mideksa, T. and S. Kallbekken, 2010: The impact of climate change on the electricity market: A review. *Energy Policy*, **38**, 3579–3585.

Mirasgedis, S., Y. Sarafidis, E. Georgopoulou, V. Kotroni, K. Lagouvardos, and D. Lalas, 2007: Modeling framework for estimating impacts of climate change on electricity de- mand at regional level: Case of Greece. *Energy Conversion and Management*, **48 (5)**, 1737–1750.

Nahmmacher, P., E. Schmid, L. Hirth, and B. Knopf, 2016: Carpe diem: A novel approach to select representative days for long-term power system modeling. *Energy*, **112**, 430–442.

Nakamura, H., T. Sampe, A. Goto, W. Ohfuchi, and S. Xie, 2008: On the importance of mid-latitude oceanic frontal zones for the mean state and dominant variability in the tropospheric circulation. *Geophysical Research Letters*, **1**, 1–4.

National Grid, 2015: Future Energy Scenarios: UK gas and electricity transmission. Tech. rep., National Grid, 112-139 pp.

National Research Council, N., (Ed.) , 1998: *Decade-to-Century-Scale Climate Variability and Change: A science strategy*. National Academy Press, Washington D.C., 193-208 pp.

NERC, 2016: Living with environmental change: How can UK energy systems be made more resilient to the impacts of climate change? Tech. rep., National Environmental Research Council, 1-4 pp. URL `http://www.nerc.ac.uk/research/partnerships/ride/lwec/ppn/ppn31/`.

Nolan, P., P. Lynch, R. McGrath, T. Semmler, and S. Wang, 2012: Simulating climate change and its effects on the wind energy resource of Ireland. *Wind Energy*, **15**, 593608.

NREL, 2010: Western Wind and Solar Integration Study. Tech. rep., NREL, 536 pp.

NREL, 2011: Eastern Wind and Transmission Integration Study. Tech. rep., NREL, 242 pp.

References

Oswald, J., M. Raine, and H. Ashraff-Ball, 2008: Will British weather provide reliable electricity? *Energy Policy*, **36**, 3212–3225.

Palutikof, J., P. Kelly, and T. D. nd J.A. Halliday, 1987: Impacts of spatial and temporal windspeed variability on wind energy output. *Journal of Applied Meteorology and Climatology*, **26**, 1124–1133.

Parkpoom, S. and G. Harrison, 2008: Using weather sensitivity to forecast Thailand's electricity demand. *IEEE*, **9**, 237–242.

PB, 2013: Elecricity generation model: Update of renewable technologies. Tech. rep., Parsons Brinckerhoff, 1-29 pp. URL https://www.gov.uk/government/publications/parsons-brinckerhoff-electricity-generation-model-2013-update.

Pelly, J. and B. Hoskins, 2003: A new perspective on blocking. *Journal of Atmospheric Science*, **60**, 743–755.

Pfenninger, S. and J. Keirstead, 2015: Renewables, nuclear, or fossil fuels? Scenarios for Great Britain's power system considering costs, emissions and energy security. *Applied Energy*, **152 (1)**, 83–93.

Pfenninger, S. and I. Staffell, 2016: Long-term patterns of European PV output using 30 years of validated hourly reanalysis and satellite data. *Energy*, **114**, 1251–1265.

Pfhal, S. and H. Wernli, 2012: Quantifying the relevance of atmospheric blocking for co-located temperatrue extremes in the Northern Hemisphere on (sub-)daily time scales. *Geophysical Research Letters*, **39 (L12807)**.

Pinto, J., S. Zacharias, A. Fink, G. Leckebusch, and U. Ulbrich, 2009: Factors contributing to the development of extreme north atlantic cyclones and their relationship with the nao. *Climate Dynamics*, **32**, 711–737.

POYRY, 2009: Impact of Intermittency: How wind variability could change the shape of the British and Irish electricity Markets. URL http://www.uwig.org/ImpactofIntermittency.pdf, URL http://www.uwig.org/ImpactofIntermittency.pdf.

Pryor, S., R. Barthemlmie, and J. Schoof, 2006: Interannual Variability of Wind indices across Europe. *Wind Energy*, **9**, 27–38.

References

Psiloglou, B., C. Giannakopoulos, S. Majithia, and M. Petrakis, 2009: Factors affecting electricity demand in Athens, Greece and London, UK: A comparative assessment. *Energy*, **34**, 1855–1863.

Quest, H., 2013: Energy meteorology: Stormy times for uk wind power. Tech. rep., University of Reading.

Rienecker, M., et al., 2011: MERRA: NASA's Modern-Era Retrospective Analysis for Research and Applications. *Journal of Climate*, **24 (14)**, 3624–3648.

Rose, S. and J. Apt, 2015: What can reanalysis data tell us about wind power? *Renewable Energy*, **83**, 963–969.

Sailor, D. and J. Munoz, 1997: Sensitivity of electricity and natural gas consumption to climate in the U.S.A. Methodology and results for eight states. *Energy*, **22**, 987–998.

Sailor, D. J., 2001: Relating residential and commercial sector electricity loads to climate evaluating state level sensitivities and vulnerabilities. *Energy*, **26 (7)**, 645–657.

Santos-Alamillos, F. J., D. Pozo-Vzquez, J. A. Ruiz-Arias, V. Lara-Fanego, and J. Tovar-Pescador, 2012: Analysis of spatiotemporal balancing between wind and solar energy resources in the southern Iberian Peninsula. *Journal of Applied Meteorology and Climatology*, **51**, 2005–2024.

Scaife, A., T. Woolings, J. Knight, G. Martin, and T. Hinton, 2010: Atmospheric blocking and mean biases in climate models. *Journal of Climate*, **23**, 6143–6152.

Schar, C., P. Vidale, D. Luthi, C. Frei, C. Haberli, M. Liniger, and C. Appenzeller, 2004: The role of increasing temperature variability in european summer heatwaves. *Nature*, **427**, 332–336.

Seidel, D., Q. Fu, W. Randel, and T. Reichler, 2008: Widening of the tropical belt in a changing climate. *Nature Geoscience*, **1**, 21–24.

Shaffrey, L., et al., 2009: UK-HiGEM: The New U.K. High Resolution Global Environment Model - Model description and basic evaluation. *Journal of Climate*, **22**, 1861–1896.

Sinden, G., 2007: Characteristics of the uk wind resource: Long-term patterns and relationship to electricity demand. *Energy Policy*, **35**, 112–127.

References

Solomon, S., D. Qin, M. Manning, Z. Chen, M. Marquis, K. Averyt, M.Tignor, and H. Miller, (Eds.) , 2007: *Near-term Climate Change: Projections and Predictability.* Cambridge University Press, Cambridge, United Kingdom and New York, NY, USA, 1-18 pp.

Staffell, I. and S. Pfenninger, 2016: Using bias-corrected reanalysis to simulate current and future wind power output. *Energy*, **114**, 1–15.

Stoft, S., 2002: *Power System Economics: Designing markets for electricity.* Wiley, 1-20 pp.

Taylor, J. W. and R. Buizza, 2003: Using weather ensemble predictions in electricity demand forecasting. *International Journal of Forecasting*, **19 (1)**, 57–70.

Thatcher, M. J., 2007: Modelling changes to electricity demand load duration curves as a consequence of predicted climate change for Australia. *Energy*, **32 (9)**, 1647–1659.

Thompson, D. and J. Wallace, 2013: The arctic oscillation signature in the wintertime geopotential height and temperature fields. *Geophyiscal Research Letters*, **8 (3)**, 1–10.

Thornton, H., B. Hoskins, and A. Scaife, 2016: The role of temperature in the variability and extremes of electricity and gas demand in Great Britain. *Environmental Research Letters*, **11 (114015)**, doi:doi:10.1088/1748-9326/11/11/114015.

Thornton, H., A. Scaife, B. Hoskins, and D. J. Brayshaw, In review: The relationship between wind power, electricity demand and winter weather patterns in Great Britain. *Environmental Research Letters*.

Tibaldi, S. and F. Molenti, 1990: A new perspective on blocking. *Tellus A: Dynamic Meteorology and Oceanogrpahy*, **42**, 343–365.

Tobin, I., et al., 2015: Assessing climate change impacts on European wind energy from ENSEMBLES high-resolution climate projections. *Climatic Change*, **128**, 99–112.

Tobin, I., et al., 2016: Climate change impacts on the power generation potential of a European mid-century wind farms scenario. *Environmental Research Letters*, **11 (3)**, 3–13.

Trigo, R., I. Trigo, C. DaCamara, and T. Osborn, 2004: Climate impact of the European winter blocking episodes from the NCEP/NCAR Reanalyses. *Climate Dynamics*, **23**, 17–28.

References

Ueckerdt, F., R. Brecha, and L. G., 2015: Analyzing major challenges of wind and solar variability in power systems. *Renewable Energy*, **81**, 1–10.

Ueckerdt, F., L. Hirth, G. Luderer, and O. Edenhoffer, 2013: System lcoe: What are the costs of variable renewables? *Energy*, **63**, 61–75.

Ulbrich, U. and M. Christoph, 1999: A shift of the nao and increasing storm track activity over europe due to anthropogenic greenhouse gas forcing. *Climate Dynamics*, **15**, 551–559.

Valor, E., V. Meneu, and V. Casselles, 2001: Daily air temperature and electricity load in Spain. *Journal of Applied Meteorology*, **40**, 1413–1421.

Wangpattarapon, K., S. Maneewan, N. Ketjoy, and W. Rakwichian, 2008: The impacts of climatic and economic factors on residential electricity consumption of Bangkok Metropolis. *Energy and Buildings*, **40**, 1419–1425.

Woollings, T., 2010: Dynamical influences of European Climate: An Uncertain Future. *Philosopghical Transactions of the Royal Society*, **368**, 3733–3756.

Woollings, T. and A. Hannachi, 2010: A Regime View of the North Atlantic Oscillation and Its Response to Anthropogenic Forcing. *Journal of Climate*, **23**, 1291–1307.

Woollings, T., A. Hannachi, and B. Hoskins, 2010: Variability of the North Atlantic eddy-driven jet stream. *Quarterly Journal of the Royal Meteorological Society*, **136**, 856–868.

Yao, R. and K. Steemers, 2005: A method of formulating energy load profile for domestic buildings in the UK. *Energy and Buildings*, **37**, 663–671.

Yin, J., 2005: A consistent poleward shift of the storm tracks in simulations of 21st century climate. *Geophysical Research Letters*, **32**, 1–4.

Zachary, S., C. Dent, and D. Brayshaw, 2011: Challenges in quantifying wind generation's contribution to securing peak demand. *Power and Energy Society General Meeting, 2011 IEEE*, **1 (1)**, 1–8.

Zappa, G., G. Masato, L. Shaffrey, T. Woollings, and K. Hodges, 2014: Linking Northern Hemisphere blocking and storm track biases in the CMIP5 climate models. *Geophysical Research Letters*, **41**, 135–139.

References

Zappa, G., L. Shaffrey, and K. Hodges, 2013a: The ability of CMIP5 to simulate North Atlantic extratropical cyclones. *Journal of Climate*, **26**, 5379–5396.

Zappa, G., L. Shaffrey, K. Hodges, P. Sansom, and D. Stevenson, 2013b: A multimodel assessment of future projections of north atlantic and european extratropical cyclones in the CMIP5 climate models. *Journal of Climate*, **26**, 5846–5862.

Zubiate, L., F. McDermott, C. Sweeney, and M. O'Malley, 2016: Spatial variability in winter NAOwind speed relationships in western Europe linked to concomitant states of the East Atlantic and Scandinavian patterns. *Quarterly Journal of the Royal Meteorolgical Society*, **143**, 552–562.